

# **Block II SRM Conceptual Design Studies Final Report**

## **Conceptual Design Package Volume I, Book 1**

(NASA-CR-179048) BLOCK 2 SRM CONCEPTUAL  
DESIGN STUDIES. VOLUME 1, BOOK 1: CONCEPTUAL  
DESIGN PACKAGE Final Report (Morton  
Thiokol) 275 p

N87-21034

CSCL 21H

G3/20

Unclas  
43354

**19 December 1986**

**MORTON THIOKOL, INC.**

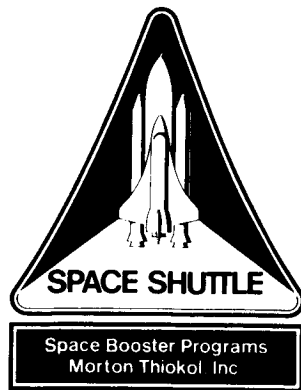
---

**Wasatch Operations**

**Space Division**

P.O. Box 524, Brigham City, Utah 84302 (801) 863-3511

*Publications No. 87354*



# **Block II SRM Conceptual Design Studies Final Report**

## **Conceptual Design Package Volume I, Book 1**

**19 December 1986**

Prepared for

National Aeronautics and Space Administration  
George C. Marshall Space Flight Center  
Marshall Flight Center, Alabama 35812

Contract No. NAS8-37296

**MORTON THIOKOL, INC.**

---

**Wasatch Operations  
Space Division**

P.O. Box 524, Brigham City, Utah 84302 (801) 863-3511

*Publications No. 87354*

## ACKNOWLEDGEMENTS

Under the programmatic direction of the Space Division, the detail design studies were conducted and reported by engineers in the Support Services Division at Morton Thiokol's Wasatch Operations. The following principal engineers completed the conceptual study under the technical management of Mr. Charles R. Voris:

Brad Smith . . . . . Case and Joint Design  
Neal Williams . . . . . Case and Joint Analysis  
John Miller . . . . . Insulation Design  
Joe Ralston . . . . . Nozzle Design  
Jennifer Richardson . . . Nozzle Materials  
Walt Moore . . . . . Ignition  
Dan Doll . . . . . Propellant  
Jeff Maughan . . . . . Ballistics and Motor Performance  
Fred Hayes . . . . . Development and Verification Plan

Morton Thiokol's Capability Assessment was led by Mr. DelRey Bjorkman. Cost estimates were developed under Mr. Grant Lindsay's direction.

PRECEDING PAGE BLANK NOT FILMED

PAGE 11 INTENTIONALLY BLANK

## CONTENTS

	<u>Page</u>
1.0 INTRODUCTION. . . . .	1-1
1.1 NOMENCLATURE. . . . .	1-3
1.2 REQUIREMENTS. . . . .	1-3
2.0 BLOCK II SRM CONFIGURATION SELECTION. . . . .	2-1
2.1 INDUSTRY EXPERIENCE . . . . .	2-2
2.1.1 Space Shuttle SRM . . . . .	2-2
2.1.2 Large SRM Review. . . . .	2-4
2.1.3 Technology Status . . . . .	2-6
2.2 MONOLITHIC MOTOR CONCEPTS . . . . .	2-7
2.3 BLOCK II SRM PERFORMANCE OPTIONS. . . . .	2-13
3.0 BLOCK II SRM CONCEPTUAL DESIGN. . . . .	3-1
3.1 BLOCK II SRM DESIGN DESCRIPTION . . . . .	3-1
3.2 MOTOR PERFORMANCE . . . . .	3-11
3.2.1 Trade Study Summary . . . . .	3-11
3.2.2 Analysis. . . . .	3-16
3.2.3 Performance . . . . .	3-31
3.3 CASE DESIGN . . . . .	3-39
3.3.1 Requirements and Scope of Study . . . . .	3-40
3.3.2 Case Design Description . . . . .	3-42
3.3.3 Material Selection. . . . .	3-44
3.3.4 Case Fabrication Trades . . . . .	3-48
3.3.5 Preliminary Analyses. . . . .	3-51
3.3.5.1 Case Membrane Design. . . . .	3-51
3.3.5.2 Fracture Mechanics Analysis . . . . .	3-53
3.3.5.3 Case Axial Growth Study . . . . .	3-54
3.3.6 Alternate Design Selections . . . . .	3-58
3.3.6.1 Material Backup . . . . .	3-59
3.3.6.2 Integral Kick Ring, Skirt Attach, and Case Joint. . . . .	3-59
3.4 JOINT DESIGN. . . . .	3-63
3.4.1 Objective/Scope . . . . .	3-67
3.4.2 Block II Clevis Joint . . . . .	3-68
3.4.3 Double-Recess Bolted Joint. . . . .	3-78
3.4.4 Single-Recess Bolted Joint. . . . .	3-80
3.4.5 Inclined Bolted Joint . . . . .	3-82
3.4.6 Nozzle Fixed Housing-to-Case Aft Dome Joint . . . . .	3-84
3.5 SEAL DESIGN . . . . .	3-89
3.5.1 Elastomeric Seal Selection for Block II Clevis Joint. . . . .	3-90



## CONTENTS (Cont)

	<u>Page</u>
3.5.2 Elastomeric Seal Design and Testing Summary (RSRM Program). . . . .	3-92
3.5.2.1 Standard Chemical and Physical Properties . . . . .	3-92
3.5.2.2 Resiliency. . . . .	3-92
3.5.2.3 Dynamic Sealing . . . . .	3-99
3.5.2.4 Case Corrosion Protection and O-ring Lubrication. . . .	3-100
3.5.2.5 Aging . . . . .	3-100
3.5.2.6 Heat Resistance . . . . .	3-101
3.5.2.7 Joint Assembly. . . . .	3-101
3.5.2.8 Leak Check. . . . .	3-101
3.5.2.9 Geometric Sizing. . . . .	3-102
3.5.2.10 Seal Producibility. . . . .	3-104
3.5.2.11 Quality Acceptance. . . . .	3-104
3.5.3 Metallic Seal Development and Testing . . . . .	3-105
3.6 NOZZLE DESIGN . . . . .	3-113
3.6.1 Requirements and Scope of Study . . . . .	3-115
3.6.2 Summary of Selected Design. . . . .	3-117
3.6.2.1 Flex Bearing. . . . .	3-119
3.6.2.2 Structures and Internal Seals . . . . .	3-119
3.6.2.3 Ablatives and Insulators. . . . .	3-122
3.6.3 Discussion. . . . .	3-123
3.6.3.1 Flex Bearing. . . . .	3-123
3.6.3.2 Structures and Internal Seals . . . . .	3-132
3.6.3.3 Ablatives and Insulators. . . . .	3-141
3.7 PROPELLANT. . . . .	3-155
3.7.1 Requirements. . . . .	3-156
3.7.2 Propellant Experience Base. . . . .	3-157
3.7.3 Propellant Raw Materials. . . . .	3-158
3.7.4 Propellant Performance. . . . .	3-161
3.7.5 Propellant Processing . . . . .	3-178
3.7.5.1 Processibility. . . . .	3-180
3.7.5.2 Labor and Energy Costs. . . . .	3-185
3.7.5.3 Safety. . . . .	3-186
3.7.6 Conclusion. . . . .	3-186
3.8 LINER . . . . .	3-189
3.8.1 Bond Strength . . . . .	3-190
3.8.2 Compatibility . . . . .	3-190
3.8.3 Maintenance of Bond Integrity With Time . . . . .	3-191
3.8.4 Previous Applications . . . . .	3-193
3.8.5 Castable Inhibitor. . . . .	3-193
3.9 INSULATION DESIGN . . . . .	3-195
3.9.1 Requirements and Scope of Study . . . . .	3-195
3.9.2 Summary of Selected Design. . . . .	3-196
3.9.2.1 Forward Segment . . . . .	3-197

## CONTENTS (Cont)

		<u>Page</u>
3.9.2.2	Center Segments . . . . .	3-197
3.9.2.3	Aft Segment . . . . .	3-198
3.9.2.4	Nozzle-to-Case Insulation . . . . .	3-198
3.9.2.5	Field Joint Insulation. . . . .	3-199
3.9.3	Discussion. . . . .	3-199
3.9.3.1	Asbestos Replacement. . . . .	3-201
3.9.3.1.1	Case Insulation Alternatives. . . . .	3-205
3.9.3.2	Nozzle-to-Case Insulation . . . . .	3-216
3.9.3.2.1	Nozzle/Aft Dome Alternatives. . . . .	3-216
3.9.3.3	Field Joint Insulation. . . . .	3-216
3.9.3.3.1	Field Joint Alternatives. . . . .	3-233
3.9.4	Manufacturing Process Alterations . . . . .	3-246
3.10	IGNITER . . . . .	3-251
3.10.1	Discussion. . . . .	3-251
APPENDIX A	SPECIFICATION NO. CPW1-1900	
APPENDIX B	COMPOSITE MOTOR CASE	
B.1	INTRODUCTION. . . . .	B-1
B.2	SUMMARY AND CONCLUSIONS . . . . .	B-1
B.3	STUDY OBJECTIVES AND APPROACH . . . . .	B-3
B.3.1	Design Requirements . . . . .	B-4
B.3.2	Heads-Up Mission Design Requirements. . . . .	B-5
B.3.3	FWC Design Description. . . . .	B-5
B.3.4	Composite Case Reuse. . . . .	B-9
B.4	BLOCK II SRM COMPOSITE CASE DESIGN. . . . .	B-11
B.4.1	Composite Configuration and Layup . . . . .	B-11
B.4.2	Composite Joint and Seal Design . . . . .	B-14
B.4.3	Block II Composite Case Analysis Results. . . . .	B-16
B.4.4	Block II Composite Case Design Summary. . . . .	B-19
B.5	HYBRID METAL/COMPOSITE CASE . . . . .	B-23
B.5.1	Design Description. . . . .	B-23
B.5.2	Hybrid Case Structural Analysis . . . . .	B-25
B.5.3	Axial Growth and Stiffness. . . . .	B-25
B.5.4	Hybrid Case Reuse . . . . .	B-28

CONTENTS (Cont)

		<u>Page</u>
B.6	JOINT TRADE STUDIES . . . . .	B-28
B.6.1	Double Steel Strap Joint. . . . .	B-28
B.6.2	Tang and Clevis Joint . . . . .	B-30
B.7	MATERIALS AND PROCESS TRADE STUDY . . . . .	B-30
B.7.1	Trade Study With/Without Axial Growth Requirements. . .	B-32
B.7.2	Composite Material Availability . . . . .	B-35
B.7.3	Wet Winding Versus Prepreg. . . . .	B-35
B.8	REFERENCES. . . . .	B-39

## ILLUSTRATIONS

<u>Figure</u>		<u>Page</u>
1	Block II SRM Study Tasks. . . . .	1-2
2	Heads-Up Thrust Versus Time Trace . . . . .	1-5
3	Process for Establishing Block II SRM Design Concept. .	2-3
4	Block II SRM Motor Layout . . . . .	3-2
5	Bonded J-Seal Field Joint Design. . . . .	3-4
6	Nozzle-to-Case Jonint and Insulated Aft Dome . . . . .	3-5
7	SRM Block II Nozzle Configuration . . . . .	3-8
8	SRM Nominal--Heads-Up Comparison Thrust Versus Time Table. . . . .	3-9
9	Adjusted Surface Area Values. . . . .	3-17
10	Heads-Down SRM Propellant Comparison. . . . .	3-21
11	Thrust Performance for Design 1A. . . . .	3-23
12	Thrust Performance for Design 2A. . . . .	3-25
13	Thrust Performance for Design 1B. . . . .	3-27
14	Thrust Performance for Design 2B. . . . .	3-29
15	Heads-Down Payload Comparison . . . . .	3-33
16	Heads-Up Payload Comparison . . . . .	3-35
17	Schematic of Block II Case Design . . . . .	3-43
18	Girth Weld Geometry . . . . .	3-50
19	Pressure Distribution . . . . .	3-55
20	Line Load Comparison. . . . .	3-56
21	Concept for Integrating Skirt Attach and Joint. . . . .	3-60

## ILLUSTRATIONS (Cont)

<u>Figure</u>		<u>Page</u>
22	Alternate Case-to-Aft Dome Joint. . . . .	3-61
23	Case Field Joint Concepts . . . . .	3-64
24	Fixed Housing-to-Aft Dome Connections . . . . .	3-69
25	Block II SRM Clevis Joint . . . . .	3-73
26	Overlay of Block II SRM Clevis Joint and RSRM Baseline Joint. . . . .	3-75
27	Comparison of Gap Motion Between Two SRM Referee Tests (with and without composite overwrap rings) . . . . .	3-77
28	Double Recess Bolted Joint. . . . .	3-79
29	Single Recess Bolted Joint. . . . .	3-81
30	Inclined Bolted Joint . . . . .	3-83
31	Welded Nozzle Joint . . . . .	3-86
32	Bolted Nozzle Joint . . . . .	3-87
33	Silicone S-650 Seal Response to Gap Growth Tests. . . . .	3-91
34	Fluorosilicone L677 Seal Response to Gap Growth Tests . . . . .	3-94
35	Viton 747 Seal Response to Gap Growth Tests . . . . .	3-95
36	Viton GLT Seal Response to Gap Growth Tests . . . . .	3-96
37	Arctic Nitrile Seal Response to Gap Growth Tests. . . . .	3-97
38	Pressure Required to Breach Grease Blockage . . . . .	3-103
39	Thermalok <sup>®</sup> T-Seal in Assembled Position for RSRM. . . . .	3-106
40a	Nozzle Insulation With Thermalok <sup>®</sup> U-Seal for RSRM . . . . .	3-107
40b	Clevis and Joint Configuration. . . . .	3-109
40c	SRM Nozzle-to-Case Joint With Thermalok <sup>®</sup> E-Seal Using Existing Aft Dome . . . . .	3-110

## ILLUSTRATIONS (Cont)

<u>Figure</u>		<u>Page</u>
41	Block II SRM Nozzle . . . . .	3-118
42	Block II Flex Bearing/Thermal Protection Configuration . . . . .	3-120
43	Block II Nozzle Structure and Internal Seals. . . . .	3-121
44	Structural Flex Bearing Design. . . . .	3-124
45	Geometry of Actuation . . . . .	3-127
46	Vectored Nozzle Clearance . . . . .	3-129
47	Elastomer Temperature Sensitivity . . . . .	3-131
48	Maximum Stress Locations. . . . .	3-131
49	Finite Element Grid . . . . .	3-134
50	Minimum Factor of Safety Locations. . . . .	3-135
51	Graphite Epoxy Overwrap Design. . . . .	3-138
52	Thermal Analysis Station Locations. . . . .	3-144
53	Ablative Rings/Materials Selection. . . . .	3-147
54	Thermal Analysis Flow Chart . . . . .	3-154
55	Uniaxial Failure Envelopes for TP-H1139 Propellant-- Mix 8657001, Aged 72 Months at 77°F . . . . .	3-164
56	Comparison of Aging Effects on Uniaxial Maximum Stress for HTPB Propellant--Aged at 77°F, Tested at 77°F and Ambient Pressure, 2 In./Min Crosshead Rate. . . . .	3-165
57	Comparison of Aging Effects on Strain at Maximum Stress for HTPB Propellant--Aged at 77°F, Tested at 77°F and Ambient Pressure, 2 In./Min Crosshead Rate. . . . .	3-166
58	Increasing Ground AP Fraction to Achieve 0.42-ips Burn Rate Results in Higher EOM Viscosities . . . . .	3-171

## ILLUSTRATIONS (Cont)

<u>Figure</u>		<u>Page</u>
59	Effect of Ground AP on Burn Rate and Exponent in 88 percent Solids/19 percent Al DL-H396 Propellant with 200/9 Micron AP . . . . .	3-172
60	Burn Rate Versus $\text{Fe}_2\text{O}_3$ in Space Shuttle Propellant (1,000 psi at 60°F) . . . . .	3-174
61	Burn Rate Requirements for "Heads-Down" and "Heads-Up" Flight Modes Achieved with <0.2 Percent, Type II, $\text{Fe}_2\text{O}_3$ , DL-H396-Type Propellant. . . . .	3-175
62	Effect of Ground AP on Burn Rate and Exponent in Trimodal 400/200/50 AP Distribution . . . . .	3-177
63	TP-H1148 Burn Rate Versus $\text{Fe}_2\text{O}_3$ (5-in. CP Data) . . . . .	3-179
64	Addition of TPB Cure Catalyst Shortens Cure Time of DL-H396 Propellant--Tooling Could Be Removed After 3-4 Days of Cure at 135°F . . . . .	3-182
65	DL-H396 Propellant Pot Life Can Be Tailored by Adjustments in TPB Content. . . . .	3-183
66	Effect of Sample Temperature on Slope of Pot Life Curves for TP-H1148 Propellant (Mix AB5154) . . . . .	3-187
67	Effect of Accelerated Aging on Tensile Adhesion . . . . .	3-192
68	Effect of Accelerated Aging on 90°F Peel Adhesion . . . . .	3-192
69	Forward Segment Design. . . . .	3-206
70	Forward Center Segment Design . . . . .	3-207
71	Aft Center Segment Design . . . . .	3-208
72	Aft Segment Design. . . . .	3-209
73	Insulated Aft Dome. . . . .	3-217
74	Aft Case-to-Nozzle Insulation . . . . .	3-219
75	Circumferential Flow Blocker (baffle) . . . . .	3-221
76	Insulation Test Section of 70-lb Charge Char Motor. . . . .	3-222

## ILLUSTRATIONS (Cont)

		<u>Page</u>
77	Material Affected Rate Versus Mach Number--Char Motor No. 107 . . . . .	3-225
78	Material Affected Rate (High Velocity)--Char Motor No. 107 . . . . .	3-226
79	Material Affected Rate (Medium Velocity)--Char Motor No. 107 . . . . .	3-227
80	Material Affected Rate (Low Velocity)--Char Motor No. 107 . . . . .	3-228
81	Bonded J-Seal . . . . .	3-231
82	Overview of Field Joint Trade Study . . . . .	3-234
83	Vented Labyrinth. . . . .	3-235
84	Bonded U-Seal . . . . .	3-236
85	Thin Line Bonded U-Seal . . . . .	3-237
86	Interference Fit U-Seal . . . . .	3-238
87	Interference Fit J-Seal . . . . .	3-239
88	Vented Interlock. . . . .	3-241
89	Casting Dome Assembly . . . . .	3-247
90	Nozzle Assembly-to-Aft Segment. . . . .	3-249
91	Comparison of Current and Block II SRM Ignition Systems . . . . .	3-252
APPENDIX A SPECIFICATION NO. CPW1-1900		
APPENDIX B COMPOSITE MOTOR CASE		
B-1	FWC-SRM Configuration . . . . .	B-6
B-2	Seal Capture Lip. . . . .	B-8
B-3	Case Acquisition Cost Versus Number of Reuses . . . . .	B-10



## ILLUSTRATIONS (Cont)

	<u>Page</u>
B-4 Composite Case Configuration. . . . .	B-12
B-5 FWC Composite Segment Construction. . . . .	B-13
B-6 Composite Case Field Joint. . . . .	B-15
B-7 Joint Concept FWC Feasibility Study . . . . .	B-17
B-8 Loading and Boundary Conditions . . . . .	B-18
B-9 Predicted Case Joint Radial Expansion . . . . .	B-20
B-10 Location of Maximum Critical Stresses in Metal Strap Components. . . . .	B-21
B-11 Hybrid Metal/Composite Case . . . . .	B-24
B-12 TASS Finite Element Model Key Membrane Stresses . . . .	B-26
B-13 TASS Finite Element Joint Model With Key Stresses . . .	B-27
B-14 Comparison Between Double Steel Strap and Standard FWC-Type Tang and Clevis Joint. . . . .	B-29
B-15 SRM Block II Composite Case Tang and Clevis Joint . . .	B-31

## TABLES

	<u>Page</u>
1        Large Solid Propellant Grains . . . . .	2-5
2        Monolithic SRM Comparisons With Segmented SRM . . . . .	2-8
3        Chamber Fineness Ratio for Large Solid Propellant Grains. . . . .	2-11
4        Block II SRM Performance Potential--Heads-Down Trajectory. . . . .	2-14
5        Block II SRM Performance Potential--Heads-Up Trajectory. . . . .	2-15
6        Block II SRM Design Baseline Performance. . . . .	3-10
7        Design Configurations Considered. . . . .	3-14
8        Heads-Down Propellant Comparison. . . . .	3-19
9        Heads-Up Propellant Comparison. . . . .	3-20
10       Heads-Down Payload Comparison (lbm) with HPML Nominal (nonasbestos insulation, SF = 1.5). . . . .	3-37
11       Heads-Up Payload Comparison (lbm) With HPML Nominal (nonasbestos insulation, SF = 1.5). . . . .	3-38
12       Design Requirements Criteria. . . . .	3-41
13       Metallic Case Trades. . . . .	3-46
14       Case Fabrication Trades . . . . .	3-49
15       Block II Case Membrane Design Criteria. . . . .	3-51
16       Block II Case Cylinders Design Summary. . . . .	3-52
17       Block II SRM Joint Trade Study. . . . .	3-65
18       Block II Clevis Joint Stress Study. . . . .	3-72
19       Block II Clevis Joint Offset Study. . . . .	3-72

## TABLES (Cont)

<u>Figure</u>		<u>Page</u>
20	Block II SRM Joint Trade Study. . . . .	3-98
21	Flex Bearing Design Parameters. . . . .	3-125
22	Maximum Predicted Torque Comparison . . . . .	3-126
23	Flex Bearing Weight Comparison. . . . .	3-130
24	Elastomer Shear Properties. . . . .	3-132
25	Flex Bearing Analysis Results . . . . .	3-132
26	Minimum Factors of Safety . . . . .	3-136
27	Rayon and PAN Mechanical Property Data. . . . .	3-145
28	Thermal Analysis Results. . . . .	3-148
29	Major Production Programs for PBAN and HTPB Propellants . . . . .	3-157
30	Basic Candidate Propellant Compositions . . . . .	3-159
31	Propellant Raw Material Elements. . . . .	3-160
32	Propellant Performance. . . . .	3-162
33	Propellant Burn Rate Tailoring. . . . .	3-168
34	Burn Rate (ips) Requirement at 1,000 psi. . . . .	3-170
35	Propellant Processing Comparison. . . . .	3-181
36	Composition of UF-2155 Liner. . . . .	3-189
37	Bond Strength Comparison. . . . .	3-190
38	Formulation for UF-2153 Inhibitor . . . . .	3-193
39	Preliminary Weight Impact Study for Silica/NBR. . . . .	3-210
40	Preliminary Sandwich Weight Impact Study for Silica/NBR Using Interchangeable Center Segments . . . . .	3-211

## TABLES (Cont)

		<u>Page</u>
41	SRM Asbestos-Free Insulation Development. . . . .	3-213
42	Insulation Material and Process Development--Char Motor Performance . . . . .	3-223
43	Char Motor Performance--Motor No. ARN 107 . . . . .	3-224
APPENDIX A SPECIFICATION NO. CPW1-1900		
APPENDIX B COMPOSITE MOTOR CASE		
B-1	Block II SRM Compoiste Case Design Requirements . . . .	B-4
B-2	Steel Rings and Capture Feature Critical Stress Data. .	B-22
B-3	Composite Case Designs--Existing FWC Axial Growth and Stiffness Requirements at 1,000 psi MEOP. . . . .	B-33
B-4	Composite Case Designs--Axial Stiffness and Strength only, 1,100 psi MEOP. . . . .	B-34
B-5	Comparison of FWC and Advanced Block II Material Technology. . . . .	B-37
B-6	Fiber Strength Variation Study. . . . .	B-38

## 1.0 INTRODUCTION

NASA interest in considering an improved SRM (Block II) for the Space Shuttle led to parallel studies by five contractors of alternative designs of the Space Transportation System (STS) Solid Rocket Motor (SRM). The conceptual design studies of a Block II SRM required elimination of asbestos-filled insulation and was open to alternate designs, such as case changes, different propellants, modified burn rate -- to improve reliability and performance. Limitations were placed on SRM changes such that the outside geometry should not impact the physical interfaces with other Space Shuttle elements and should have minimum changes to the aerodynamic and dynamic characteristics of the Space Shuttle vehicle.

The Space Division of Morton Thiokol, Inc., has completed a conceptual design study of the Block II SRM for the George C. Marshall Space Flight Center (MSFC) in accordance with contract NAS8-37296. The study, as described in this report, is based on a careful assessment of previous Space Shuttle SRM experience and on new design concepts combined to define a valid approach to assured flight success and economic operation of the STS. Covering approximately 120 days, September through December 1986, the study effort included the tasks outlined in Figure 1. As the study progressed interim reviews were held with the NASA Block II SRM Study Manager and a mid-term (60-day) briefing was presented at MSFC. The 60-day briefing included details of SRM segment joint design concepts and was supplemented with preliminary versions of the Conceptual Design Package and the Development and Verification Plan.

This report presents the results of Morton Thiokol's Block II SRM Conceptual Design Study. The report documents trade studies, preliminary designs, analyses, plans, and cost estimates in two volumes. In Volume I, Book 1 comprises the Conceptual Design Package including a Preliminary Part 1 Contract End Item (CEI) Specification as an appendix, and Book 2 comprises the Preliminary Development and Verification (D&V) Plan. Volume II includes Morton Thiokol's Capability Assessment Report as Book 1 and ROM Cost Estimates as Book 2.

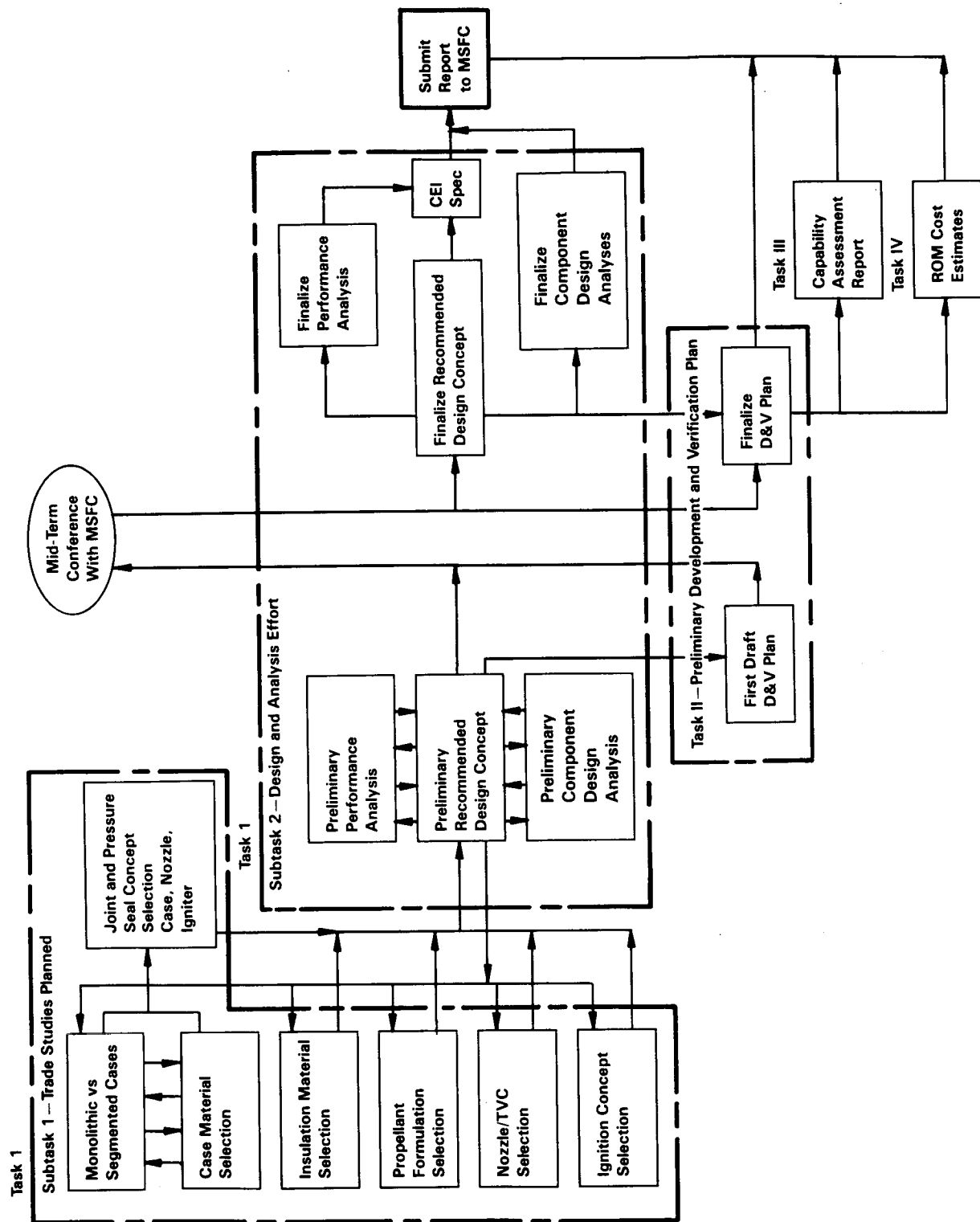


Figure 1. Block II SRM Study Tasks

## 1.1 NOMENCLATURE

Throughout this report references to various versions of the STS SRM are made in the following manner:

- SRM is a categorical item referring to any of the individual configurations.
- High Performance Motor (HPM) refers to the SRM configuration, manufactured by Morton Thiokol, and used on all Shuttle flights from STS-8 onward.
- Redesigned Solid Rocket Motor (RSRM) refers to the redesigned configuration recently approved by MSFC at the Preliminary Design Review which is now proceeding toward the Critical Design Review scheduled for August 1987.
- SRM II or the Block II SRM refers to the baseline design culminating from Morton Thiokol's Block II SRM Conceptual Design Study.

## 1.2 REQUIREMENTS

Groundrules for the Block II SRM Conceptual Design Studies were established to ensure compliance with existing STS requirements while allowing flexibility for design concepts that offered potential improvements in reliability, performance, and cost. The Block II SRM studies were conducted in parallel with the qualification of a Redesigned Solid Rocket Motor (RSRM) and requirements were adjusted to agree with the applicable new criteria. In addition, previous studies have projected increased payload capability for the Space Shuttle flown in a "heads-up" launch trajectory with a new thrust-time history provided by the SRM. The heads-up thrust versus time criteria for the SRM were included as a desirable goal for Block II SRM concepts as long as reliability and safety were not compromised.

A preliminary Part I Contract End Item (CEI) specification, CPW1-1900, is included as an appendix to this volume. The preliminary CEI specification presents the performance, design, and verification requirements for Morton Thiokol's Space Shuttle Block II SRM. The requirements in the CEI specification

are traceable to the groundrules defined in the statement of work for Contract NAS8-37296 which are summarized below:

- a. The existing performance, design, and verification requirements contained in Specification Number CPW1-3300, Part I, for the Space Shuttle High Performance Solid Rocket Motor shall be the baseline requirements document for proposed design concepts except as changed and/or amplified below. References to specific design characteristics such as segmented cases and other motor design characteristics and/or specification requirements unique to the present design are deleted. Where these references are deleted the contractor shall interpret that he has the option to select the specific design characteristics that best suit his overall Block II motor design concept. (The baseline requirements document is supplemented with preliminary CEI specification CPW1-3600 for the RSRM and an applicable Review Item Discrepancy (RID) package. These items were provided for information and guidance during the course of the study.)
- b. Design concepts must essentially duplicate the outside geometry of the current Space Shuttle SRM and its interfaces with other Space Shuttle elements such that impact to the aerodynamic and dynamic characteristics of the Space Shuttle vehicle is minimized.
- c. Design concepts shall not use asbestos-filled insulation materials.
- d. Design concepts are not constrained to the current propellant formulation but shall provide the capability to successfully perform over an equivalent PBAN propellant formulation burn rate range of 0.360 to 0.400 in./sec (at 625 psi and 60°F). For information, the performance data contained in CPW1-3300 is based on a PBAN propellant formulation with a target burn rate of 0.368 in./sec (at 625 psi and 60°F).

(The performance envelope was defined by thrust versus time traces for the nominal HPM and for a "heads-up" thrust versus time trace. The Block II SRM studies should determine performance capability within that envelope. See Figure 2.)

- e. Performance shall be in accordance with the requirements contained in CPW1-3300 from the sea level to 200,000 ft over a propellant mean bulk temperature (PMBT) range of +40 to +90°F after being subjected to the natural and induced environments specified in paragraphs 3.2.7.1 and 3.2.7.2, respectively, of CPW1-3300 to the extent that the PMBT range of +40 to +90°F is not violated.
- f. Any Criticality 1, 1R, 2, and 2R pressure seal shall be fully redundant and verifiable (inspected and leak tested in prescribed functional location). Further, no seal shall require pressure actuation to perform its designed function.
- g. Verification methods prescribed in Section 4.0, Table V, of CPW1-3300 are deleted and method of verification shall be a product of this study contract.
- h. Appendix 10, deviations, and any references to approved deviations are deleted from CPW1-3300.



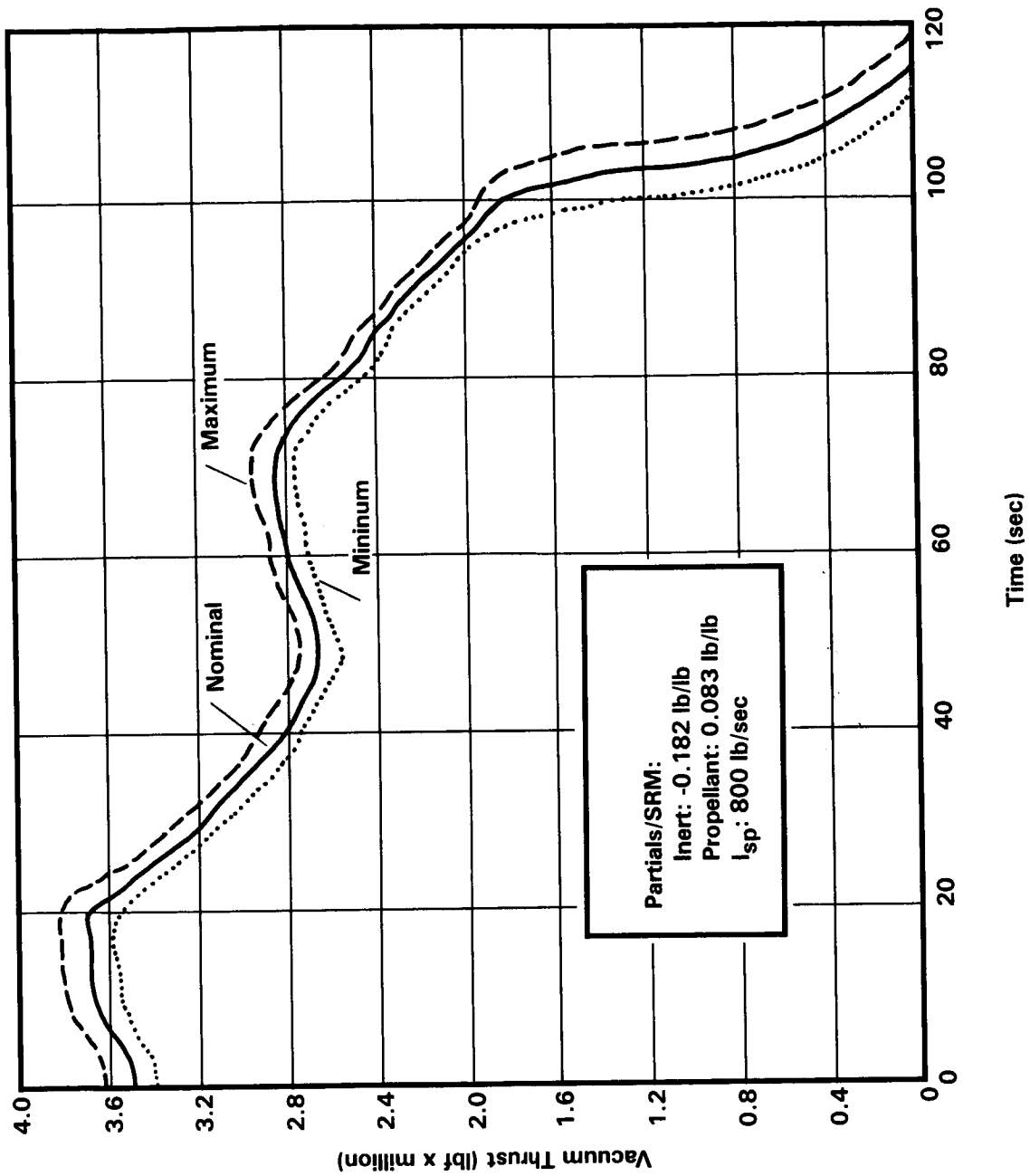


Figure 2. Heads-Up Thrust Versus Time Trace

87354-25

## **2.0 BLOCK II SRM CONFIGURATION SELECTION**

As the incumbent contractor for the Space Shuttle SRM, Morton Thiokol has a complete understanding of program issues that must be handled in the development, verification, production, and flight of this important element of the Space Transportation System. We have drawn on this experience and associated important events to develop concepts for a Block II SRM. This background also lends confidence to the Development and Verification (D and V) approach; credibility to the assessment of our Space Division's D and V and production capability; and realism to the ROM cost estimates -- items which are treated in other books of this report.

In completing this study and recommending a Block II SRM concept we have recognized that a new design could have great impact on the existing infrastructure for development production and operation of the SRM. Elements of this infrastructure include the analysis tools; management, engineering, and production team; component test capability; motor test facilities; review procedures; material suppliers; subcontractor teams; quality assurance and NDE systems; safety assessments and procedures; production facilities and tools; manufacturing plans and documentation; logistics support; storage facilities; transportation system; launch site facilities and GSE; launch support team; recovery equipment; disassembly facilities, and refurbishment facilities and equipment. One consideration in judging design concepts was the degree to which they could utilize the previous investments in these demonstrated capabilities.

The study was influenced by implications that changes from demonstrated successful solid rocket industry experience would have an uncertain influence on system safety, reliability, performance, cost, and development risk (schedules and cost). For this reason a review of industry experience was completed early in the study and was a factor in selecting the preferred motor configuration.

This previous experience and the ongoing efforts to qualify the RSRM and resume Space Shuttle flights provide the solid rocket industry with a technology

base to propose Block II SRM concepts. Morton Thiokol's criteria for selecting the SRM II configuration were prioritized as follows:

1. Assure system reliability
2. Maintain/increase performance
3. Enhance cost effectiveness

The study approach used to establish our recommended concept is illustrated in Figure 3.

## **2.1 INDUSTRY EXPERIENCE**

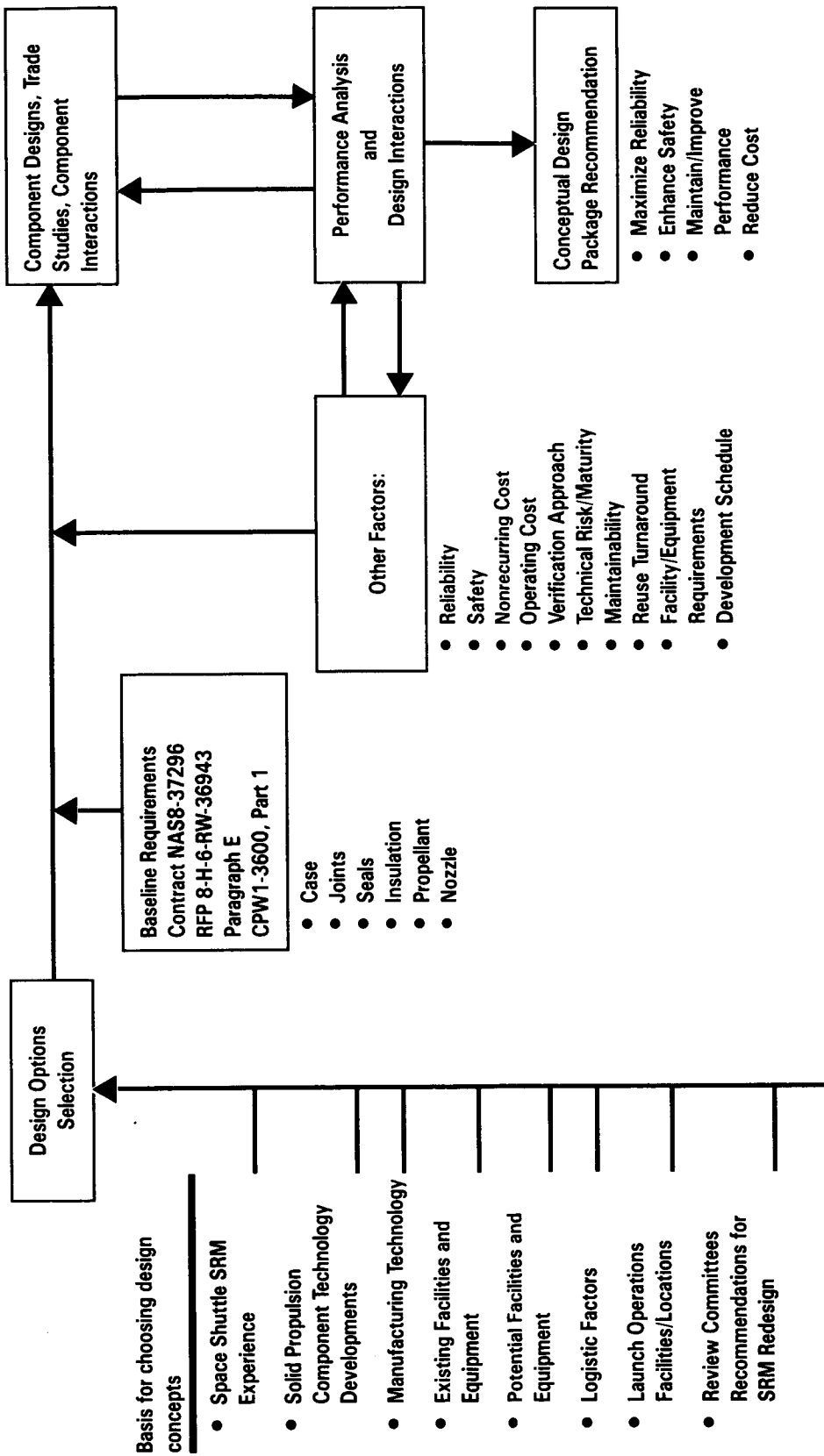
Since the 1960s, interest in the high thrust levels available in efficiently-sized solid rocket motors has led to technology demonstration programs for large boosters to support space launch systems. The relatively simple solid rocket design and cost effectiveness were key factors in selecting large solid rocket motors for strategic missile applications and for space launchers such as Titan and Space Shuttle. These technology demonstrations and production operations form the most applicable experience base of the solid rocket industry.

### **2.1.1 Space Shuttle SRM**

Development of the Space Shuttle SRM was started by Morton Thiokol in 1974 leading to an initial static test in 1977 and delivery of the first flight set of SRMs to KSC in 1979. Seven full scale static tests were conducted in the development and qualification effort and six flight sets of motors were delivered. A modified design, called the high performance motor (HPM), was qualified with two additional static tests, and the HPM was used for Shuttle flights from STS-8 onward. A filament-wound case (FWC) version of the SRM was also designed and carried through two static tests to date.

Facilities are in place at Morton Thiokol's Space Division to produce the HPM to support Shuttle flights at rates of more than 24 flights per year. Through 1985 more than 60 motors had been manufactured for flight.

The HPM configuration consists of four motor segments with a separate aft exit cone assembly. The ignition system is installed in the forward segment and a movable nozzle is attached to the aft segment. The four segments and exit cone



A004013

Figure 3. Process for Establishing Block II SRM Design Concept

are assembled at the launch site to complete the 146-in.-diameter motor. The HPM is 126 ft long and weighs 1,255,750 lbm including 1,110,000 lbm of propellant. The largest unitary propellant grain is cast in the forward segment which contains 300,000 lbm of PBAN propellant.

The Shuttle SRM development and production project achieved several important goals including:

- o Largest solid rocket motor brought to operational status
- o Successful recovery and reuse of major metal components
- o Thrust-time trace reproducibility and flight pair thrust matching to meet design specifications
- o Largest vectoring nozzle used for flight control

These achievements and the success of most aspects of the manufacturing and operations processes form an important base for substantiating proposed Block II SRM concepts.

Following the 51-L flight failure of the aft-center-to-aft-segment joint leading to the destruction of the Challenger, an intensive review and redesign program is underway. The redesigned motor (RSRM) development and qualification is being supported by extensive analysis tools and new full scale component test vehicle. The program will include six static tests leading to RSRM qualification.

The RSRM project will verify the reliability of a new field joint concept before Space Shuttle flights resume. Subsequent production and flight operations will accumulate an expanding demonstrated database. Block II SRM concepts that can benefit from this experience in manufacturing and operations will have additional credibility for successful development and reliable flight performance.

#### **2.1.2 Large SRM Review**

The experience of the solid rocket industry with large solid rocket motors was reviewed to establish the range of capabilities previously demonstrated. An

understanding of this background is useful in estimating the degree of certainty to assume for the success of a new Block II SRM concept. The following Table 1 summarizes industry experience with solid rocket motors requiring more than 50,000 lbm of propellant cast in a single grain.

**Table 1. Large Solid Propellant Grains**

<u>Motor Designation</u> <u>(Diameter)</u>	<u>Number</u> <u>Produced</u>	<u>Approximate</u> <u>Propellant</u> <u>Weight</u> <u>(Klbm)</u>	<u>Transported to</u>	
			<u>Test</u> <u>Site</u>	<u>Launch</u> <u>Site</u>
Titan Segment (120)	> 500	70	Y	Y
Peacekeeper (92)	> 50	100	Y	Y
156 Segment (156)	19	200	Y	N
156 Monolithic (156)	3	300	Y	N
Shuttle Segment (146)	> 300	300	Y	Y
260 Monolithic (260)	3	1,650	N	N

The most extensive usage of large solid propellant grains has occurred in the Titan program with the production of 120-in.-diameter segments containing in excess of 70,000 lbm of propellant. The largest propellant grains to be cast on a production basis are the Shuttle SRM segments which contain approximately 300,000 lbm of propellant.

The 260-in. motor program cast the largest propellant grain to date (1,650,000 lbm). This technology demonstration program assembled, cast, and tested the motors in a vertical pit. None were moved after the propellant casting was complete. The third motor of the series experienced operating anomalies apparently related to breakup of the grain and ejection of unburned pieces of propellant.

All of the motors in the table used PBAN propellant, except for the more recently-developed Peacekeeper Stage I motor which uses an HTPB propellant.

### 2.1.3 Technology Status

In addition to understanding the experience level for design, manufacture, inspection, test, transport, handling, and launch of large solid rocket motors, the Block II SRM concept study should recognize the available technology for the mid-1980s. Design decisions based on the technology available at the beginning of the Shuttle SRM project were revisited to determine if new options are pertinent.

Propellant selection for the Shuttle SRM was driven by the extensive success with PBAN formulations in earlier strategic missile applications. HTPB formulations with higher energy were considered, but not selected because of limited experience. Today the PBAN propellant still has an unmatched history of production quantity, but the HTPB formulations have reached a mature status and are used in many production programs. The largest motor using HTPB propellant is the Peacekeeper Stage I produced at Morton Thiokol's Strategic Division. The total annual production of HTPB propellant in the industry is presently measured in millions of pounds annually. An HTPB propellant could provide performance benefits for a Block II SRM and could be introduced without significant risk. An extensive database exists to support the development and the production reliability.

A D6AC steel was chosen for the segmented Shuttle SRM case. Maraging 200 steels were not chosen even though they had been used in several of the previous large motor demonstration programs. Among the factors ruling them out was concern over their availability and cost stability. This issue was caused by the strategic metal cobalt which was a critical constituent of the maraging steels in the 1960s. New maraging steels that use titanium for strengthening and no cobalt are now available such as MAR T-250. This steel offers improved design properties and new options for case fabrication. A new case material could be introduced for a Block II SRM with completion of material characterization using well-established test procedures.

Nozzle ablative materials were selected in the original Shuttle SRM design based on extensive previous history with rayon-based carbon phenolics. More recent testing and demonstration of improved PAN materials indicate better material performance in the nozzle environment. A Block II SRM nozzle could take advantage of these newer materials to ensure the integrity of the ablative insulators.

New requirements for a Block II SRM forbid the use of materials containing asbestos. While an impressive list of candidate materials is available, additional data are needed to substantiate the performance of nonasbestos insulation materials for all the environments in the motor. These data are forthcoming from aggressive research and testing programs within the industry. While several candidates may be available soon, present knowledge leads to recommendation of previously-used asbestos-free NBR and EPDM formulations with known success in fabricating high quality insulators and achieving adequate bond strength with case and propellant.

## **2.2 MONOLITHIC MOTOR CONCEPTS**

A monolithic motor, with a unitary propellant grain, is one concept considered for the Block II SRM. This configuration could most easily be achieved by assembling existing or redesigned steel segments into a complete case. After the case is insulated and lined the 1.1 million pound propellant grain is cast in the motor. Subsequent assembly, test, transport, and launch operations would handle the motor as a single piece. A new one-piece case of steel or composite materials is an option for the monolithic motor with additional development effort.

Our study evaluated the attributes of the monolithic concept relative to the demonstrated segmented SRM. Issues of feasibility, reliability, performance, and cost were considered. This assessment is summarized in Table 2 for SRM Design Features and Performance; for SRM Manufacture and Critical Processes; and for Facilities and Equipment.

A key issue facing the monolithic motor concept is the total lack of a database for production of and operations with a unitary propellant grain in a motor of the size required for a Block II SRM. To produce a monolithic SRM



Table 2. Monolithic SRM Comparisons With Segmented SRM

<b>A</b>	<b>B</b>	<b>C</b>	<ul style="list-style-type: none"> <li>• No Change      ? TBD</li> <li>+ Improvement    ✓ Concern</li> </ul>
			<b>SRM Design Features and Performance</b>  <ul style="list-style-type: none"> <li>•      •      +      Case Inert Weight</li> <li>•      •      +      Case Joint Structure</li> <li>•      +      +      Case Joint Seals</li> <li>•      •      •      Nozzle/Igniter Joints and Seals</li> <li>•      ?      ?      Propellant Grain Integrity</li> <li>•      ?      ?      Ballistic Performance</li> </ul>

**A. Segmented motor design (similar to PDR baseline)**

**B. Monolithic motor design — Segmented case**

**C. Monolithic motor and case design**

Table 2. Monolithic SRM Comparisons With Segmented SRM (Cont)

A	B	C	<div> <div>• No Change + Improvement</div> <div>? TBD ✓ Concern</div> </div>
			<b>SRM Manufacture and Critical Processes</b>  <div> <div>•</div> <div>•</div> <div>✓</div> <div>Case Fabrication</div> </div> <div> <div>•</div> <div>✓</div> <div>✓</div> <div>Case Preparation Process</div> </div> <div> <div>•</div> <div>✓</div> <div>✓</div> <div>Case Insulation Process</div> </div> <div> <div>•</div> <div>✓</div> <div>✓</div> <div>Propellant Grain Casting Methods</div> </div> <div> <div>•</div> <div>✓</div> <div>✓</div> <div>Motor Handling</div> </div> <div> <div>•</div> <div>✓</div> <div>✓</div> <div>Discrepant Motor Disposition</div> </div>

**A. Segmented motor design (similar to PDR baseline)**

**B. Monolithic motor design— Segmented case**

**C. Monolithic motor and case design**

Table 2. Monolithic SRM Comparisons With Segmented SRM (Cont)

A	B	C	<div> <div>• No Change + Improvement</div> <div>? TBD ✓ Concern</div> </div>
•	?	?	Facilities and Equipment
•	?	?	Manufacturing Location
•	✓	✓	Transportation Methods
•	✓	✓	Delivery Access to Both STS Launch Sites
•	✓	✓	Cost for SRM Processing Facilities/Equipment
•	✓	✓	Cost for Launch Site Facilities/Equipment
•	•	✓	Cost for Case Refurbishment Facilities/Equipment

**A. Segmented motor design (similar to PDR baseline)**

**B. Monolithic motor design— Segmented case**

**C. Monolithic motor and case design**

substantially altered manufacturing processes are required, new facilities must be qualified, transportation and handling methods must be developed, and launch site operations must be demonstrated. With essentially no experience with these methods at this scale it is difficult to project a high system reliability with confidence. Critical processes including total case insulation, lining operations, and propellant casting are areas where consistent integrity of the product must be demonstrated at full scale. An example of this concern is the erratic operation of the third 260-in. monolithic test motor apparently due to a progressive propellant grain failure.

The process control issues are increased by the configuration of the Shuttle SRM if the case is handled as a monolithic unit. The fineness ratio (L/D) of the motor and propellant grain would be much greater than any of the large solid rocket motors previously manufactured (Table 3). The tooling and equipment to control the manufacturing process would increase in complexity accordingly.

**Table 3. Chamber Fineness Ratio for Large Solid Propellant Grains**

<u>Motor Designations (Diameter)</u>	<u>Approximate Propellant Wt. (Klbm)</u>	<u>Chamber (L/D)</u>
Peacekeeper (92)	100	3.0
Titan Segment (120)	70	1.0
Shuttle Segment (146)	300	2.6
260 Monolithic (260)	1,650	2.8
Shuttle Monolithic (146)	1,100	9.5

These producibility issues and the high cost associated with conducting the necessary D and V effort to provide the substantiating data for a monolithic motor led to a decision to continue with the segmented approach in the Block II SRM study.

No facilities are in place to handle the complete fabrication of monolithic motors for development and test facility access is an issue. We assessed the cost of acquiring monolithic grain manufacturing capability by assuming a new plant could be activated at a coastal location. Costs for facilities and tooling to support the development and production of the monolithic SRM were estimated at \$325M. This estimate assumed use of existing Space Division facilities for individual case segment insulation prior to assembly, for all refurbishment operations, for nozzle and igniter manufacturing. A substantial additional investment is necessary for barge transportation and transportation support equipment, and for new facilities, handling equipment, and GSE at the KSC and VAFB launch sites.

Our assessment of the monolithic SRM concept concluded that configurations could be proposed to meet the necessary thrust versus time requirements and that grain stress analyses would predict adequate margins. The development of a monolithic SRM is feasible, but would require a substantial D and V effort. Key demonstrations are necessary at full scale including: ballistic reproducibility and motor pair thrust balance; consistency in processing and casting propellant to produce acceptable mechanical properties with control of voids and porosity; and maintaining insulation quality and bonding integrity during extended motor processing.

Although the insulated joints of the monolithic SRM is a method of improving case joint reliability, the total reliability increase of this concept is uncertain. Questions relative to the ability of manufacturing processes to control the integrity of the propellant grain and other critical features exist because the monolithic SRM represents a substantial departure in scale from previous successful experience.

A Block II SRM concept is best assured of success if it builds on a substantial base of experience. Segmented designs can benefit from the production and operations experience of the Shuttle SRM and other large motor programs. No large deviation is required from demonstrated facilities, processes, transport, and launch site handling if a new segmented design is selected. The specific

reliability improvements being developed and demonstrated for the RSRM case and insulation joint can be enhanced for a Block II SRM design that can consider a wider range of options.

### **2.3 BLOCK II SRM PERFORMANCE OPTIONS**

The baseline Block II SRM design concept recommended from this study is discussed in detail in Section 3. A segmented design was selected to take advantage of the substantial successful experience with this approach for large solid rocket motors. A new case design is proposed with the potential for improvement in the integrity of assembly joints. The steel case material will ensure reusability and maintain the cost benefits demonstrated from recovery and refurbishment of large metal components in the Shuttle program. Nozzle and propellant changes are also proposed for the Block II SRM.

The selected configuration and component designs were chosen to provide the largest payload increase for the Space Shuttle (9,900 lbm) based on rough performance estimates using constant exchange ratios. The Block II SRM concept presupposes a benefit for Shuttle capabilities from delivering the heads-up thrust versus time profile. This higher performing configuration can be developed with no significant loss in design reliability, but the development effort is increased by implementing changes in all the major elements of the motor. More modest payload gains are available with a reduced development effort.

A range of performance gains was estimated for various combinations of case design, nozzle design, and propellant formulation. The data were prepared for both the nominal STS launch mode (Table 4) and the heads-up launch mode (Table 5).

Table 4. Block II SRM Performance Potential--  
Heads-Down Trajectory

PROPELLANT NOZZLE CONFIGURATION	PAYLOAD INCREMENT FROM HPML PERFORMANCE		
	PBAN TP-H1148	PBAN TP-H1148	HTPB DL-H396
CASE OPTION 1 D6AC SEGMENTED	HPM NOZZLE	BLOCK II NOZZLE	BLOCK II NOZZLE
	300	1,300	3,500
CASE OPTION 2 T250 SEGMENTED	3,300	4,300	6,500
CASE OPTION 3 T250 WELDED INTO CASTING SEGMENTS	4,600	5,600	7,600

ASSUMES NOMINAL STS TRAJECTORY

NONASBESTOS INSULATION SAFETY FACTOR = 1.5

Table 5. Block II SRM Performance Potential---  
Heads-Up Trajectory

PROPELLANT NOZZLE CONFIGURATION	PAYLOAD INCREMENT FROM HPML PERFORMANCE		
	PBAN TP-H1148 HPM NOZZLE	PBAN TP-H1148 BLOCK II NOZZLE	HTPB DL-H396 BLOCK II NOZZLE
CASE OPTION 1 D6AC SEGMENTED	2,100	3,000	6,000
CASE OPTION 2 T250 SEGMENTED	4,500	5,500	8,600
CASE OPTION 3 T250 WELDED INTO CASTING SEGMENTS	5,900	6,900	9,900

ASSUMES HEADS-UP TRAJECTORY ADDS 3,500 LBM PAYLOAD WITH HPML PROPELLANT AND  
INERT WEIGHT WHEN BURN RATE IS INCREASED TO 0.392 IN./SEC.



### 3.0 BLOCK II SRM CONCEPTUAL DESIGN

In the following discussions, we describe many of the details of our conceptual Block II SRM design. The selections of the detail concepts are supported by described trade studies or rationale. The design studies and concept selections have exploited the many years of personal experience of the SRM design and management team at Morton Thiokol. The lessons learned during the past 12 years of SRM development, manufacture, and flight have been observed. Further, the design analyses and tests of the ongoing SRM redesign (culminating recently in the RSRM PDR configuration) have provided many inputs to this Block II SRM study, and have been a synergistic benefit to the definition of a Block II SRM configuration.

### 3.1 BLOCK II SRM DESIGN DESCRIPTION

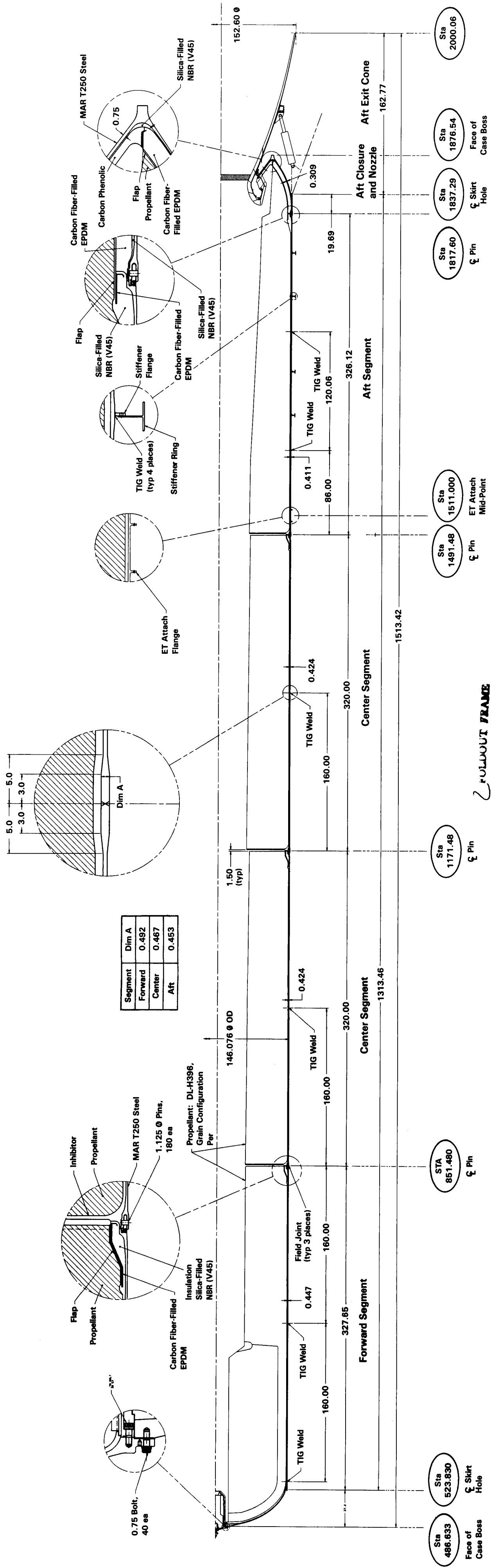
Morton Thiokol's Block II SRM design (Figure 4) is a segmented steel case motor which meets the outline envelope and interface requirements of the HPM. This Block II SRM could be substituted directly into the STS flight configuration with no modifications to the solid rocket booster (SRB) or attaching hardware. The overall motor weight is 1,260,929 lb; it produces a vacuum total impulse of 296,468,090 lbf-sec, and meets the heads-up thrust versus time requirement. Using this motor configuration would result in a payload increase of 9,877 lbm with an assumed heads-up Space Shuttle flight mode. A similar motor design concept, using a lower propellant burn rate to duplicate the HPM thrust-time trace, would provide a payload increase of 7,593 lbm for the current standard Space Shuttle launch trajectory (heads-down). The payload increases come from several features of the design as shown below:

<u>Area Affecting Payload</u>	<u>Payload Increase (lbm)</u>	
	<u>Heads-up</u>	<u>Heads-down</u>
Inert Weight Reduction	3,485	5,121
Propellant (HTPB)	2,044	1,688
I <sub>sp</sub> (HTPB Improved Performance)	848	784
Heads-up Flight Mode	<u>3,500</u>	<u>0</u>
Total	9,877	7,593

ORIGINAL PAGE IS  
OF POOR QUALITY

ORIGINAL PAGE IS  
OF POOR QUALITY

ORIGINAL PAGE IS  
OF POOR QUALITY



A004668

FOLDOUT FRAME

Figure 4. Block II SRM Motor Layout

The Block II SRM is manufactured in four segments of the same length as presently used for the HPM. For launch site assembly of the three mating joints between segments, the design employs a tang and clevis plus capture feature field joint (Figure 5). The configuration is similar to the RSRM design, but improvements are incorporated and accommodated by the new case forgings. The design details also consider the higher strength steel and the higher motor operating pressure necessary for the heads-up thrust-time trace.

The selected case material, maraging T250 steel, offers several advantages to a Block II SRM. First, the design allowable strengths for T250 steel are 20 percent greater than that provided by the D6AC steel used in the present case. With this material, longer case segments can be fabricated by circumferentially welding two steel case sections together. Welding will replace the tang and clevis configuration and the pins used at the current HPM factory joints at the forward dome and case cylinder interfaces. Thus, the additional inert weight of the six factory joints is eliminated. Using this concept, a Shuttle payload increase of 2,292 lbm is attributable to the case weight reduction achieved by using the higher strength material and the longer welded case segment configuration.

Although the final configuration of the aft segment is the same, the aft dome and nozzle are assembled to the aft casting segment in a different manner than used previously with the HPM. For the Block II SRM an integral one-piece aft dome and conical fixed nozzle housing is used to close the aft end of the case and provide structural support for the movable nozzle. This maraging T250 steel component is fully insulated and combined with the forward section of the nozzle to form an aft closure subassembly. This aft closure subassembly is attached to the aft segment after the propellant is cast and cured. The attachment joint for the aft closure is located at the outer diameter of the motor behind a split flap that is bonded to the propellant grain (Figure 6). At this location the joint is exposed to a less erosive environment than the present nozzle-to-case joint. The aft closure is assembled to the aft segment at the factory using a tang and clevis structural joint that is identical to the Block II SRM field joints.

ORIGINAL PAGE IS  
OF POOR QUALITY

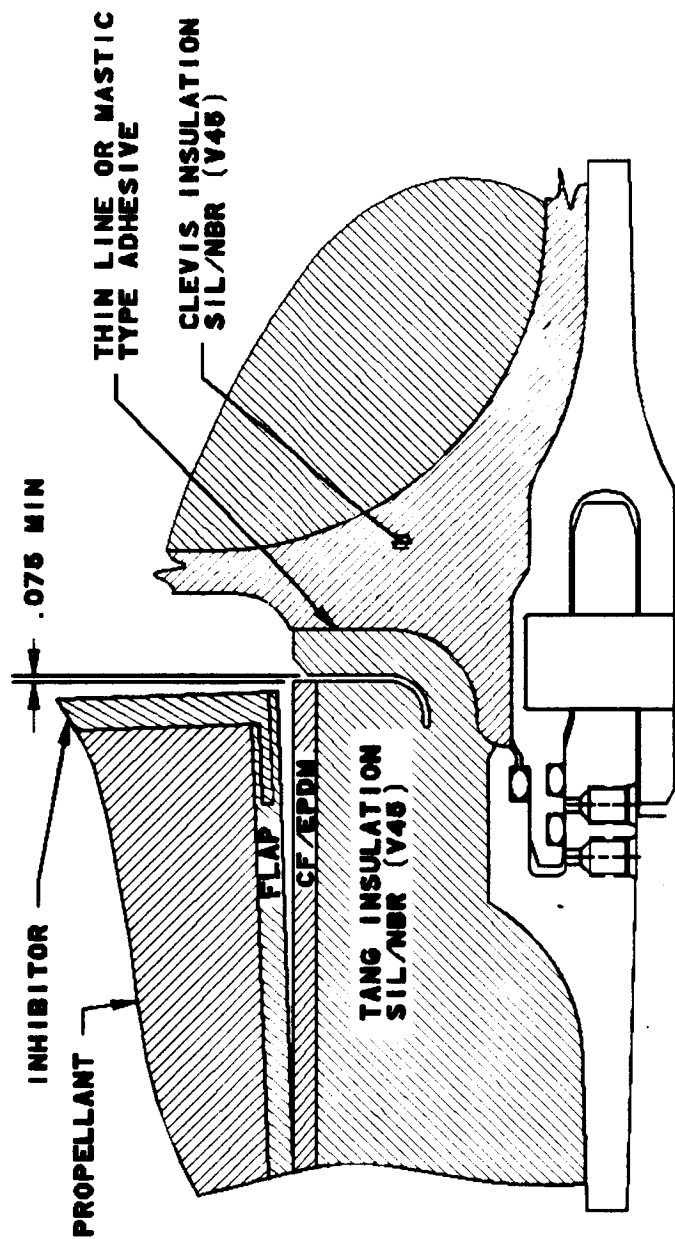


Figure 5. Bonded J-Seal Field Joint Design

ORIGINAL PAGE IS  
OF POOR QUALITY

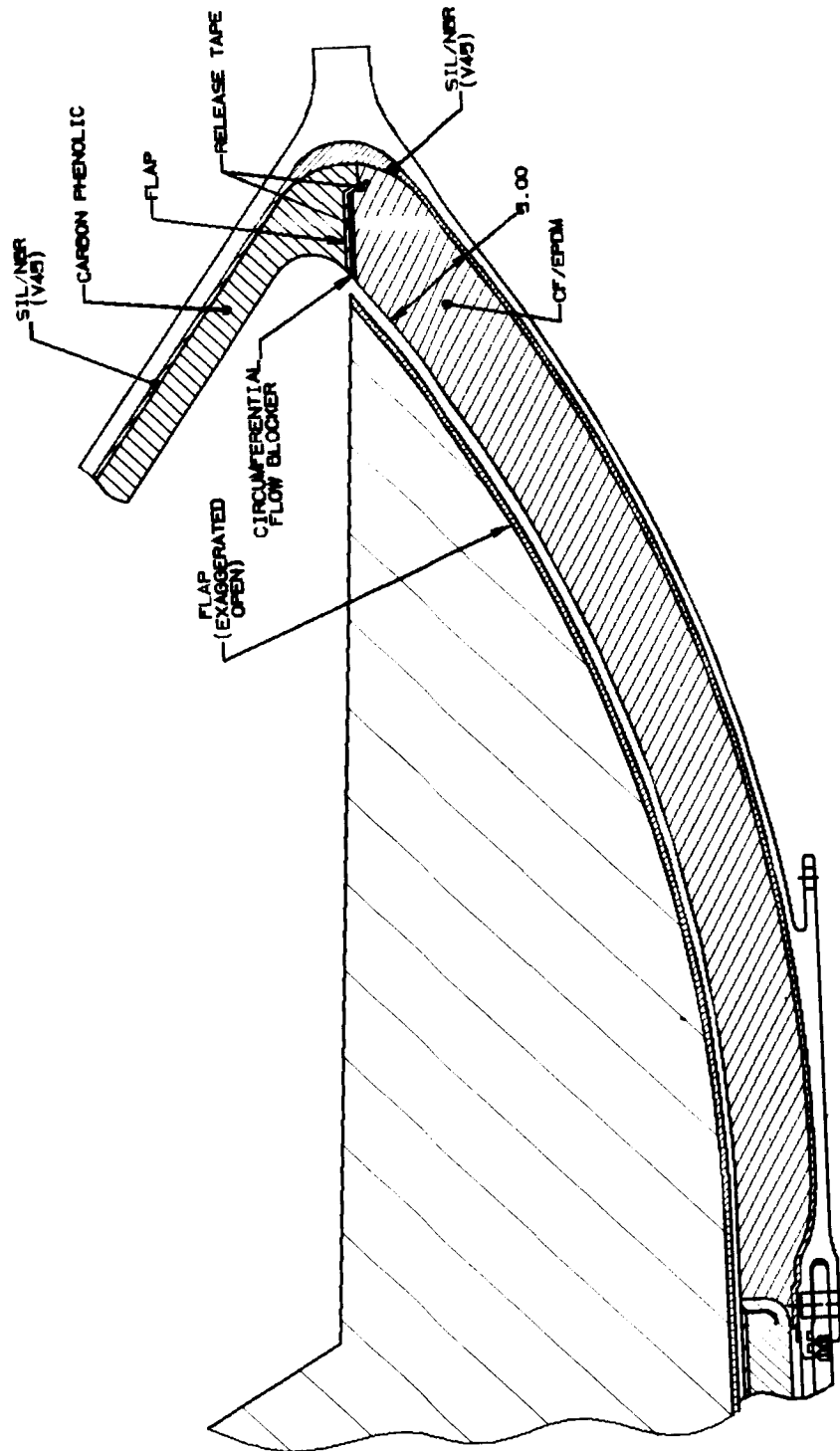


Figure 6. Nozzle-to-Case Joint and Insulated Aft Dome

The case insulation selected for the Block II SRM is a silica-filled NBR with carbon fiber-filled EPDM used in the areas where higher erosion resistance is required. These two nonasbestos materials have been used in the current HPM motor and have well known characteristics for bonding to case and propellant. Extensive material development is avoided and additional processing development will be minimal.

The solid propellant grain configuration will be identical to the HPM. For the Block II SRM the propellant will be Morton Thiokol's DL-H396 HTPB formulation containing 88 percent solids. This propellant formulation uses an iron oxide burn rate catalyst and is a variant of the 88 percent solids HTPB propellant used successfully in the Peacekeeper Stage I motor. The HTPB polymer selected is the commercial HT material produced by ARCO, and the aziridine bonding agent HX-752 will be used. Raw material costs and propellant processing cycles are very close to those for the PBAN propellant used in the HPM. The more dense and more energetic HTPB formulation produces a performance improvement over the PBAN propellant with a density and  $I_{sp}$  gain that results in a Shuttle payload increase of 2,750 lbm for the heads-up (2,177 lbm for heads-down) flight mode due to these factors alone.

To assure reliable bonds of the propellant grain to the NBR insulation, a well-demonstrated HTPB liner formulation (UF-2155) will be used. This liner, used in many HTPB propellant motors (e.g., Peacekeeper, PAM D-II, MK-104), contains no asbestos floats.

The ignition system for the Block II SRM design is similar to that used by the HPM. No changes are planned in igniter propellant, thermal insulation, or structural materials. To reduce the inert weight, a shorter housing and a more efficient grain design are proposed. The igniter is also modified to simplify the assembly and reduce the number of seals.

The Block II SRM nozzle complies with the external envelope requirements for the Shuttle motor and maintains the 7.72 expansion ratio and nozzle throat diameter presently used by the HPM. Significant changes are made in materials

and components to meet the structure and ablative design safety factors while achieving a net reduction in weight. The nozzle weight change accounts for 1,010 lbm of the total Shuttle payload increase noted in earlier paragraphs.

The proposed nozzle design (Figure 7) includes these features:

1. Flexible bearing TVC (omniaxial  $\pm$  8-deg vectoring).
2. "Conical" bearing with a separate sacrificial bearing for thermal protection (polyisoprene elastomer with no asbestos for both bearings).
3. Polyacrylonitrile (PAN) carbon-cloth phenolic ablative insulators.
4. Graphite filament wound exit cone structure.
5. Steel (D6AC) nozzle structure components.
6. Dual verifiable seals at all internal joints of steel structure.

The revised geometry of the flexible bearing changes the nozzle's center of rotation, which, in turn, will impact the stroke requirements of the actuators (shorter stroke required). This bearing, with its sacrificial thermal protection bearing, however, requires less actuation torque. Consequently, the existing actuators and TVA system should provide the requisite thrust vector control for the Shuttle system. The materials used in the bearings -- steel shims and polyisoprene rubber in the main bearing and carbon cloth phenolic shims and polyisoprene rubber for the sacrificial bearing -- have been proven in some of the following motors: Peacekeeper Stage I; current HPM; C-3 Stages I, II, and III; C-4 Stages I, II, and III; D-5 Stages I and II; and Small ICBM Stage I. The ablative materials lining the nozzle are of spun PAN (for the inlet rings and the throat) and lightweight PAN (for the nose cap, stationary shell, and exit cone). These materials permit attaining the requisite factors of safety without impacting the external configuration or the expansion ratio.

One of the goals of the Block II SRM design was to produce a thrust time curve greater than the HPM motor produces, approaching that desired for the heads-up concept (Figure 8). To increase the performance of the Block II SRM (Table 6), it was found necessary to increase the maximum expected operating pressure (MEOP) to 1,129 psia by increasing the burning rate of the propellant (the nozzle throat is the same as for the HPM motor). With no change in the

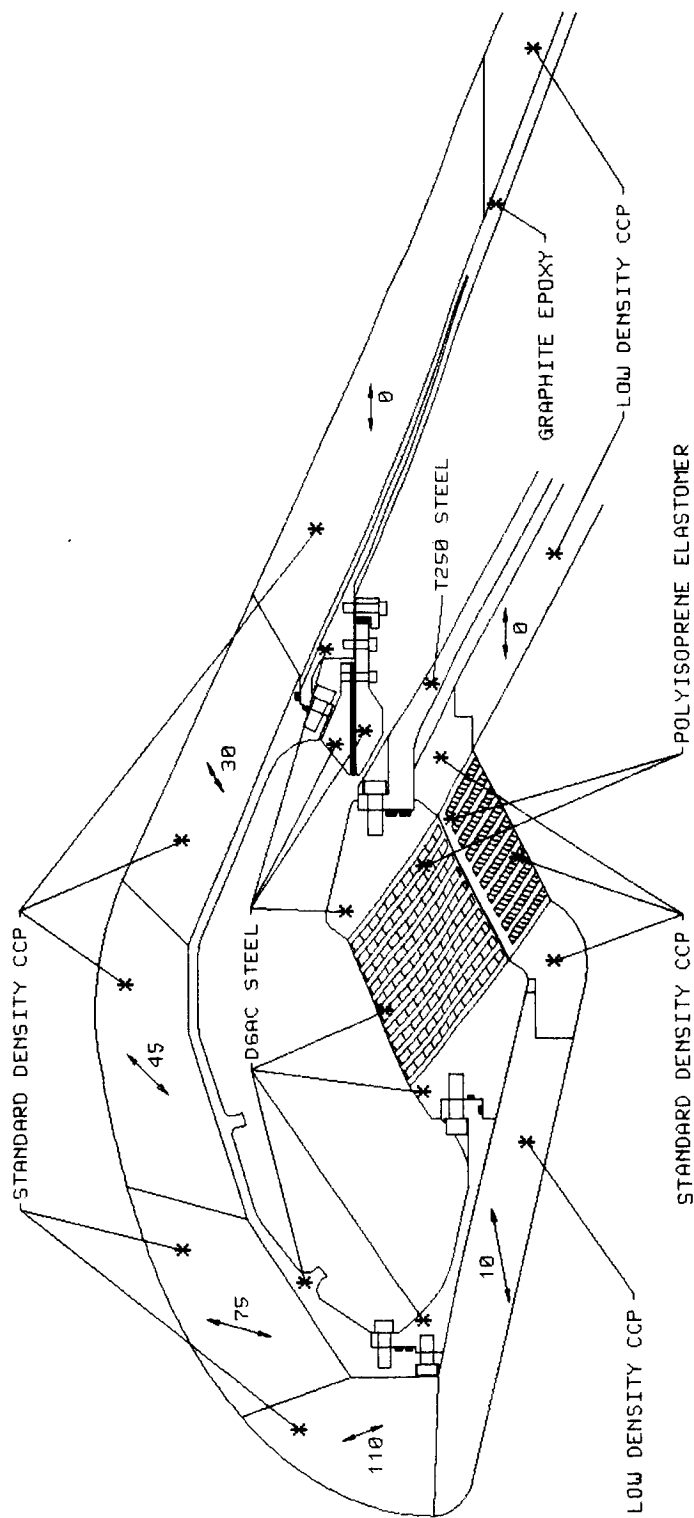
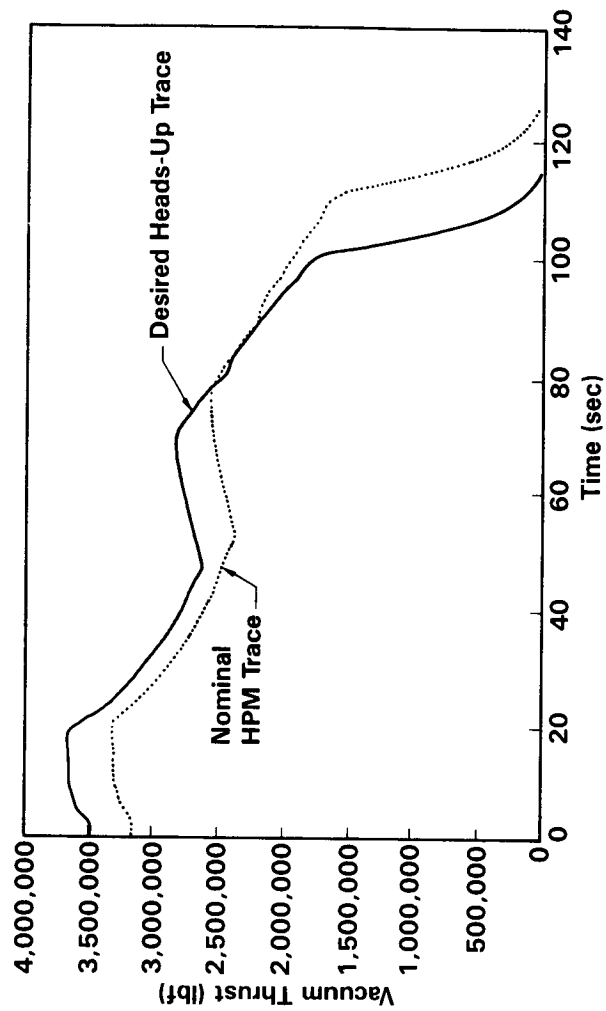


Figure 7. SRM Block II Nozzle Configuration





4004012

Figure 8. SRM Nominal--Heads-Up Comparison Thrust Versus Time Table

physical dimensions of the propellant grains, the higher burn rate results in a shorter motor duration than exhibited in the HPM. Using these approaches, a near match of the heads-up requirement is attained as shown in Section 3.2.

**Table 6 . Block II SRM Design Baseline Performance**

<u>Parameter</u>	
Web Time (sec)	104.2
Web Time Average Pressure (psia)	727.7
MEOP (psia)	1129.5
Max Sea Level Thrust (Mlbf)	3.442
Vacuum Delivered Specific Impulse (lbf-sec/lbm)	268.16
Burn Rate at 625 psia (in/sec)	0.38
Throat Radius (in.)	26.93
Initial Expansion Ratio	7.720

### **3.2 MOTOR PERFORMANCE**

This section presents the ballistics and performance characteristics for the Block II SRM design concepts. The Block II SRM must meet, as a minimum, the performance requirements documented in CPW1-3600 for the Space Shuttle RSRM. NASA has also provided an alternate thrust-time trace requirement for a heads-up flight mode which is estimated to increase Space Shuttle payload capability. The heads-up requirement was used as a goal for the ballistics of the Block II SRM.

Performance screening was based on changes in Space Shuttle payload capability resulting from each Block II SRM concept. The relative payload capability was estimated by a simplified process of adjustment using exchange ratio constants provided by NASA-MSFC. Space Shuttle payload capability using the HPM configuration was the basis for comparison. Heads-up design concepts were credited with a 3,500-lb payload benefit based on previous NASA studies.

#### **3.2.1 TRADE STUDY SUMMARY**

Motor ballistics and Space Shuttle payload performance increments were established in an iterative process. Initial requirements were allocated for design trade assessments of major SRM components. As the component design concepts were developed, their evaluation included establishing the impact on the motor's performance parameters and resulting implications for vehicle payload capability. Performance comparisons were among the factors used to arrive at the recommended component configurations; first by ensuring that the integrated Block II SRM design would meet specification requirements, and second by providing a discriminator for selection among otherwise equivalent options.

Important component design considerations that were evaluated in performance assessments included:

**Insulation design and material selection** - to establish the inert weight of the asbestos-free insulator and the effect on internal case volume for displacing propellant or altering burning area-versus-web characteristics.

**Propellant selection** - to evaluate propellant density and specific impulse contributions and determine burn rate characteristics to produce the required thrust trace; also establish design parameters such as MEOP flow rates and burn time.

**Case design** - to determine the weight of the largest component of the motor's inert weight and to account for changes in propellant loading due to case thickness or configuration adjustments. (Outside diameter of the case was unchanged from the HPM configuration.)

**Nozzle design** - to establish the inert weight of the nozzle and the influence of nozzle area ratio and material erosion on delivered performance.

Insulation materials that have extensive experience in solid rocket motors and have been employed in the HPM were selected. The silica-filled NBR and carbon fiber-filled EPDM contain no asbestos and provide an effective insulator when configured in a sandwich layup. The insulator design for each motor segment accounts for the local environment and utilizes the data obtained from previous HPM flights to confirm that safety factors meet design requirements in all areas. A slight decrease in insulation weight is projected for the Block II SRM. The insulator is designed to meet the 1.5 safety factor, and the insulation in the two center segments is the same to allow interchange of the segments if necessary.

Four propellants were considered for the Block II SRM design and the two most promising were evaluated for compliance with both the RSRM thrust requirements and the heads-up thrust requirements. For these evaluations the propellant grain design was not altered from the present design, but propellant burn rate or nozzle throat size were adjusted to produce the desired thrust trace.

The propellants were:

- TP-H1148 (86 percent solids, PBAN used in HPM)
- DL-H396 (88 percent solids, HTPB similar to Peacekeeper, Stage I)
- TP-H3340 (89 percent solids, HTPB used in Star 37X)
- DL-H397 (88 percent solids, HTPB with low HCl in exhaust)

All of these propellants appeared satisfactory for meeting the performance requirements for specification CPW1-3600 (RSRM), but two were eliminated as candidates during the trade studies. The TP-H3340 formulation was dropped because of material cost considerations and because of concern with propellant processing after the formulation was tailored to the higher burn rates required for the Block II SRM. The "clean" propellant, DL-H397, is being developed in an ongoing technology program, but was eliminated from consideration because the formulation is not mature and there is no database for a similar propellant.

The Space Shuttle HPM propellant (TP-H1148) and the HTPB propellant (DL-H396), which is similar to that used in the Peacekeeper Stage I motor, have an extensive experience base and can meet the performance needs for a Block II SRM. These two formulations can be tailored to meet the thrust-time requirements that duplicate the HPM or that satisfy the heads-up flight scenario.

Motor and vehicle performance were evaluated for various case design options. Case configurations ranged from the D6AC segmented case from the RSRM to new case materials and segment concepts. Nozzle options were also included in the trade studies to determine the effects of changing from the RSRM configuration to new nozzle designs and new nozzle materials.

The several motor configurations that can be derived from the foregoing options on insulation, propellant, case, and nozzle were evaluated to determine feasibility and performance. Two configurations are discussed below because they bound the possible combinations that were evaluated. Configuration 1 represents the minimum change from the Shuttle RSRM in terms of component and material selection. Configuration 2 incorporates more extensive changes in components and materials to achieve improved performance. Each configuration was selected for designs to meet the CPW1-3600 thrust-versus-time requirement and for designs to meet the heads-up thrust-versus-time requirement. Estimated increases in the Space Shuttle payload capability for these design configuration options are summarized in Table 7.

**Table 7. Design Configurations Considered**

	<u>Shuttle Payload Deltas* (lb)</u>	
	<b>Configuration 1</b> TP-H1148 Propellant D6AC Steel Case <u>HPM Nozzle</u>	<b>Configuration 2</b> DL-H396 Propellant MAR-T250 Steel Case <u>Block II Nozzle</u>
Design A - Heads-down thrust versus time	+ 332	+ 7,593
Design B - Heads-up thrust versus time	+ 2,063	+ 9,877**

---

\*Payload deltas based on HPM nominal capability.

\*\*Recommended Block II configuration.

The major characteristics of each configuration are:

Configuration 1. Minimum change to meet thrust requirements with minimized costs.

- TP-H1148 propellant (PBAN)
- D6AC segmented steel case
- Improved joint design
- Nonasbestos insulation (1.5 safety factor)

Configuration 2. Highest performance consistent with thrust and CPW1-3600 requirements.

- DL-H396 propellant (HTPB)
- Steel case (four welded segments)
- Increased case design strength (T250 maraging steel)
- Improved joint design
- Nonasbestos insulation (1.5 safety factor)

Design 1A meets all requirements with a small payload gain and minimum cost impact. This design is essentially the same as the RSRM except for the change in insulation. A non-asbestos insulation (1.5 safety factor) is used in all the Block II configurations which decreases insulation weight and volume (allowing an increase in propellant weight). Design 1A with TP-H1148 propellant gives an increase of 332-lb payload weight for heads-down flight mode compared with the HPM nominal.

Design 1B meets all requirements with payload gain and minimum cost impact. The increase in burn rate with the TP-H1148 propellant, to meet the heads-up flight mode requirements, causes an increase of 97 psia in MEOP. As a result, the D6AC steel case membrane is thickened, causing an increase in inert weight and a decrease in propellant weight. Design 1B gives an increase of 2,063-lb payload weight for a heads-up flight mode compared with the HPM and nominal Shuttle launch mode.

Design 2A uses the DL-H396 propellant. With greater energy (higher solids content) than the TP-H1148 propellant, an MEOP increase of 19 psia results when the nozzle throat area is not changed. The T250 maraging steel case exhibits a significantly decreased inert weight, and a new lighter Block II nozzle is included. Design 1A gives an increase of 7,593-lb payload weight for heads-down flight mode compared with the HPM nominal.

Design 2B has the highest payload gain and meets heads-up thrust requirements. The increase in burn rate with the DL-H396 propellant to meet heads-up flight mode requirements causes an MEOP increase of 114 psia. Even with the higher pressures, the T250 maraging steel has improved physical properties and fewer joints, causing inert weights to go down. Propellant weight and  $I_{sp}$  improve, and the new lighter Block II nozzle is used. Design 2B gives an increase of 9,877-lb payload weight for a heads-up flight mode compared with the HPM and nominal Shuttle launch mode.

### 3.2.2 ANALYSIS

Performance data were calculated by several means: (1) case design program evaluated the case weight changes between the D6AC and the MAR T250 steel cases as MEOP and design strength varied; (2) the Automated Design Program (ADP) calculated nozzle weights at different pressures, erosion rates, and throat sizes using thermochemical and ballistics data as the input; and (3) the NASA-Lewis Thermochemical Program (SDA03) provided thermochemical analysis and, coupled with a nozzle efficiency analysis, estimated changes in delivered specific impulse ( $I_{sp}$ ). Changes in inert weight, propellant weight, and  $I_{sp}$  make up the change in payload (along with heads-up payload increment of 3,500 lbm) compared with the HPM nominal configuration. Changes in payload capability were calculated by means of partials received from NASA-MSFC.

The NASA-Lewis Thermochemistry Program (SDA03) was used to calculate theoretical rocket performance for equilibrium composition during adiabatic expansion down the nozzle. An added model, the Hawkins Loss Correlation, includes these losses in the nozzle:

- 2-Phase
- 2-D
- Kinetic
- Boundary Layer
- Erosion
- Submergence

The reactant composition for the propellants was input into this thermochemical program to calculate ballistic characteristics, erosion rates, and nozzle losses.

The preliminary ballistics pseudo-steady-state code was modified to include the effects of a surface area burn rate error (hump), and pressure transition down the bore. This was accomplished by modifying the surface area versus web trace at constant volume for the HPM as shown in Figure 9. This results in proper pressure versus time history calculations based on actual HPM performance data.



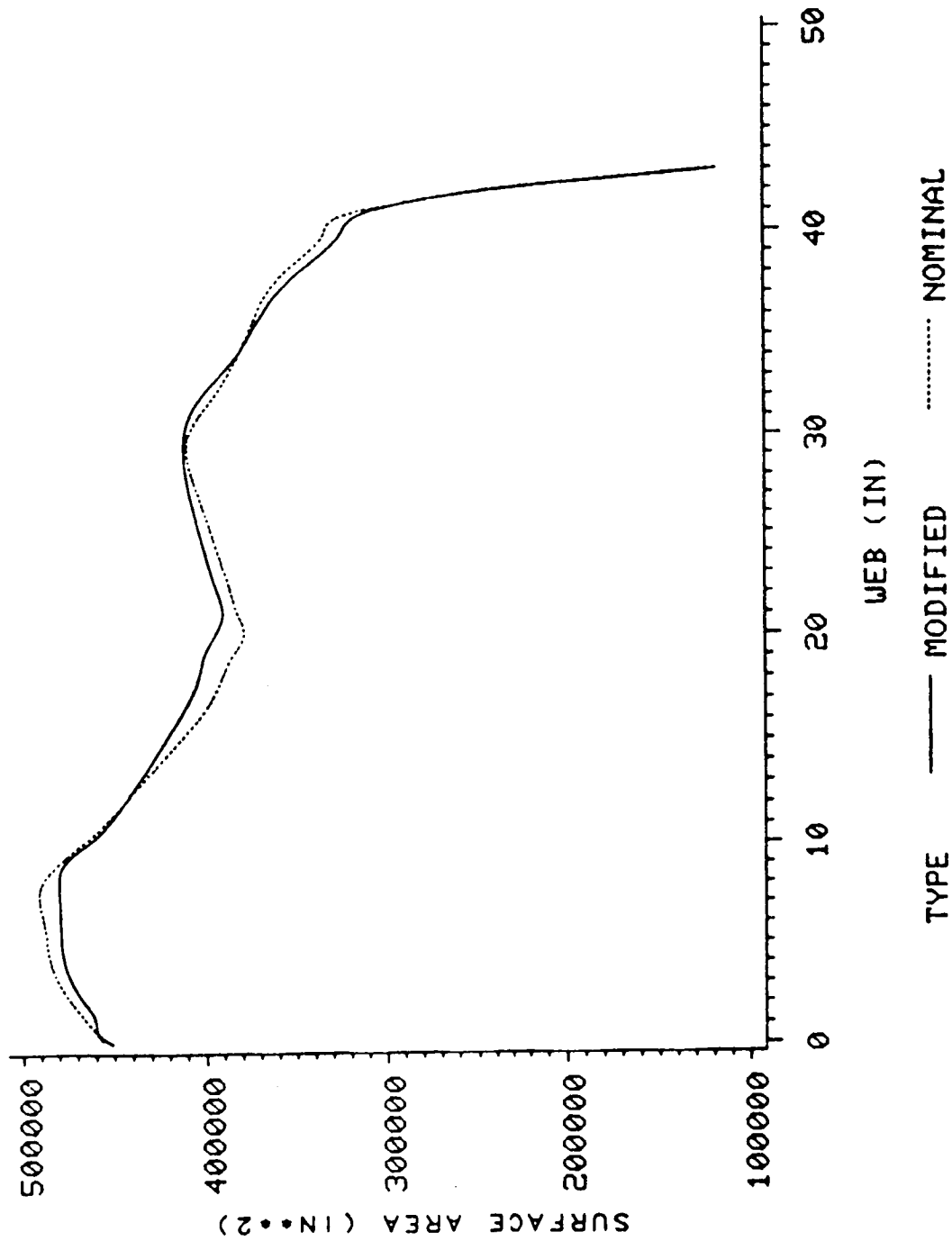


Figure 9. Adjusted Surface Area Values

Ballistics analyses were completed on the four propellants denoted above. These propellants were initially analyzed in the heads-down configuration with the current asbestos-filled insulation. Figure 10 shows how these propellants compared with the CEI nominal requirements and the HPM with TP-H1148 propellant. The DL-H397 propellant was eliminated due to immature development for application in a Block II design. The TP-H3340 propellant was also not accepted because of its low burn rate and higher ingredient costs. Table 8 presents the ballistic propulsion characteristics for the TP-H1148 and DL-H396 propellants in heads-down flight mode. Respective thrust performance traces are shown in Figures 11 and 12. Insulation weights using nonasbestos materials and safety factors were developed and adjusted surface area versus web trace was incorporated into the appropriate ballistics analyses.

To increase performance, the heads-up flight mode requirements were considered and two options evaluated to achieve the higher thrust requirements. Either the burn rates for the TP-H1148 and DL-H396 propellants were increased or the nozzle throat diameters were reduced. Iron oxide is added to the propellant formulations to meet the higher burn rates needed for heads-up thrust requirements. The resultant changes in propellant density, specific impulse, and burn rate slopes were included in the studies.

When the throat diameter is reduced the nozzle expansion ratio increases which significantly improves the specific impulse for this approach. The expansion ratio increases because the exit area remains fixed at the HPM geometry. When the throat radius is decreased, MEOP increases more than that resulting from increased burn rate. This requires a thicker and heavier case wall resulting in a consistent propellant weight loss. Accordingly, the approach using increased burning rates offers the most system advantages. For this selected approach, Table 9 presents the propulsion characteristics for the two propellants formulated to satisfy the heads-up flight mode.

Figures 13 and 14 show the thrust time trace for Designs 1B and 2B, for heads-up flight. The Design 2B thrust-time trace represents Morton Thiokol's baseline SRM II design.

Table 8. Heads-Down Propellant Comparison

Parameter	ALTERNATE PROPELLANTS	
	HPML Nominal	DESIGN A
		TP-H1148
Web Time (sec)	111.7	111.7
Web Time Avg. Pressure (psia)	660.8	660.9
MEOP (psia)	1016.0	1016.5
Max Sea Level Thrust (Mlbf)	3.06	3.06
Web Time Avg Vac Thrust (Mlbf)	2.59	2.59
Vacuum Delivered Specific Impulse (lbf-sec/lbm)	267.1	267.1
Web Time Vac Total Impulse (Mlbf-sec)	288.9	289.1
Burn Rate @ 1000 psia (in/sec)	0.4338	0.4338
Throat Radius (in)	26.93	26.93
Initial Expansion Ratio	7.720	7.720
Propellant Weight (Mlbm)	1.11**	1.111
% Iron Oxide	0.28	0.28
Density (lbm/in <sup>3</sup> )	0.06348	0.06348
Throat Erosion @ Time Avg. (in/sec)	0.00863	0.00864

\* Based on a PMBT of 60°F

\*\* Nominal propellant weight 1,110,136 lbm

Table 9. Heads-Up Propellant Comparison

Parameter	ALTERNATE PROPELLANTS		
	HPML <sup>*</sup> Nominal	TP-H1148	DL-H396
DESIGN B			
Web Time (sec)	111.7	101.1	104.2
Web Time Avg. Pressure (psia)	660.8	728.5	727.7
MEOP (psia)	1016.0	1112.7	1129.5
Max Sea Level Thrust (Mlbf)	3.06	3.395	3.442
Web Time Avg Vac Thrust (Mlbf)	2.59	2.855	2.851
Vacuum Delivered Specific Impulse (lbf-sec/lbm)	267.1	266.5	268.16
Web Time Vac Total Impulse (Mlbf-sec)	288.9	288.0	296.5
Burn Rate @ 1000 psia (in/sec)	0.4338	0.4627	0.4540
Throat Radius (in)	26.93	26.93	26.93
Initial Expansion Ratio	7.720	7.720	7.720
Propellant Weight (Mlbm)	1.11**	1.112	1.135
% Iron Oxide	0.28	0.66	0.10
Density (lbm/in <sup>3</sup> )	0.06348	0.06362	0.06479
Throat Erosion @ Time Avg. (in/sec)	0.00863	0.00931	0.00890

\* Based on a PMBT of 60°F

\*\* Nominal propellant weight 1,110,136 lbm

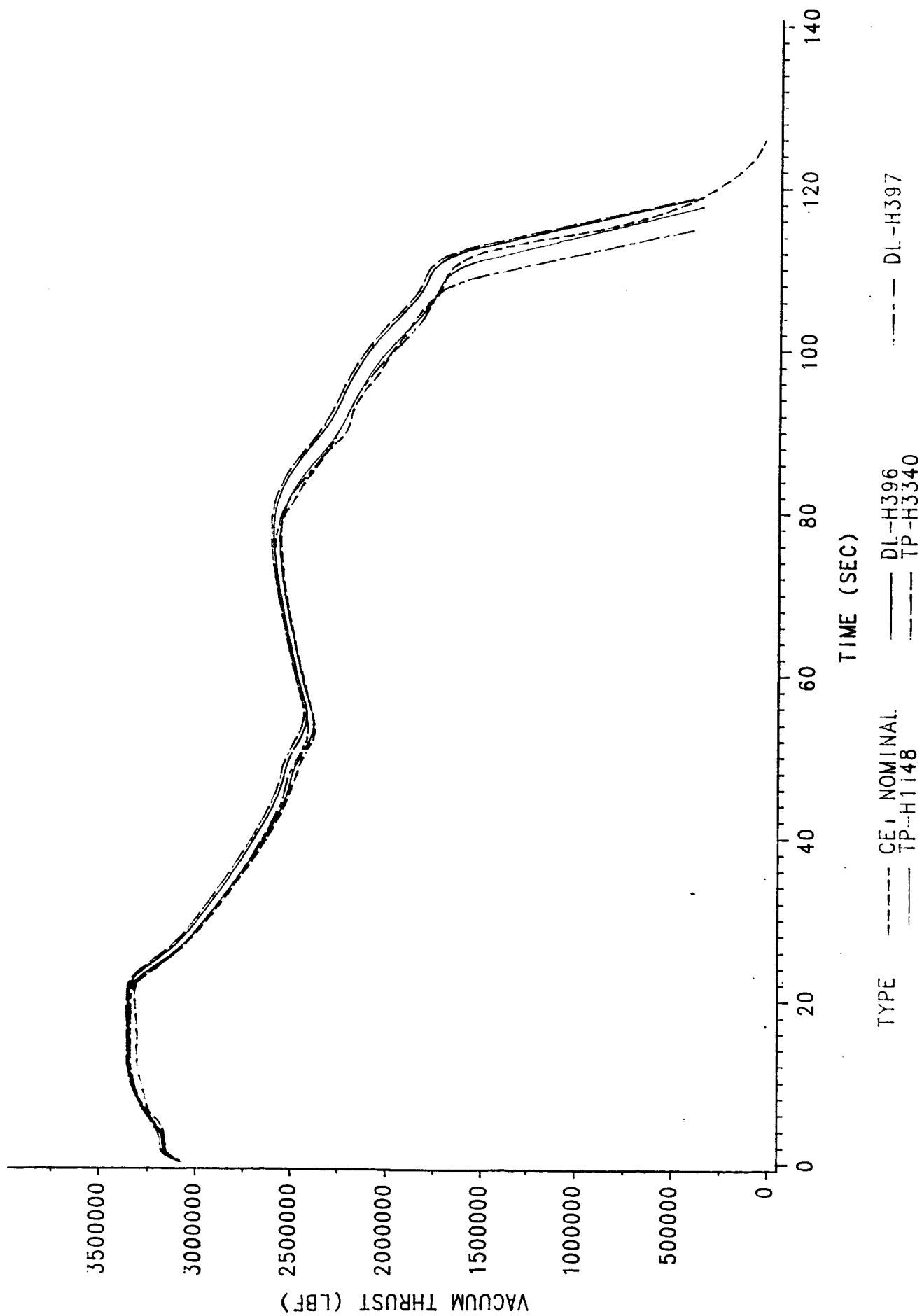


Figure 10. Heads-Down SRM Propellant Comparison

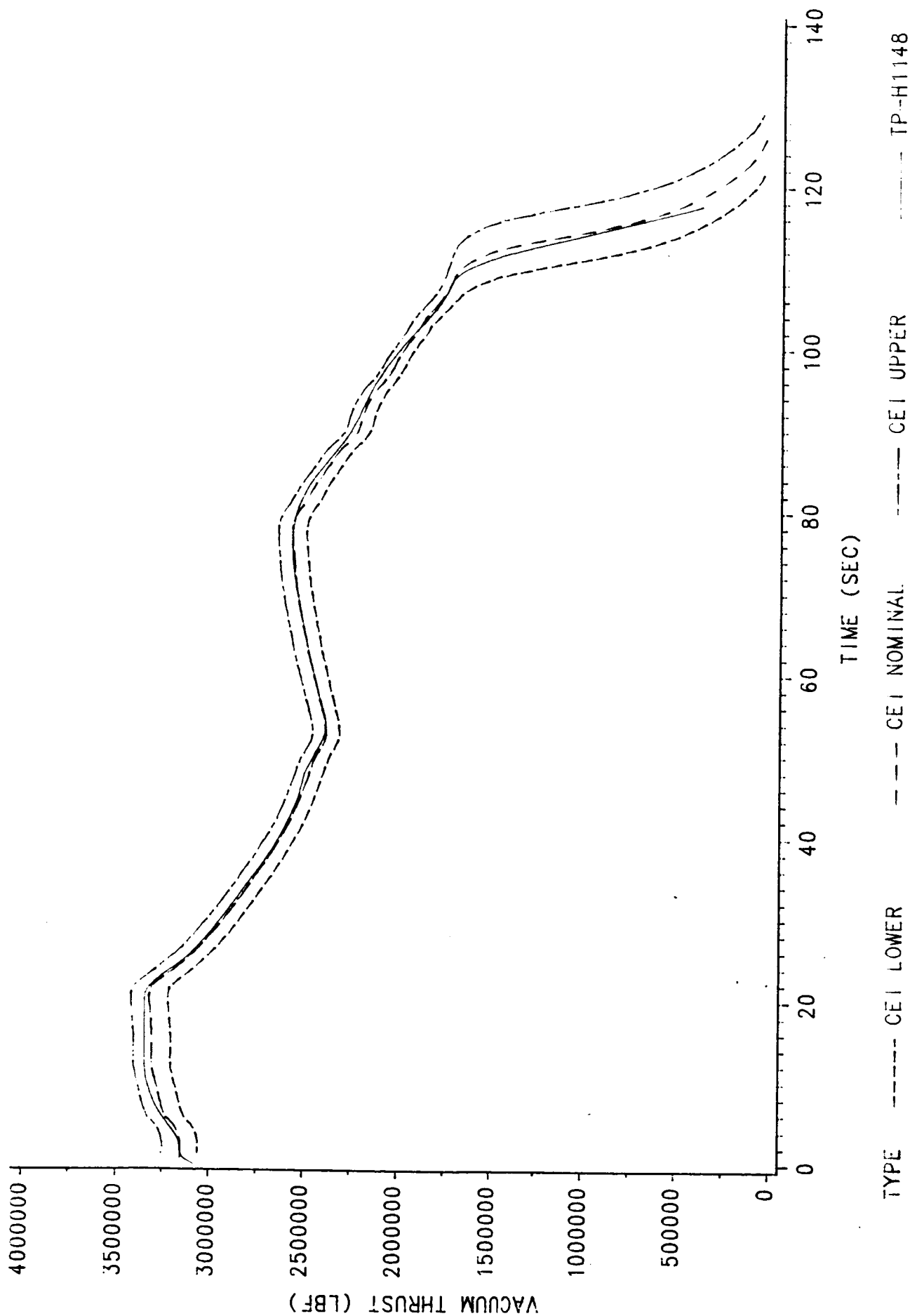


Figure 11. Thrust Performance for Design 1A

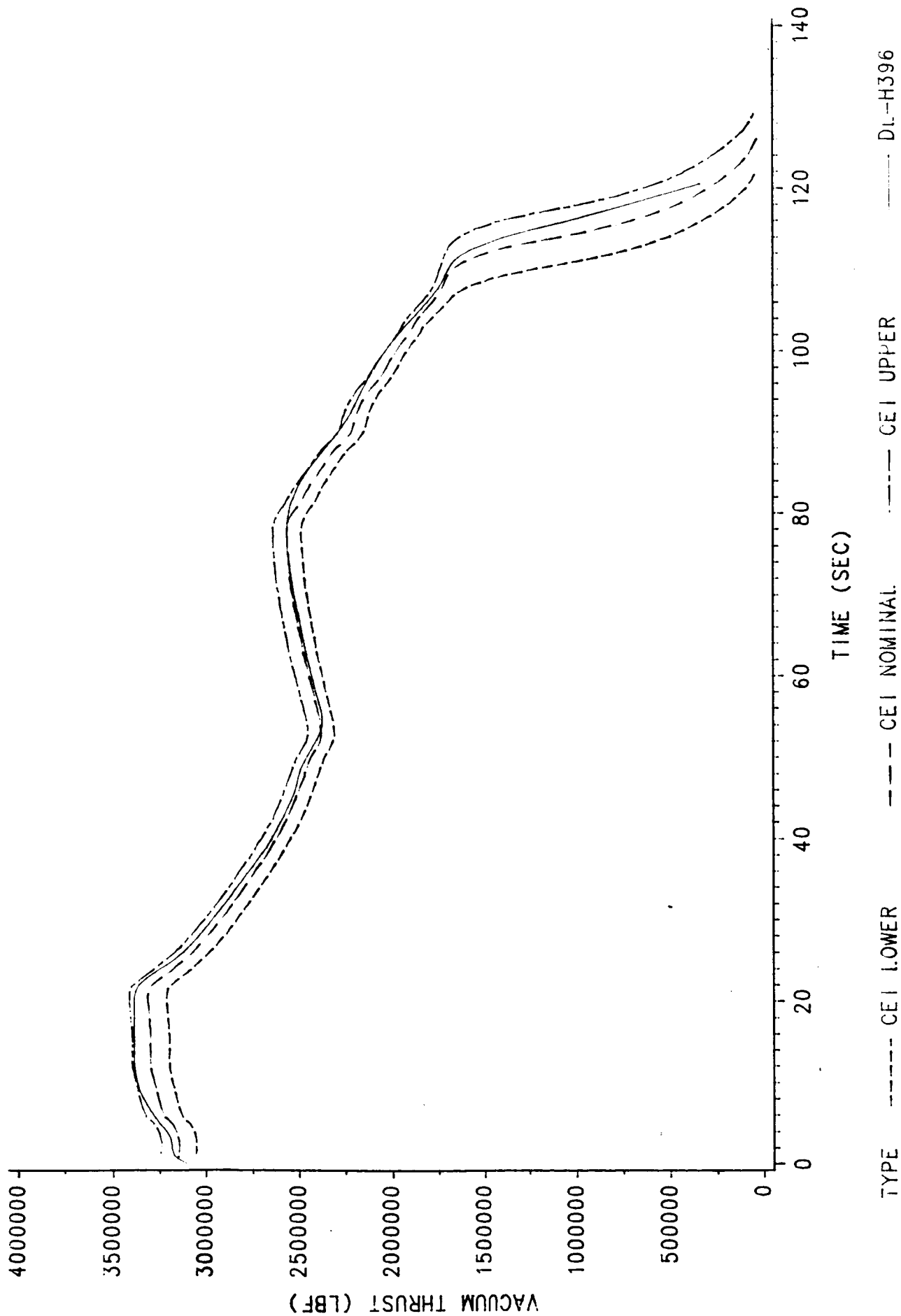


Figure 12. Thrust Performance for Design 2A

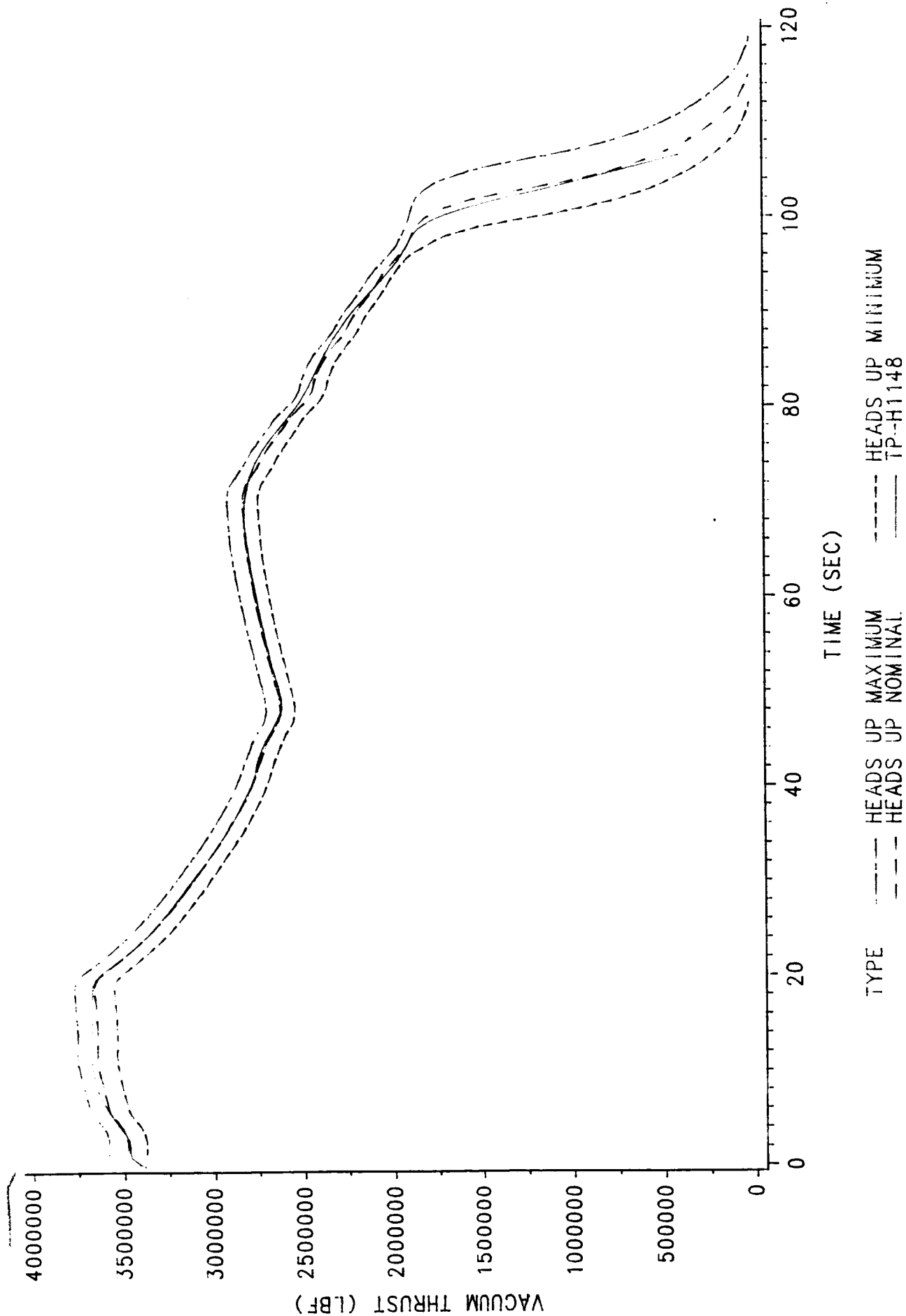


Figure 13. Thrust Performance for Design 1B



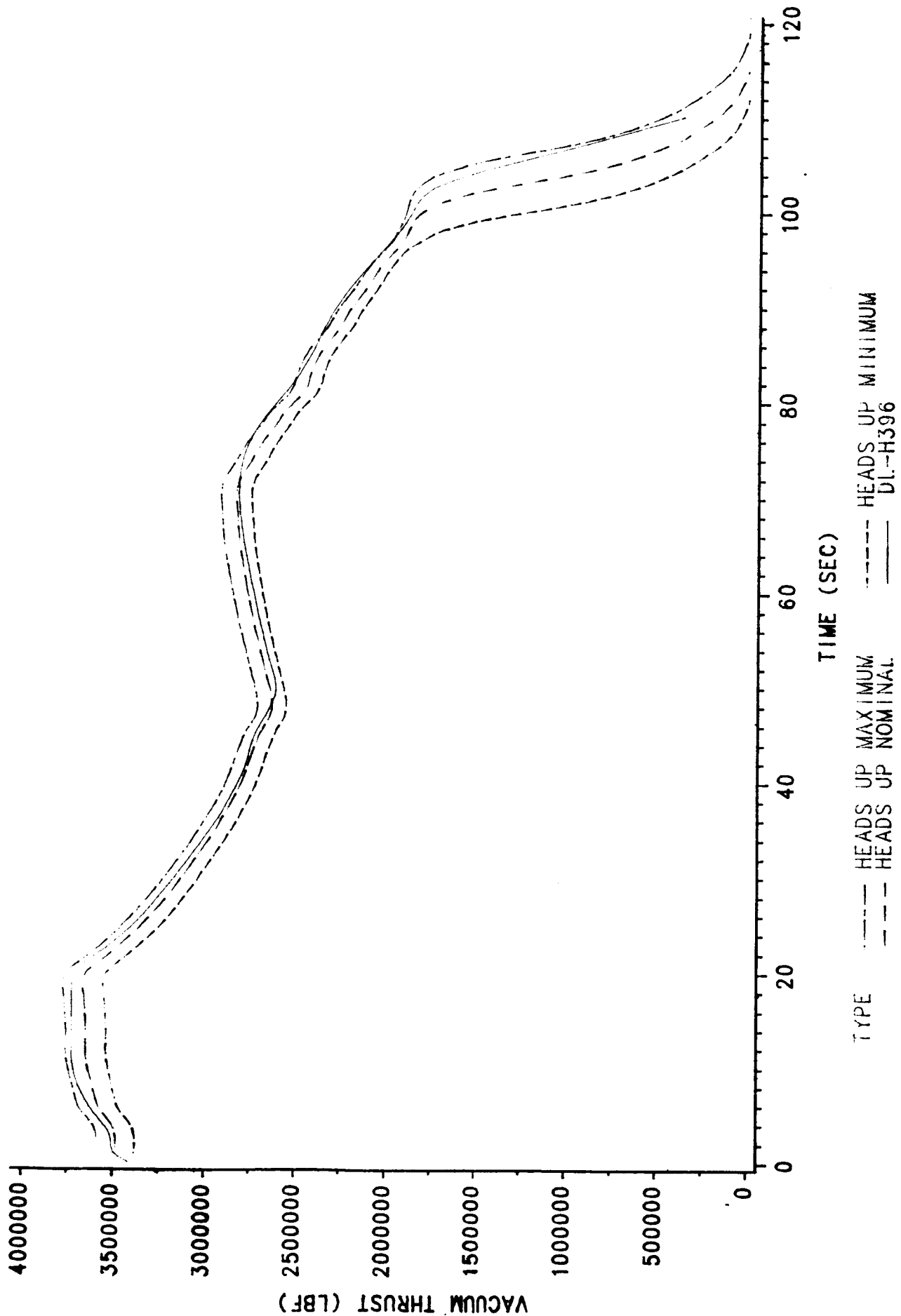


Figure 14. Thrust Performance for Design 2 B

### 3.2.3 PERFORMANCE

Figure 15 is a representation of the heads-down payload comparison for Designs 1A and 2A. Figure 16 depicts a heads-up payload comparison for Designs 1B and 2B. These figures identify the contribution of inert weight changes, propellant weight changes, and specific impulse changes to the total estimated payload increment. Shuttle payload increments were calculated by the use of partials received from NASA-MSFC which are:

Inert: -0.182-lbm payload/lbm inert  
Propellant: 0.083-lbm payload/lbm propellant  
Specific Impulse: 800-lbm payload/second  $I_{sp}$   
(Partials Per SRM for the Vehicle)

The payload assessments are only meant to provide a measure for relative comparisons between design concepts since they are not derived by vigorous methods. In addition to adjusting payload capability to account for changes in inert weight, propellant weight, and propellant specific impulse, the configurations providing a heads-up thrust-time trace were given the benefit of a 3,500-lb payload increase attributed to the improved launch trajectory. This assumption is based on earlier studies for Shuttle heads-up flight that used HPM inert weights and propellants weights while optimizing the thrust-versus-time requirement.

In addition to two different propellants we considered two case designs. The first case, for Design 1A or 1B, uses the D6AC steel with ten joints, similar to the current RSRM configuration except for the improved joint design. The second case, for Design 2A or 2B, uses T250 maraging steel and has four total joints. A case design program was used to calculate the case weight changes between the D6AC and MAR T250 steel cases and these weights were correlated with the detailed design assessments. The ADP calculated nozzle weights at different pressures and erosion rates with thermochemical and ballistic data as inputs. These weights accurately reflect the HPM nozzle actual weights used in Design 1A or 1B and agree with the Block II nozzle weights for Design 2A or 2B developed from detailed evaluation. Those configurations with the higher MEOP pay a cost in payload reduction due to necessary inert weight increases. For example, Design 1B provides a payload increase of 2,063 lb. Because of increased inert

weight, this represents a 1,134-lb payload reduction from the previous heads-up performance studies which assumed HPM weights were held constant.

Tables 10 and 11 summarize the potential performance gain and the contributing factors for the design configurations discussed in this section.

For increased performance, Design 2B, using a new steel case material, reduced number of joints, a Block II nozzle, and HTPB propellant, is an attractive design approach meeting all heads-up requirements. This design offers significant performance improvements through use of higher performing propellant and lighter weight, reusable steel cases, and has been selected as the Block II SRM concept.

**Delta Payload Analysis**

Configuration	Type	Delta Payload
Configuration 1	INERT	~4500
	SP	~1000
	TOTAL	~5500
Configuration 2	INERT	~-8500
	SP	~-1000
	TOTAL	~-9500

### Figure 15. Heads-Down Payload Comparison

TYPE	HEADS	INERT	SP	TOTAL	WP
TP-H1148	1	1	1	3	1
DL-H396	1	1	1	3	1

**Figure 16. Heads-Up Payload Comparison**

PAGE 3-34 INTENTIONALLY BLANK

Table 10. Heads-Down Payload Comparison (lbm) With HPML Nominal  
(nonasbestos insulation, SF = 1.5)

Parameter	DESIGN A	
	Configuration 1	Configuration 2
	TP-H1148 <sup>2</sup>	DL-H396 <sup>3</sup>
Nozzle Weight	23,306	17,755
Case Weight	98,648	77,379
Insulation	21,829	20,059
Other	1,536	1,988
Total Inert Weight	145,319	117,181
Delta Inert Weight	±0	-28,138
Propellant Weight	1,110,136	1,130,470
Delta Density	±0	+16,788
Delta Case Thick.	±0	+2,440
Delta Non-Asbes.	±0	+1,106
Insulation		
Delta Propellant Weight	±0	+20,334
Delta ISP	267.1	±0.98
		DELTA PAYLOAD <sup>1</sup>
Inert	+240	+5,121
Propellant	+92	+1,688
Isp	±0	+784
Total	+332	+7,593

- Notes: 1. Partial/SRM  
Inert: 0.182 lb/lb  
Propellant: 0.083 lb/lb  
ISP: 800 lbs/sec
2. D6AC Segmented Steel Case
3. T250 Maraging Steel Case with 4 Joint Design

Table 11. Heads-Up Payload Comparison (lbm) With HPML Nominal  
(nonasbestos insulation, SF = 1.5)

Parameter	DESIGN B		
	Configuration 1	Configuration 2	
	HPML	TP-H1148 <sup>2</sup>	DL-H396 <sup>3</sup>
Nozzle Weight	Nominal	23,306	17,755
Case Weight	23,306	106,194	86,056
Insulation	98,648	20,059	20,374
Other	21,829	1,988	1,988
Total Inert Weight	145,319	151,547	126,173
Delta Inert Weight	±0	+6,228	-19,146
Propellant Weight	1,110,136	1,112,262	1,134,756
Delta Density	±0	+2,448	+22,909
Delta Case Thick.	±0	-1,430	+1,050
Delta Non-Asbes.	±0	+1,108	+661
Insulation			
Delta Propellant Weight	±0	+2,126	+24,620
Delta ISP	267.1	-0.60	+1.06
DELTA PAYLOAD <sup>1</sup>			
Inert		-1,134	+3,485
Propellant		+177	+2,044
ISP		-480	+848
Heads-Up Flight Mode	+3,500.0	+3,500	+3,500
Total		+2,063	+9,877

Notes: 1. Partials/SRM

Inert: 0.182 lb/lb

Propellant: 0.083 lb/lb

ISP: 800 lbs/sec

2. D6AC Segmented Steel Case

3. T250 Maraging Steel Case with 4 Joint Design

### **3.3 CASE DESIGN**

The objective of the Block II case conceptual design study effort is to provide a design for a reliable, high-performance case suitable for the Space Shuttle SRBs. The definition of an optimal case design requires the selection of concept, materials, and fabrication techniques that offers the potential to provide reliability and performance gains over the RSRM while satisfying all of the requirements of the CEI specification. The Block II case is designed to a head-end MEOP of 1,100 psig. Trade studies included consideration of composite materials (Appendix B) and various metal alloys.

The preliminary design trade studies conducted for the Block II case concluded that a segmented steel case would best meet the reliability, performance, cost, and reuse requirements. In this section we present the case design with results of supporting studies and analyses which illustrate the feasibility of the recommended design concept. The issues of mechanical joint design and sealing are discussed in Sections 3.4 and 3.5 of this report.

The trade studies conducted for the Block II case focused on selecting compatible material and processing methods for producing the large-diameter, thin-wall case segments. High strength steels with good fracture toughness and high ratio of yield strength-to-ultimate strength are required to meet the reliability, safety, and performance requirements of a reusable rocket motor case. The combination of material and processing methods selection must be carefully considered since the large size of the case limits heat treatment and process selection.

The case design report is the result of optimization of material selection, process selection, membrane thickness, case segment length, and integration of aft closure and nozzle fixed housing. The resulting design meets all interface and performance requirements. Further optimization is possible during the design phase of the development program. The aft segment stiffener design, to resist collapse loads during splashdown, must be optimized during the development program.



### **3.3.1 REQUIREMENTS AND SCOPE OF STUDY**

Many of the design features of the Block II case are logical extensions of the SRM, HPM, and RSRM design concepts and criteria. The SRM development and production programs provide extensive test and analytical procedures to apply to the design and verification of the Block II case assembly.

The SRM case must provide structural capability for pad loads, motor operation (including all flight loads), water impact loads, and handling loads. Further requirements are associated with the interfacing of the SRB and external tank (ET) components.

Motor operation requires a factor of safety of 1.4 in the material strength through detailed design using a high strength steel. Case pressurization, SRB weight and design, ET attachment loads, and flight loads all require detailed investigation and design to insure proper case performance during the Shuttle ascent. Case recovery and recycle requirements are established by accounting for the water penetration, cavity collapse, splashdown, salt water environment, refurbishment, and handling effects.

The production of a reliable, safe, high-performance SRM necessitates a case with precise dimensions to allow consistent loading, fitting, and interfacing. The requirement of 19 reuses produces increased emphasis on cyclic and environmental flaw growth. Fracture mechanics is one of the design tools used to assure the reliable performance of the Shuttle SRM case in connection with reuse. Table 12 summarizes the basic design requirements for the case.

**Table 12. Design Requirements Criteria**

- Factor of Safety
  - 1.4 on ultimate Before separation
  - 1.20 on yield Before separation
  - 1.25 on ultimate\* After separation
  - 1.10 on yield\* After separation
- Minimum of 19 reuses.
- Proof test factor will demonstrate the capability for four flights.
- Service life factor of 1 on total life requirement.
- Service life factor of 4 on low cycle fatigue requirements.
- Interface, pad, flight, and splashdown loads.
- Case material resistant to or protected from:
 

Stress corrosion	General corrosion
Hydrogen embrittlement	Temper embrittlement
Creep	Galvanic corrosion
- Case temperature limit = 400°F maximum (established to prevent damage to internal insulation to case bond).

\*This is a design goal only for water impact loads. Analysis will be conducted on the effects of water impact loads for the following water entry conditions:

1. Nominal vertical velocity of 85 fps
  2. Horizontal velocity of 0 to 45 fps
  3. Impact angle of -5 to +5 degrees
- Results of these analyses will be evaluated, and the calculated factors of safety will be the basis of attrition rate determination.

The successful design and production of large, flightweight rocket motor cases require careful consideration of both material and manufacturing process to achieve a high reliability design within reasonable facility and economic constraints. The basic case design is a straightforward application of well-established, thin-wall pressure vessel membrane analysis methods. The production design includes selection of forging shapes and sizes that remain within the available melting and forming capabilities. The full detailed design analyses for the asymmetric attach and splashdown loads have been deferred to the developments programs to allow greater emphasis on the joint deflection and integrity studies in this project. In addition to the basic sizing analyses, preliminary fracture mechanics analyses were conducted to estimate the service life cycles obtainable before undetectable flaws would grow to critical size and to estimate the proof test load that would assure four additional uses. An additional special requirement of the STS that was considered in detail was the case axial growth during ignition that is limited to insure safe level dynamic loading for

the STS. This criterion restricts the design of composite cases and may even have restricted the strength utilization of a high-performance steel.

### 3.3.2 CASE DESIGN DESCRIPTION

The Block II SRM case is fabricated from 18 percent nickel, titanium-strengthened, 250 grade maraging steel in a segmented configuration. The segment concept consists of an aft closure with integral nozzle fixed housing, a stiffened aft cylindrical segment with ET attach provision, two cylindrical segments and a forward segment as shown schematically in Figure 17. Block II tang and clevis joints allow field assembly while girth welds join shear formed cylinders into casting segments.

High-strength (250 ksi), 18 percent nickel, titanium-strengthened maraging steel (MAR-T250) was selected for the Block II case development because of its higher yield and ultimate strengths with the same fracture toughness as the D6AC low alloy steel that has been proven successful in the HPM cases. The maraging steel develops its full strength by a solution annealing and aging process which offers potential for improved consistency over the quench and temper processes for low alloy steels.

The 146-in.-diameter, 116-ft-long case is made up from 12 forgings joined by girth welds into four segments and an aft closure which includes the nozzle fixed housing. These segments are joined with tang and clevis joints at final assembly. The aft closure-to-aft segment joint (the nozzle-to-case joint) is assembled prior to shipment from Wasatch Operations. The other three field joints are assembled at the launch site.

The forward segment consists of two cylindrical segments and a 1.6:1 elliptical dome. Two cylindrical segments are required due to the limitations on the length of the present shear-forming equipment. The forward dome will be forged and machined from a pancake billet and will include the forward stub skirt and the flange for the ignition system attachment. The aft closure will be assembled from two ring rolled forgings with a girth weld near the ring which reinforces the cone-to-sphere transition. The cone and reinforcement ring may be combined in one forging. This closure interfaces with the aft segment with a

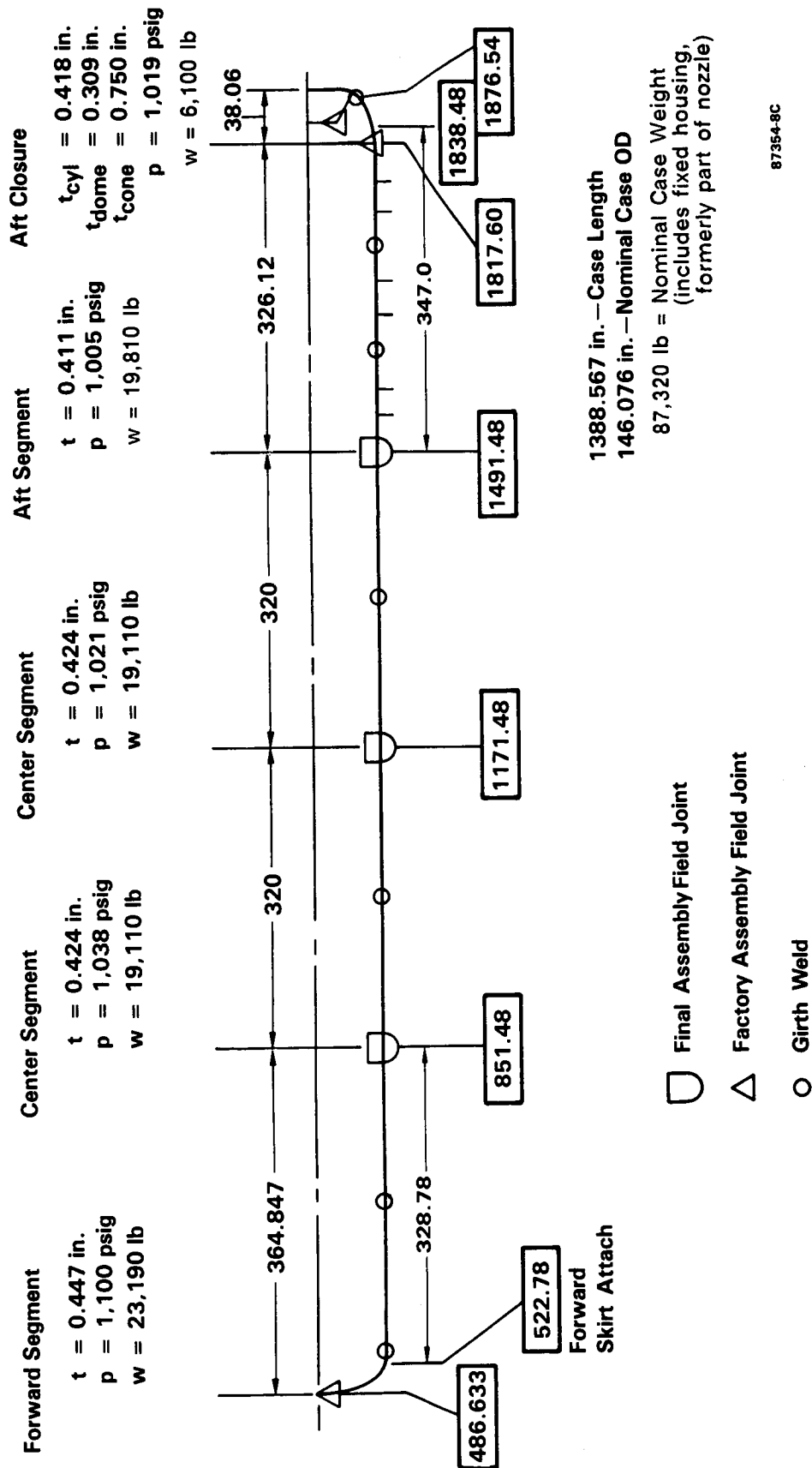


Figure 17. Schematic of Block II Case Design

clevis joint and interfaces with the aft end ring of the nozzle flex seal with a face-sealed bolted joint. The cylindrical segments are fabricated by girth welding two cylindrical shear-formed segments, heat-treating the assembly, and finish machining the tang and clevis details. The aft segment is fabricated by girth welding three shear-formed cylinders which include rolled-in buildups for ET and stiffening ring attachments. The ET attach stub rings will be machined from a thickened region of the cylinder, but the stiffening ring stubs may be welded to buildups on the case.

The case membrane thickness design follows the high performance motor design with 1.07 biaxial improvement and 90 percent of the predicted pressure drop down the length of the motor. In addition to the minimum membrane thickness we include 0.020 in. for shear forming tolerance and 0.009 for refurbishment material removal to obtain the nominal wall thickness. For the MAR-T250 alloy the ultimate strength criteria (with the 1.4 factor of safety) govern the design size. The yield criteria with a factor of safety of 1.2 is satisfied when the ultimate criteria are satisfied.

### **3.3.3 MATERIAL SELECTION**

An objective of this study was to identify the most promising material candidates for the development of a highly reliable, improved-performance solid rocket motor case. Initially, we considered carbon fiber composite cases as well as those fabricated of high strength steels. Our studies concerning the composite materials are included in Appendix B. The result of these studies showed the composite case to offer good performance advantages, but reliability respective to component reuse had not been demonstrated. Until this technology is developed, the preferable SRM case material is one of the high strength steels.

Candidate steel case materials were compared on strength, fracture toughness, experience, process effects, and cost. To maintain the booster performance, only steels with ultimate tensile strength equal to or greater than the present D6AC steel were considered. To maintain reliability, only materials with fracture toughness equal to or better than the present D6AC are admissible. The steels that survive shear forming operations must be substantially inclusion and defect free. Consequently, the process of shear forming provides an effective

defect detection and billet rejection criterion early in the processing of every case component. The combined costs of both raw material and fabrication processes must be considered to provide an equitable basis to select the most cost-effective approach.

Based on all considerations, 18 percent nickel, titanium-strengthened, 250 grade maraging steel was selected as the case material with the low-alloy D6AC steel as a more mature backup. The primary factors and data summary for comparing the candidate materials are presented in Table 13. The maraging steel offers the advantages of higher yield and ultimate strength<sup>(1,2)</sup> with the same fracture toughness as the alternative D6AC steel.<sup>(3)</sup> The titanium-strengthened maraging steels were first introduced in 1981. These alloys use no cobalt and consequently can be expected to remain available and nonvolatile in cost. The comparative youth of the MAR-T250 steel leaves the database less developed than the D6AC steel database. This will require completion of the detailed characterization testing and evaluation as a key element of the Block II design substantiation.

The extensive material trade studies conducted for the original SRM development<sup>(4)</sup> identified two good candidate materials as a baseline and alternate. D6AC, a low-alloy steel, and MAR-200, an 18 percent nickel maraging steel, were closely compared. The primary discriminators in that decision were cost, cost and schedule credibility, and performance. The ultimate strengths were about equal but the MAR-200 steel's fracture toughness exceeded that of D6AC steel. The D6AC steel case was expected to be 10-15 percent cheaper than the MAR-200 steel case and that material had a slightly broader experience base which was seen to support the credibility of the cost and schedule estimates.

---

<sup>1</sup>Product Information Sheet, "VascoMax<sup>®</sup> T-250," Teledyne Vasco, Latrobe, Pennsylvania, 1982.

<sup>2</sup>Product Information Sheet, "VascoMax<sup>®</sup> T-200/T-250/T-300," Teledyne Vasco, Latrobe, Pennsylvania, 1985.

<sup>3</sup>TWR-10891, "Mechanical Properties of D6AC Steel As Used on the SRM Program," 20 February 1976, R. H. Gercke.

<sup>4</sup>TWP-077326, "Design, Development, and Verification for Solid Rocket Project for the Space Shuttle Program," 27 August 1973.

Table 13. Metallic Case Trades

Material	Experience	Cost Matl/SRM	Fracture Toughness K <sub>IC</sub> (ksi $\sqrt{\text{in.}}$ )	Cleanliness	Fabrication	Heat Treatment	Strength (ksi) Ftu/Fty
D6AC	High	Low/low	90	Excellent VAR	Shear spin, no welds	Q&T	200 180
MAR-C200	Moderate	High/moderate	120	Excellent VIM-VAR	Shear spin, girth welds	900°F age 3 hr	210 200
MAR-T250	Moderate	High/moderate	90	Excellent VIM-VAR	Shear spin, girth welds	900°F age 3 hr	250 240
HY-180	Low	High/high	200	Excellent VIM-VAR	Roll and weld	Q&T in plate, weld in Q&T cond	195 180

The maraging steel of that time (MAR-C200) required the strategic material cobalt as an alloying element. The limited supply and consequent volatility of the cost and availability were judged to unfavorably degrade the cost and schedule credibility in the long term Space Shuttle program. In 1981, titanium-strengthened grades of maraging steel were introduced. These steels have properties as good as or slightly better than the cobalt-strengthened grades introduced in the 1960s. With the removal of cobalt, the cost and availability of these new maraging steels are expected to be stable. This removes the strategic material cost and supply risk.

The D6AC material meets the essential requirements of the Shuttle system. It has proven adequate to meet the strength and toughness requirements so essential for the reusable cases. The specified heat treatment was selected by carefully balancing the fracture toughness gain against the ultimate strength reduction.<sup>(4)</sup> This requires close tolerances on the critical quench and temper processes.

The age hardening steels achieve the strength and toughness characteristics through the less complex process of solution treating and aging. Since they are practically carbon free, no protective atmosphere is necessary during their heat treatment. The MAR-T250 alloy offers the opportunity for a 25 percent increase in ultimate strength, a 33 percent increase in yield strength, and no loss in fracture toughness when compared to the D6AC material. Other advantages of the MAR-T250 steel are gained by the removal of the critical quench and temper process. Since no slack quench problems are encountered, heat treatment of full segment length cases may be accomplished. This allows the development of high-reliability automated welding processes. Properly welded and aged maraging steel will exhibit weld efficiencies close to 100 percent with fracture toughness similar to the parent material. (A 90 percent weld efficiency was assumed for preliminary analysis.) Welding does not require preheat or postheat treatment and allows full strength development through re-solution annealing and aging. Compared to the critical quench and temper of the D6AC material, the solution anneal and age hardening offers potential for reduced variation of finished part properties which translates into less performance penalty to allow for random variation of material strength.



The raw material cost for the maraging steel is currently three to four times the cost of the low-alloy D6AC steel. The baseline design will offset this cost increase by using a simpler heat treatment process and by minimizing the precision machining operations with the reduction of the number of mechanical joints. Further cost reductions may be encountered because of the potential to develop and qualify welding procedures for the repair of segments damaged during their service life of 20 flights and the associated handling operations.

### 3.3.4 CASE FABRICATION TRADES

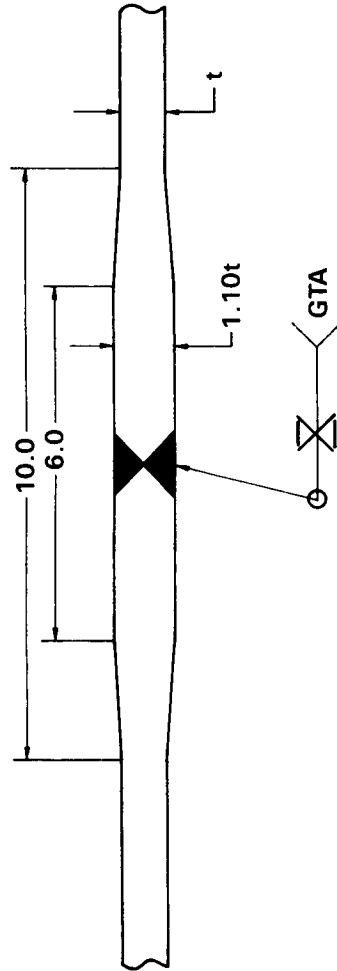
Three different fabrication approaches were considered in deciding the primary approach to build the Block II SRM metallic case. These approaches are: (1) nonwelded segmented (existing method); (2) roll and welded cylinder; and (3) shear-formed cylinders assembled with girth welds into casting length segments. Table 14 summarizes the advantages and disadvantages of each. The roll and weld approach was ruled out due to the longitudinal welds which are fully stressed by the cylinder hoop stresses. Removal of the six factory joints of the HPM case offers substantial performance gains over the existing fabrication approach. Welding of the proposed MAR-T250 steel is a less complex process than for the D6AC steel. It requires no preheating or postheating and nearly 100 percent efficiency is achieved by re-solution annealing and aging. The recommended fabrication sequence is:

- Prepare VIM-VAR ingot
- Upset and punch forging
- Hot roll ring forging
- Solution anneal
- Shear forming operation
- Rough machine
- Perform girth welds
- Solution anneal
- Heat treat (age)
- Final machine

Figure 18 shows the proposed buildup in the girth weld area which has a 10 percent thicker section for the welds to allow for mismatch, any reductions in  $K_{IC}$ , or reductions in strength due to welding. The proposed welding technique is

Table 14. Case Fabrication Trades

<u>Approach</u>	<u>Advantages</u>	<u>Disadvantages</u>
1. Segmented (nonwelded)	<ul style="list-style-type: none"> <li>• No welds and associated QA scope increase</li> </ul>	<ul style="list-style-type: none"> <li>• More mechanical joints required</li> <li>• Geometry restricted by shear spinning capability</li> <li>• Higher inert weight</li> </ul>
2. Welded (roll and weld, longitudinal, and girth welds)	<ul style="list-style-type: none"> <li>• Low cost</li> <li>• Not constrained by shear spinning capabilities</li> <li>• Reduced inert weight</li> </ul>	<ul style="list-style-type: none"> <li>• Longitudinal welds are fully stressed</li> <li>• QA scope increase on welds</li> </ul>
3. Welded (shear spin cylinders, assembly with girth welds)	<ul style="list-style-type: none"> <li>• Welds in reduced stress environment</li> <li>• Reduced inert weight</li> </ul>	<ul style="list-style-type: none"> <li>• QA scope increase on welds</li> </ul>
	<ul style="list-style-type: none"> <li>• Welded design reliability assured by NDI, proof test, and proven fracture mechanics design procedures</li> <li>• The third approach with MAR-T250 offers reliability and highest performance potentials</li> </ul>	



- Gas tungsten arc welding
  - Argon gas shielding
  - Stringent controls on filler wire cleanliness
  - No preheating or postheating required
  - Weld efficiencies near 100 percent by resolution annealing and reaging
- Also consider plasma arc welds during development
- Consider development of weld automation

A004039

Figure 18. Girth Weld Geometry

gas tungsten arc which has argon gas shielding and stringent controls on filler wire cleanliness. Also, plasma arc welding should be investigated as a lower cost (time) alternate during development.

### 3.3.5 PRELIMINARY ANALYSES

#### 3.3.5.1 Case Membrane Design

The case membrane region thicknesses were selected to satisfy the design criteria listed in Table 15. The design pressure for each segment is based on the criteria used for the HPM case stress analysis.<sup>(5)</sup> This allows varying the segment MEOP to account for the pressure drop along the length of the motor at the time of maximum headend pressure. The Block II design used 90 percent of the calculated pressure drop for conservative sizing of the membrane thickness. The design pressure, nominal thickness, and girth weld reinforcement thickness are listed for each cylindrical case segment in Table 16. The nominal thickness includes a dimensional tolerance of  $\pm 0.020$  in. and a refurbishment allowance of 0.009 in. to allow for grit blast material loss during the 19 reuses of the case.

**Table 15. Block II Case Membrane Design Criteria**

Material:	18 Percent Ni Maraging Steel MAR-T250
Specified Minimum Properties	
	$F_{TU} = 250$ ksi
	$F_{TY} = 240$ ksi
	$E = 27$ msi
Design Factors	
	Biaxial Improvement (2:1 stress field) = 1.07
	Factor of Safety = 1.4
Nominal Case Outer Diameter	= 146.076 in.
Maximum Case Outer Diameter	= 146.146 in.

---

<sup>5</sup>S. R. Stein, "Space Shuttle HPM SRM Case Analysis," TWR-12968, Rev. A, January 1983.

**Table 16. Block II Case Cylinders Design Summary**

<u>Segment</u>	<u>Nominal MEOP (psig)</u>	<u>Nominal Membrane Thickness</u>	<u>Weld Reinforcement Thickness (in.)</u>
Forward	1,100	0.447	0.492
Center	1,038	0.424	0.467
Center	1,021	0.424*	0.467
Aft	1,005	0.411	0.453
Aft Closure	1,019	0.418	0.460

\*Not minimum to allow full interchange of center segments

The forward dome membrane thickness was sized originally to provide uniform membrane stress throughout the 1.6:1 ellipse. For the Block II design the tabulated thicknesses were scaled to account for the increase in MEOP and for the increase of strength of the material. A conservative factor of 0.901 was used.

The aft dome membrane is a spherical shell with tapered reinforcements to manage the discontinuity stresses resulting from the cylinder and Y-joint transition and from the nozzle fixed housing cone to sphere transition. Axisymmetric finite element models were used to design appropriate tapers and to select the 0.309-in. required membrane thickness to assure a 1.4 factor of safety with minimum strength and thickness. The arc length of the shell is short enough that the effects of the discontinuity stresses are visible over its entire length.

The aft closure includes the nozzle fixed housing and a reinforcement ring which reduce the discontinuity stresses at the cone-to-sphere transition. The conical region of the aft closure is in a compressive axial and circumferential stress state and is consequently subject to failure by buckling before failure by general yield or rupture. The buckling factor of safety for conservative

combination of bending moment from nozzle vectoring, chamber pressure and an axial load resulting from proof test closure axial loading was 1.92 using the referenced methods.<sup>(6,7)</sup>

### 3.3.5.2 Fracture Mechanics Analysis

A preliminary fracture analysis was conducted on the Block II SRM proposed design. This analysis was performed to determine:

1. If hardware meets four times crack growth expected in one service life (20 uses).
2. If proof test can ensure four additional uses.

The approach used was the same approach defined for the HPM<sup>(8)</sup> which utilizes the Collipriest-Ehret equation:

$$\frac{da}{dN} = \exp \left[ n \cdot \frac{\ln K_C - \ln \Delta K_0}{2} \cdot \operatorname{arctanh} \left\{ \frac{\ln \Delta K - \frac{\ln [K_C (1 - R)] + \ln \Delta K_0}{2}}{\frac{\ln [K_C (1 - r)] - \ln \Delta K_0}{2}} \right\} + \ln \left\{ C \exp \left( \frac{\ln K_C + \ln \Delta K_0}{2} \cdot n \right) \right\} \right]$$

$da/dN$  = Crack growth due to fatigue cycling (inches growth/stress cycle)

$n$  = Paris equation exponent

$C$  = Paris equation coefficient

$\Delta K_0$  = Threshold stress intensity range for growth (ksi  $\sqrt{\text{in.}}$ ).

$K_C$  = Stress intensity for fracture =  $K_{IC}$  at the temperature of interest (ksi  $\sqrt{\text{in.}}$ ).

<sup>6</sup>Roark, Formulas for Stress and Strain, 5th Edition.

<sup>7</sup>ANS, Rockwell Structures Manual, p. 9.23.08.

<sup>8</sup>R. M. McCaskey, "Fracture Control Plan for Space Shuttle SRM High Performance Motor Case," TWR-13236, December 1981.

The input variables are:

R = Load ratio ( $P_{\min}/P_{\max}$ ) = 0 (normally)

$\Delta K$  = Cyclic stress intensity range of interest (ksi  $\sqrt{\text{in.}}$ ).

Assuming a minimum detectable flaw size by NDI of  $2a_0 = 0.100$  in., and using a nominal  $K_{IC}$  of 95,000 psi  $\sqrt{\text{in.}}$  and material constants for 18 percent Ni maraging steel,<sup>(9)</sup> the analysis indicated that the design would survive greater than 250 life cycles. Crack depth and critical crack size after 250 cycles were 0.1071 and 0.1217 in., respectively. Further analysis<sup>(10)</sup> determined that a proof test factor of 1.08 will ensure a minimum of six reuses.

The MAR-T250 material appears to be acceptable from a fracture mechanics aspect pending more detailed design and material evaluations which would be conducted during the Block II SRM development stage.

### 3.3.5.3 Case Axial Growth Study

Axial growth of the SRB is constrained to 0.9 in. for a metallic chamber. The proposed design will meet this requirement although the MEOP has increased. The selected material has a higher strength and lower elastic modulus (which suggests higher strain at pressure). These lead toward an expectation that the pressurized case axial growth would constrain the design. The proposed case eliminates six joints and uses a material with a higher Poisson's ratio. These attributes lead toward the expectation of reduced axial growth. With these changes, a detailed analysis was required to sum the offsetting effects while recognizing that the growth requirement is less than one part in 1,300.

The growth study used the conventional membrane equations and accounted for the variation of pressure (Figure 19) and axial load (Figure 20) along the

---

<sup>9</sup>R. H. Gercke and R. F. Zeigler, "Final Report: Space Shuttle SRM Case Materials Study, Project Numbers 93219 and W3219," IT-T7-17-699, December 1973.

<sup>10</sup>R. M. McCaskey, "Revised Proof Pressures for Space Shuttle SRM High Performance Motor Case, TWR-13695, 21 February 1983.

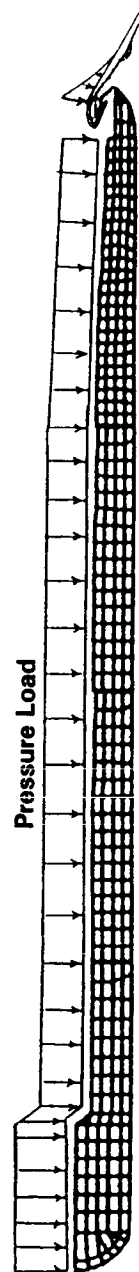
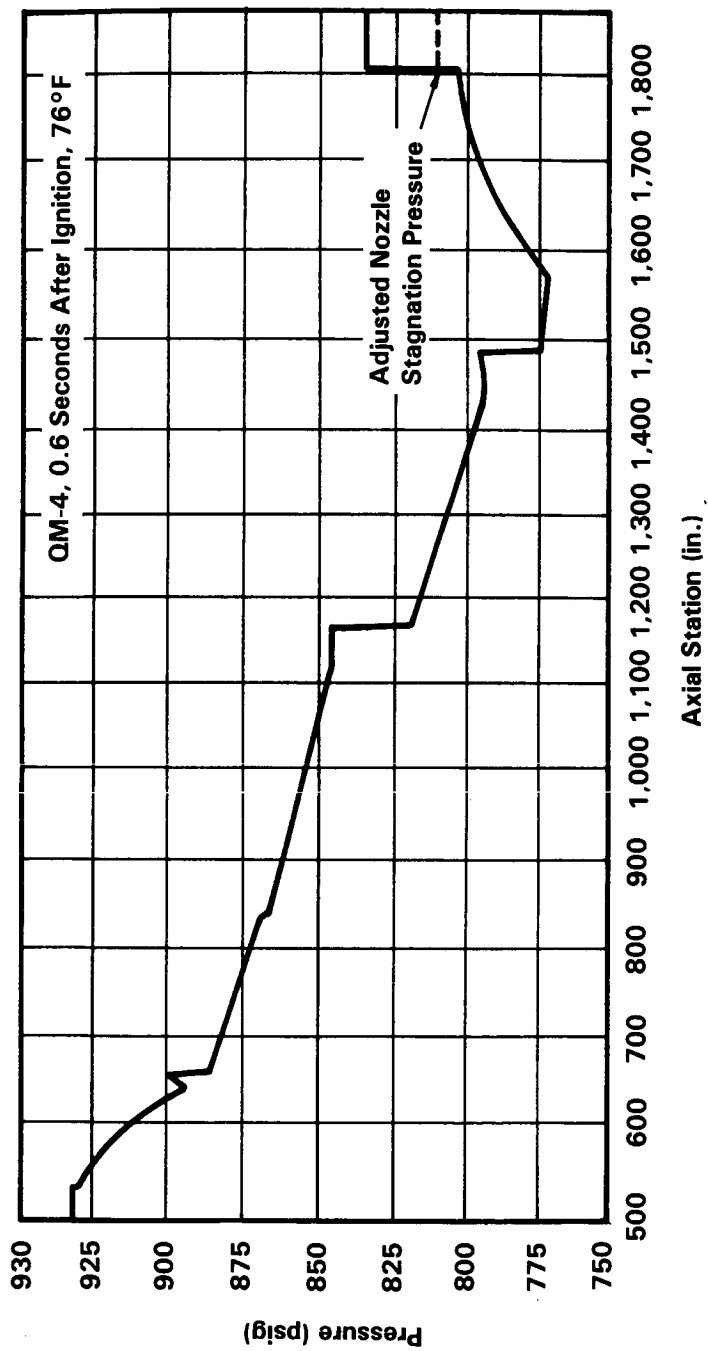


Figure 19. Pressure Distribution



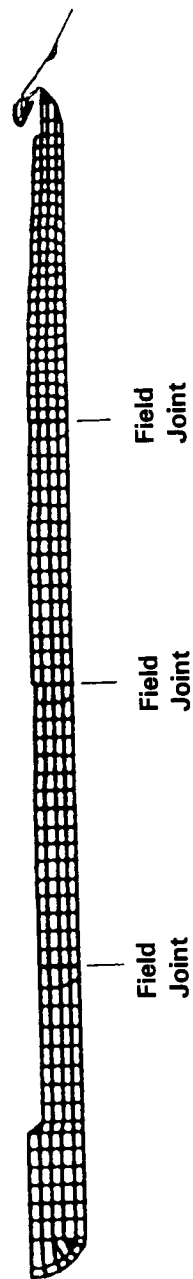
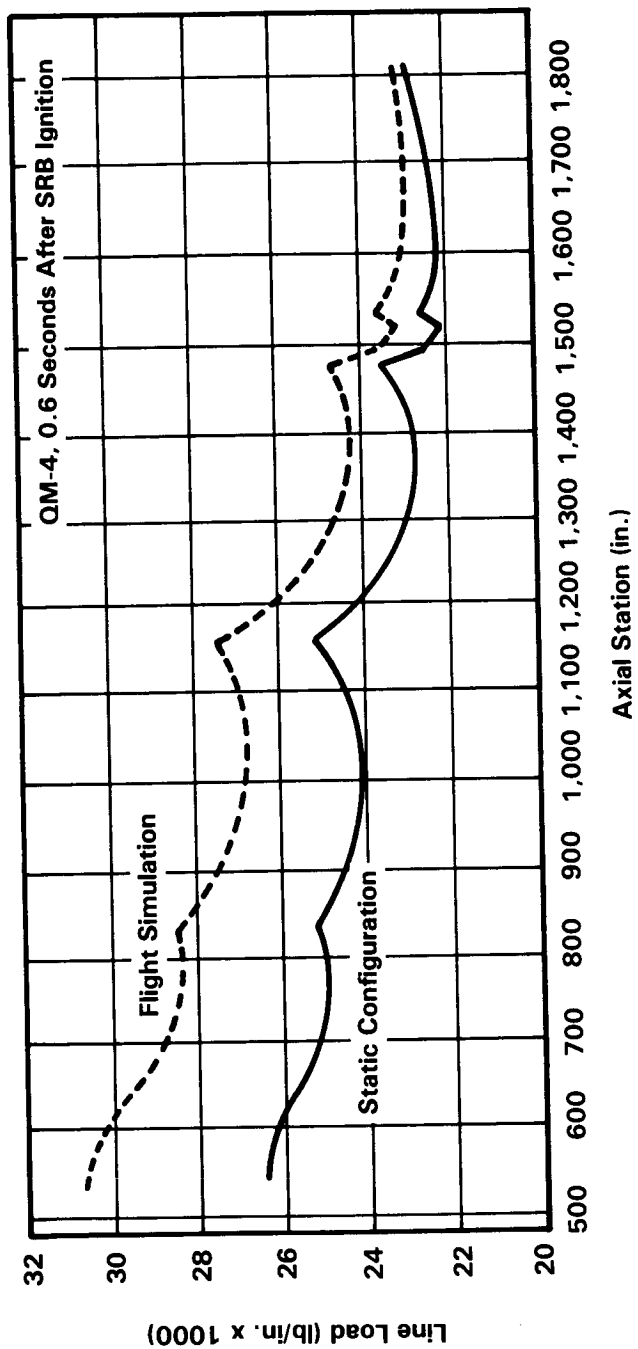


Figure 20. Line Load Comparison

length of the SRB. A loaded motor static test analysis<sup>(11)</sup> at 0.6 sec after ignition analytically compares axial growth in static test to the flight axial growth with a 1.6-g acceleration. The significant result of that analysis is the variation of the axial membrane load along the case shown in Figure 20. The "scalloping" of the load within a segment is due to the sharing of the axial load with the grain through a simple shear lag mechanism. The difference in axial membrane load from the grain inertia loading is also illustrated in this figure. The effect of the thrust compression is offset by the inertial load of the grain on the case. The greatest difference is about 15 percent in the forward segment.

One effect of the case membrane loading is the change of length in the case. This is evaluated using a conventional pressure vessel membrane design approach. Starting from the equilibrium line loads, geometry, and material properties, the axial and radial growth of uniformly loaded cylinders are:

$$\Delta L = \frac{L}{Et} (N_1 - \nu N_2) \quad (1)$$

$$\Delta R = \frac{R}{Et} (N_2 - \nu N_1) \quad (2)$$

Where:

$\Delta L$	=	Cylindrical membrane length change
$\Delta R$	=	Cylindrical membrane radius change
$L$	=	Initial cylinder length
$R$	=	Initial cylinder radius
$E$	=	Elastic modulus of case material
$\nu$	=	Poisson's ratio for case material
$t$	=	Membrane thickness
$N_1$	=	Axial line load
$N_2$	=	Circumferential line load

---

<sup>11</sup>G. L. Hurst, "Space Shuttle SRB Axial Growth Comparison Static Fire Configuration vs Flight Simulation," 21 July 1986.

Note how the length change depends on both the axial and circumferential loading through the Poisson's ratio term in equation (1). Since the hoop load is typically two to three times the axial load in a rocket motor chamber (compared with a closed tank where the load ratio is 2:1), the axial length change must always include the biaxial effects. The fact that the  $N_2/N_1$  ratio is two for a closed tank leads to the observation that the length growth will be significantly influenced by the Poisson's ratio. In a rocket motor where  $N_2/N_1$  is greater than 2, the influence of the Poisson's ratio is greater than in a closed tank. For example, at  $N_2/N_1 = 3$  then a Poisson's ratio of  $1/3$  would result in zero elongation of the case. Similarly, when a closed tank is examined, zero elongation would only be obtained when Poisson's ratio is  $1/2$ .

The D6AC material has a Poisson's ratio of 0.286 while the Block II MART250 steel has a Poisson's ratio of 0.31. These data are very important in meeting the length growth requirement because the working stress will be increased and the modulus decreased, which will amplify strains by about 35 percent. The increase of Poisson's ratio of 8 percent with the 2.5:1 typical load ratio in the Space Shuttle static test motor gives a 22 percent reduction in displacement that adds to the 25 percent reduction due to the joint elimination to predict an expected net 17 percent reduction of  $\Delta L$  for the Block II SRM. Without the change of material the axial growth would be slightly less than in the RSRM because of the larger pin size and the joint stress reduction. The membrane deflection would not change because the working stress does not change. Consequently, the axial growth of the D6AC steel case at the Block II MEOP would be a few percent less than the axial growth of the RSRM.

The important conclusion of this evaluation is that the Block II case and alternate designs will exhibit less axial growth than the current HPM.

### 3.3.6 ALTERNATE DESIGN SELECTIONS

As backup design options to the key features of the recommended design, D6AC steel is recommended in a segmented case. Also recommended is to retain the

segment lengths of the HPM case with mechanically joined case segments forming the casting segments. The backup design provides proven materials and fabrication methods but reduces the structural efficiency.

In addition to the backup design alternates, a concept is presented to integrate the skirt attach ring into the case design with a bolted, face-sealed, aft case segment-to-aft closure joint.

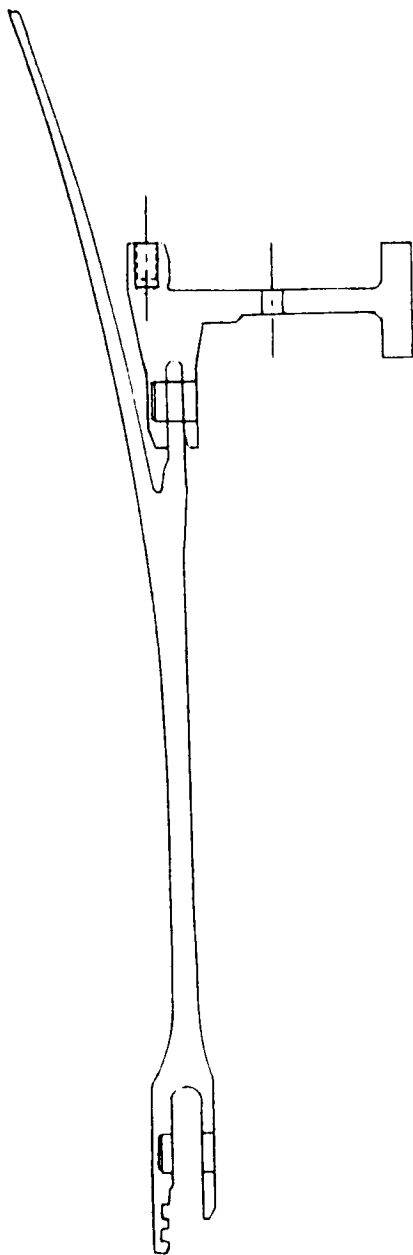
#### **3.3.6.1 Material Backup**

As a conservative backup, the D6AC steel can be used for the Block II case. The low-alloy case would be substantially heavier than the MAR-T250 steel because the case segment length would be limited by the quench requirements. The higher MEOP of the Block II design would cause the case weight to increase by about 10 percent over the HPM case, or increase by about 20 percent over the Block II baseline. The D6AC case would retain the weld-free case design of the HPM and would require using the bolted fixed housing-to-case aft closure.

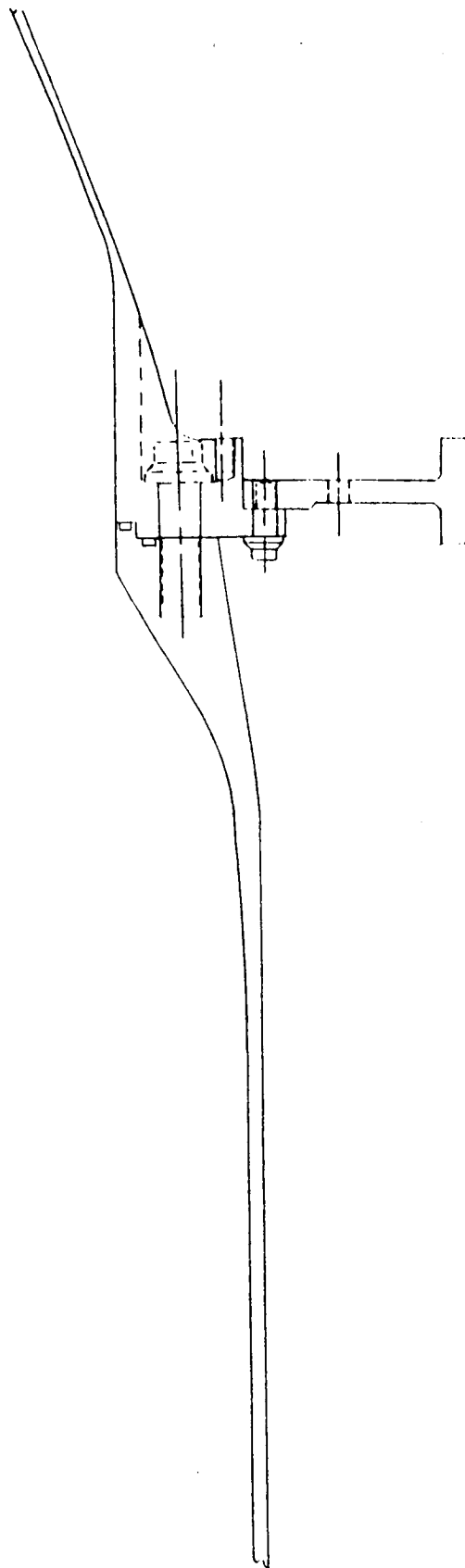
#### **3.3.6.2 Integral Kick Ring, Skirt Attach, And Case Joint**

One concept that emerged during the Block II study was the possibility of combining the functions of the kick ring, skirt attach ring, and case-to-dome joint into a single design feature of the case. The present configuration is compared to the proposed concept in Figure 21. Analysis results for this integrated joint are shown in Figure 22.

This design shows merit over the Block II baseline but does not conform to the interface requirements of the CEI specification. Since this involves components that are beyond the range of the case assembly it is simply presented as a feasible idea, but will not become a part of the Block II case without the coordination of the MSFC.

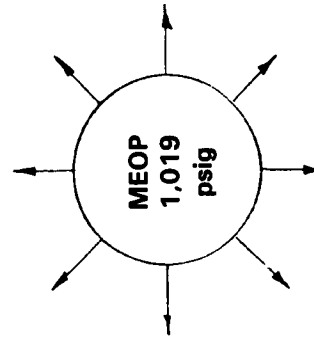
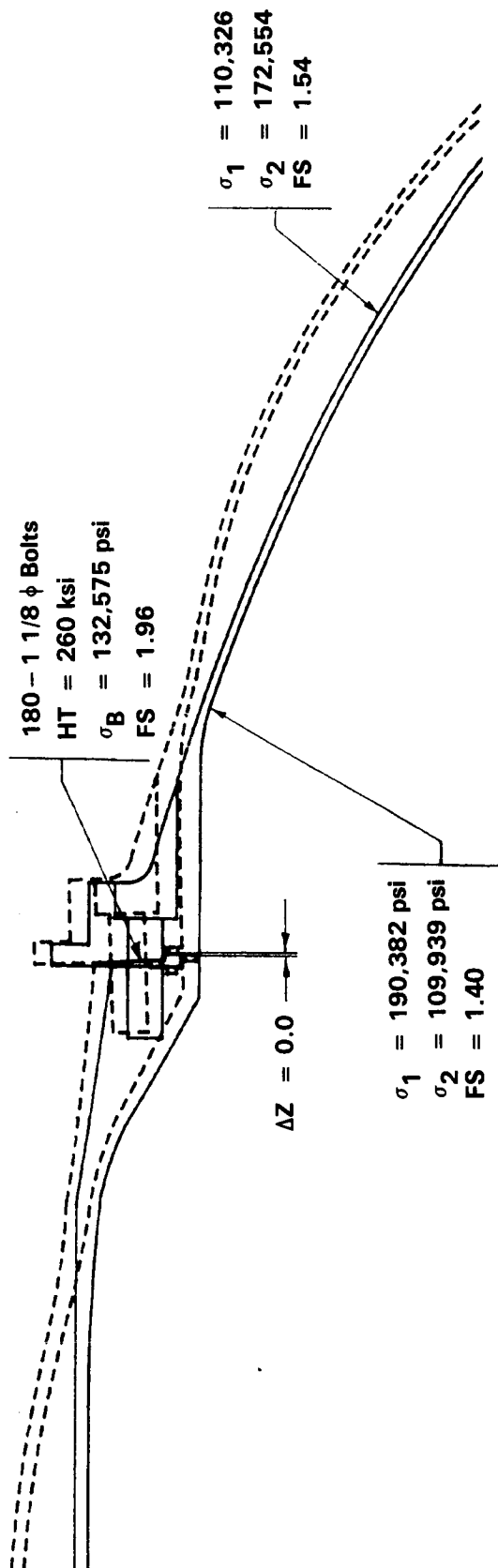


EXISTING SKIRT ATTACH RING DETAIL



SUGGESTED DESIGN

Figure 21. Concept for Integrating Skirt Attach and Joint



87354-9C

Figure 22. Alternate Case-to-Aft Dome Joint

### 3.4 JOINT DESIGN

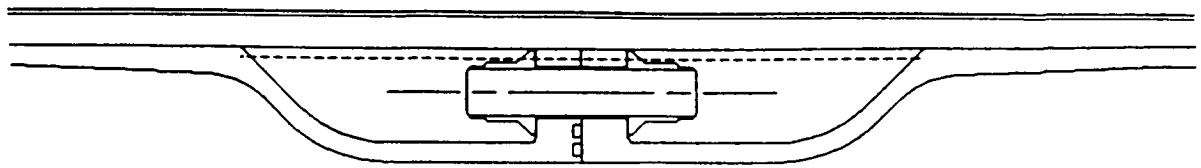
Development of a capable and reliable segmented SRM design revolves around the ability to design an intersegment joint insensitive to flight loading and environments. Pursuant to this goal a variety of case field joints were evaluated. Of these designs, four designs were determined to have sufficient merit for detailed consideration (Figure 23). These four designs include:

- a. Double-recess bolted joint (originally developed by NASA Langley Research Center). This joint features face seals in a bolted configuration. The joint is offset from the membrane line of action to insure that all seal gaps remain closed.
- b. Inclined bolted joint. A bolted joint which incorporates both face and bore seals.
- c. Single-recess bolted joint. This joint has all the advantages of the double-recess bolted joint plus the added advantage of higher structural margins of safety.
- d. Modified pin-clevis joint (hereafter referred to as Block II clevis joint). Though similar to the RSRM configuration, there are two important improvements. One, the joint is sized to use larger diameter pins resulting in reduced stresses/strains around the pin holes. Two, the joint is offset from the membrane line of action resulting in a reduction of seal gap growth. For elimination of seal gap growth the filament wound overwrap was included in the comparison as a modification to the Block II clevis joint.

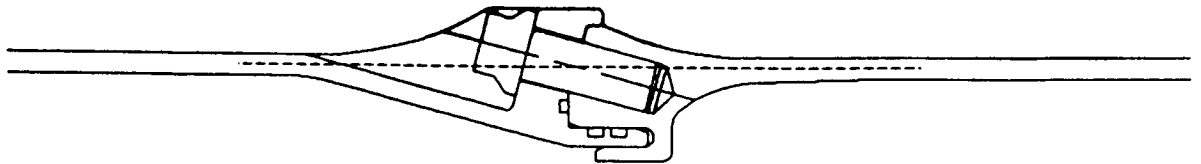
Each joint was sized using 2-D axisymmetric analyses and assuming an MEOP of 1,100 psi and material properties for MAR-T250 steel. The joints were traded based on the following criteria:

- a. Seal performance (gap growth under pressurization and flight loads)
- b. Structural adequacy
- c. Motor performance based on internal volume changes and inert weight effects
- d. Ability to manufacture and assemble

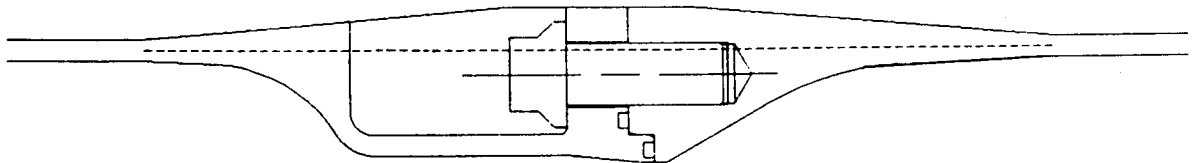
Analyses results showed that all Block II joint designs control seal gap growth within acceptable limits (see Table 17). Analysis of the Block II clevis joint predicts better seal gap performance than currently attained by the RSRM baseline joint. Studies by the SRM redesign team indicate that the clevis seal



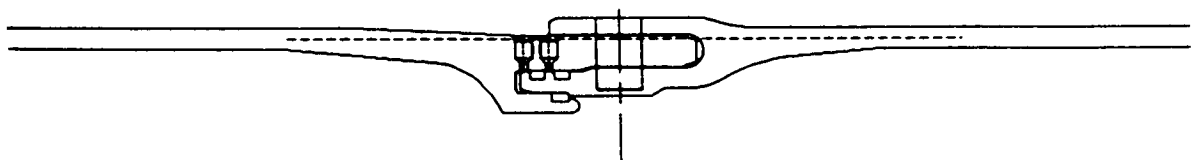
**Double Recess Bolted**



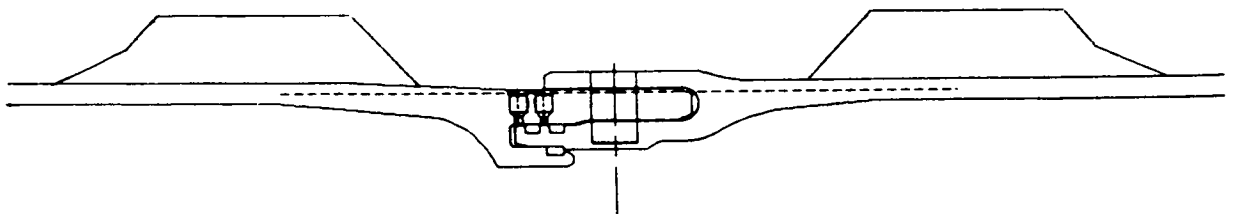
**Inclined Bolted**



**Single Recess Bolted**



**Block II SRM Clevis**



**Block II SRM Clevis  
With Overwrap Stiffeners**

87354-10G

**Figure 23. Case Field Joint Concepts**



Table 17. Block II SRM Joint Trade Study

	Units	HPM*	RSRM Baseline*	Block II Clevis**	with optional Overwrap	Inclined Bolted**	Double Recess Bolted**	Single Recess Bolted**
Weight Delta Over Cylinder***	(lb) per joint	730	794	1,176	2,276	1,643	1,859	2,031
Internal Volume Displacement	(cu in.) per joint	1,788	2,745	4,173	4,173	5,114	15,311	7,700
Weight of Displaced Propellant	(lb) per joint	113	173	263	263	322	965	485
Seal Gap Growth Primary Secondary Tertiary Capture Feature	(in.)	0.034 (B) 0.030 (B) NA NA	0.007 (B) 0.009 (B) NA 0.000 (B)	0.006 (B) 0.006 (B) NA 0.000 (B)	0.000 (B) 0.000 (B) NA 0.000 (B)	0.008 (B) 0.006 (B) 0.000 (F) NA	0.000 (F) 0.000 (F) NA NA	0.000 (F) 0.000 (F) NA NA
Payload Reduction Per Joint + Inert Weight Propellant Loss Total	(lb)	133 10 143	145 14 159	214 22 236	414 22 436	299 27 326	358 20 413	371 40 411

Notes: \*Designed for MEOP = 1,004 psig; D6AC steel

\*\*Designed for MEOP = 1,100 psig; MAR-T250 steel

\*\*\*Metal parts only

+Used heads up exchange ratios

(B) = Bore seal

(F) = Face seal

gap opening could be completely eliminated in this joint by the addition of overwrap stiffeners. Both the single- and double-recess bolted joint face seals remain closed under pressure loads. The bore seal gaps of the inclined bolted joint open under pressure loads, but less than the RSRM baseline joint, while the face seal gap remains closed.

The structural adequacy of each joint was determined by using 2-D axisymmetric finite element analysis. Margins of safety are based on the maximum normal stress theory. Of all the considered joints, the Block II clevis joint is the most efficient and predictable. This joint demonstrates good margins of safety and yet is the lightest of the joints considered. The single-recess bolted joint also demonstrates good margins of safety but is the heaviest of the joints. Analysis of both the double-recess and inclined bolted joints predicts high levels of stress while the joints are relatively heavy.

The effect of each joint on the motor's performance was evaluated based on the increase in inert weight over a continuous cylinder weight and the displaced volume of propellant. It is noted that less propellant is displaced at the field joint locations than at the factory joint locations. This is less true for the recessed bolt designs because of the increased length of the joint. A performance penalty for both inert weight gain and propellant displaced is calculated using the following heads-up exchange ratios:

- -0.182-lbm payload/lbm inert case.
- 0.083 lbm payload/lbm propellant

The weight/performance penalty is compared on a per joint basis (see Table 17). The Block II clevis joint provides the lowest payload reduction or highest performance with the inert weight being the most significant factor.

Manufacturing and assembly procedures appear to be much more simple and predictable for the Block II clevis joint than for the bolted joints. The bolted joint designs will be difficult to assemble, particularly in the horizontal position which is required for motor static testing because the face seals will

be extremely difficult to keep in position. The vertical assembly and breakover for static test is not within current facility capability nor has this been demonstrated.

Based on performance, structural integrity, and ease of manufacturing and assembly, the Block II clevis joint is preferred over the bolted configurations. Since the Block II clevis joint proposes a capture feature seal which always remains in contact, and two backup seals that are predictable in their response, sealing reliability is fully assured. For these reasons, the Block II clevis joint is selected as the proposed Block II SRM joint with either the single-recessed bolted joint or the Block II clevis joint with overwrap stiffeners as favorable alternatives.

Of the nozzle fixed housing-to-aft dome joints that were studied, a welded joint option was finally selected as the proposed baseline for the Block II SRM (Figure 24). The use of a welded fixed housing-to-aft dome joint presupposes the existence of a factory assembled joint at the case cylinder-to-aft dome junction. The proposed alternative joint is the bolted concept featuring an interference sealing surface, ensuring no initial seal gap. It also has a capture feature to minimize the seal gap growth and to prevent sudden gap deflections or skip.

The igniter attachment and seal provisions are described in Section 3.10.

### **3.4.1 OBJECTIVE/SCOPE**

The primary objective of this study was to determine a case joint design, for a segmented Block II SRM design, which would be insensitive to flight loading and environments, and maintain its structural and seal integrity.

To find the optimum joint, a variety of joint configurations were considered. These joints were evaluated based on attributes related to:

- a. Redundant and verifiable seals
- b. Seal gap control
- c. Structural capability
- d. Producibility

- e. Reuse potential
- f. Assembly ease and leak check verification (checking two seals in the sealing direction)
- g. Handling ease
- h. Performance
- i. Cost

Four designs, as discussed earlier, were selected for detailed studies. These joint designs were sized based on the MAR-T250 steel case material properties using hand analyses. Detailed 2-D axisymmetric finite element analyses were performed on each joint configuration to predict deflections and stress levels under combined pressure and axial loading. An internal pressure of 1,100 psi, and an axial load of  $Pr/2$  lb/in. was applied to each model. Bolted joint models included a bolt preload of 60 percent of the bolt tensile capacity. Twenty inches of cylinder were modeled on either side of the joint buildup to dampen out the discontinuity bending. An effort was made to optimize each of the joints analyzed. Subsequent to joint optimization each joint was evaluated on motor performance loss.

### 3.4.2 BLOCK II CLEVIS JOINT

Design of a clevis type joint for Block II SRM centered around improving the RSRM clevis joint without requiring the design to mate with existing hardware. Some design changes were required to meet the increased Block II performance requirements, specifically an increase of MEOP from 1,004 to 1,100 psi. The design goals of the Block II clevis joint were as follows:

- Demonstrate better margins of safety at 1,100 psi than the RSRM joint at 1,004 psi
- Reduce plastic deformation in the joint pinhole regions
- Minimize the seal gap response

Structural predictions were determined using 2-D axisymmetric linear finite element analysis. Previous experience of the SRM redesign team verifies this type of analysis will give good gap predictions. The trends in stress and strain predictions will accurately be depicted and are sufficient for comparative

ORIGINAL PAGE IS  
OF POOR QUALITY

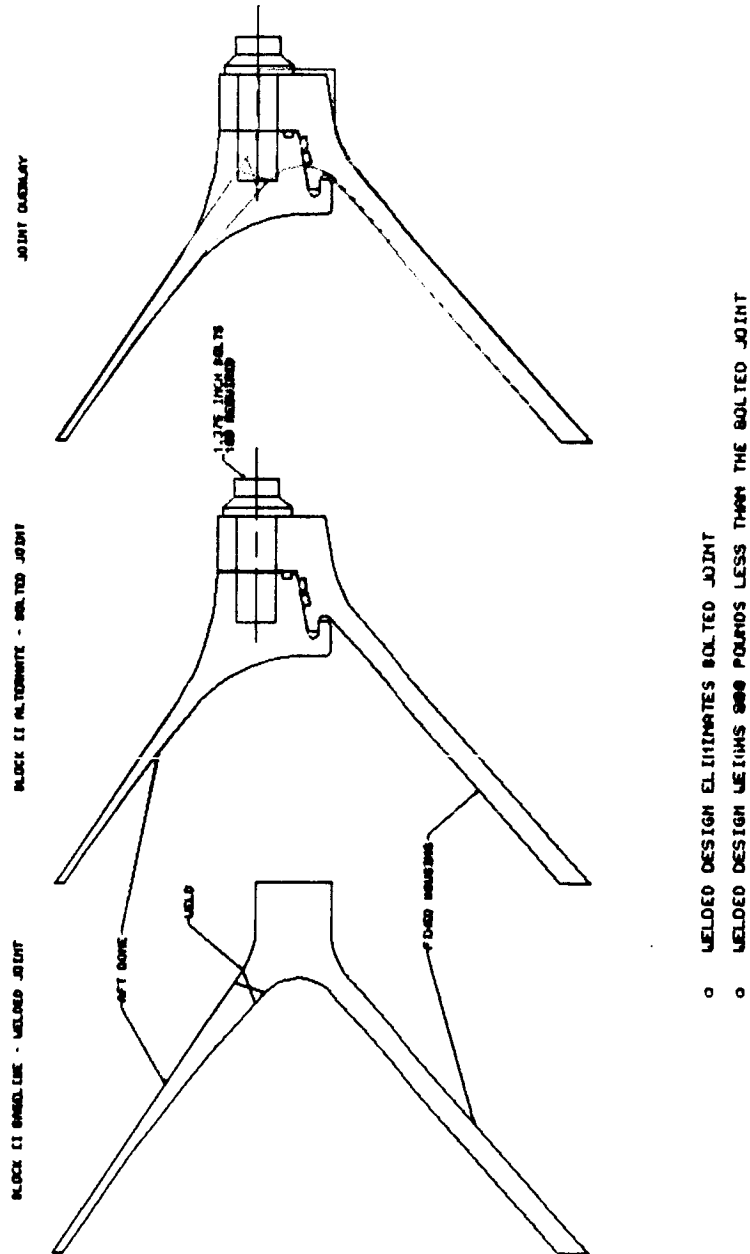


Figure 24. Fixed Housing-to-Aft Dome Connections

studies. However, because the joint is not axisymmetric, precise predictions of stress and strain in the pinhole regions can only be obtained using 3-D nonlinear finite element techniques.

Structural analysis of the Block II clevis joint predicts higher margins of safety than predicted in the RSRM joint. Increasing the thicknesses of the clevis legs and the tang resulted in lower stress predictions (see Table 18). Stresses were further reduced by increasing the pin diameter to 1.125-inch. In spite of the increase in MEOP (1,004 to 1,100 psi), the stresses are less than those experienced by the RSRM clevis joint. The plastic action currently observed in the existing HPM hardware will also be reduced by the reduction in stress and also by trading the current material (D6AC) for a higher strength material (MAR-T250) with a 33 percent higher yield strength. The Block II joint stresses at 1,100 psig are shown in Figure 25. The comparison of pin stresses between the RSRM and the Block II joint configuration are also shown in this figure.

Seal gap opening is minimized by offsetting the joint inward from the membrane line of action by 0.25 inch. Most of the gap deflection is due to bending at the joint under pressure loads. Offsetting the joint creates an opposite bending effect under axial tension loads, thus reducing the gap opening. Predicted clevis seal gap openings of 0.0059 and 0.0060 in. at 1,100 psi are smaller than 0.0067 and 0.0091 in. for the RSRM design at 1,004 psi. The capture feature seal remains closed for all pressure loads. The differences between the RSRM and the Block II clevis are illustrated in Figure 26. The joint offset can be seen more clearly in Figure 25 where the dashed line indicates the membrane line of action.

A parametric study was performed to find the optimal joint offset using a preliminary Block II joint design. The results of this study, which are summarized in Table 19, indicate that gap opening is reduced as the joint is moved inward. Too much inward offset begins to cause stress problems and thus limits the amount of offset that can practically be enforced. An offset of 0.25 in. produces good reductions in both the gap opening and stress values; therefore, this amount of offset was incorporated in the Block II clevis joint.

Table 18. Block II Clevis Joint Stress Study

Increase in Inner Clevis Leg Thickness	Critical Stresses (ksi)				
	Max Eff	Max Axial (tang)	Max Axial (clevis)	Max Axial (pin)	Max Hoop (tang)
<u>RSRM*</u>					
0.00 (in.)	162.4	141.1	138.9	190.1	121.4
<u>Preliminary Block II*</u>					
0.00 (in.)	176.5	134.5	161.0	135.6	113.2
0.06	158.6	125.8	140.1	136.4	112.9
0.12	143.1	124.3	121.7	132.7	112.9
<u>Baseline Block II**</u>					
0.12 (in.)	130.0	110.2	95.6	123.1	117.2

\*Assumed 1,004 psi internal pressure

\*\*Assumed 1,100 psi internal pressure

Table 19. Block II Clevis Joint Offset Study

Line of Action Offset	Gap Opening at		Critical Stress Max SIGE <sup>†</sup> (ksi)	Pin Stress Ratio*** Outer/Inner
	First Clevis Seal	Second Clevis Seal		
<u>RSRM*</u>	0.0067	0.0091	162.4	0.62
<u>Preliminary Block II*</u>				
0.00	0.0060	0.0063	143.1	0.56
0.25	0.0054	0.0055	123.4	0.69
0.50	0.0050	0.0052	154.1	0.70
<u>Baseline Block II**</u>				
0.25	0.0059	0.0060	130.0	0.72

\*Assumed 1,004 psi internal pressure

\*\*Assumed 1,100 psi internal pressure

\*\*\*A ratio of 1.0 indicates balanced pin stresses

<sup>†</sup>Von Mises equivalent stress

Material: MAR-T250 Steel

$F_{tu} = 250 \text{ ksi}$

$F_{ty} = 240 \text{ ksi}$

$\sigma_1 = \text{Max In-Plane Stress}$

$\sigma_2 = \text{Hoop Stress}$

$\sigma_{vm} = \text{Von Mises Stress}$

Block II Joint

177 — 1 1/8 Pins

$\sigma_{BR} = 132.3 \text{ ksi}$

$\tau_s = 77.9 \text{ ksi}$

FS = 1.86

RSRM Joint at 1,004 psig

177 — 1.0 Pins

154.3 ksi

93.5 ksi

FS = 1.55

$\sigma_2 = 92.9 \text{ ksi}$

$\sigma_1 = 119.1 \text{ ksi}$   
FS = 2.09

Gap Opening = 0.0059 in.

Gap Opening = 0.0060 in.

$\sigma_{vm} = 135.2 \text{ ksi}$

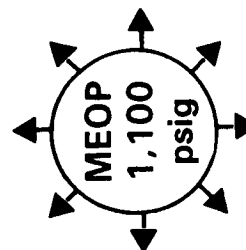
$\sigma_1 = 98.6 \text{ ksi}$

FS = 1.84

$\sigma_2 = 129.0 \text{ ksi}$

FS = 1.93

$\sigma_2 = 90.0 \text{ ksi}$



A004041

Figure 25. Block II SRM Clevis Joint



Important advantages of the clevis joint concept include: 1) ease of manufacturing, 2) ease of assembly, and 3) reusability. Each of these advantages has been **demonstrated** in current Shuttle hardware. Joint dimensions can be turned to within very tight tolerances. Assembly in both vertical and horizontal configurations is made easy since the clevis is a natural guide for the tang. Reusability of a clevis/tang joint has been **demonstrated** via tests and actual refurbishment of SRM flight hardware. The improvements proposed in the Block II clevis joint preserve these advantages and further increase the reusability of the hardware.

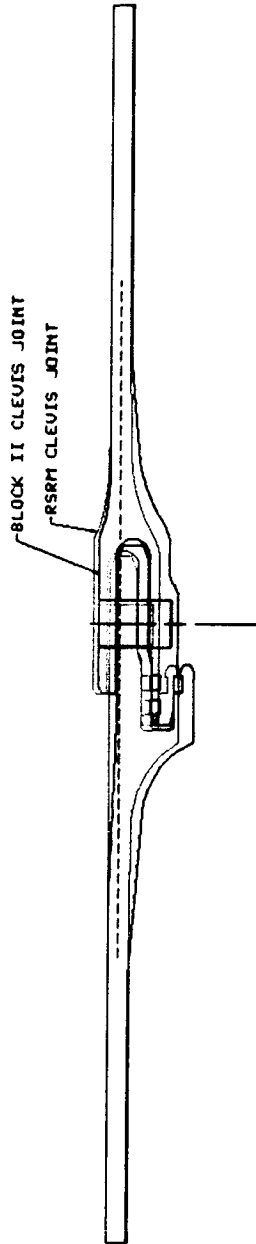
In summary, the proposed Block II clevis joint is a more robust version of the RSRM design. Joint dimensions are strategically increased and a higher strength steel is specified. The joint is offset from the membrane line of action to reduce the gap openings. The joint has improved structural safety factors and seal gap control while servicing 10 percent higher pressure loads.

Based on its high degree of structural integrity, reliable sealing mechanism, and acceptable weight increase the Block II clevis joint design is recommended as the baseline for the Block II SRM.

Optional Overwrap Stiffeners. An overwrap stiffener concept has been studied which, when added to a clevis/tang joint, will effectively prevent gap growth under pressure loads. Because the bore seal surfaces generally have an initial gap, the intent of the overwrap is to prevent that gap from changing throughout the entire operating pressure range. This technology, though developed on the HPM and RSRM clevis joints, applies directly to the proposed Block II clevis joint as well.

Stiffeners are typically made of composite material rather than steel because of the composite stiffness to-weight-ratio. The composite stiffener can be wound directly onto the case or fastened as a removable bolt-on feature. Overwrap test results from the RSRM redesign effort successfully demonstrated the effectiveness of this concept (Figure 27).

ORIGINAL PAGE IS  
OF POOR QUALITY



- o CHANGES
- o LINE OF ACTION MOVED
- o PIN DIAMETER INCREASED TO 1.125 IN.
- o TANG LENGTH AND THICKNESS INCREASED
- o CLEVIS LEGS THICKENED
- o PIN ENGAGEMENT INCREASED

	GAP OPENING 1ST SEAL	2ND SEAL	CRITICAL STRESS (KSI)	PIN STRESS RATIO (KSI)	MEOP (PSIG)
RSRM	0.0067	0.0091	162.4	0.62	1004
BLOCK II	0.0059	0.0068	130.0	0.72	1100

Figure 26. Overlay of Block II SRM Clevis Joint  
and RSRM Baseline Joint

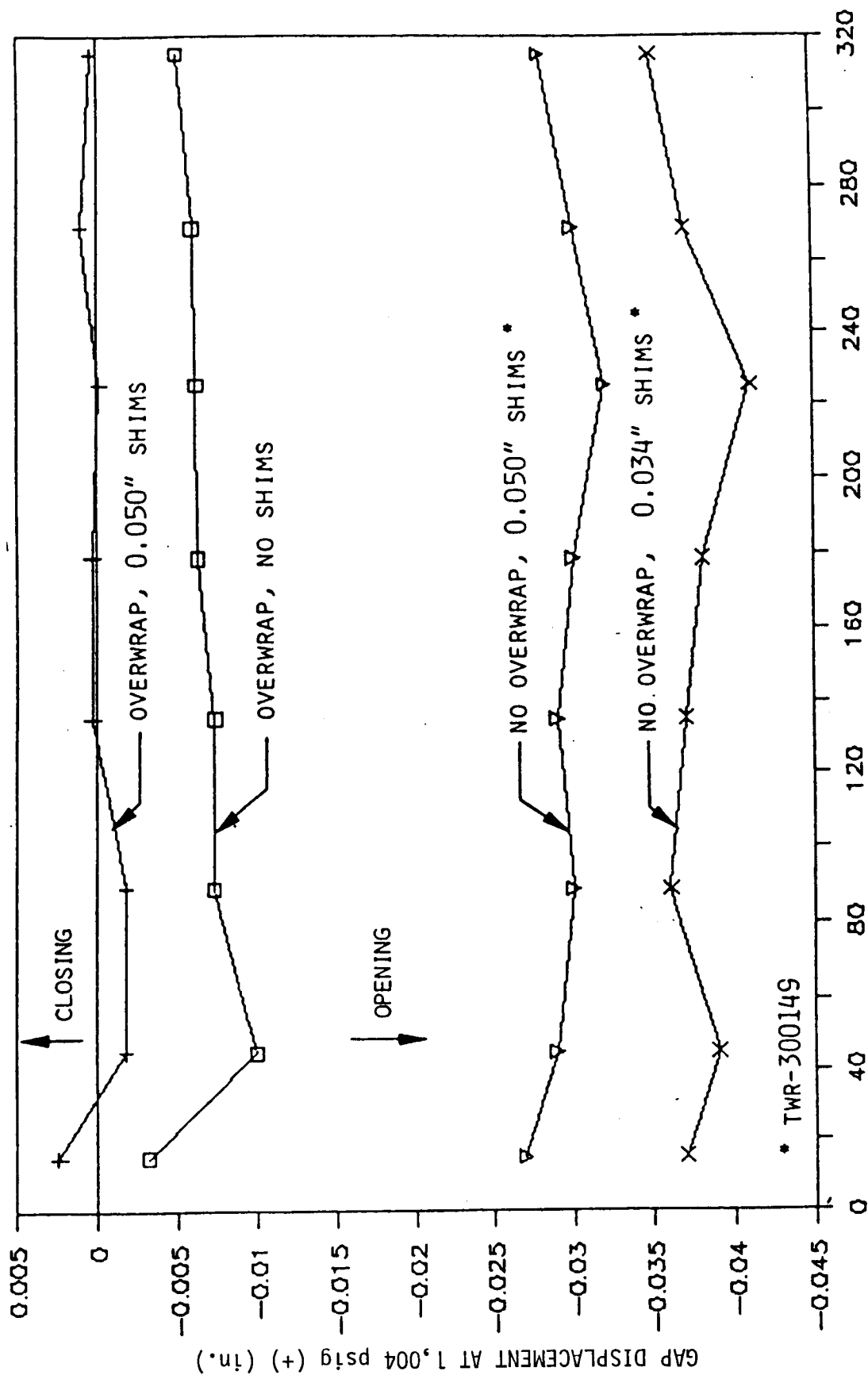


Figure 27. Comparison of Gap Motion Between Two SRM Referee Tests (with and without composite overwrap rings)

The main disadvantage of using overwraps with the clevis joint is the substantial weight/performance penalty (see Table 17). The combined clevis with overwraps suffers the greatest performance reduction of all the joint designs considered.

In light of these studies, the proposed Block II clevis joint combined with overwraps would make a very predictable alternative design. Aside from the weight/performance penalty, all of the advantages of the clevis joint are preserved. Should design limitations require that all seal gaps remain neutral during pressurization, then this joint configuration should be considered as an alternative design.

### **3.4.3 DOUBLE-RECESS BOLTED JOINT**

The double-recess bolted joint is a unique bolted joint originally proposed by personnel from NASA-Langley. Two face seals are used to achieve redundant and verifiable sealing. Both mating halves of the joint have clearance bolt holes. Joining is achieved with one-hundred forty-four 1.129-in.-diameter MP35N studs inserted through the clearance holes with nuts installed on both ends (Figure 28).

The strength of this design is clearly the predictability of the face seal concept. Milled recesses move the bolt circle to a smaller diameter than the membrane line of action. This offset introduces a moment due to line load which offsets the moment due to pressure and hoop discontinuity at the joint. The result is that seal gap surfaces, which are initially in contact, remain in contact for all pressurization loads.

The sealing concept is the major advantage of this design. Structurally, this design transfers all loads through the bolts as axial stress. From a failure standpoint it is generally better to transfer loads through bolts in shear, as in the clevis joint. Block II studies indicated high stresses in the webs between recesses, in the bolts, and high hoop stresses in the flanges containing the clearance bolt holes. Note that the seal gap remains closed under pressure. The 146.8-ksi hoop stress in the flange does not reflect the stress concentration effects around the holes since this is only a two-dimensional analysis. However, a stress concentration factor of about 2.0 is typical around

Material: MAR-T250 Steel

$F_{tu} = 250 \text{ ksi}$

$F_{ty} = 240 \text{ ksi}$

$\sigma_1 = \text{Max In-Plane Stress}$

$\sigma_2 = \text{Hoop Stress}$

144—1 1/8 Studs

HT = 260 ksi

$\sigma_B = 219.8 \text{ ksi}$

FS = 1.18

$\sigma_1 = 183.3 \text{ ksi}$

FS = 1.36

$\sigma_2 = 146.8 \text{ ksi}$

$\sigma_1 = 27.5 \text{ ksi}$

$\sigma_2 = 150.5 \text{ ksi}$

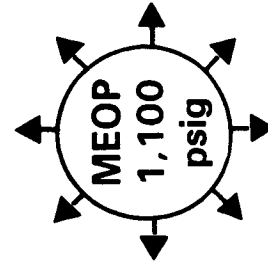
FS = 1.66

Gap Opening = 0.0 in.

$\sigma_1 = 143.3 \text{ ksi}$

$\sigma_2 = 139.4 \text{ ksi}$

FS = 1.74



A004043

Figure 28. Double Recess Bolted Joint

this type of hole. Detailed studies conducted by NASA-Langley indicate that the web stresses and bolt stresses can be reduced to acceptable levels; however, their analyses still show the high flange hoop stresses and subsequent stress concentrations around the holes. Stresses in the flange could be reduced by increasing flange thickness but this both reduces bolt stiffness and increases joint hoop discontinuity. Both of these would tend to increase joint opening.

It has not yet been determined how this joint would successfully be assembled, particularly in the horizontal position. It appears difficult because loaded case segments will not be round in a horizontal position and the forces required to mate two segments can be a problem. There is no obvious method for joining two segments, a process which is inherently simple with the clevis/tang concept. The handling and assembly of segments with this joint would be difficult.

Due to the milled recess at each bolt hole, this joint is more difficult to manufacture than the clevis/tang joint. This joint also suffers from relatively high inert weight, thus reducing the overall motor performance (Table 17).

In summary, the double-recess bolted joint should have predictable seal gap response; however, it poses structural, manufacturing, and handling problems that the clevis joint does not have. A much more detailed study of this joint is required before it can be properly developed as an alternative Block II design concept.

#### **3.4.4 SINGLE-RECESS BOLTED JOINT**

The single-recess bolted joint (Figure 29) is a variation of the double-recess bolted joint which mates a clearance hole on the top segment with a tapped hole on the bottom segment. One-hundred forty-four 1.25-in.-diameter MP35N bolts are used to secure the segments. This joint is the heaviest of the four joints studied in detail but displaces half as much propellant as the double-recessed design. The design has two face seals to meet the redundant and verifiable seal requirement. The seals are located on two different sealing surfaces to preclude the probability that one flaw on either joint surface could cross both seals.

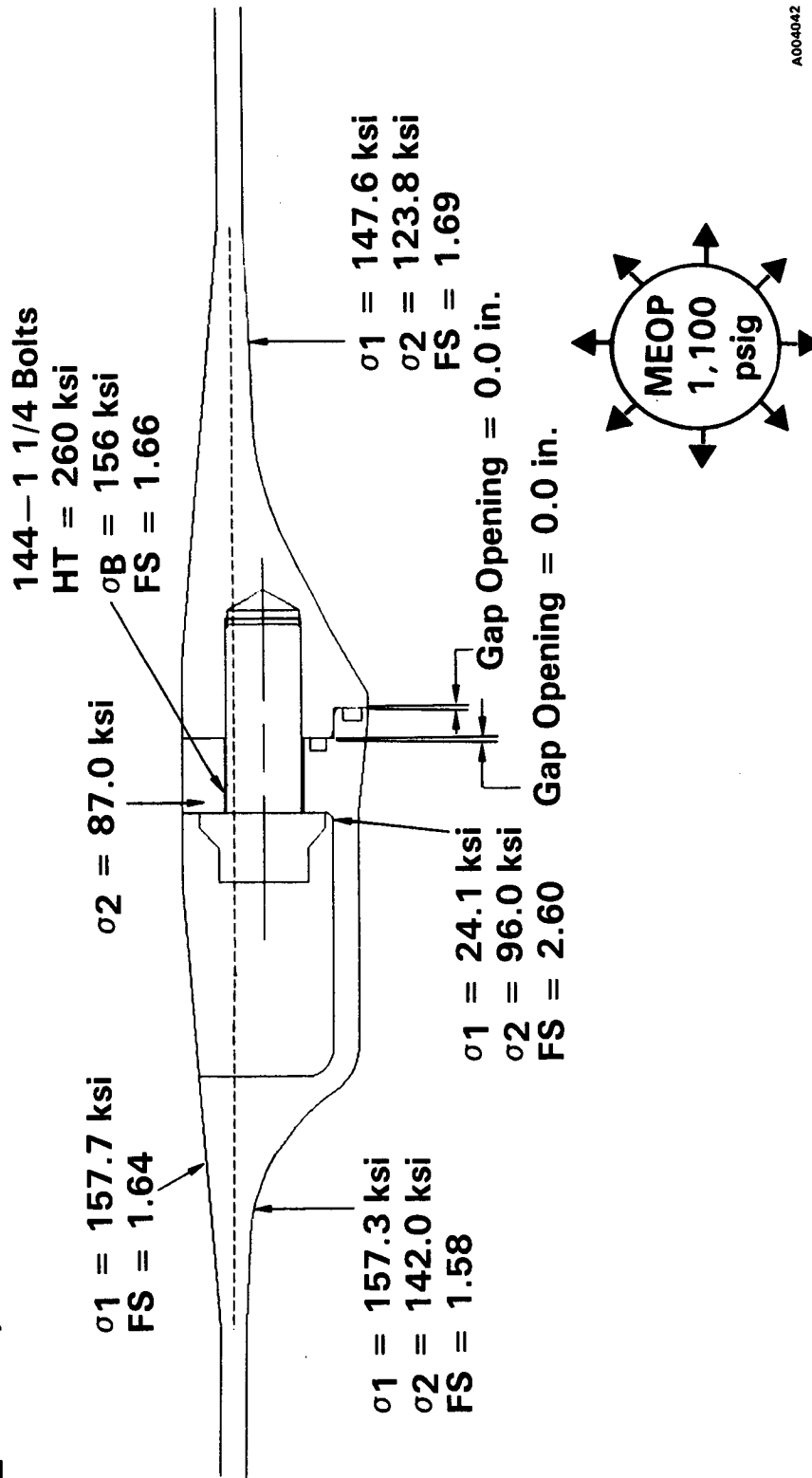
**Material: MAR-T250 Steel**

**$F_{tu} = 250$  ksi**

**$F_{ty} = 240$  ksi**

**$\sigma_1 = \text{Max In-Plane Stress}$**

**$\sigma_2 = \text{Hoop Stress}$**



A004042

Figure 29. Single Recess Bolted Joint

Though similar to the double-recess bolted joint, the single-recess design performs better structurally because of the increase in material resulting in reduced hoop stress. Analysis results are summarized in Figure 29. All factors of safety are well above the required 1.40, including the bolt factors of safety.

The offset of the bolt line from the membrane line of action prevents seal gaps from opening under pressure. Sealing attributes are similar to those of the double-recess joint. Basic hoop stress near the holes was 87.0 ksi (not including stress concentration effects), which has the lowest of all four designs analyzed.

The introduction of tapped holes to the design may raise concerns about reusability. However, refurbishment of tapped holes has been demonstrated on the current SRM in the aft dome segment where threaded holes are successfully repaired by using or replacing threaded helical inserts.

In summary, the single-recess bolted design has all the advantages of the double-recess design while demonstrating better structural integrity. The single-recess bolted concept could be considered as an alternative Block II design.

### **3.4.5 INCLINED BOLTED JOINT**

In an attempt to design a bolted configuration which minimizes inert weight and loss of propellant volume, the inclined bolt joint concept was developed. This design (Figure 30) uses one-hundred sixty 1.25-in.-diameter MP35N bolts on a 15-deg incline to fasten the case segments together. The incline allows the bolt circle to be at the membrane line of action diameter without requiring a milled recess for bolt installation. Redundant sealing is achieved with two bore seals and one face seal. Verification in the proper sealing direction is obtained for one bore seal and the face seal. Deflections of the bore seals are controlled with a capture feature which mechanically forces the seals to follow the sealing surface throughout pressurization. Shear in the bolts is controlled with a shear lip on the joint outside diameter. Reusability of this design will be similar to that of the single-recess bolted joint.



Material: MAR-T250 Steel

$F_{tu} = 250 \text{ ksi}$

$F_{ty} = 240 \text{ ksi}$

$\sigma_1 = \text{Max In-Plane Stress}$

$\sigma_2 = \text{Hoop Stress}$

$\sigma_1 = 129.1 \text{ ksi}$   
 $FS = 1.93$

$\sigma_2 = 89.8 \text{ ksi}$

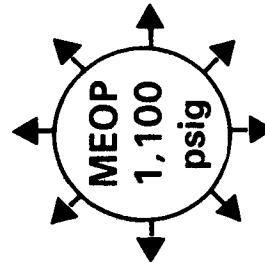
160-1 1/4 Bolts  
 $HT = 260 \text{ ksi}$   
 $\sigma_B = 201.3 \text{ ksi}$   
 $FS = 1.29$

$\sigma_1 = 154.1 \text{ ksi}$   
 $\sigma_2 = 139.5 \text{ ksi}$   
 $FS = 1.62$

$\sigma_1 = 140.5 \text{ ksi}$   
 $\sigma_2 = 113.4 \text{ ksi}$   
 $FS = 1.77$

Gap Opening = 0.0076 in.

Gap Opening = 0.0 in.



A00-6040

Figure 30. Inclined Bolted Joint

Figure 30 summarizes the analysis results for the inclined bolted joint. Note that all factors of safety are in excess of the required 1.40 except for the bolts. The high bolt stresses are a result of the bolt incline which introduces double curvature bending into the bolt. More or larger bolts could be installed but this would reduce the material left between bolts below acceptable levels. Under pressure the face seal gap remains at zero while the bore seals open up slightly (0.006 and 0.008-in.). The basic hoop stress around the holes is 89.8 ksi (not including stress concentration effects), which is much lower than for the double-recess bolted joint. The inclined bolted joint has the lowest weight impact of the bolted joints considered but was not selected for the Block II SRM due to high bolt stresses.

#### **3.4.6 NOZZLE FIXED HOUSING-TO-CASE AFT DOME JOINT**

The Block II SRM design proposes a clevis joint near the cylinder-to-aft dome transition that is assembled after casting the propellant grain in the aft segment. This allows inert assembly of the nozzle-to-aft closure, followed by live assembly of the clevis joint in the aft case segment prior to shipping the aft segment. The aft casting segment, as delivered to the launch site, is thus the same as that currently delivered for the HPM.

The factory assembly sequence is altered and special tooling is required for casting the aft segment but launch site assembly operations are not changed. The forward nozzle subassembly is attached to the aft closure when shipped.

This concept allows trading a bolted fixed housing-to-aft dome joint for a welded, enlarged aft closure that includes a short cylinder, the Y-joint and skirt attach strut, the aft dome, and the fixed housing. This moves the nozzle-attachment interface to the flex bearing aft end ring instead of the previous dome-to-fixed housing interface. The nozzle attachment is achieved by the same procedure currently used for assembly of the fixed housing-to-aft end ring in the HPM nozzle.

Changing from a bolted joint to a welded juncture not only eliminates complex sealing problems, but also reduces the inert weight and increases the motor performance. Consequently, the trade study concluded that the lightest,

most reliable design is obtained by replacing the bolted fixed housing-to-aft dome joint with a girth weld and a reinforcing ring at the cone-to-sphere juncture. These designs were compared in Figure 24 in the introduction. In this section the analysis and trade study results are presented for the two designs.

The welded baseline concept design analysis is summarized in Figure 31. This shows the greatly exaggerated deformation and the location and magnitude of the maximum stresses in each of the design elements.

The analysis summary of an alternative bolted concept is presented in Figure 32. The objective of this bolted joint design study was to:

- Minimize joint opening at seal locations
- Provide redundant and verifiable seals
- Isolate joint from the flow environment
- Provide positive alignment for the nozzle assembly

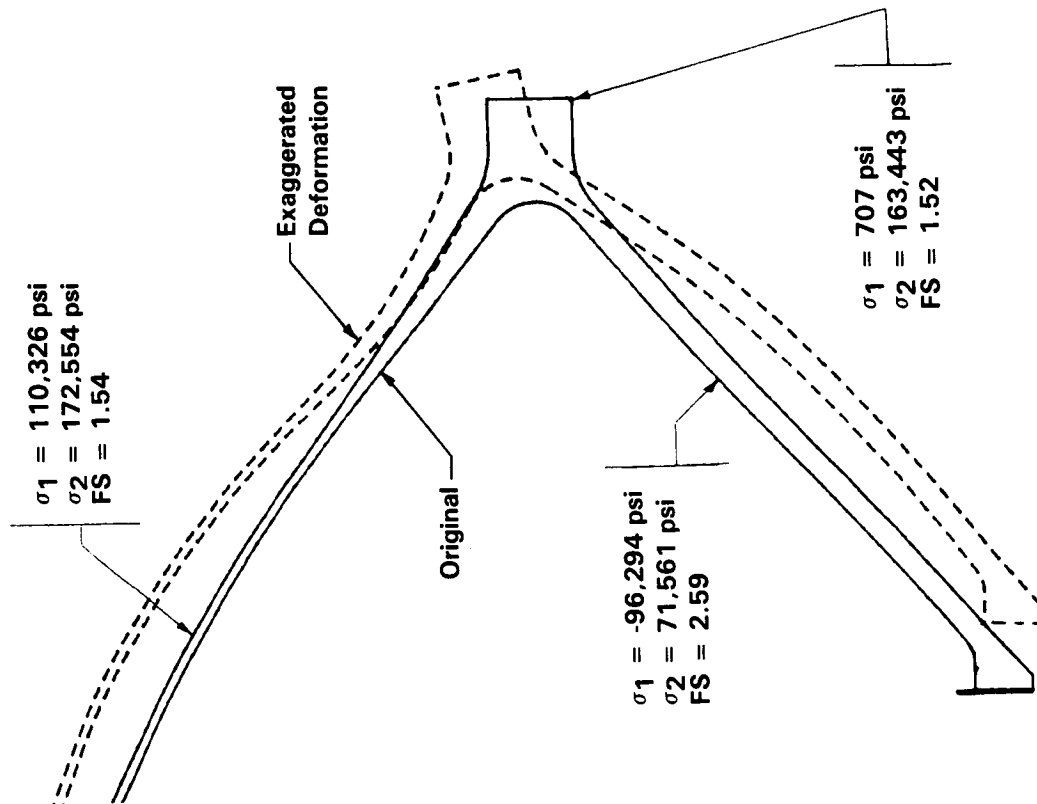
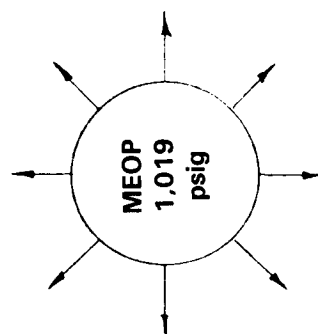
This alternative bolted configuration for the Block II SRM aft closure-to-nozzle fixed housing joint would be assembled and insulated as a single component prior to mating with the forward nozzle section. The nozzle and dome assembly would be attached to the cylindrical aft segment case where there is a much less severe environment than at the HPM nozzle-to-case joint location. This attachment joint would be mated at the factory and the aft segment would be shipped in its current shipping configuration.

In addition to insulating over the aft dome-to-fixed housing joint the alternative design would change the metal parts to the configuration shown. This joint has an inclined sealing surface that has a small radial interference which is drawn up when torquing the bolts such that the unpressurized seal gap is zero. One-hundred 1.375-in.-diameter Inconel 718 bolts are used to secure the joint just as in the HPM assembly. Figure 32 summarizes the preliminary two-dimensional analysis. All factors of safety are adequate and the maximum seal gap opening is 0.006-inch.

Material: MAR-T250 Nickel Alloy Steel

$F_{tu} = 250 \text{ ksi}$   
 $F_{ty} = 240 \text{ ksi}$

$\sigma_1 = \text{Max In-plane Stress}$   
 $\sigma_2 = \text{Hoop Stress}$



87354-9B

Figure 31. Welded Nozzle Joint

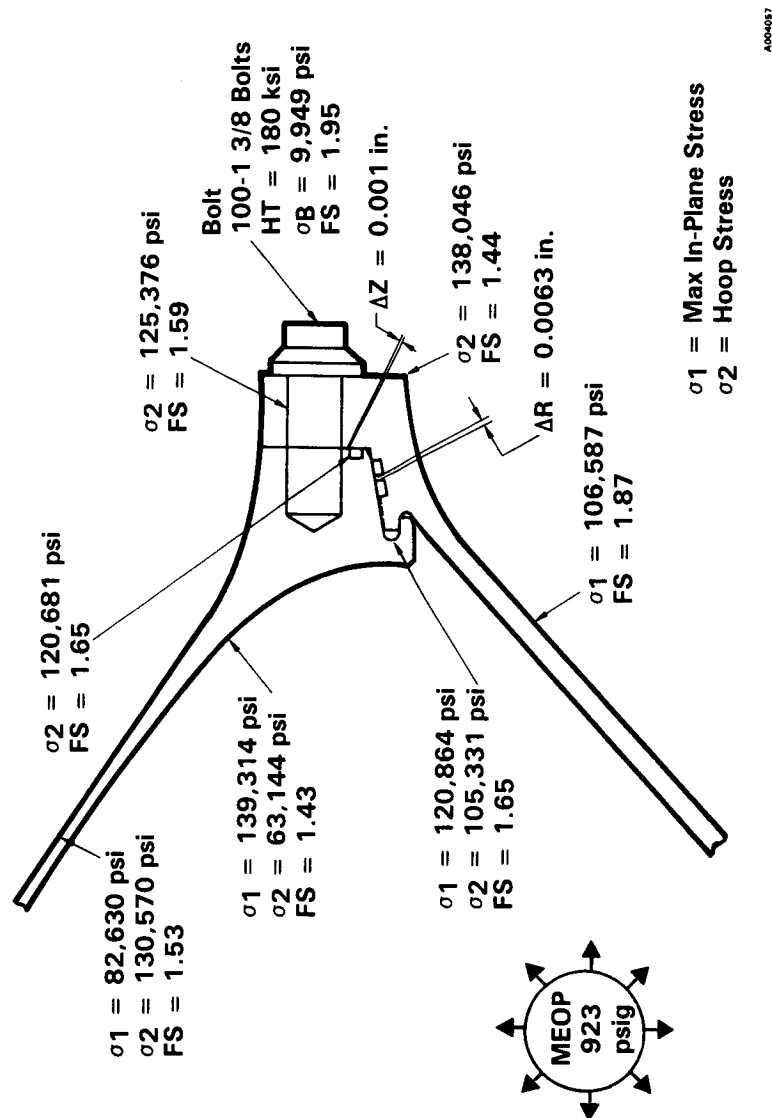


Figure 32. Bolted Nozzle Joint

### 3.5 SEAL DESIGN

The purpose of the seals in the three case field joints and the aft dome-to-case joint is to close the gap between the mating metal components and maintain pressure integrity during motor operation. The material selected must provide closure in the joint while accommodating the relative motion between the mating surfaces and the environment at the joint. The O-ring seals and materials proposed for the Block II clevis joint are designed to maintain its sealing capability during the motion of the joint over the entire range of operating conditions. The seal design will be extensively tested to verify acceptable performance using the recently-developed methods such as the Joint Environment Simulator (JES) test and Transient Pressure Test Article (TPTA).

Major design requirements/objectives for the case field joints and the aft closure-to-case joint are the following:

- O-rings must have 15 percent minimum squeeze assuming no compression set and at least 10 percent squeeze when compression set is considered.
- O-rings must have at least 0.002-in. clearance to prohibit contact with both side walls.
- Seal must maintain contact with the gland even at twice the expected displacement or twice the expected displacement rate.
- Seals must meet requirements over an ambient temperature range of 20° to 120°F.
- Seals must not be damaged during joint assembly.
- Seals must be verified after assembly by a leak check that seats the seal in the seating direction.
- Seal performance must not be jeopardized by the joint corrosion prevention system or the seal lubricant.

Design studies by the RSRM team are considering both elastomeric and metallic seals to arrive at a design which satisfies all requirements. The Block II SRM design is following the RSRM program's conclusions wherever applicable.

### 3.5.1 ELASTOMERIC SEAL SELECTION FOR BLOCK II CLEVIS JOINT

As discussed in Section 3.5.2, a major O-ring material evaluation and selection program is nearing completion. Final selection of the optimum elastomeric material for the RSRM will be made after completing all the planned testing. Preliminary results indicate that polysiloxane S-650 O-ring material will meet the design requirements for the Block II clevis joint. The O-rings would be molded into 18-ft lengths, then ground to the proper OD and spliced to obtain the correct length. Testing to date shows that this material has adequate resiliency to maintain contact with the gland at twice the expected displacement and twice the expected displacement rate over the required temperature range of 20° to 120°F, without the need for auxiliary heaters. Figure 33 shows the S-650 O-ring material's location to track a contact plate that opens 0.0206 in. during the pressure rise time of 0.55 sec. This is about three times the maximum seal gap growth of 0.006 in. predicted for the primary and secondary seals on the Block II clevis. This exceeds the requirement that the O-ring material maintains contact at twice the expected displacement or twice the expected displacement rate. The polysiloxane material has excellent aging characteristics, which will be beneficial on the shelf and installed in the joint. Compatibility with the case corrosion inhibiting grease must be fully tested (which is under way at Morton Thiokol).

The capture feature seal has a different set of design requirements. The capture feature seal gap growth is zero, but the seal located closer to the internal motor environments. As a result, the requirement for this seal to provide some degree of thermal protection is an important consideration. Two of the candidates considered for this location were an ablative-coated, fluorocarbon polypak-type seal and an aramid fiber-reinforced delta-type seal. These are both in the development stage and could not be selected as a baseline. As a result, Viton 747 was selected for the capture feature seal because of its demonstrated higher tolerance to heat and jet impingement compared with the other O-ring materials tested to date.

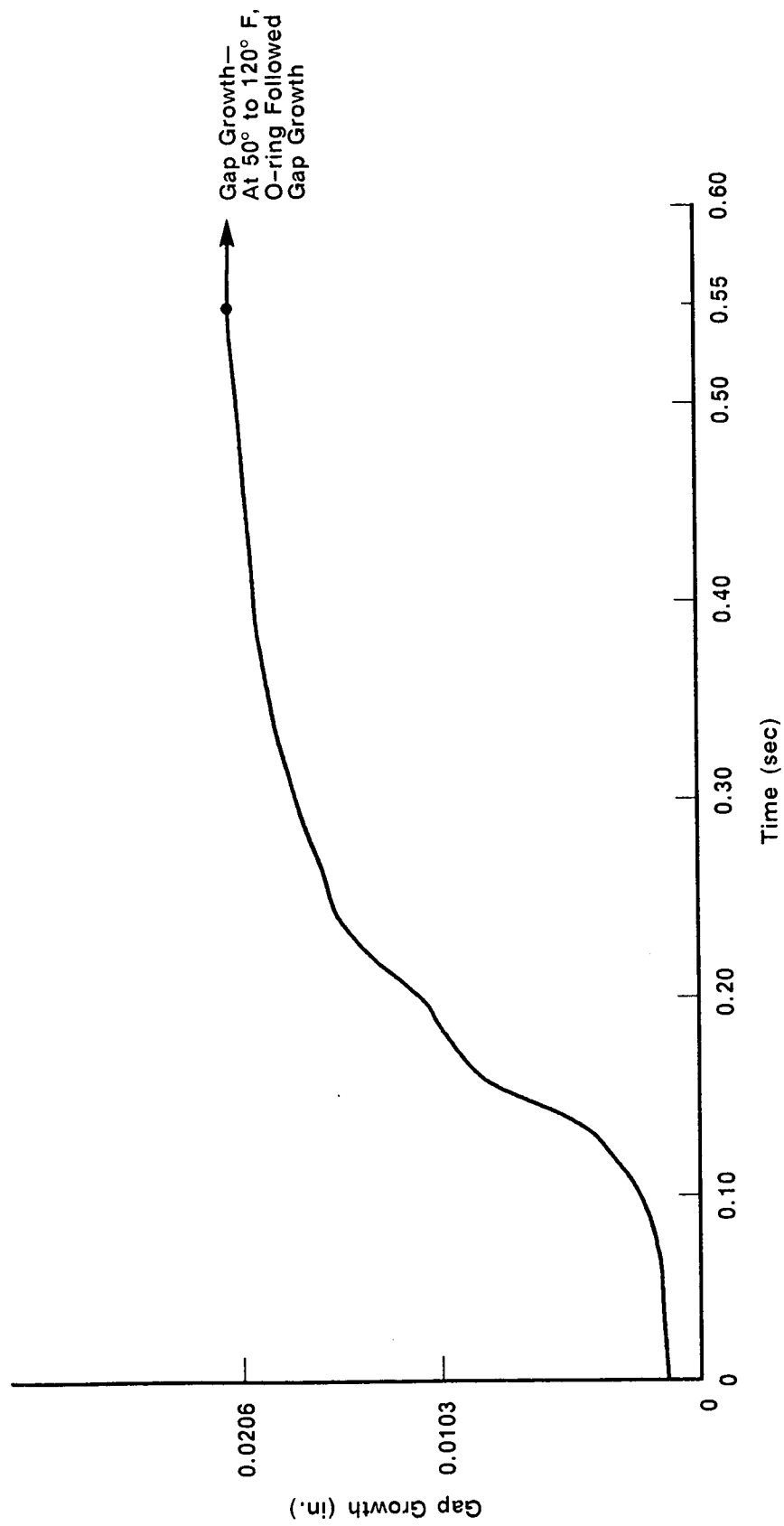


Figure 33. Silicone S-650 Seal Response to Gap Growth Tests

A004599a



### **3.5.2 ELASTOMERIC SEAL DESIGN AND TESTING SUMMARY (RSRM PROGRAM)**

There are many factors that determine proper seal material selection, many of which overlap, and almost all of which can impact each other. This summary of these factors addresses the following topics:

1. Standard Chemical and Physical Properties
2. Resiliency
3. Dynamic Sealing
4. Case Corrosion Protection and O-ring Lubrication
5. Aging
6. Heat Resistance
7. Joint Assembly
8. Leak Check
9. Geometric Sizing
10. Seal Producibility
11. Quality Acceptance

#### **3.5.2.1 Standard Chemical and Physical Properties**

All the O-rings that Morton Thiokol has investigated to date have basic properties that render the O-rings usable in this application. They have the strength, elongation, and hardness properties that are within design targets. These properties can change, however, when subjected to the SRM environments over a period of time. For this reason it is necessary to monitor these properties consistently in the test programs.

#### **3.5.2.2 Resiliency**

Resiliency is one of the key material properties of a seal used in a joint that has any tendency to open during pressurization. All elastomeric seal materials have the capability to spring back to some extent when the mating surfaces are separated. This property is temperature-dependent. Fluorocarbon O-rings do not have good resiliency at temperatures below 50°F, whereas the silicone O-rings maintain good resiliency at temperatures as low as 10°F and below.

Due to SRM pressurization at ignition, relative displacement of field joint components occurs (joint rotation) causing the O-ring gland depth (distance between the sealing surfaces) to increase rapidly. The ability of a nonpressurized O-ring to respond and remain in contact with the increasing gland depth is a key factor in key field joint reliability.

It is imperative that the seal be capable of maintaining contact with its adjacent surfaces without the need for pressure actuation for the complete distance of separation with a positive safety factor. Morton Thiokol recommends a safety factor of 2.0, i.e., the O-ring be capable of maintaining adjacent surface contact at twice the separation rate and twice the distance. If a joint does not open upon pressurization, resiliency ceases to be an issue.

A test configuration has been designed to provide data concerning the ability of various proposed seal materials to keep up with the expanding gland. The effect of temperature variations on the material's performance was determined by varying the test temperature from 20° to 75°F. Several materials have been tested under the same conditions, thus providing comparisons of the materials based on their performance under test conditions.

Resiliency screening testing was conducted over a range of temperatures using the gap growth curve shown in Figures 33 through 37. The data from these curves define the rate at which the platens of test setup separate. The first curve (CF19) assumed a gap growth of 0.019-inch. This was based upon a capture feature that limits growth of the expanding gap to 0.019-inch. This curve assumed a metal-to-metal condition at  $t=0$ . The second curve (CF10) used a 0.010-in. gap growth with a 0.009-in. initial gap.

Requirements for pressure seals established in CPW1-3600, Section 3.2.1.2(E), require each seal to maintain a sealing margin of 100 percent (based on seal/metal tracking velocities) without pressure assistance. Seal gap openings shown in Table 20 indicate a maximum opening of 0.009. Sealing margin of 100 percent would give a total gap opening of 0.018. Tests were conducted with 0.019 gap to include this condition. Tests were also run with an initial gap of 0.009 and 0.010 growth as the joint design had not been finalized at the time of testing.

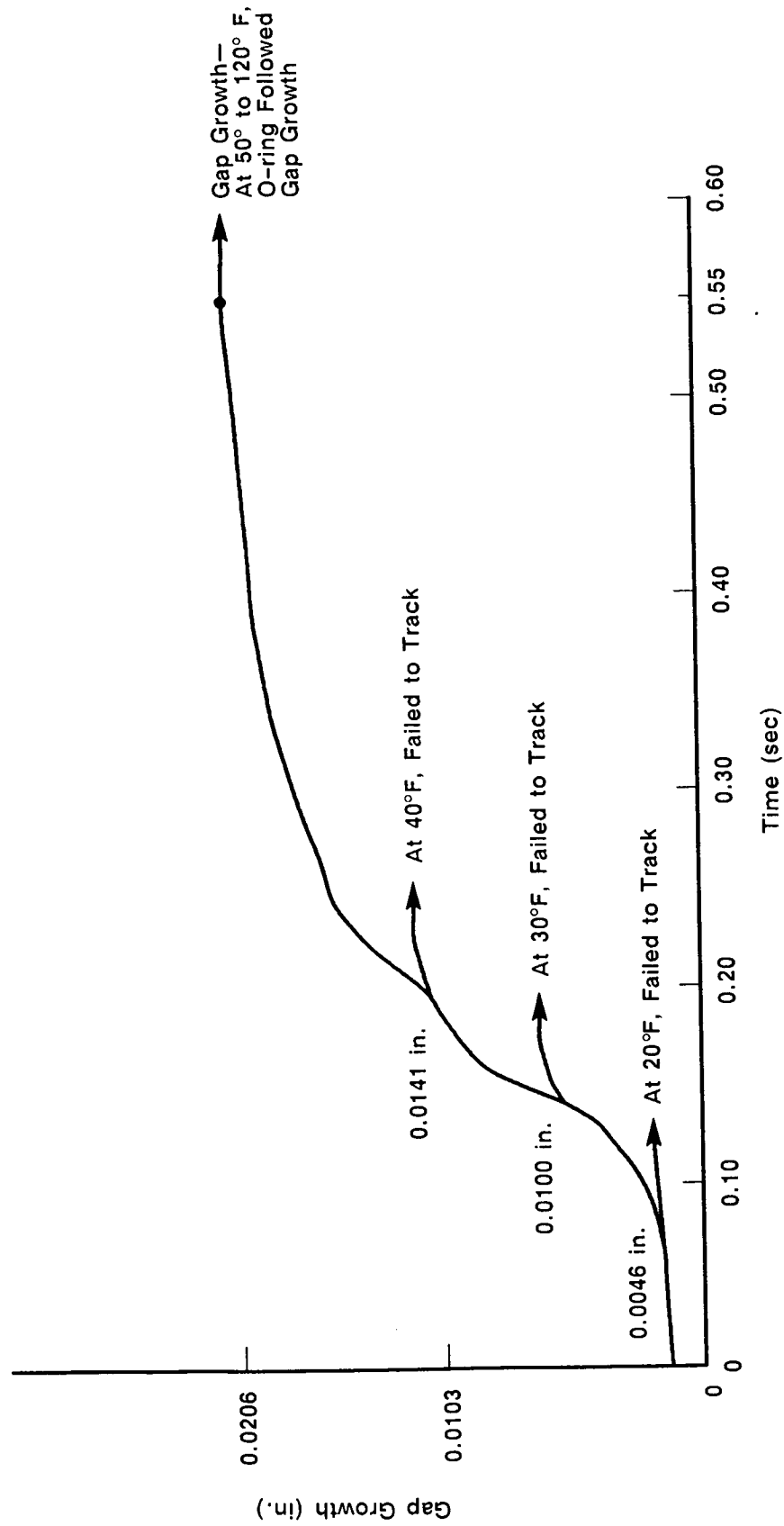


Figure 34. Fluorosilicone L677 Seal Response to Gap Growth Tests

A004595a

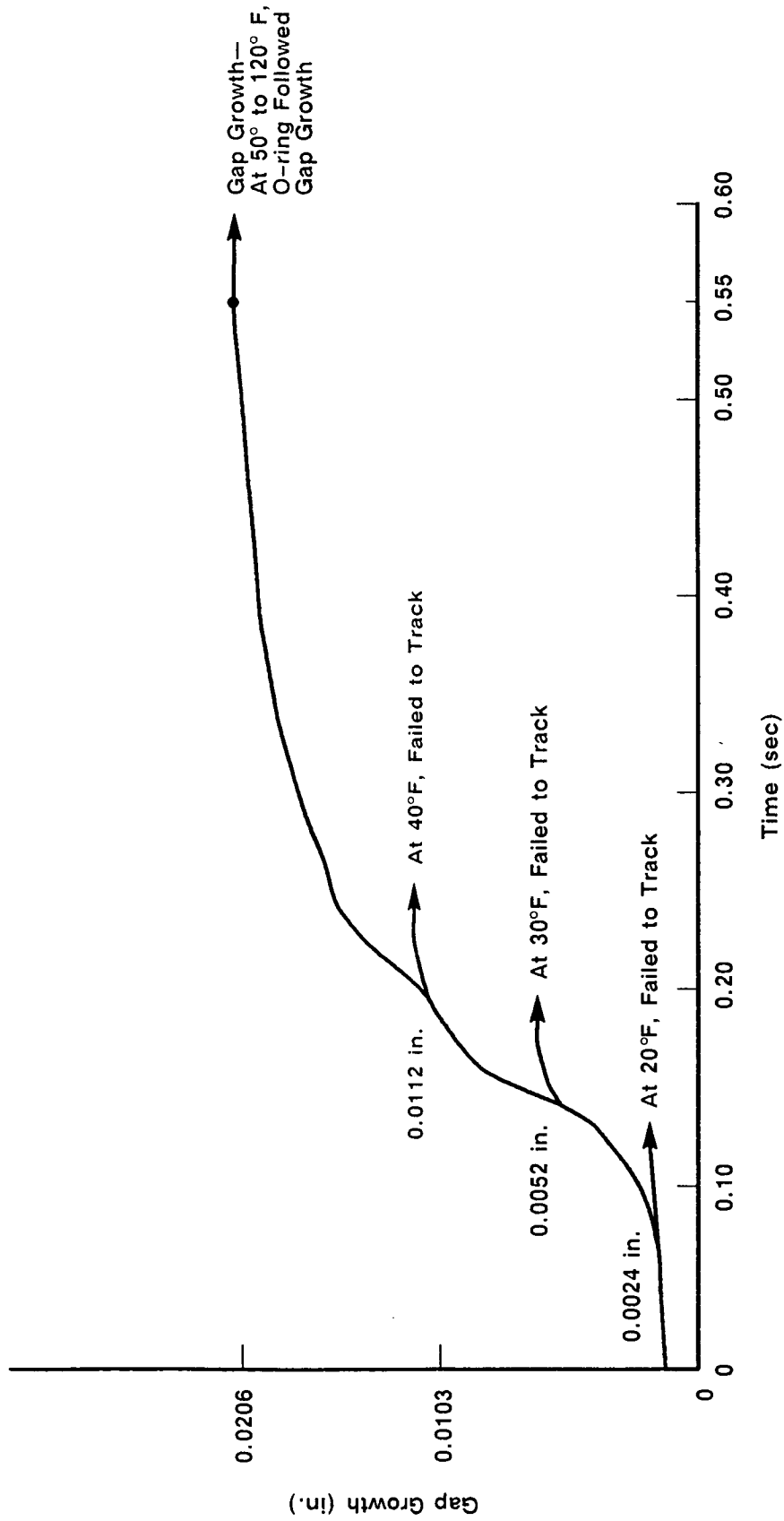


Figure35. Viton 747 Seal Response to Gap Growth Tests

A004596a

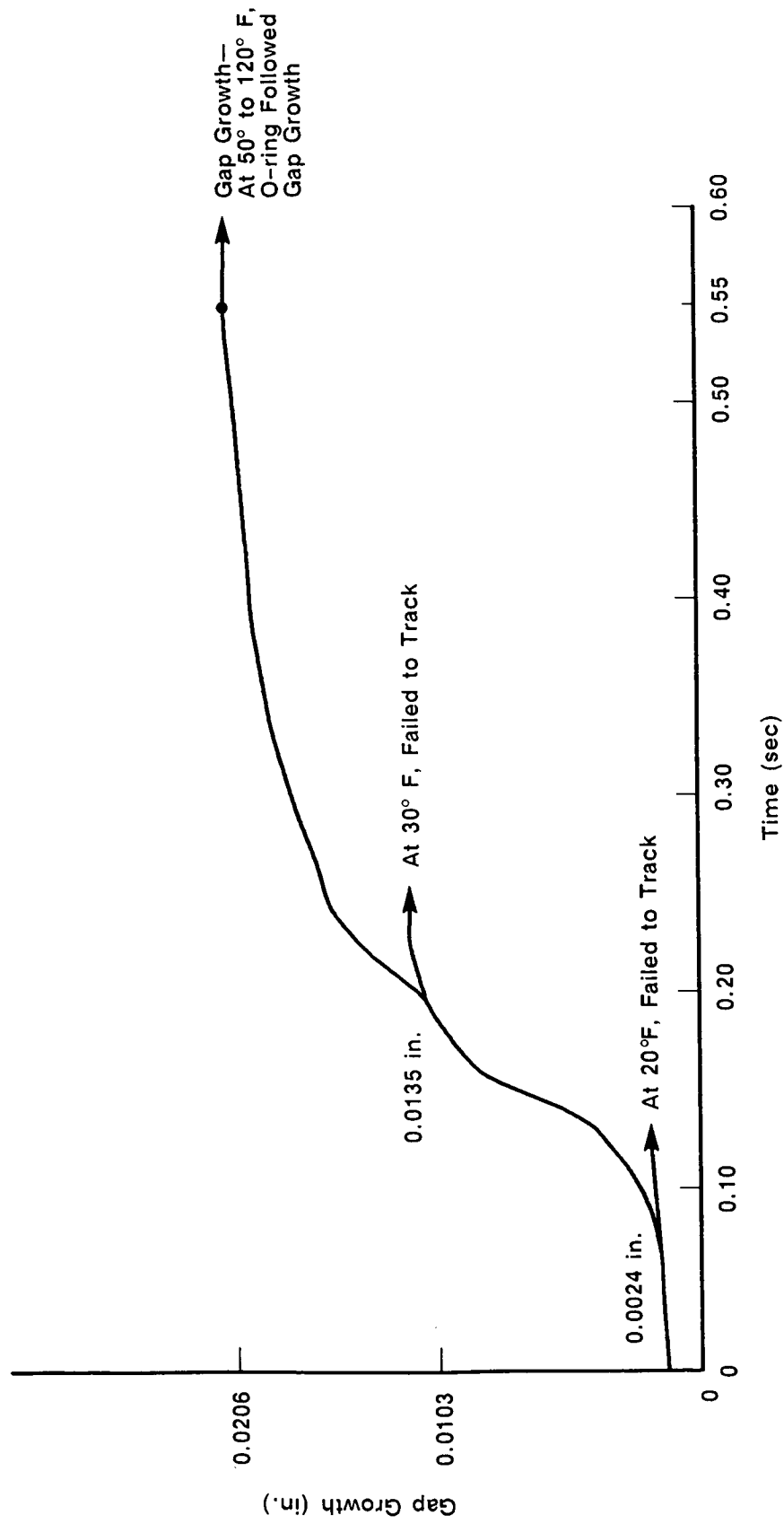


Figure 36. Viton GLT Seal Response to Gap Growth Tests

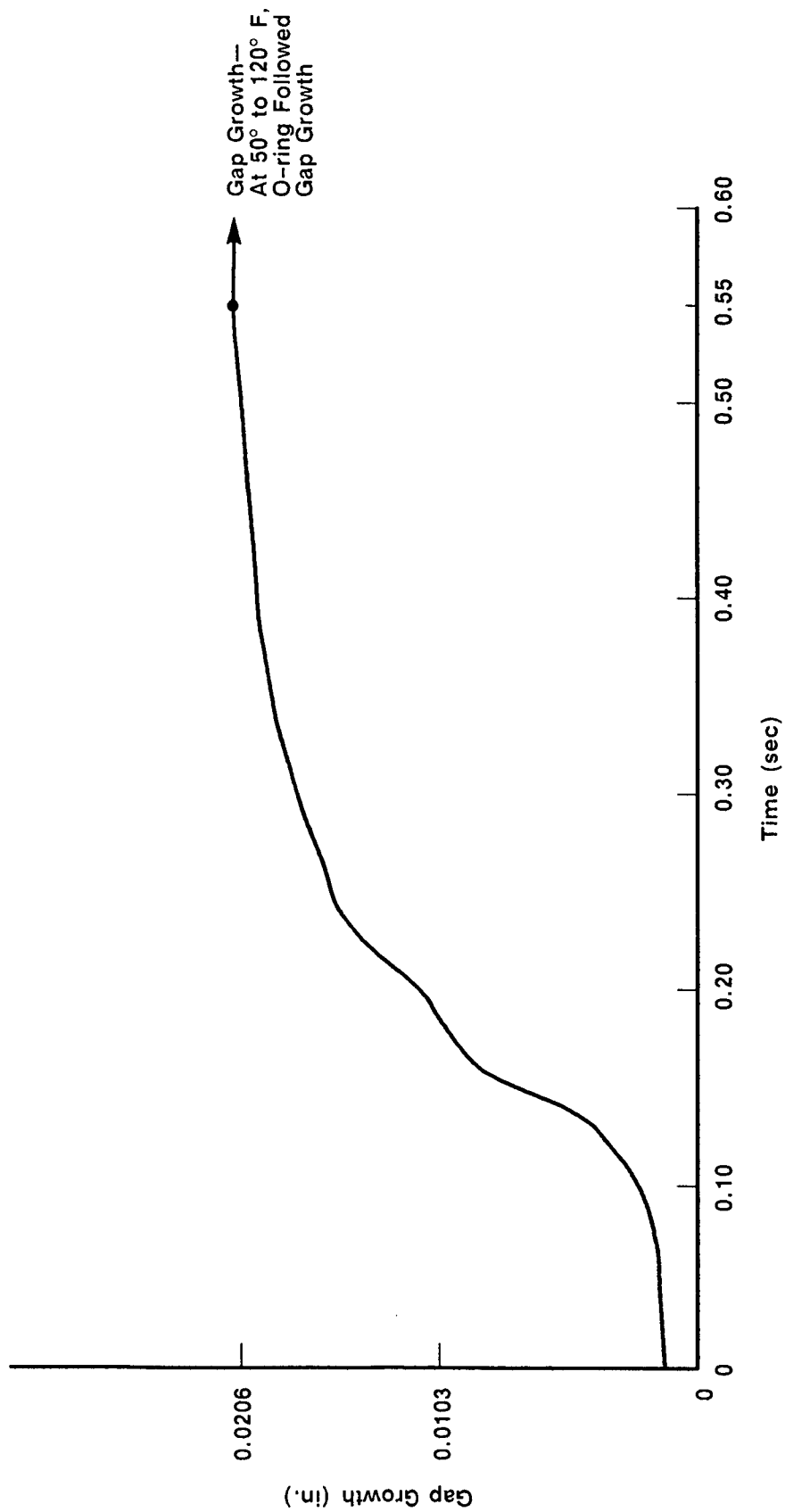


Figure 37. Arctic Nitrile Seal Response to Gap Growth Tests

A004598a

Table 20. Block II SRM Joint Trade Study

	Units	HPM*	PDR Baseline*	Block II Clevis**	With optional Overwrap	Inclined Bolted**	Double Recess Bolted	Single Recess Bolted
	-----	----	-----	-----	-----	-----	-----	-----
Weight Delta Over Cylinder***	(lb) per joint	730	794	1,176	2,276	1,643	1,859	2,031
Internal Volume Displacement	(cu in.) per joint	1,788	2,745	4,173	4,173	5,114	15,311	7,700
Weight of Displaced Propellant	(lb) per joint	113	173	263	263	322	965	485
Seal Gap Growth	(in.)							
Primary		0.034 (B)	0.007 (B)	0.006 (B)	0.000 (B)	0.008 (B)	0.000 (F)	0.000 (F)
Secondary		0.030 (B)	0.009 (B)	0.006 (B)	0.000 (B)	0.006 (B)	0.000 (F)	0.000 (F)
Tertiary		NA	NA	NA	NA	0.000 (F)	NA	NA
Capture Feature		NA	0.000 (B)	0.000 (B)	0.000 (B)	NA	NA	NA
Payload Reduction	(lb)							
Per Joint +								
Inert Weight		133	145	214	414	299	338	371
Propellant Loss		10	14	22	22	27	80	40
Total		143	159	236	436	326	418	411

Notes: \*Designed for MEOP = 1,004 psig; D6AC steel  
 \*\*Designed for MEOP = 1,100 psig; MAR-1250 steel  
 \*\*\*Metal parts only  
 +Used heads up exchange ratios  
 (B) = Bore seal  
 (F) = Face seal

Resiliency can change in a material over time, in compression, and/or when the material is altered by contact with another material. Effects of aging (in free state, under compression, and at temperature) and effects of the case corrosion inhibitor and the O-ring lubricant need to be assessed as they affect resiliency. The silicones are the most resilient O-rings that Morton Thiokol has found over the 20<sup>0</sup> to 120<sup>0</sup>F temperature range, but as discussed in Section 3.5.2.4 the Conoco HD-2 grease used for case corrosion protection causes the silicones to swell. Though the fluorocarbon material has inadequate resiliency at lower temperatures, it is conceivable that it could be the best material choice because it is impervious to the grease, and at higher temperatures (75<sup>0</sup>F) its resilience can meet the 2:1 safety factor. The resultant choice may be to fly fluorocarbon O-rings with joint heaters.

Test results are shown in Figures 33 through 37 with materials tested at various temperatures showing that with temperatures below 50<sup>0</sup>F, Viton GLT, Viton 747, and fluorosilicone L677 require heaters and silicone S-650 and arctic nitrile perform well at all temperatures tested. These tests were conducted using double the expected gap growth and double the rate as required for the RSRM.

### **3.5.2.3 Dynamic Sealing**

This test is of extreme importance to verify performance of the O-rings in the Block II clevis joint. The test can be run with both cold and hot gas. The dynamic environment encompasses all of the motions within the joint just prior to and during the SRM action time. Twang, vibration, axial joint expansion, radial joint rotation, O-ring sliding or rolling, and max q all cause motion within the joint. These phenomena must be simulated and tested with and without pressure on the seal to verify that the O-ring will seal at all times.

This test interrelates with resiliency, material compatibility, leak check, and geometric sizing. Changes to any of these would require dynamic sealing retests. Also, results of this testing may cause changes in those categories.



#### **3.5.2.4 Case Corrosion Protection and O-ring Lubrication**

Conoco HD-2 grease is used to prevent corrosion in the SRM joint area. This concern for corrosion is magnified by splashdown in salt water and the possibility of salt water being trapped for long periods of time in the joint area. HD-2 grease is the best corrosion inhibitor Morton Thiokol has found to date; however, recent testing has revealed too much grease may create problems in leak testing of joints and O-ring performance at SRM ignition. Amounts and methods of application are currently under investigation at Morton Thiokol.

There is evidence that HD-2 grease is not an optimal O-ring lubricant, particularly at lower temperatures, and tests have shown that it can mask flawed O-rings during leak testing. Morton Thiokol and some of its subcontractors are investigating alternate O-ring lubricants that could be used with the HD-2 grease to enhance the ability of the O-ring to respond quickly when pressurized. Material compatibility between the grease, the lubricant, and the O-ring must be fully tested and understood. None of the materials can degrade the performance of the other during assembly, leak check, storage, flight, and recovery.

#### **3.5.2.5 Aging**

Because all the SRM joints, except the three field joints and the one exit cone field joint, are mated prior to segment shipment from the Morton Thiokol, Wasatch facility, the O-rings have to perform as intended with all required margins of safety for 5 years. The field joints have to be capable of performing for 6 months after stacking. All this is required after some finite O-ring shelf life. Since many elastomers are age sensitive, testing must be done to demonstrate performance capability after real-time aging at specified environments in the compressed and uncompressed state. Material tests, resiliency, dynamic sealing, material compatibility, heat resistance, and O-ring size can be affected and must be investigated. A complete aging program plan is required to assure that all factors sensitive to aging are appropriately evaluated and that test data exist for materials from batches older than those to be flown.

#### **3.5.2.6 Heat Resistance**

The SRM O-rings must be expected to withstand gases at temperatures of 500°F, and possibly gas jets at temperatures higher than that. Most elastomeric O-rings that Morton Thiokol has investigated can survive this environment for two minutes, so this design factor becomes a nonissue for them. However, Morton Thiokol has tested some noncircular, spring-loaded seals in a hot gas environment. Some of these seals melted or became badly disfigured and lost their ability to seal. Though these seals met the resiliency requirement, they would likely not hold up a motor environment if hot gas reached them.

Morton Thiokol has investigated some fiber-filled elastomers and some ablative coated seals to increase the seal safety margin when subjected to hot gas flow or a gas jet. These materials tend to be less resilient, but in certain applications they may be desirable. Further development of such seals may be desired for the Block II SRM design, but it would probably not be required.

#### **3.5.2.7 Joint Assembly**

Any new design should prevent the tendency to damage the seals during assembly. Morton Thiokol has tested many elastomeric materials and seal configurations for resistance to tearing. There are differences in material toughness, but all seals tested to date are adequate to be assembled consistently without damage. Morton Thiokol recommends, however, that any new joint design be assembled a number of times to gain confidence that the mating operation will not result in damage to the seals.

#### **3.5.2.8 Leak Check**

An important feature in a joint design is the capability to verify the presence of undamaged seals in the assembled joint and to demonstrate that the seals will perform as intended at or after ignition of the SRM. Leak checking between two seals has been performed on all HPM field and nozzle-to-case joints in the past. The development of the leak check procedure must take issues into account such as placing the seals in the proper sealing direction, masking of the leak check by grease or by metal-to-metal contact, or damage to other motor components as a

result of the leak check. Testing by NASA, Morton Thiokol, and their subcontractors has shown that the leak test can be masked by grease adjacent to the O-ring (this is also temperature-dependent) and by face-to-face metal contact. A leak test development program would be required to minimize or eliminate this possibility.

Due to the use of Conoco HD-2 grease in the SRM joint for both an O-ring lubricant and protection against corrosion, testing has been performed to determine the effect of HD-2 grease on the seal verification test performed at assembly. Testing performed by Morton Thiokol, MSFC, Cameron Iron Works, and AECL has concluded HD-2 grease does block pressure communication around the joint at low temperatures and has the ability to mask flaws in the O-ring and its sealing surface at low temperatures (Figure 38).

The question of whether to perform a high-pressure and/or a low-pressure leak test would have to be resolved. O-rings tend to seal better as the pressure increases up to the point of physically failing. (The failure point of the O-ring is well above 1.4 times MEOP.) A relatively low pressure check (50 psig) has been used on the HPM and will be used on the RSRM. Any surface flaws on the metal or on the seal itself would be most reliably detected by the low pressure check. It might also be desirable to perform a pressure check at higher pressures to assure that any tendency to mask the leak check is minimized. This is an issue that is highly dependent on the overall joint design and would have to be developed in conjunction with the design configuration, O-ring lubrication and case corrosion protection materials, and the assembly procedures.

For the alternate joint configurations studied for Block II both the single- and double-recess bolted configuration have only two O-rings with a metal-to-metal fit. There is a concern that the metal-to-metal fit may result in a seal and the O-rings may not be verifiable. The inclined bolted configuration has the same concern on the outer O-ring, but the two inner O-rings would be verifiable.

#### **3.5.2.9 Geometric Sizing**

O-ring and groove dimensions including allowable tolerances are critical to seal function. Groove depth, O-ring cross-sectional size, O-ring stretch, compression

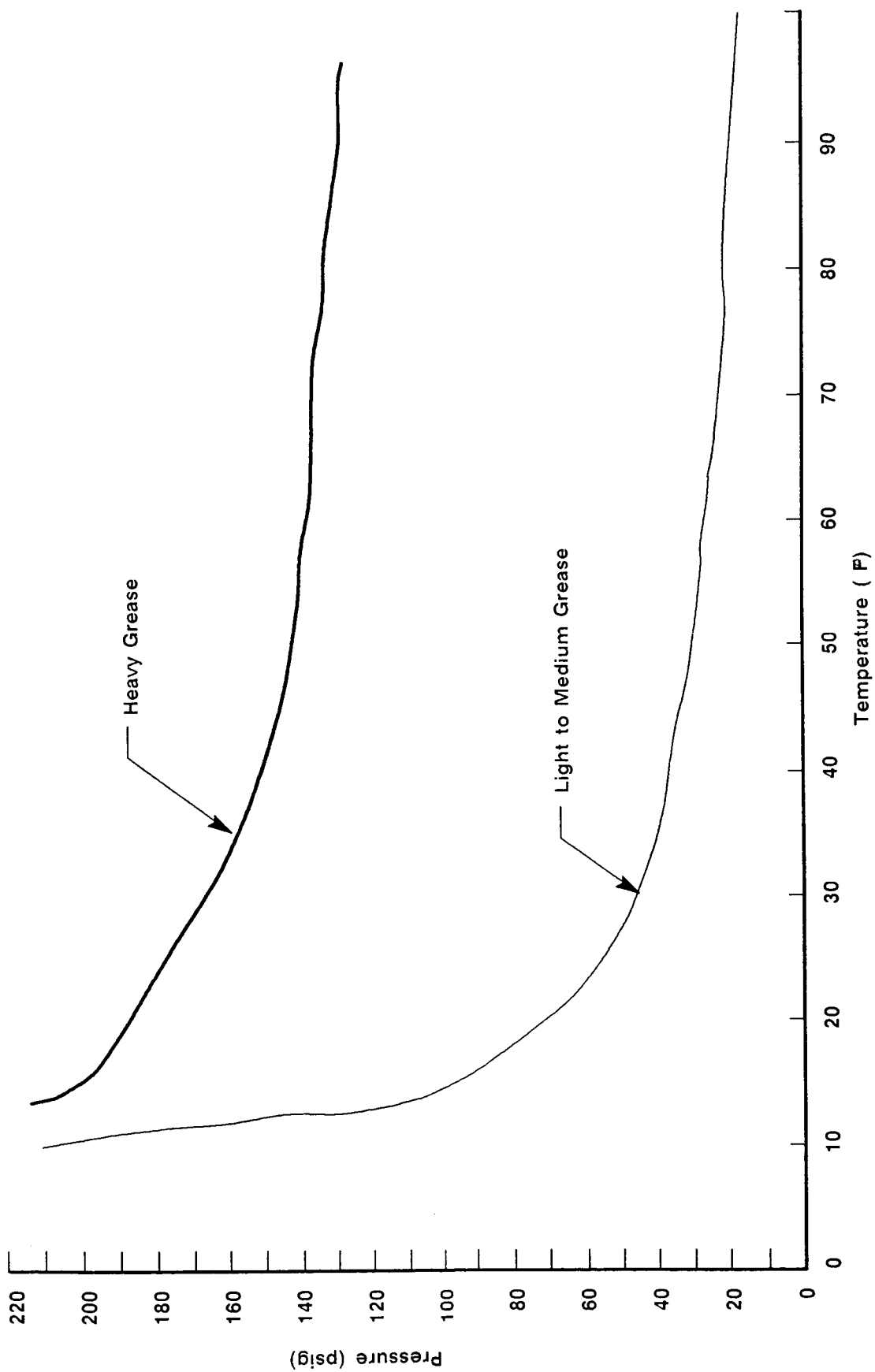


Figure 38. Pressure Required to Breach Grease Blockage

A004600a

set, and metal gap width result in O-ring squeeze. Once squeeze has been determined, the groove width is adjusted to assure the cavity fill meets the required value and to assure that the compressed O-ring does not contact both groove walls.

Depending on the joint design, it may be desirable to configure the inlet gap to pressurize at the center of the O-ring rather than at one side. Test data indicate that such a design is desirable to enhance O-ring seal response at ignition, but potential damage during installation may dictate that a more traditional O-ring groove design would be required.

#### **3.5.2.10 Seal Producibility**

Since the steel hardware is so large, tolerance control of the sealing surfaces can only reach a certain level. Tight tolerances are also required on the O-rings, which necessitate controlled centerless grinding of the O-ring. This operation is performed on a cord stock prior to the splicing operation. Morton Thiokol is investigating new technology to grind O-rings after splicing, but it is not known at present whether this will be possible or practical. Some O-ring material that may be desirable because of good physical properties, such as resilience and compression set, may be difficult to splice. Single-piece, net-molded O-rings may have such a high rejection rate (even if the dimensional control could be achieved) because of defects such as mold mismatch, backrind, and surface voids, that there may not be enough O-rings produced to maintain program schedules. The producibility issues must also be addressed in material selection to assure that the program will not be hampered by unavailability of acceptable O-rings.

#### **3.5.2.11 Quality Acceptance**

Morton Thiokol is working with various subcontractors to develop O-ring inspection techniques to verify that the flight O-rings will perform as intended. Standard O-ring tests such as tensile strength, elongation, tear resistance, and hardness will continue to be performed. Newly developed tests such as resiliency (recovery capability) will also be incorporated. This test is a function of the joint design, and the 2:1 safety factor within the specified environmental range

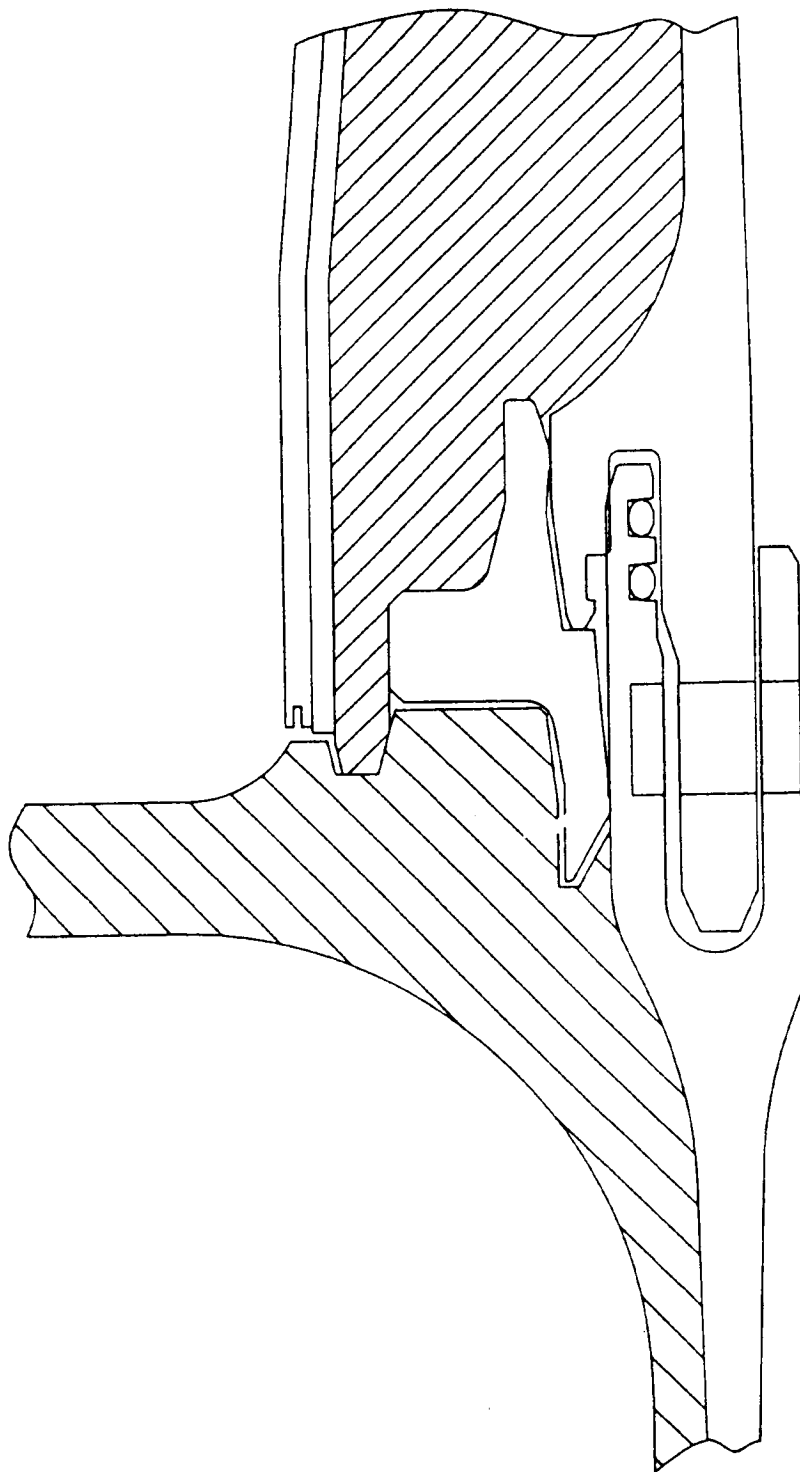
will be demonstrated by acceptance testing. Atomic Energy of Canada Limited (AECL) is developing methods for subsurface NDT inspection, such as tomography and elastodynamic inspection. A minimum of one subsurface NDT procedure will be incorporated into the acceptance procedures to detect voids and inclusions. AECL is also conducting tests to determine the allowable level of voids and inclusions that does not impact the sealability of the O-ring.

Dimensional inspection has been enhanced by using laser micrometers to check cross-sectional size. Morton Thiokol is also developing procedures to assure that splices are acceptably strong and dimensionally within the parent stock envelope.

### 3.5.3 METALLIC SEAL DEVELOPMENT AND TESTING

Among the seal candidates that are being evaluated in the SRB redesign program are metal-to-metal seals. Vetco Gray, an oil tool company, has used metal sealing technology for the past 60 years and developed their Grayloc<sup>®</sup> metal seal 35 years ago for applications of high temperature and high pressure (2,000<sup>°</sup>F external flame temperature, 20,000 psi). Vetco Gray has designed ThermaLok<sup>®</sup> T-seals for use in the SRM case-to-case joint and ThermaLok<sup>®</sup> U-seals for the SRM nozzle-to-case joint (Figures 39 and 40a). The seal rings are made of D6AC steel, heat treated to the proper strength level based on safety factors of 1.2 on yield and 1.4 on ultimate. The sealing surfaces are coated with silver, which serves as a lubricant to prevent galling at assembly and also exhibits excellent high-temperature lubricity. The metal-to-metal seal is achieved by creating an interference fit up to 0.220-inch, which results in elastic bending of the seal legs to provide the required bearing load to prevent leakage. A 32- $\mu$ in. RMS surface finish is required for leak tightness in the  $1 \times 10^{-4}$  scc/sec range.

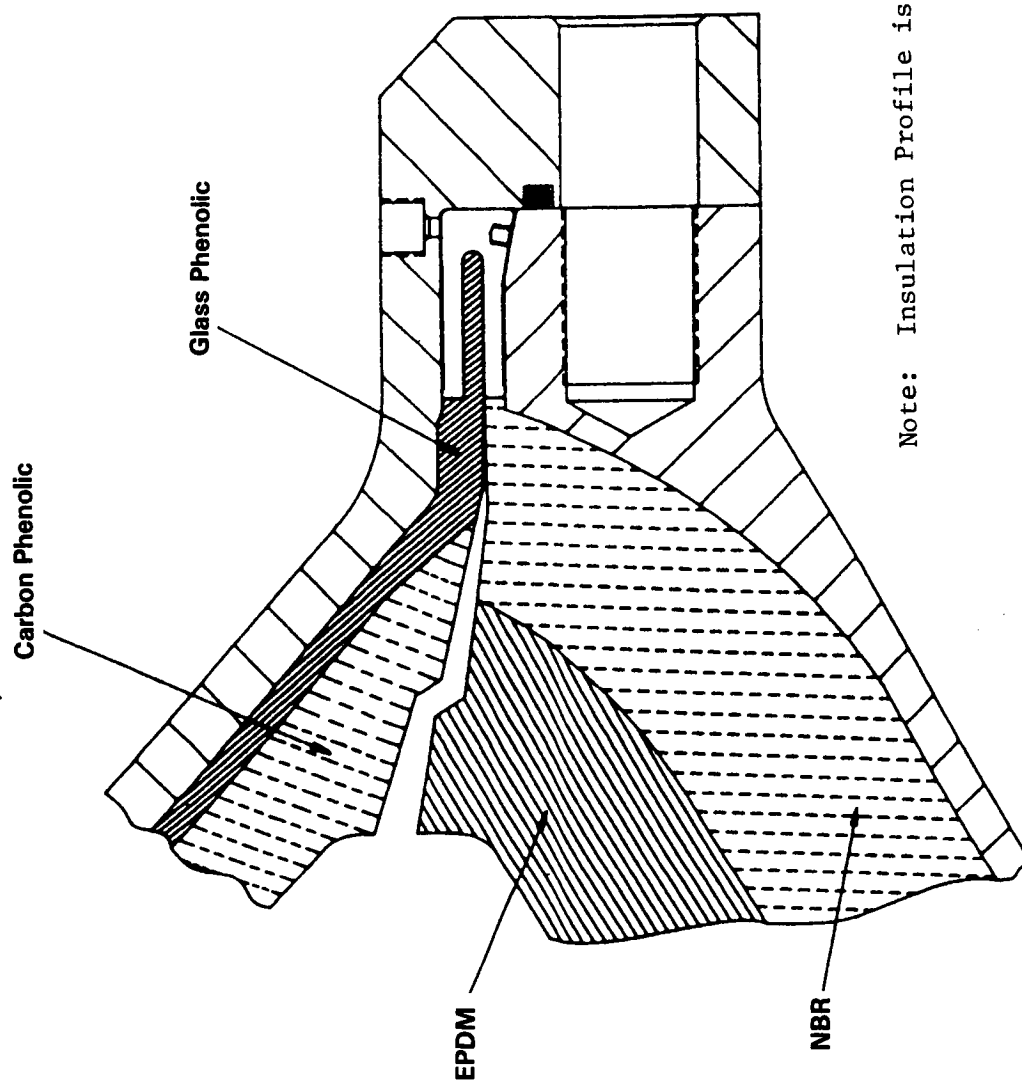
An important feature in the metal seal design is the ability of the seal to maintain the bearing load at the sealing points throughout all dynamic motions of the joint. For example, as the case expands under pressure, the T-seal follows this movement because of the interference in the assembled, but unpressurized condition. Because the seals are affected on cylindrical surfaces, axial expansion of the joint does not affect the line load or the sealability at the seal footprints. (An O-ring bore seal is affected similarly in that axial joint



Note: Insulation profile is illustrative only

Figure 39. Thermallok® T-Seal In Assembled Position for RSRM

87354-10A



Note: Insulation Profile is illustrative only

Figure 40a. Nozzle Insulation With Thermalok<sup>®</sup> U-Seal for RSRM

87354-100



growth causes the O-ring to slide, but not to lift off the seal surface.) Other ThermaLok<sup>®</sup> T-rings have maintained seals when the axial growth of the cylinders due to pressure and temperature has been as high as 0.125 in., more than three times the axial opening expected on any of the SRM joints.

An assembly and hydroproof test is planned for late December 1986 on the T-seal in an SRM case joint with a capture feature, similar to the RSRM design. The U-seal will be tested hydrostatically in the nozzle joint evaluation simulator hydroproof (NJES-H) test series in the first quarter of 1987.

Design issues that need to be addressed on the metal seals are stress corrosion and galvanic action. When the metal seals are installed, they are in a state of stress and remain in that state until they are removed. Analyses are in work to optimize the seal ring and joint designs to assure that this stress level is below the threshold where stress corrosion becomes a concern. Galvanic action will also be evaluated by analysis and test to assure that no hardware damage will result.

Vetco Gray has also proposed an optimized design using a T-ring with a capture feature, which significantly reduces the joint opening at the clevis seals (Figure 40b). This is accomplished by moving the contact point between the OD of the capture feature and the ID of the inner clevis leg aft, thus reducing the tendency of the inner clevis leg to bend. In the nozzle-to-case joint, Vetco Gray has proposed an alternate concept of a metal E-seal (Figure 40c). It is not reusable since it yields inelastically at assembly, whereas the T- and U-seals are reusable.

The impact on performance of the case joint T-seal is that its inert weight is 350 lb per ring. It displaces 1,350 in.<sup>3</sup> of propellant. The U-seal weighs 85 lb, but metal removed from the nozzle fixed housing equals 135 lb for a net weight savings of 50 lb. The U-seal displaces no propellant. The total impacts of these designs per SRM is 1,000 lb of additional weight and 255 lb of propellant lost for a total payload penalty of 298 lb over the RSRM baseline.

The advantage of this design regarding joint reliability is that it eliminates the concern of combustion gases reaching an elastomeric primary seal. A

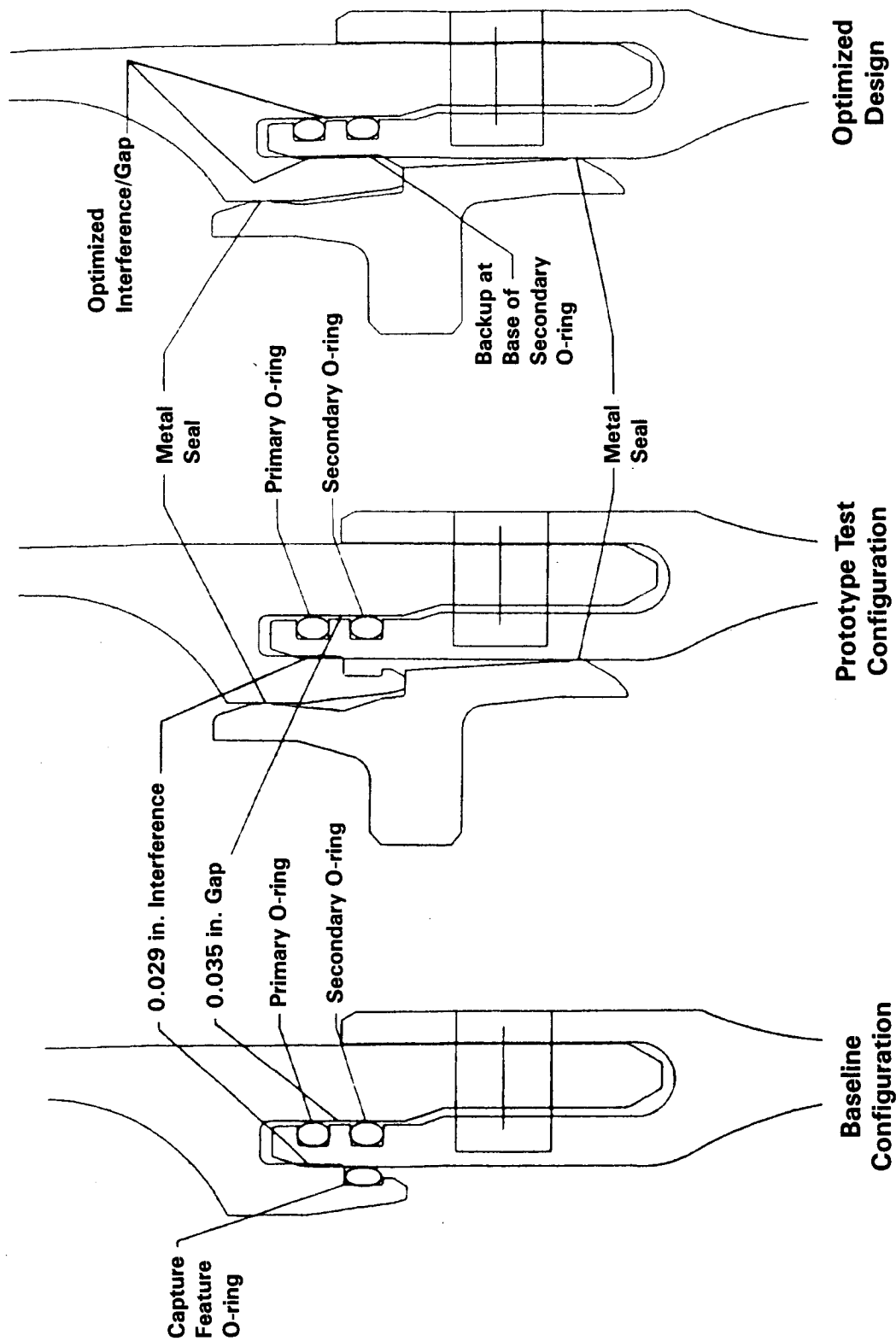
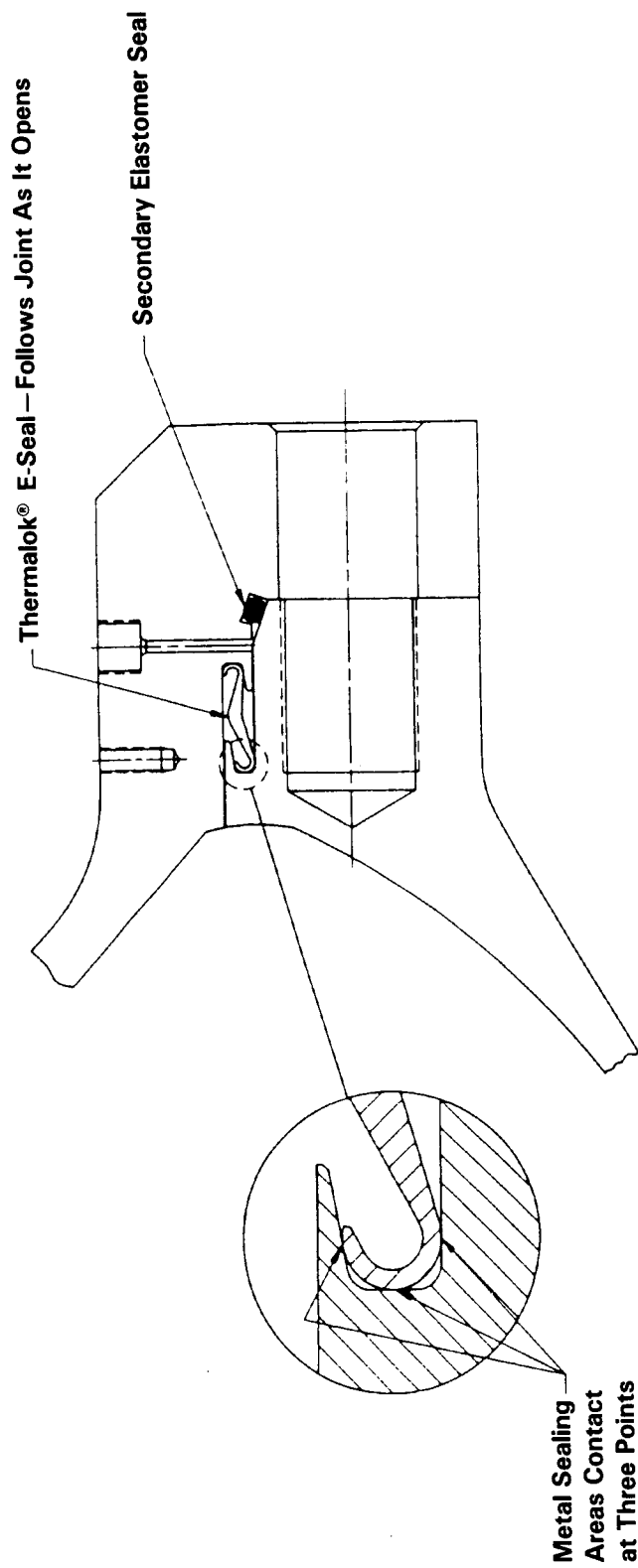


Figure 40b. Clevis and Joint Configuration

87354-108



354-10C

Figure 40c. SRM Nozzle-to-Case Joint With Thermalok® E-Seal Using Existing Aft Dome

metal seal is much more highly resistant to erosion caused by hot gas jet impingement or recirculating circumferential flow. The seals are leak checkable and are not affected adversely by joint rotation. They are energized at installation and are pressure-assisted rather than pressure-actuated. A maintainability advantage is that the ring could be replaced at a relatively low cost if the seal footprints are irreparably damaged. The flat seal surfaces on the SRM case and fixed housing hardware could be blended out as is presently done.

Because of the attractive characteristics of these proposed metal seals, Morton Thiokol's RSRM Team is continuing to test them for potential use in the case-to-case and nozzle-to-case joints.

### 3.6 NOZZLE DESIGN

The proposed design for the Block II SRM nozzle is a significant improvement over the HPM or RSRM nozzle configurations. Changes are made to accommodate the higher pressure requirements of the Block II SRM while increasing nozzle reliability, optimizing the performance of the total system and removing all asbestos materials. Increases in reliability are realized by using higher quality ablative materials, incorporating redundant and verifiable seals and selecting superior structural materials. The performance of the system is optimized on two fronts. First, a reduction in total system weight is accomplished by changing the overall configuration of the nozzle structure/flex bearing. Secondary weight savings are realized by the careful selection of ablative and structural materials. The performance is also increased by using a lower erosion throat material.

By far, the most extensive change in the Block II design over the current design is in the configuration of the flex bearing. The angle of the flex bearing, relative to the equatorial axis of the bearing, is increased and the size of the bearing reduced. The overall change in the configuration of the flex bearing is based in large part on experience gained through the Peacekeeper and Trident programs which use similar high-angle bearing systems. This change in the flex bearing design was accompanied by a change in the flex bearing thermal protector. The flexible boot/cowl system of the current design using an asbestos filled material is replaced with a tandem, sacrificial flex bearing requiring no asbestos. This sacrificial flex bearing acts as a thermal protector for the structural flex bearing and is superior to the boot/cowl system previously used because it requires far less actuation torque.

Changes are also made in the configuration of the structural members. The most obvious result of this alteration in the structural members is in the placement of the nose. The nose has moved almost 5-in. aft (toward the throat) and over 2-in. inboard. This change initiated a redesign of the remaining structural members, as well, and reduced the weight of the structural system considerably. Another effect of redesigning the structural members is the

incorporation of redundant and verifiable internal seals. Steel has been selected for all metal structural members to increase the reliability of the system.

The extent of the metal structure in the exit cone is also reduced. In the Block II design, the steel structure ends at the exit cone attach point. From that point aft, the structure is a graphite epoxy, filament wound overwrap. This replaces the aluminum shell and glass phenolic overwrap used on the current SRM. The filament wound overwrap reduces the weight of the nozzle considerably. This is accomplished in two ways. First, the graphite/epoxy system density is lower than that of the aluminum and glass phenolic currently used. Second, the stiffness of the graphite epoxy is higher so the required exit cone overwrap thickness is reduced. Since the Block II design is required to meet more stringent erosion and char safety factors in the aft end of the exit cone, the thinner filament wound exit cone overwrap allows more liner material to be added without sacrificing performance. Graphite epoxy overwrap systems are currently being used on the Trident I (C-4) and Trident II (D-5) programs, and were, at one time, considered for use on the HPM nozzle.

Another change being implemented to reduce the loss in performance due to the higher erosion and char requirements is the change to PAN-based, carbon-cloth phenolic, ablative liner materials. The PAN-based materials have a slightly higher thermal conductivity than the rayon based materials currently being used. This results in a lower erosion rate with only a slightly greater char depth. Another advantage of the PAN-based materials is their low sodium content. There is some indication that increased localized erosion in the forward throat and nose regions of the HPM nozzle can be attributed to the high sodium content of the rayon-based materials.

A PAN-based material is also being used as the ablative liner on the stationary shell. The stationary shell is insulated with silica-filled nitrile butadiene rubber (NBR) and is a continuation of the case insulation material.

Another change is the removal of all glass phenolic insulation in the nozzle. This results in a small sacrifice in performance (more ablative thickness is required in some areas of the nozzle) but is considered a positive trade because of the reduced manufacturing, material, and machining costs.

Experience gained over the past 15 to 20 years on programs such as Trident I (C-4), Trident II (D-5), and Peacekeeper has been integrated into the Block II SRM nozzle design. In addition, the extensive experience base of the HPM is drawn upon. This experience base applies extensively to such areas as fabrication and reusability, the selection of ablative liner ply angles, the use of an outer cork thermal protector, and the nozzle plug design.

### **3.6.1 REQUIREMENTS AND SCOPE OF STUDY**

The Block II SRM nozzle was designed to meet the requirements outlined in specification CPW1-3600.<sup>(1)</sup> A synopsis of the requirements that pertain to the nozzle design are as follows:

- Pressure Seals - ...Redundant and verifiable seals shall be provided for each pressure vessel leak path except for the flex bearing...
- Vectoring - The nozzle assembly shall be movable and be capable of omniaxial vectoring to a minimum of 8 deg from the nozzle null position...
- Flex Bearing Protection - The nozzle assembly shall incorporate a nozzle snubbing device suitable for preventing flex bearing damage resulting from water impact. This device shall limit the flex bearing axial travel to approximately one inch...
- Environmental Protection - The nozzle assembly shall contain a covering and/or plug to protect the SRM from the environments...

---

<sup>1</sup>Specification No. CPW1-3600 for Space Shuttle Solid Rocket Motor Project, 16 November 1986.

- TVC Actuator Attach Points - The nozzle assembly shall have attach points for the government furnished TVC actuators...
- Nozzle Assembly/Aft Segment Interface - The nozzle assembly without the exit cone assembly, shall be capable of being inserted into an assembled SRB aft skirt...
- Aft Exit Cone Severance Ordinance Ring - The aft exit cone severance ordinance ring shall sever a portion of the nozzle exit cone. Severance shall be accomplished by using a detonator cartridge, and a Linear Shaped Charge (LSC)...
- Reusability - The reusability goals are...

<u>Component</u>	<u>Number of Reuses</u>
Nozzle metal parts	19
Nozzle flex seal reinforcement shims and end mounting rings	19
Nozzle flex seal assembly (elastomer material)	9

- Safety Factors for Metallic Flight Structures - Manned<sup>(2)</sup>

Ultimate Pressure = 1.40 x limit pressure  
(verified by analysis and static test)

= 2.00 x limit pressure  
(verified by analysis only)

---

<sup>2</sup>MSFC-HDBK-505, Rev. A, Structural Strength Program Requirements, January 1981.



- Nozzle Safety Factors - The minimum design safety factors for the nozzle assembly primary ablative materials shall be...
  - Erosion: 2.0 times maximum predicted local final erosion depth
  - Char: 1.25 times maximum predicted local final (end of action time) char thickness

In addition to the design requirements outlined in CPW1-3600, the added requirement that no asbestos-filled materials be used is imposed.

### 3.6.2 SUMMARY OF SELECTED DESIGN

The Block II SRM nozzle features a state-of-the-art convergent-divergent aft pivot movable nozzle which provides 8 deg of omniaxial vectoring capability. The Block II nozzle layout is shown in Figure 41. Vectoring capability is provided by a flex bearing consisting of spherical elastomer pads sandwiched between spherical steel reinforcements. The elastomer pads are deformed in shear allowing the nozzle to rotate about the center of the spherical bearing. Thermal protection is provided by a sacrificial flex bearing in tandem with the structural flex bearing. The thermal bearing has elastomer pads and carbon cloth phenolic reinforcements and end rings.

All structural members are made from D6AC steel with the exception of the aft exit cone structure which features a lightweight filament wound graphite epoxy overwrap. The stationary shell structure of the nozzle which uses the Mar T250 material, has been made an integral part of the case aft dome in the SRM II concept. All internal seals are redundant and verifiable.

PAN-based carbon-cloth phenolic is used for all ablative materials. In highly erosive environments (inlet, throat, and forward and mid exit cone) standard density (1.55-gm/cc) PAN materials are used; in less erosive areas (aft portion of the exit cone, nose cap, and stationary shell) low density (1.20-gm/cc) PAN materials are used to reduce system weight. The stationary shell is insulated with a continuation of the case insulation material, silica-filled NBR.

The Block II nozzle is equipped with a snubbing device to preclude the possibility of damage to the flex bearing during splashdown.

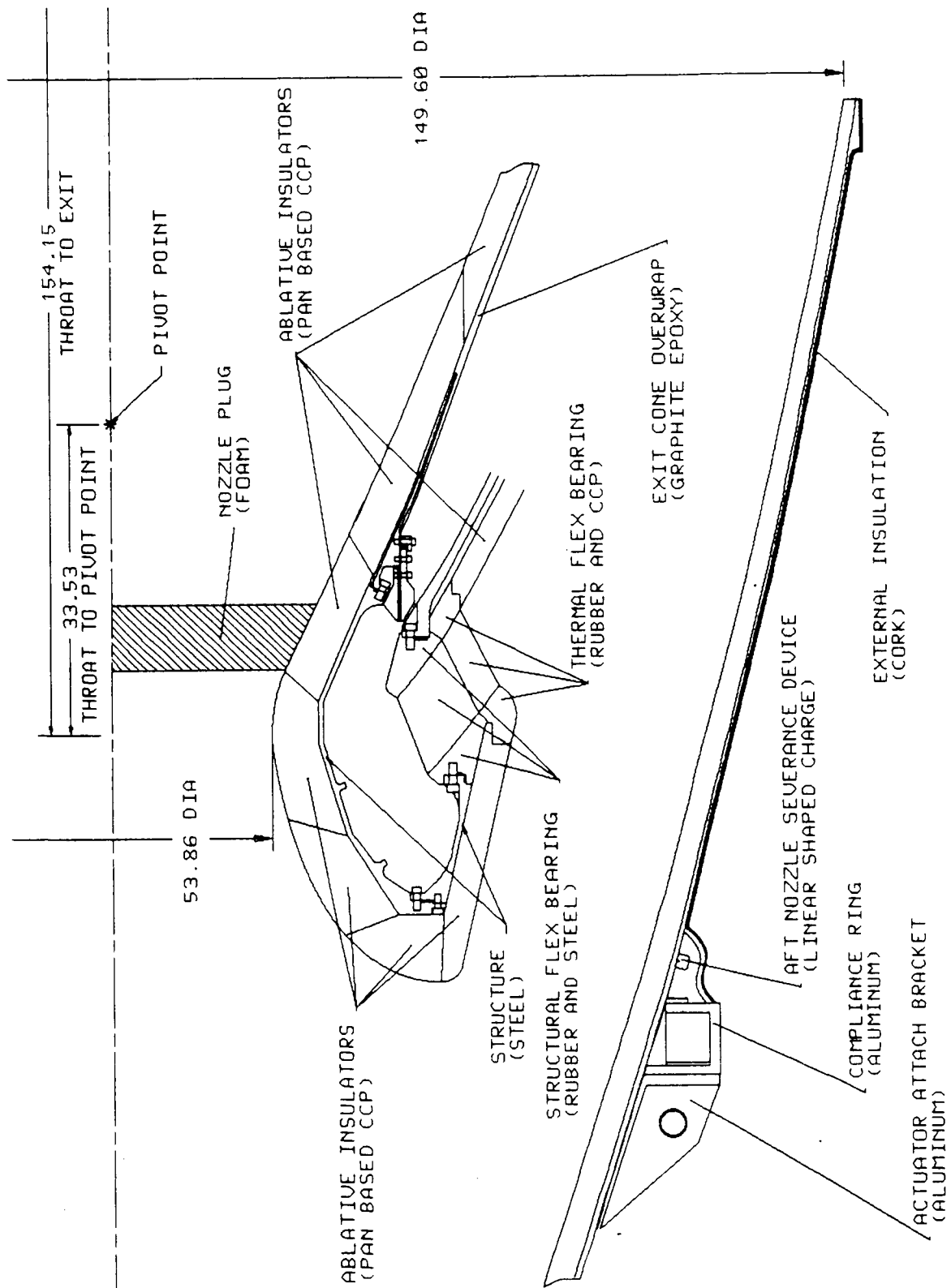


Figure 41. Block II SRM Nozzle

A foam nozzle plug protects the Block II SRM propellant from radiant and/or convective heating during SSME flight readiness firing tests or potential launch pad aborts.

The exit cone is covered with a layer of cork aft of the compliance ring for thermal protection from the SSME exhaust and from plume radiation and recirculation of the SRM exhaust.

#### **3.6.2.1 Flex Bearing**

The Block II nozzle structural flex bearing consists of a reinforced elastomer core and steel end rings. The core has eleven 0.220-in.-thick elastomer pads separated by ten, 0.327-in.-thick steel reinforcing shims. The shims, elastomer and end rings are vulcanized together to form the assembly shown in Figure 42. The end rings and reinforcing shims are fabricated from D6AC steel. The elastomer chosen for the Block II flex bearing is a polyisoprene formulation, DL-1514.

The thermal bearing consists of eleven 0.220-in.-thick pads of the same polyisoprene elastomer used in the structural bearing and ten 0.327-in.-thick reinforcing shims. The end rings and reinforcing shims are made of carbon-cloth phenolic. The shims, end rings, and elastomer are vulcanized together to form the assembly shown in Figure 42.

The snubber assembly (shown in Figure 41) is similar in design to the one used on the HPM nozzle. The snubber will limit axial travel of the nozzle to approximately 0.5-in. and will not interfere with vectoring the nozzle. The assembly contains provisions for shimming to obtain the clearances necessary to achieve the above-noted axial travel.

#### **3.6.2.2 Structures and Internal Seals**

The support structure of the Block II nozzle, other than the flex bearing and the exit cone overwrap, is made from D6AC steel. D6AC steel is used for some structural members in the HPM and RSRM nozzles. The structure is composed of the three members shown in Figure 43. This is one less structural member than in

ORIGINAL PAGE IS  
OF POOR QUALITY

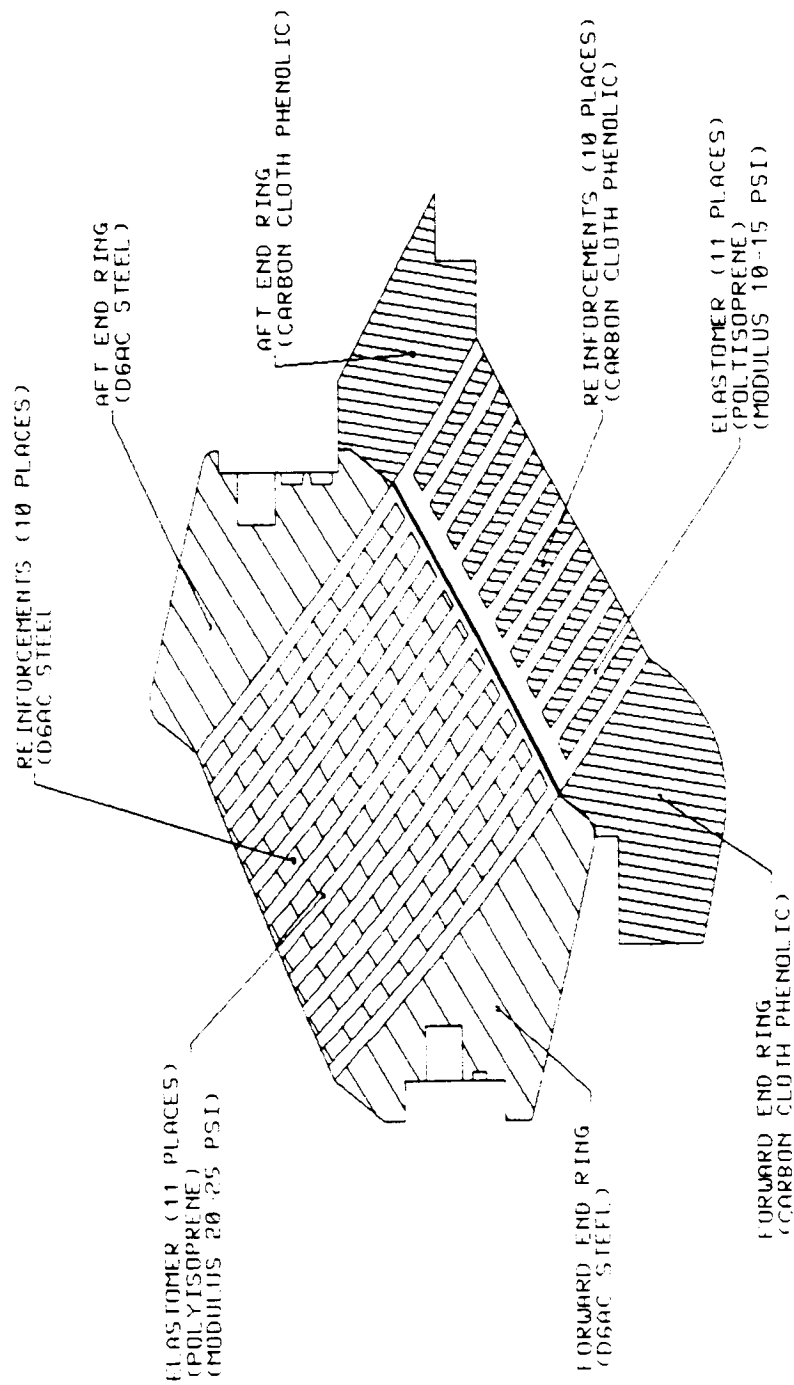


Figure 42. Block II Flex Bearing/Thermal Protection Configuration

ORIGINAL PAGE IS  
OF POOR QUALITY

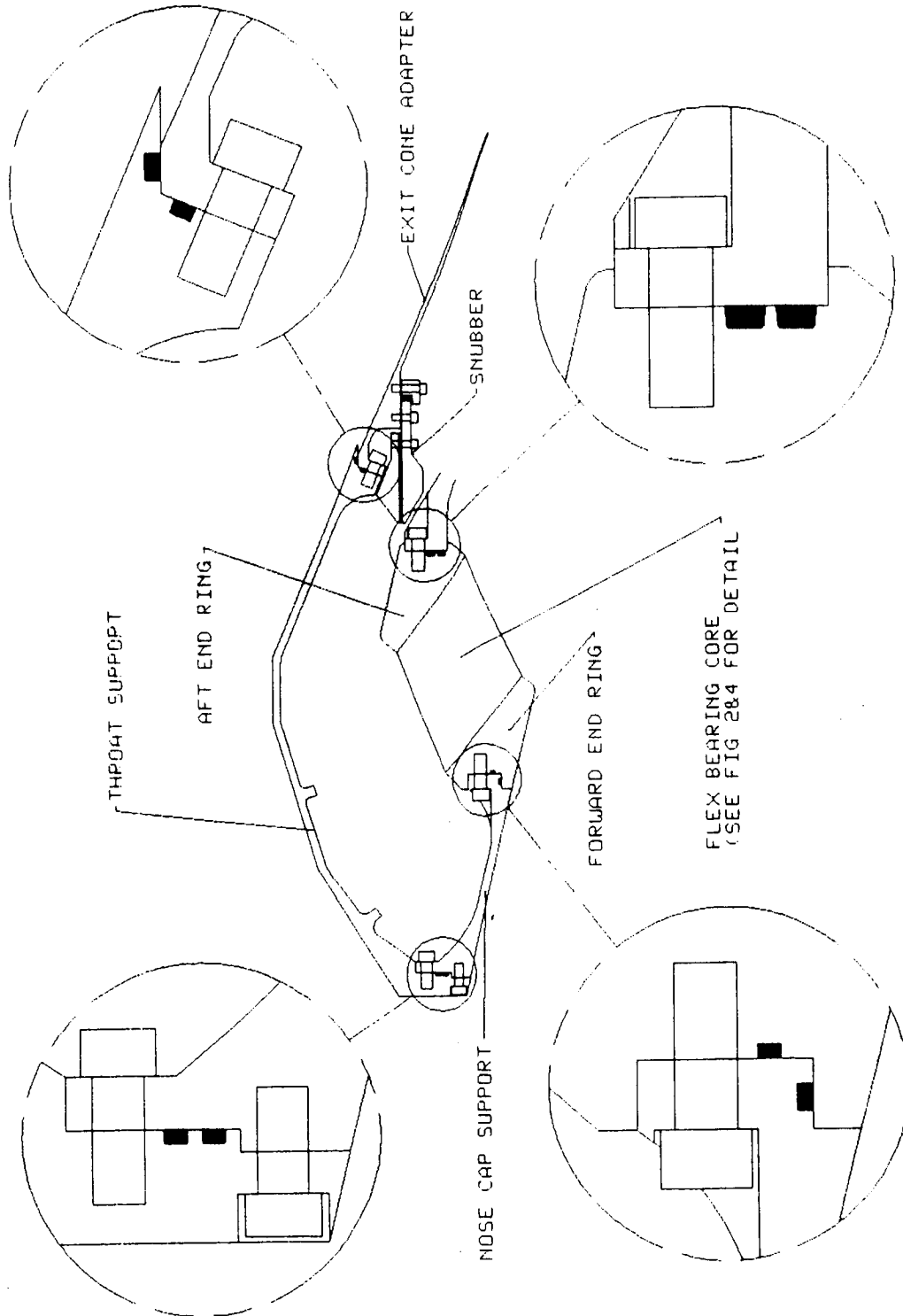


Figure 43. Block II Nozzle Structure and Internal Seals

the current nozzle. In addition to eliminating one member and one joint, the structure is simplified and contains no joints which connect more than two structural members. This has caused some problems in the HPM nozzle.

All joints are designed with redundant, verifiable seals as a requirement. Where possible, dual face seals are employed. At least one face seal is employed in all joints. Details of the joints/seals are shown in Figure 43.

The aluminum housing and glass phenolic overwrap exit cone structure used on the HPM nozzle has been replaced by a short steel adapter and a graphite epoxy, filament wound overwrap. The graphite epoxy consists of Hercules AS4, 12 thousand filament, graphite fibers impregnated with Fiberite 982 epoxy resin. This fiber/resin system is the same combination used on the Trident II (D-5) program. A similar system is also used on Trident I (C-4). Based on preliminary analysis, the required overwrap thickness at the exit plane is approximately 0.140 inches. This represents a thickness savings of 43.3 percent over the HPM design. The required overwrap thickness just aft of the compliance ring is 0.200 inches. This represents a thickness savings of 60 percent over the HPM design.

#### **3.6.2.3 Ablatives and Insulators**

PAN-based, carbon-cloth phenolic ablative materials have been selected for the Block II SRM nozzle. Standard density (~1.55-gm/cc) materials will be used in areas of high erosion such as the inlet, throat, and forward exit cone regions. Low density materials (~1.20-gm/cc) will be used in less erosive environments such as the nose cap, stationary shell, and aft exit cone. The low density materials have been shown to perform similarly to the standard density materials in these areas, yet represent over an 11 percent savings in the weight of the ablatives.

The standard density PAN-based materials proposed for the Block II SRM nozzle include both continuous PAN fiber and spun PAN fiber materials. The low-density materials are made of continuous PAN fibers in open weaves with microballoon fillers to yield densities in the range of 1.0 to 1.3 gm/cc. Multiple vendors are available for all of these PAN materials.

Based on available data, the spun PAN, continuous PAN, and low-density PAN materials have relatively equivalent material properties, although the spun PAN materials show superior erosion performance and char integrity.

Ply angles for the Block II ablative liners are chosen that emulate the ply angles of the RSRM ablative liners. The ply angle selection is based on studies<sup>(3)</sup> on the effect of ply angles on erosion and on manufacturing experience.

The aft portion of the exit cone is protected from SSME exhaust heating, and SRM plume radiation, and hot gas recirculation by the same cork TPS used on the HPM nozzle.

The nozzle plug is the same design as the HPM nozzle foam plug with the exception that the density of the foam is increased from 2 to 3 lb/ft<sup>3</sup> as it is for the RSRM nozzle plug.

### 3.6.3 DISCUSSION

#### 3.6.3.1 Flex Bearing

The design of the structural flex bearing for the Block II SRM nozzle (shown in Figure 44) is based on experience gained from the HPM flex bearing and several other systems, principally, the Peacekeeper and Trident I (C-4) and II (D-5) programs. Table 21 compares some of the pertinent design parameters for the Block II flex bearing to several other flex bearings currently in use.

---

<sup>3</sup>TWR-14360, Nose/Inlet (403/404) Preliminary Redesign Thermostructural Evaluations, 27 April 1981

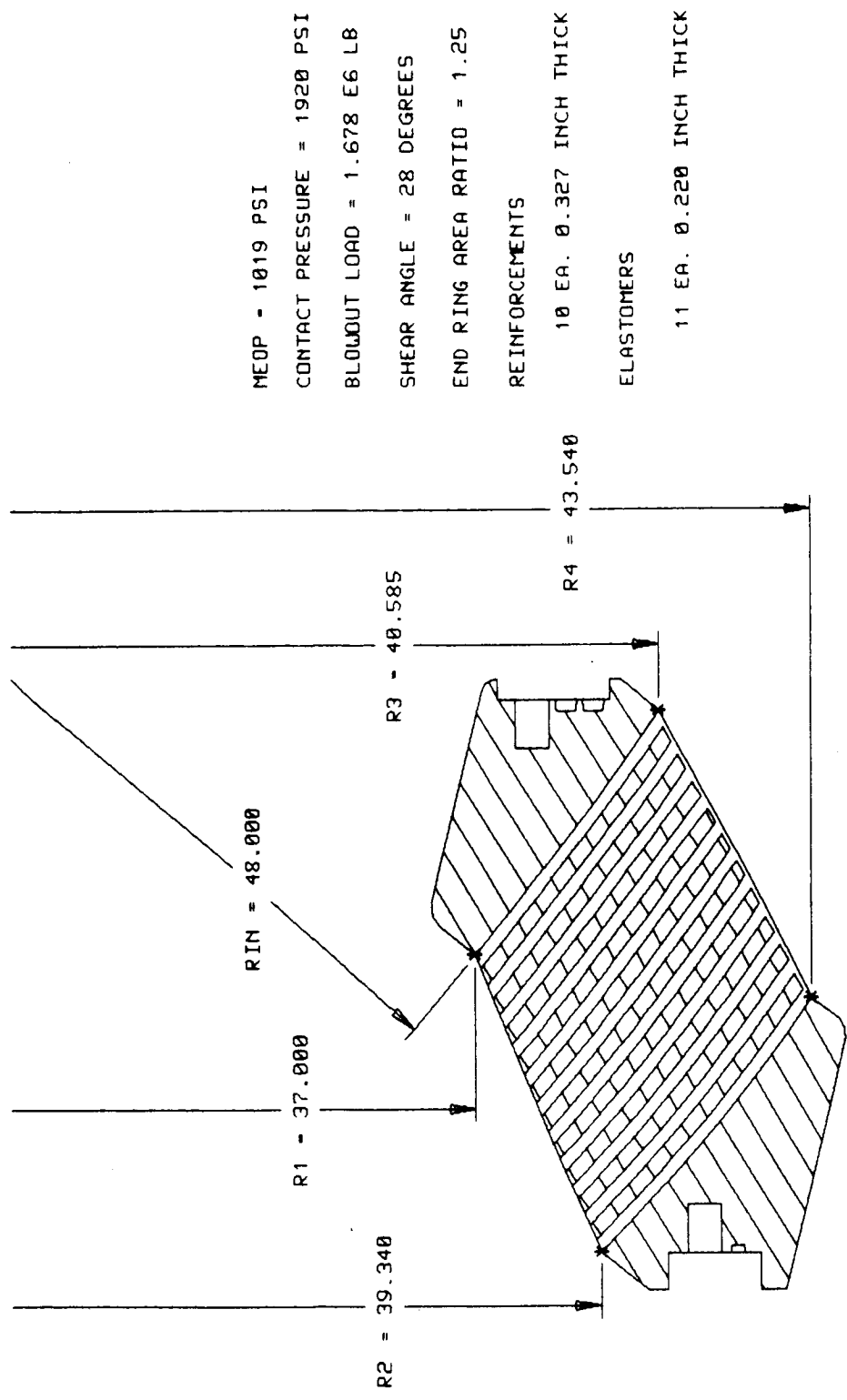


Figure 44. Structural Flex Bearing Design



**Table 21. Flex Bearing Design Parameters**

	<u>Blk II</u>	<u>HPM</u>	<u>PK</u>	<u>C-4</u>	<u>D-5</u>
Contact Pressure (psi)	1,920	1,630	3,160	3,580	2,700
Average Shear Strain* (%)	240	133	262	148	241
Shear Stress (psi)	385	222	550	580	500
$R_{in}/R_1$	1.29	1.11	1.58	1.27	1.27

---

\*Shear strain due to vectoring

All of the design parameters shown in Table 21 fall well within the demonstrated experience base. The shear stress and strain levels, while higher than on the HPM, are less than those demonstrated on other operating systems. Increasing the contact pressure slightly over the level used in the HPM flex bearing reduces the size of the bearing significantly. The contact pressure is increased by moving the flex bearing to a higher angle on the bearing envelope.

The  $R_{in}/R_1$  ratio (see Figure 44 for definition) in the table is a measure of the position of the flex bearing on the hemispherical envelope. A large ratio is a bearing near the pole; a value near 1.0 is a bearing near the equator (such as the HPM bearing). Increasing the angle of the bearing reduces the stresses in the bearing at a given load, making it possible to increase the design pressure.

The higher angle also makes attachment of a thermal protection system for the structural flex bearing easier and allows the use of a thermal protector which requires much less torque. All this is at the expense of the torque level of the flex bearing. Increasing the angle of the bearing requires increasing the spherical radius of the bearing and torque is proportional to the fourth power of the spherical radius. This increase in torque is partially offset by the reduced size of the bearing, and partially by the reduction in torque required for the thermal protection system.

The predicted torque levels for the Block II structural and thermal flex bearings are compared with the torque levels for the flex bearing and thermal

boot system used on the HPM in Table 22. The much lower total torque level of the system will allow use of the same TVA system for both flex bearings even though the moment arm is slightly reduced on the Block II system. Although the pivot point is moved aft 15.96 in. on the Block II bearing, the effect on the system is minimal. The moment arm is reduced by 5.8 percent and the required stroke is reduced by the same amount. Assuming that the actuator stall force is the same as on the current SRM, the maximum allowable torque for the Block II system would be  $4.16 \times 10^6$  in.-lb. The geometries of the two systems are shown in Figure 45.

**Table 22. Maximum Predicted Torque Comparison**

	<u>Maximum Torque (<math>\times 10^6</math> in.-lb)</u>	
	<u>Block II SRM</u>	<u>HPM</u>
Structural Flex Bearing	3.253	3.525*
Thermal Bearing or Boot	<u>0.677</u>	<u>1.707</u>
Total	3.930	5.232

---

\*Predicted value - Measured maximum is  $3.670 \times 10^6$  in.-lb

The higher angle of the flex bearing also increases its stiffness. The axial deflection is predicted to be approximately 80 percent of the HPM axial deflection of 1.0 in. at MEOP or 0.80 inch.

Because of the change in geometry of the flex bearing the movement of the pivot point under pressure and actuation forces will change also. The axial movement of the pivot point will be reduced by an amount proportional to the axial stiffness increase. The size of the radial pivot point box dimension will change due to several factors, principally the higher angle (increase), small size (increase), and thinner pads (decrease). The cumulative effect of these factors is to increase the size of the pivot point box in the radial direction by a factor of nearly 2.0.

Examination of the results of several HPM flex bearing bench tests revealed maximum pivot point movements of 0.75 in. forward, 1.25 in. aft, and +0.55 and -0.75 in. in the radial direction. Applying the above factors to these values

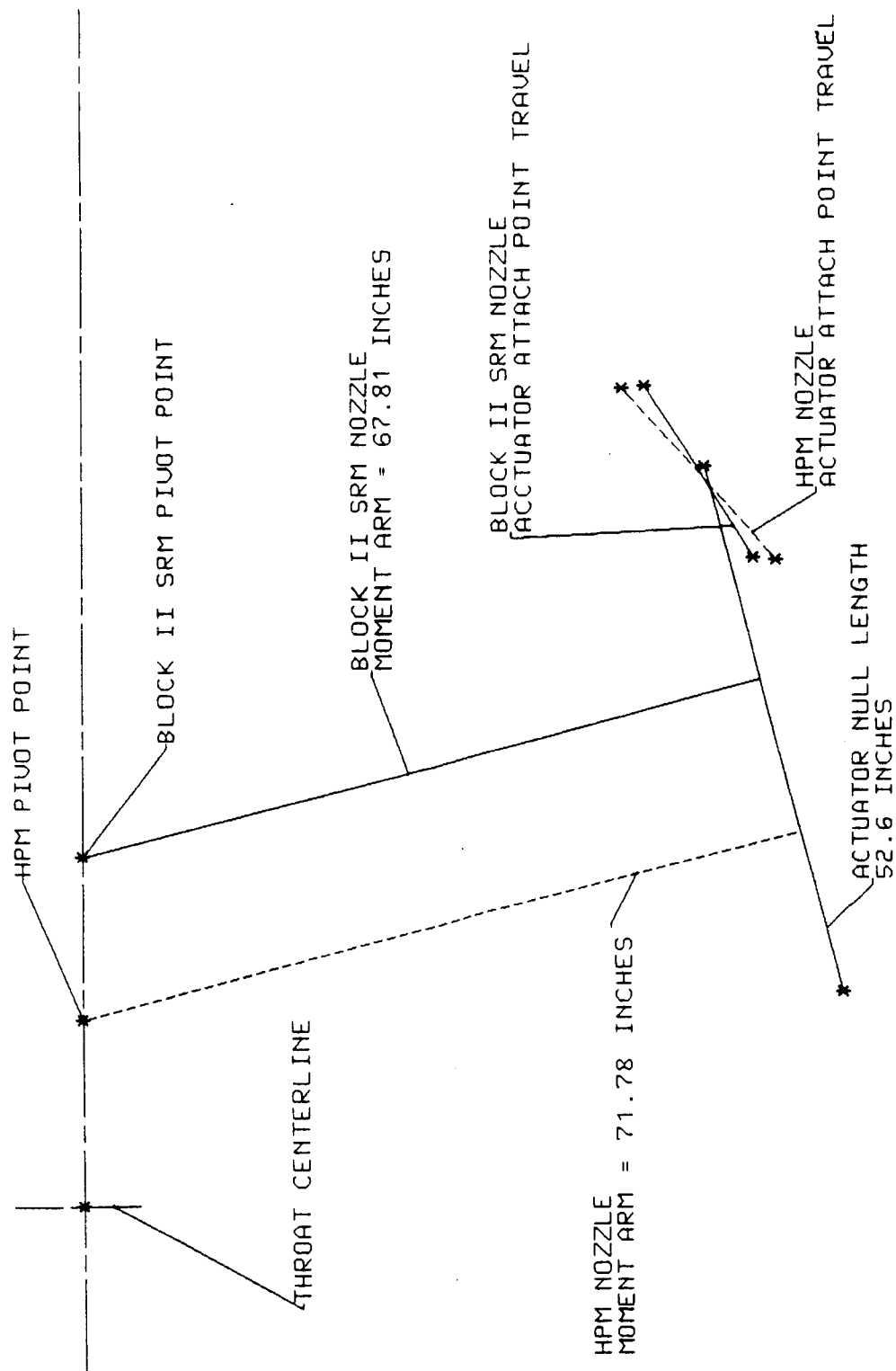


Figure 45. Geometry of Actuation

gives maximum axial pivot point shifts of 0.61 in. forward and 1.01 in. aft. The maximum radial shifts are +1.10 in. and -1.50 in., all of which comply with the current specification (STW7-2740[F]).

To satisfy concerns that moving the pivot point 15.96 in. aft would cause clearance problems, a vectored nozzle clearance study was conducted using CAD/CAM layouts of the Block II and HPM nozzles. The nozzles were vectored about their respective pivot points to the maximum allowable 8-deg vector angle and superimposed along with the ICD clearance envelope. Figure 46 shows the results of this clearance study.

Due to the pivot point moving aft, the Block II exit cone travels a smaller distance, providing greater clearance than on the HPM nozzle. The nose of the Block II nozzle is further from the pivot point than the nose of the HPM nozzle and moves a greater distance. However, due to its smaller size the vectored position of the Block II nozzle lies within the vectored position of the HPM nozzle.

The thermal protection flex bearing draws on experience gained in several strategic missile motor programs which utilize flex bearings made from composites.

For the thermal bearing a 2-D thermal analysis using the axisymmetric ablation and charring program (ASCHAR) was necessary due to the CCP/rubber-laminated structure of the component. The results of the analysis predicted 0.124 in. of erosion and 0.861 in. of char. This gives a margin of safety of 0.70 based on the required factors of  $2 \times \text{erosion} + 1.25 \times \text{char}$  and an initial thickness of 2.25 inches. There is an additional 0.25 in. of rubber on the inboard side of the thermal bearing which yields final temperatures at the interface between the two flex bearings of 85/212°F at end-of-burn/splashdown (113 sec/400 sec). The thermal analysis procedure is described at the end of Section 3.6.3.3.

The carbon-cloth phenolic reinforcements selected for this bearing will not support the same stress levels as the steel reinforcements in the structural flex bearing. To reduce the amount of load that the thermal protection flex bearing

ORIGINAL PAGE IS  
OF POOR QUALITY

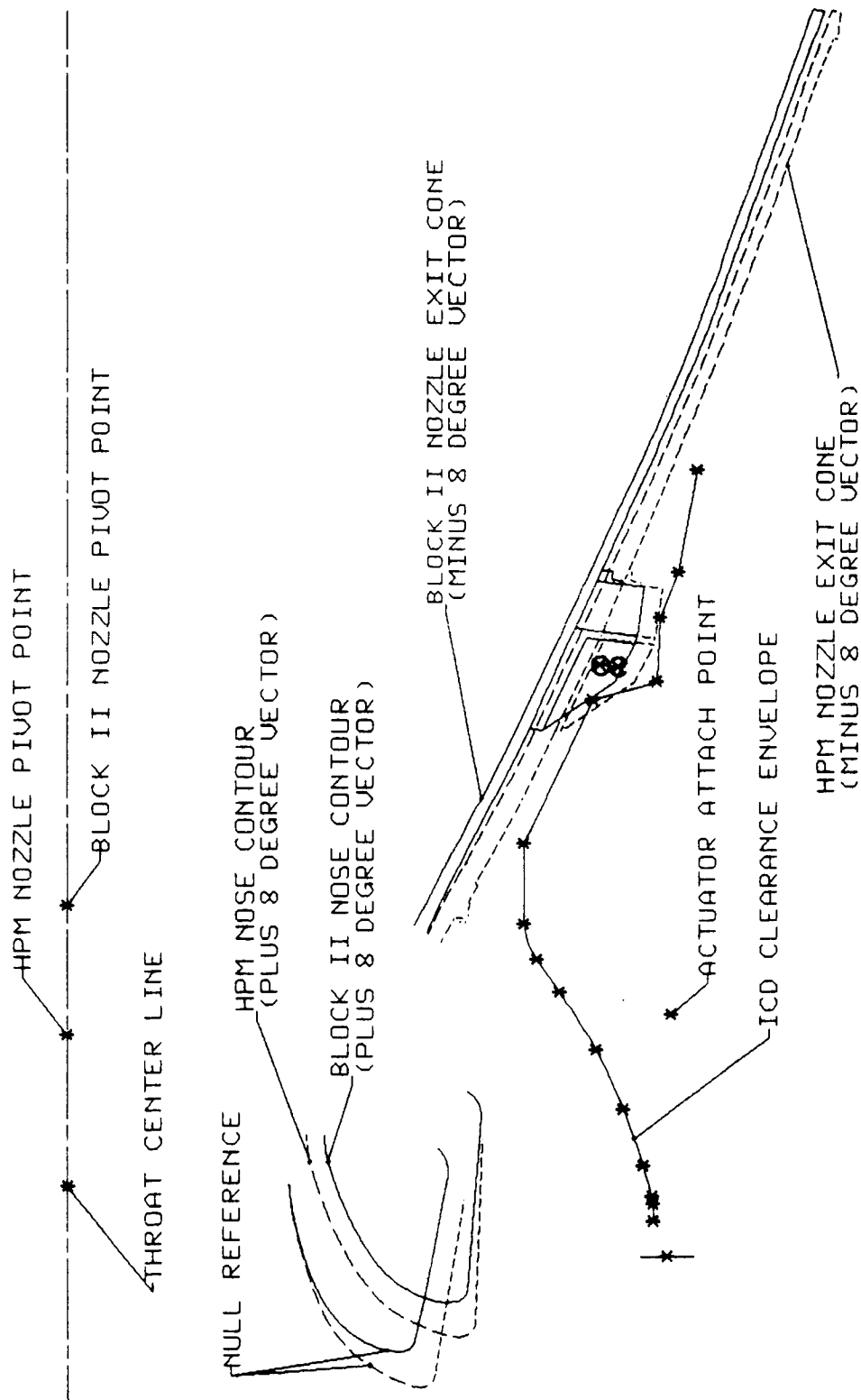


Figure 46. Vectored Nozzle Clearance

is required to support, the modulus of the elastomer will be lowered to approximately half that of the structural bearing elastomer. This will be accomplished by vulcanizing the structural bearing assembly at an elevated temperature (320° versus 290°F for the thermal bearing). This will also serve to reduce the torque which is needed to actuate the thermal protection flex bearing.

The overall flex bearing/thermal protection system is significantly lighter than the HPM flex bearing/thermal boot system, as shown in Table 23.

**Table 23. Flex Bearing Weight Comparison**

	<u>Weight (lb)</u> <u>Block II SRM</u>	<u>HPM</u>
Structural Flex Bearing	3390	7026
Thermal Bearing or Boot	<u>440</u>	<u>1280</u>
Total	3830	8305

A flex bearing operates by deforming the elastomer pads in shear. To perform over a broad temperature range the elastomer must have stable shear properties over that temperature range. Figure 47 is a comparison of the shear modulus of the polyisoprene elastomer chosen for use in the Block II flex bearing and the current natural rubber elastomer as a function of ambient temperature. The natural rubber elastomer is temperature sensitive and subject to strain-induced crystallization at temperatures below 45°F. Polyisoprene is less sensitive to temperature and is unaffected by strain-induced crystallization to temperatures well below the minimum operational temperature for the Block II SRM.

Table 24 compares the mechanical properties of the polyisoprene elastomer used in the Block II flex bearing to the natural rubber elastomer used in the HPM nozzle flex bearing. Polyisoprene is equivalent or superior in all areas. The superior mechanical properties and superior temperature performance led to the selection of the polyisoprene for the Block II flex bearing.

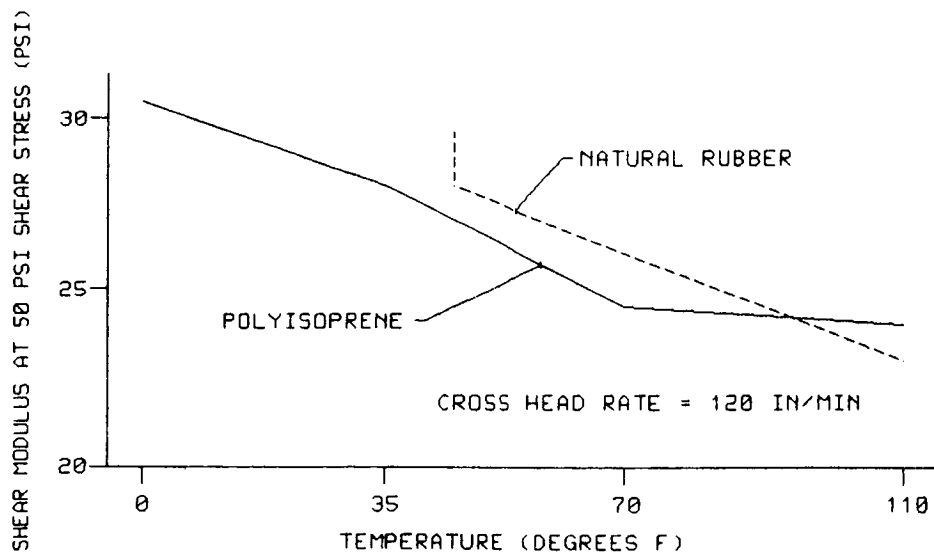


Figure 47. Elastomer Temperature Sensitivity

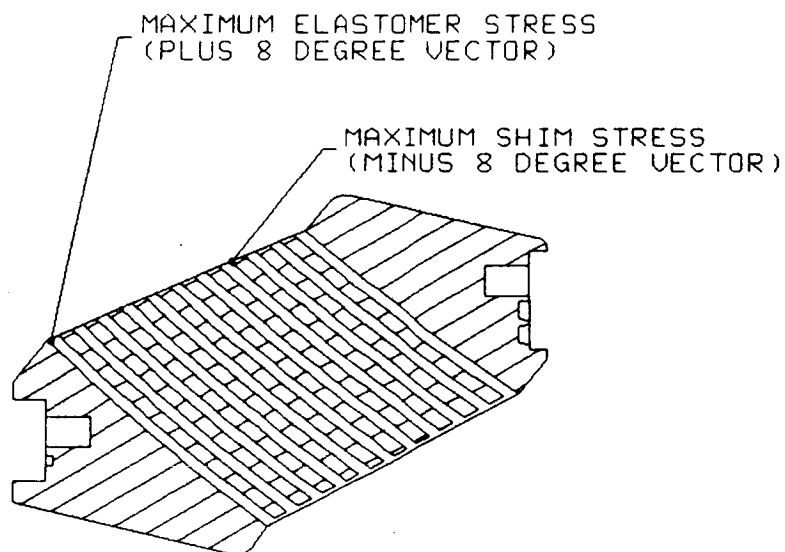


Figure 48. Maximum Stress Locations

**Table 24. Elastomer Shear Properties**

	<u>Modulus (psi)</u>	<u>Ult Stress (psi)</u>	<u>Ult Strain (%)</u>
Natural Rubber -- 0.5 ipm	22.2	740	950
-- 120 ipm	25.9	780	1,115
Polyisoprene Rubber -- 0.5 ipm	20.5	930	1,280
-- 120 ipm	25.0	960	1,280

<sup>1</sup>Shear modulus at 50 psi shear stress

<sup>2</sup>All data at ambient temperature

A preliminary structural analysis of the Block II structural flex bearing was conducted using TASS routine SGA01. SGA01 is an axisymmetric finite element model developed to analyze flex bearings. The flex bearing core is modeled using a fixed aft boundary and a radially restrained plate on the forward boundary. Analyses were conducted for null and maximum positive and negative vectored cases. Table 25 gives a brief summary of the worst-case stress predictions of this analysis along with minimum margins of safety at the locations shown in Figure 48.

**Table 25. Flex Bearing Analysis Results**

<u>Component</u>	<u>Stress</u>	<u>Mode</u>	<u>Margin of Safety</u>
Elastomer	385 psi	In-Plane Shear	0.30
Shims	137 ksi	Hoop Compressive	0.02

The quoted margins of safety are based on the 1.4 factor of safety required for structural members which can be proof tested. Predicted axial deflection of the flex bearing at MEOP is 0.507 inch.

### **3.6.3.2 Structures and Internal Seals**

**Steel Structure.** The steel structure of the Block II nozzle was designed to be as simple and lightweight as possible while maintaining the structural integrity of the nozzle (Figure 43).



After the inlet and exit contours were generated, a heat transfer analysis was conducted to determine necessary ablative and insulation thicknesses and thereby establish the inner boundary of these materials. Once this surface had been established the supporting structure was designed to minimize excess weight, while maintaining positive margins of safety under maximum conditions of the two load sources. The two load sources are the internal motor pressure and the nozzle vectoring loads.

An initial analysis was conducted to confirm the integrity of the structural components of the nozzle. The nozzle was modeled using TASS, Morton Thiokol's in-house axisymmetric finite element code. The finite element grid used in the analysis is shown in Figure 49. To ensure conservative results, the phenolic materials were modeled using low stiffnesses and high Poisson's ratios. The effect of this is that the pressure load is transferred to the structural components with the phenolics providing no structural support. A chamber pressure of 1,019 psi, the MEOP for the aft end of the motor, was used.

To determine the net axial and shear loads that the bolted interfaces must support, single-bolt elements were placed in the finite element model joining the appropriate components. The material model used for the bolt elements was the same as that used for steel, with a low hoop modulus. Pivot elements capable of supporting only normal compressive loads were placed on the inner and outer diameters of each interface.

The stresses for the forward and aft end rings were increased by a factor of 2.0 to account for the increase in stress due to vectoring.

The results of the analysis show that the structural components of the nozzle meet the required factors of safety. The minimum factors of safety are summarized in Figure 50 and Table 26. These safety factors were calculated using the uniaxial equivalent stress and an ultimate strength of 195 ksi. A minimum factor of safety of 1.4 is required for the forward and aft end rings, since these components can be proof tested. All other components require a minimum factor of safety of 2.0.

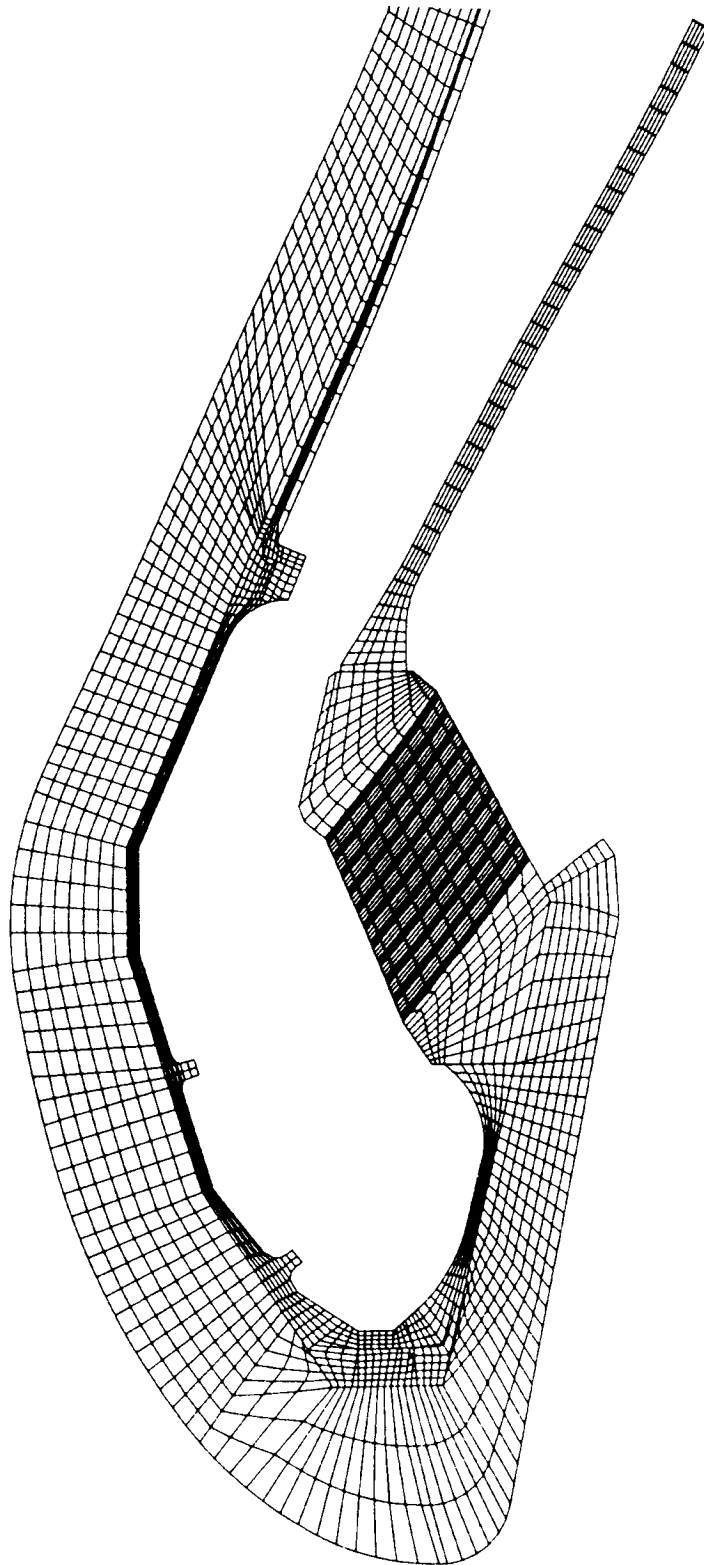


Figure 49. Finite Element Grid

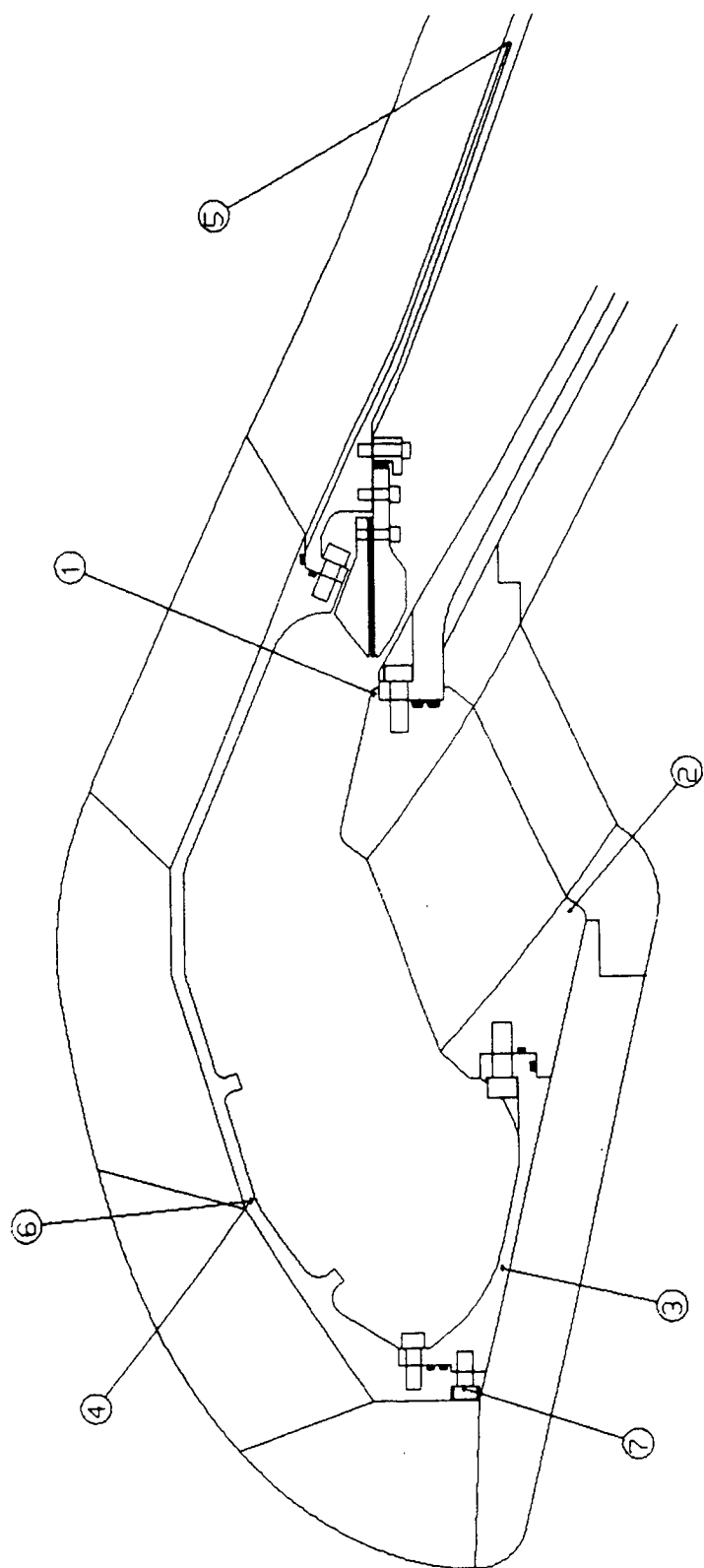


Figure 50. Minimum Factor of Safety Locations

The maximum predicted strain for the support structure adjacent to the phenolic components was used with the room temperature carbon-cloth fiber strain allowable to calculate a factor of safety. The resulting safety factor is equal to 6.85, and demonstrates that no excessive deformation occurs in the structure.

The results of the analysis show that all of the bolts, with the exception of those at the outer diameter of the forward interface, are loaded in compression. Since the shear loading in the bolts is limited by the diametrical tolerances of the mating components, the factor of safety for those bolts loaded in compression is dependant only on the preload torque. It is recommended that one-hundred 3/8-in., 180-ksi bolts be used in each location. The resulting factor of safety for the bolts loaded in tension is 7.38.

**Table 26. Minimum Factors of Safety**

<u>Location</u>	<u>Stress (psi)</u>	<u>Strain (in./in.)</u>	<u>Factor of Safety</u>
1	101200		1.93
2	65100		2.99
3	73950		2.64
4	72560		2.69
5	84925		2.30
6		0.0020	6.85
7	24440		7.38

**Internal Seals.** All internal nozzle seals were designed with dual O-rings using dual face seals where possible and at least one face seal in all cases (Figure 43). A more detailed structural analysis must be conducted to determine joint deflections to confirm that the selected seal arrangements will perform as intended.

The aft end ring-to-stationary shell joint uses two face seals located inboard of the bolt circle. Placing both seals inboard of the bolts eliminates the need for Stat-O-Seals<sup>®</sup> on the bolts and reduces the number of seals required. The line of action of the stationary shell was selected to minimize joint rotation during motor pressurization and vectoring; however, a more detailed analysis is needed to confirm actual joint rotations.

The forward end ring-to-nose cap support joint presents the greatest challenge from a sealing standpoint. There is a limited amount of room in which to place the seals and it is much more difficult to vary the line of action of the joint to minimize deflections. One face seal and one diametral seal are employed on this joint. By using large diameter seals and a double shear lip to limit radial deflections of the two structures relative to one another, a high degree of confidence in the joint is obtained.

The nose cap support-to-throat support joint uses two face seals captured between two concentric bolt rings. This design minimizes joint deflection and gives a high degree of confidence.

The throat support-to-exit cone adapter joint also has limited room to place seals. One diametral seal and one angled face seal is used on this joint. The location of the joint in a relatively low stress area and the close proximity of the seals to the bolt ring give a high degree of confidence in the seal integrity.

**Exit Cone Support Structure.** A graphite epoxy, filament wound exit cone overwrap has been selected as the structural material for the SRM Block II exit cone. This selection is based on a reduced nozzle weight, savings in performance, and on Trident I and II experience.

The exit cone support structure is shown in Figure 51. The graphite epoxy overwrap is attached to the steel throat support using an adapter that is integrally wound and cured into the structure. The compliance ring for the TVC is the same design used on the current SRM nozzle and is integrated in the same manner. A graphite epoxy stiffener ring at the exit plane will consist of a buildup of hoop ply layers.

The structure will have a minimum of four dual polar layers (one polar layer equals two plies). The thickness of the graphite epoxy will be controlled by varying the number of hoop plies applied (a minimum of four hoop plies). Based on preliminary analysis<sup>(4)</sup> the required overwrap thickness at the exit plane is approximately 0.140 in. (polar layers = 0.080 in., hoop layers = 0.060 in.). The required overwrap thickness just aft of the compliance ring is approximately

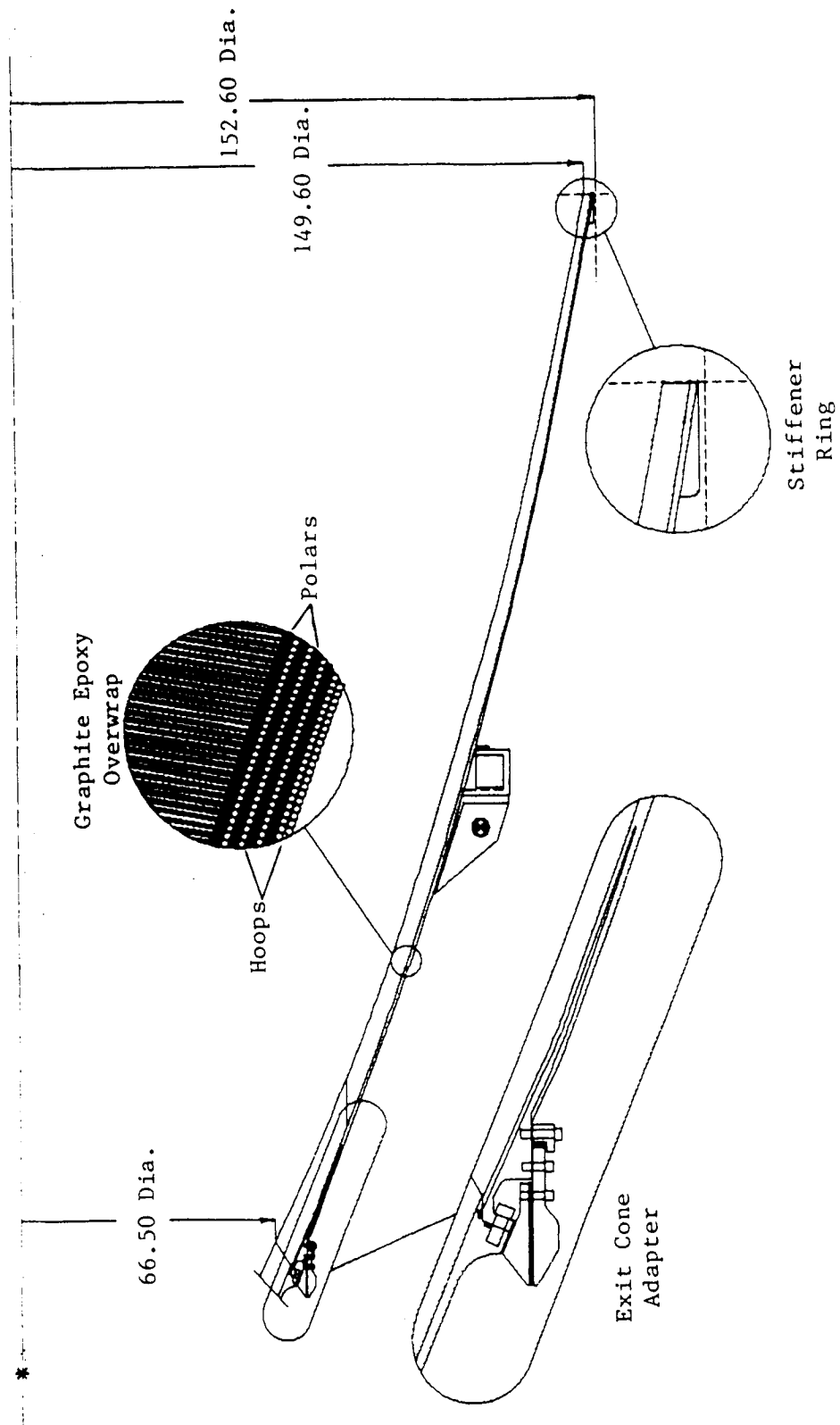


Figure 51. Graphite Epoxy Overwrap Design

0.200 in. (polar layers = 0.140 in., hoop layers = 0.060 in.). These represent a thickness savings of 43 percent and 60 percent over the HPM design and a weight savings of at least 50 percent if the thicker, heavier glass phenolic were to be used. Additional analysis needs to be performed to define the required filament wound overwrap thickness in the adapter region and to verify the preliminary aft exit cone overwrap thickness.

The reduced thickness is also important because the aft exit cone ablative thickness must be increased to assure meeting erosion and char requirements and to counteract the elimination of the glass phenolic insulation. With a thinner support structure, the erosion, char, and temperature requirements can be met without sacrificing performance due to a reduced exit diameter (the inner diameter contour of the Block II design is the same as the HPM nozzle contour).

The graphite epoxy system selected for use on the Block II design is an AS-4 (Hercules) graphite fiber impregnated with a Fiberite 982 epoxy resin system. The laminate will have a fiber volume fraction greater than 55 percent, a resin content of approximately 33 percent and a cured density of 1.55 gm/cc. The selection was based on static test results, fabrication studies, and analyses conducted on the graphite epoxy system during the NASA "Alternate Nozzle Ablative Materials Program."<sup>(5)</sup> This system was selected because analysis showed it to have the lowest required thickness and highest margin of safety, it performed well in a subscale static test environment, and because of the experience base developed from its use on Trident II.

A short review of the trade study,<sup>(4)</sup> conducted during the early stages of this program, comparing the various graphite epoxy systems -- AS4/982, Hitex/E742 and T300/Epoxy -- follows.

---

<sup>4</sup>"SRM Block II Trade and Design Studies, Nozzle," TWR-32667-07, 4 November 1986.

<sup>5</sup>"Alternate Nozzle Ablative Materials Program," JPL Publication 84-58, 1 September 1984.

**Static Test Evaluation** - An AS4/982, filament wound, graphite epoxy exit cone structure was tested on a JPL nozzle during the NASA Alternate Materials Program. Post-test inspection showed that the graphite epoxy overwrap on the exit cone liner was totally intact and unaffected by the internal or external environments.

**Fabrication Study** - Two graphite epoxy systems were evaluated for their fabrication and processing ease and laminate properties. The first was the AS4/982 system. The other was Hitex, 12K fiber impregnated with USP E742 epoxy resin. Laminates of both materials were filament wound on flat aluminum mandrels and autoclave cured for 1 hour at 176°F and 8 hours at 200°F. Test specimens were machined from these laminates and tested for mechanical properties at room temperature and at 250°F. Results showed that at room temperature the Fiberite system had slightly higher longitudinal tensile and compressive strengths. The shear strengths of the two materials were similar. At the elevated temperature the Fiberite system showed considerably higher material strengths in all directions.

**Analysis** - The original analysis on the graphite epoxy overwrap structure was conducted using the HPM nozzle design. These numbers can be translated easily to the Block II design because the forward and aft exit cone overwrap contours are similar to the HPM design.

The thickness required for the AS4/982 system was compared with the thickness required for a T300/epoxy system. These required thicknesses were also compared with the HPM glass phenolic thickness. The comparisons were conducted on the free standing portion of the exit cone (from the LSC to the aft exit plane) using equivalent stiffness matrices comparisons to determine the required thickness of the replacement material.

Both graphite epoxy systems showed major reductions in required thickness and weight over the glass phenolic system. The AS4/982 laminate showed slightly better improvement than the T300/epoxy system because of its higher stiffness and lower density (1.412 gm/cc versus 1.744 gm/cc). The overwrap stress analysis results, also comparing AS4/982 to T300/epoxy, showed significant positive margins of safety (based on a safety factor of 1.4) for both systems.



### **3.6.3.3 Ablatives and Insulators**

**Ablatives.** PAN-based, carbon-cloth phenolic ablative materials are selected for the Block II SRM nozzle design to: 1) increase the nozzle performance by reducing erosion in the throat, 2) optimize the Shuttle payload by using lightweight PAN materials wherever possible, and 3) avoid the delamination and pocketing erosion anomalies experienced earlier with the rayon-based, carbon-cloth phenolic materials.

At this stage of the project, the best selections for each area of the exit cone are: 1) a spun PAN inlet, throat, and forward exit cone for increased performance by reducing erosion and 2) a low-density PAN nose, stationary shell, and aft exit cone liner for reduced nozzle weight and increased payload. Figure shows the location of each of the ablative liner rings and the material selection for each. Continuous PAN materials are alternates to the spun PAN materials until additional material property data and processing evaluations can be obtained. A description of the alternate PAN-based materials follows:

#### **Spun PAN**

- |         |   |
|---------|---|
| K411    | This Fiberite Corporation material is a phenolic resin-impregnated, balanced, eight-harness, satin weave fabric. The phenolic resin contains 5-16 percent by weight carbon powder filler. The carbon fabric is a product of Stackpole Fibers Co., known as Panex SWB-8. The fabric is woven from carbon yarn PANEX 30Y/800d which is made by spinning long staple PAN filaments prior to carbonization. |
| FM5834A | This U.S. Polymeric material is a phenolic resin-impregnated, balanced, eight-harness, satin weave fabric. The phenolic resin contains 13-18 percent by weight carbon powder filler. The carbon fabric is a product of Polycarbon Incorporated, designated PSCA. The fabric is woven from carbon yarn which is made by spinning long staple PAN fibers prior to carbonization.                          |

## **Low Density PAN**

**MX134LD** This Fiberite Corporation material is a phenolic resin-impregnated, open plain weave fabric. The 38-44 percent by weight rubber (NBR), butadiene-acrylonitrile, modified phenolic resin contains 10-13 percent by weight carbon microballoon filler. The fabric is a plain weave with Union Carbide T300 Grade WYP 30-1/0 carbon yarn. The yarn contains 3,000 filaments that are made by carbonizing PAN continuous filament.

**FM5908** This U. S. Polymeric material is a phenolic resin-impregnated, mock Leno weave fabric. The phenolic resin contains 10 percent by weight carbon microballoon filler. The fabric is woven with three Hitco Hi-Tex carbon yarns. Each yarn contains 6,000 filaments that are made by carbonizing PAN continuous filament.

## **Continuous PAN**

**MX4961** This Fiberite Corporation material is a phenolic resin-impregnated, eight-harness, satin weave fabric. The phenolic resin contains no filler. The fabric is woven with Union Carbide T300 Grade WYP 30-1/0 carbon yarn. The yarn contains 3,000 filaments that are made by carbonizing PAN continuous filament.

**FM5879** This U. S. Polymeric material is a phenolic resin-impregnated, eight-harness, satin weave fabric. The phenolic resin contains 10-18 percent by weight carbon powder filler. The fabric is woven with Hitco's Hi-Tex carbon yarn. The yarn contains 3,000 filaments that are made by carbonizing PAN continuous filament.

The selection of low-density and spun PAN materials for use in the Block II SRM is reinforced by thermal analysis. Comparisons of predicted erosion and char depths were made using the Block II design configuration. Predictions are made based on material data available on FM5908 (low density PAN material) and K411 (spun PAN material) and are compared with predictions based on FM5055 (baseline rayon) material properties.

The low-density material and the rayon material were compared in the nose cap. Predictions indicate that the low density material will erode 32 percent deeper than the rayon material, but the char depth of the low-density material is considerably lower and the required material thickness ( $2 \times \text{erosion} + 1.25 \times \text{char}$ ) for the low-density PAN is 22 percent less. Based on experience with the Alternate Materials Program,<sup>(5)</sup> the erosion and char of the low-density PAN in the aft exit cone will be similar to that of the rayon.

The spun PAN- and rayon-based material comparisons indicate that the spun PAN required thickness ( $2E + 1.25C$ ) is, on average, only 3 percent less than the rayon material, but the lower erosion and proven superior char integrity of the spun PAN makes it a better selection for the high-erosion regions of the Block II design. A 4 percent decrease in erosion was used for calculations with the PAN material. This is a conservative assumption since test data show 13 to 22 percent less erosion with PAN materials.

Erosion, char, and temperature predictions at several locations (see Figure 52) for a definition of station locations) on the stationary shell and along the nozzle contour are shown in Table 27. Stations 1 to 5 in the nose cap, Stations 15 to 18 in the aft exit cone, and the stationary shell were modeled using FM5908 material properties. The remaining stations were modeled using K411 material properties. Positive margins of safety for erosion and char are predicted at all locations based on designed ablative thicknesses.

All steel temperatures at the end-of-burn/splashdown (400 sec) are within the specified requirements of  $+10^{\circ}\text{F}$  rise/ $450^{\circ}\text{F}$ , respectively. The graphite epoxy temperature requirements were set at  $350^{\circ}\text{F}$  at 400 sec based on experience and a predicted cure temperature of  $300^{\circ}\text{F}$ ; however, the limit on the graphite epoxy temperature may be reduced pending processing study results conducted during the D&V phases of this program. The 400-sec graphite epoxy temperatures at Stations 17 and 18 are not applicable because the severance of that portion of the exit cone is soon after the end of burn. Details of the thermal analysis procedure are presented at the end of this section.

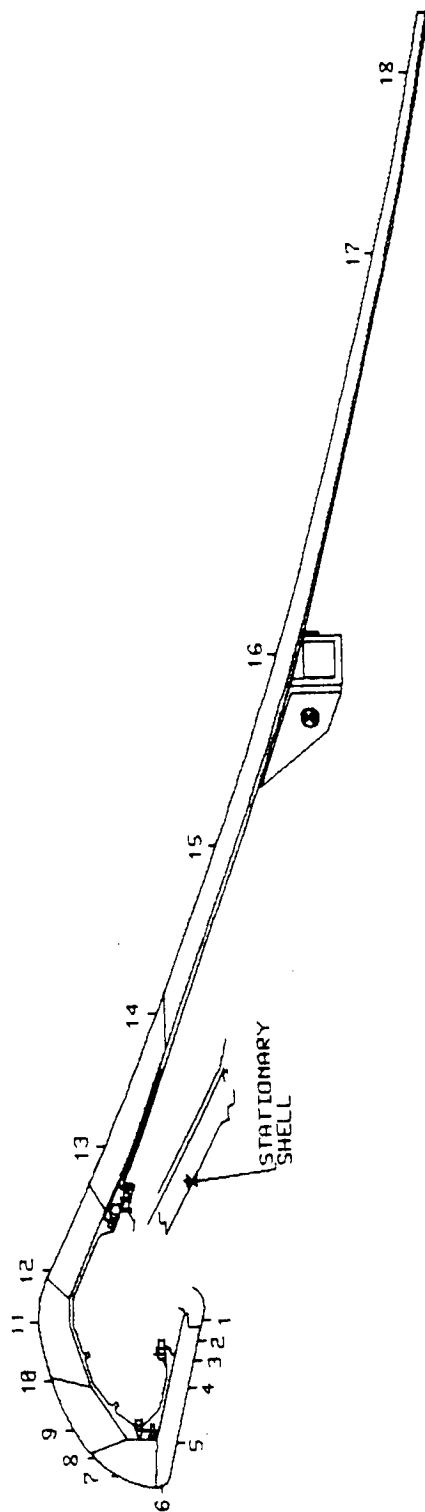


Figure 52. Thermal Analysis Station Locations

The low-density material and the rayon material were compared in the nose cap. Predictions indicate that the low density material will erode 32 percent deeper than the rayon material, but the char depth of the low-density material is considerably lower and the required material thickness ( $2 \times \text{erosion} + 1.25 \times \text{char}$ ) for the low-density PAN is 22 percent less. Based on experience with the Alternate Materials Program,<sup>(5)</sup> the erosion and char of the low-density PAN in the aft exit cone will be similar to that of the rayon.

The spun PAN- and rayon-based material comparisons indicate that the spun PAN required thickness ( $2E + 1.25C$ ) is, on average, only 3 percent less than the rayon material, but the lower erosion and proven superior char integrity of the spun PAN makes it a better selection for the high-erosion regions of the Block II design. A 4 percent decrease in erosion was used for calculations with the PAN material. This is a conservative assumption since test data show 13 to 22 percent less erosion with PAN materials.

Erosion, char, and temperature predictions at several locations (see Figure 52) for a definition of station locations) on the stationary shell and along the nozzle contour are shown in Table 27. Stations 1 to 5 in the nose cap, Stations 15 to 18 in the aft exit cone, and the stationary shell were modeled using FM5908 material properties. The remaining stations were modeled using K411 material properties. Positive margins of safety for erosion and char are predicted at all locations based on designed ablative thicknesses.

All steel temperatures at the end-of-burn/splashdown (400 sec) are within the specified requirements of  $+10^{\circ}\text{F}$  rise/ $450^{\circ}\text{F}$ , respectively. The graphite epoxy temperature requirements were set at  $350^{\circ}\text{F}$  at 400 sec based on experience and a predicted cure temperature of  $300^{\circ}\text{F}$ ; however, the limit on the graphite epoxy temperature may be reduced pending processing study results conducted during the D&V phases of this program. The 400-sec graphite epoxy temperatures at Stations 17 and 18 are not applicable because the severance of that portion of the exit cone is soon after the end of burn. Details of the thermal analysis procedure are presented at the end of this section.

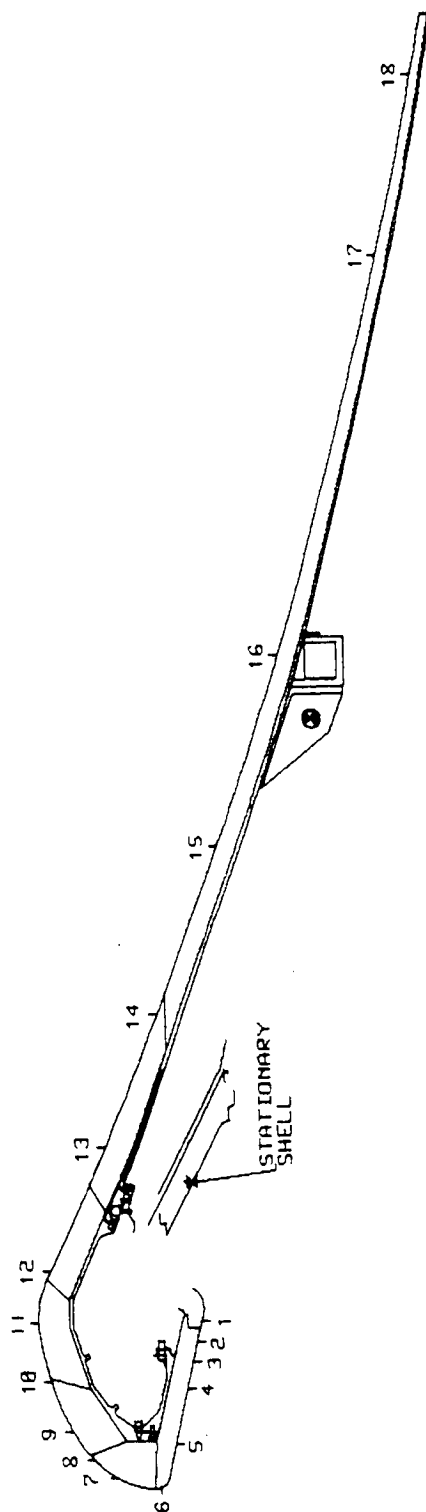


Figure 52. Thermal Analysis Station Locations

The low-density material and the rayon material were compared in the nose cap. Predictions indicate that the low density material will erode 32 percent deeper than the rayon material, but the char depth of the low-density material is considerably lower and the required material thickness ( $2 \times \text{erosion} + 1.25 \times \text{char}$ ) for the low-density PAN is 22 percent less. Based on experience with the Alternate Materials Program,<sup>(5)</sup> the erosion and char of the low-density PAN in the aft exit cone will be similar to that of the rayon.

The spun PAN- and rayon-based material comparisons indicate that the spun PAN required thickness ( $2E + 1.25C$ ) is, on average, only 3 percent less than the rayon material, but the lower erosion and proven superior char integrity of the spun PAN makes it a better selection for the high-erosion regions of the Block II design. A 4 percent decrease in erosion was used for calculations with the PAN material. This is a conservative assumption since test data show 13 to 22 percent less erosion with PAN materials.

Erosion, char, and temperature predictions at several locations (see Figure 52) for a definition of station locations) on the stationary shell and along the nozzle contour are shown in Table 27. Stations 1 to 5 in the nose cap, Stations 15 to 18 in the aft exit cone, and the stationary shell were modeled using FM5908 material properties. The remaining stations were modeled using K411 material properties. Positive margins of safety for erosion and char are predicted at all locations based on designed ablative thicknesses.

All steel temperatures at the end-of-burn/splashdown (400 sec) are within the specified requirements of  $+10^{\circ}\text{F}$  rise/ $450^{\circ}\text{F}$ , respectively. The graphite epoxy temperature requirements were set at  $350^{\circ}\text{F}$  at 400 sec based on experience and a predicted cure temperature of  $300^{\circ}\text{F}$ ; however, the limit on the graphite epoxy temperature may be reduced pending processing study results conducted during the D&V phases of this program. The 400-sec graphite epoxy temperatures at Stations 17 and 18 are not applicable because the severance of that portion of the exit cone is soon after the end of burn. Details of the thermal analysis procedure are presented at the end of this section.



Figure 52. Thermal Analysis Station Locations



Table 27. Rayon and PAN Mechanical Property Data

MATERIAL WITH PLY PROPERTIES	Units	Temp(°F)	Rayon		K411		MF5834A		MX134		FM5908		MX4961		FM5879	
			Rayon	Spun PAN	Spun PAN	Spun PAN	Spun PAN	Spun PAN	LDPAN	LDPAN	LDPAN	LDPAN	Cont. PAN	Cont. PAN	Cont. PAN	Cont. PAN
TENSILE MODULUS	Msi	70 1,000	2.5 0.98(2)	5.76 2.72	2.8 --	4.69 --	3.67 --	8.8 --								
TENSILE STRENGTH	ksi	70 1,000	16.2 7.0(2)	29.5 11.7	15.8 --	40.05 --	19.9 --	71.75 --								
COMPRESSIVE MODULUS	Msi	70 1,000 2,500	2.6 1.2(1) --	5.3 2.9 3.8	4.3 -- --	5.12 -- --	3.89 -- 1.35	9.8 -- --							6.6 -- --	
COMPRESSIVE STRENGTH	ksi	70 1,000 2,500	42.7 8.2(1) --	25.0 3.45 8.0	29.8 -- 8.6	36.45 -- --	17.67 -- 2.23	44.35 -- --							32.1 -- --	
ACROSS PLY PROPERTIES																
TENSILE MODULUS	Msi	70 1,000 2,500	2.24 0.68 0.01	0.95 0.14 --	1.4 -- 0.2	0.90 -- --	-- -- --	-- -- --							-- -- --	
TENSILE STRENGTH	ksi	70 1,000 2,500	3.88 0.16 0.42	0.84 0.32 --	2.2 -- --	1.8 -- --	-- -- --	0.12 -- --							-- -- --	
COMPRESSIVE MODULUS	Msi	70 2,500	2.09 0.5	1.1 0.3	1.68 0.17	0.91 --	0.46 --	-- --							-- --	
COMPRESSIVE STRENGTH	ksi	70 2,500	71.2 16.3	87.0 36.0	39.7 25.2	47.2 --	16.04 --	103.15 --							60.15 --	
INTERLAMINAR SHEAR PROPERTIES																
MODULUS	Msi	70	--	0.55	1.4	0.63	0.39	--							--	
STRENGTH	ksi	70	3.23	3.12(3) 5.79(4)	4.2	3.86	1.74 2.12(4)	3.46							2.49	

Notes: 1) Interpolated, 2) At 900°F, 3) Double Notch Shear, 4) Direct Shear

The ply angles for the ablative liners (Figure 53) are chosen to emulate the ply angles of the RSRM ablative liners. The ply angle selection was based on recent studies<sup>(3)</sup> concerning the effect of ply angles on erosion and on manufacturing experience. Numbers in parentheses after the Block II ply angles are the ply angles for the corresponding RSRM ablative rings.

Specific materials selections are based on fabricability, motor performance, critical properties, and predicted erosion and char. All of the PAN-based materials were considered acceptable with respect to fabrication considerations and with respect to motor performance (erosion/char). The spun PAN exhibited superior char integrity; no sign of delaminations. Of the critical material properties: 1) the PAN- and rayon-based materials have similar interlaminar shear strengths, 2) the PAN materials have slightly lower across-ply tensile strength, 3) the standard density PANs have similar CTEs except that there is less shrinkage with the spun PAN in the with-ply and across-ply directions, and 4) the low-density materials have CTEs similar to rayon. Table 28 presents a summary of the room-temperature and elevated-temperature mechanical property data available on the rayon- and PAN-based materials.

The selection of PAN-based materials is based on data from the recent NASA program, "Alternate Nozzle Ablative Materials."<sup>(4,5)</sup> During the Alternate Materials Program, standard density and low-density PAN-based materials were evaluated and compared for erosion and char performance in subscale static tests, processibility in fabrication studies, and for critical thermal and mechanical properties in material characterization testing. A short review of the data presented in that report follows.

During the NASA "Alternate Nozzle Ablative Materials Program," fifteen alternate PAN-based, carbon-cloth phenolic, tape-wrapped materials were tested as nozzle ablative liners. Four of the PAN carbon-cloth phenolic materials were made using carbon microballoons as a filler in the phenolic resin to achieve a low density (1.21 to 1.30 gm/cc) in the as-cured state. The remaining PAN materials had densities, in the as-cured state, that ranged from 1.50 to 1.56 gm/cc.

ORIGINAL PAGE IS  
OF POOR QUALITY

	MATERIAL	PLY ANGLE	MAX ANGLE TO FLOW
NOSE CAP	LT. WT. PAN	10° (10°)	---
NOSE INLET RING	SPUN PAN	110° (105°)	68°
THROAT INLET RING	SPUN PAN	75° (75°)	59°
THROAT RING	SPUN PAN	45° (60°)	69°
FORWARD EXIT CONE	SPUN PAN	30° (30°)	---
MID EXIT CONE	SPUN PAN	0° (0°)	---
AFT EXIT CONE	LT. WT. PAN	0° (0°)	---
STATIONARY SHELL	LT. WT. PAN	0° (0°)	---

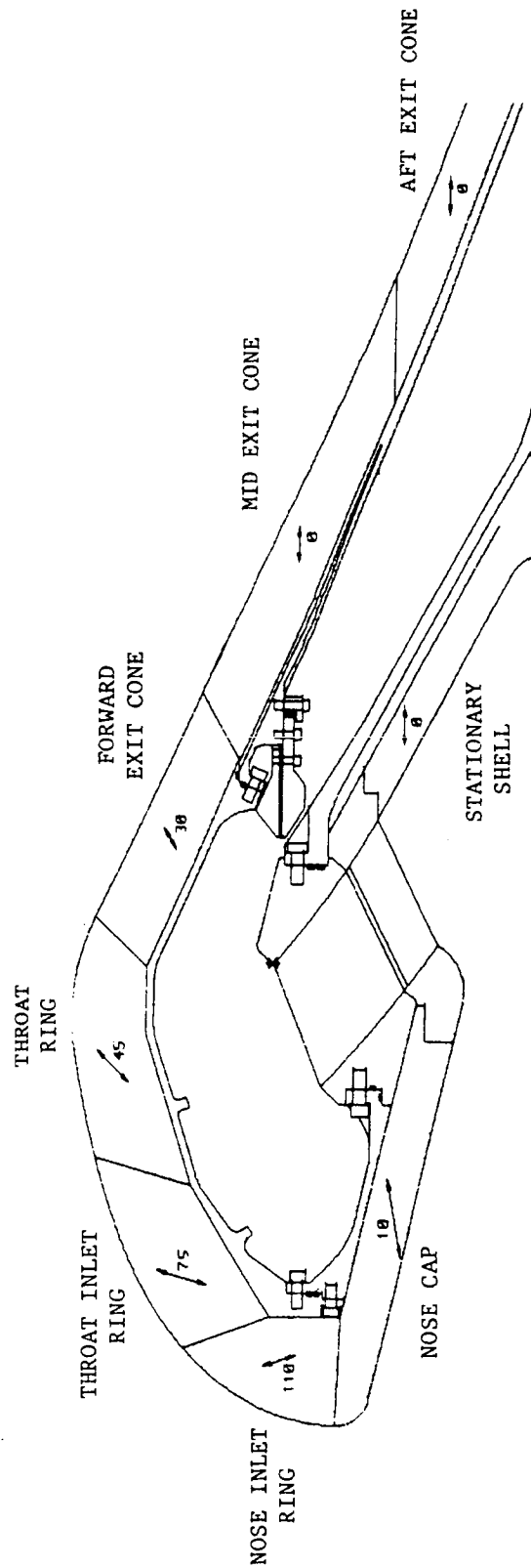


Figure 53. Ablative Rings/Materials Selection

Table 28 . Thermal Analysis Results

STATION #	EROSION (in)	CHAR (in)	2E + 1.25C	ABLATIVE		M. S.	STEEL TEMP (°F)
				THICKNESS	THICKNESS		
-1	0.141	0.444	0.837	2.49		1.97	70/80
-2	0.141	0.444	0.837	2.41		1.88	70/89
-3	0.141	0.444	0.837	2.38		1.84	70/93
-4	0.187	0.417	0.895	2.34		1.61	70/114
-5	0.554	0.282	1.460	2.31		0.58	70/183
+6	1.83	0.240	3.960	5.14		0.30	70/72
+7	1.19	0.320	2.780	4.34		0.56	70/142
+8	1.48	0.290	3.320	4.46		0.34	72/418
+9	1.64	0.270	3.617	4.65		0.29	70/219
+10	1.62	0.270	3.577	4.19		0.17	72/416
+11	1.31	0.290	2.982	3.73		0.25	72/385
+12	0.705	0.355	1.850	3.39		0.83	78/335
+13	0.514	0.387	1.512	3.05		1.02	73/266(1)
-SHELL	0.148	0.412	0.811	1.74		1.15	70/75
STATION #	EROSION (in)	CHAR (in)	2E + 1.25C	ABLATIVE		M. S.	G.E. BOND TEMP (°F)
				THICKNESS	THICKNESS		
+14	0.417	0.391	1.323	2.36		0.78	71/243
-15	0.347	0.272	1.030	2.15		1.08	70/207
-16	0.247	0.293	0.860	2.00		1.32	70/333
-17	0.237	0.286	0.830	1.38		0.66	72/NA
-18	0.285	0.265	0.900	1.06		0.18	129/NA

- FM5908 CCP  
+ K411 CCP

(1) Sandwicheed by 0.20" Graphite Epoxy  
Notation xxx/xxx = E.O.B.(113sec)/400sec  
Initial Temperature = 70°F

**Static Test Evaluation** - The spun PAN and the baseline FM5055 carbon cloth were all tested in the throat. The spun PAN exhibited the lowest throat erosion rate and exhibited superior char integrity; the Stackpole and Polycarbon materials performed equally well. Based on pre/post-test diametrical measurements, the spun PAN eroded 13 and 22 percent less than the baseline (8.88 and 7.97 mils/sec versus 10.18 mils/sec).

The continuous PAN materials exhibited the best erosion resistance in the nose, inlet, and forward exit cone region. In one test, the spun PAN showed greater erosion than the continuous PAN in the nose and inlet regions. The filled PAN materials demonstrated lower thermal conductivity than the unfilled PAN materials -- lower char depth. Erosion in the aft exit cone varied between 0 and 4.5 mils/sec and was variable down the cone. The continuous PAN, baseline material, and low-density PAN materials eroded approximately the same in this environment. The mock Leno and plain weave low-density PAN materials performed equally well in these tests.

**Fabrication Evaluation** - Fabrication studies included tape-wrapping rings for process evaluations and nozzle parts for static testing. Wrap speed, roller pressure, cure parameters, and tag end data were evaluated. All of the PAN materials were processed with the same wrapping and cure cycles as the rayon-based materials.

All of the PAN materials were found acceptable as alternates to the baseline rayon material. All processed equally well with two exceptions:

- The spun PAN material contaminates the wrapping area with carbon particles during wrapping; protective clothing and filters must be used.
- The low-density materials exhibit some variation in density from part to part.

Edgewise compressive strength was determined from tag ends from nozzle components. The baseline rayon precursor carbon-cloth phenolic measured 31,722-psi compressive strength. This compares to an average of 25,585 psi for the continuous PAN materials, with a high of 57,022 psi and a low of 11,722 psi. The

spun PAN materials averaged 21,033 psi with very little variation. The low-density PAN materials had an average compressive strength of 19,501 psi, with a high of 39,227 psi and a low of 7,222 psi.

**Material Properties** - Thermal and mechanical properties were obtained for selected materials. Southern Research Institute reports, SORI-EAS-85-831-5086<sup>(6)</sup> and SORI-EAS-85-501-5086,<sup>(7)</sup> present the data fully. The materials tested were:

- Continuous PAN phenolics (MX4961 and FM5879)
- Spun PAN phenolic (K411 and FM5834A)
- Lightweight PAN phenolic (MX134LD and FM5908)
- Rayon phenolic (FM5055)

The low-density MX134LD has the lowest thermal conductivity (similar to the rayon) with the spun PAN K411 having the highest due to its higher heat treatment.

The spun PAN materials (K411 and FM5879) showed greater across-ply shrinkage than the low-density MX134LD or the rayon material. In the with-ply direction the rayon material expands much more than any of the PAN materials.

Generally, the PAN materials exhibit higher with-ply tensile and compressive strengths and associated modulus at room temperature than the rayon material. The interlaminar shear strengths are similar. The across-ply tensile strengths of the PAN materials are somewhat lower. Overall, the low-density MX134LD material has exceptional properties.

At elevated temperatures the across-ply tensile strength and modulus of the PAN and rayon materials appear to be similar. The rayon material has only slightly higher strain capability in the across-ply direction up to 1500°F. In interlaminar shear, the PAN- and rayon-based materials are equivalent at elevated temperatures. There was very little elevated temperature data generated for the low density materials.

---

<sup>6</sup>Volume I, Shuttle Rocket Motor Alternate Materials Testing Program - Part I: Thermal Properties, SORI-EAS-85-501-5086, May 1985.

<sup>7</sup>Volume II, Shuttle Rocket Motor Alternate Materials Testing Program - Part II: Mechanical Properties, SORI-EAS-85-831-5086, September 1985.

In review: 1) the PAN- and rayon-based materials have similar interlaminar shear strengths, 2) the PAN materials have slightly lower across-ply tensile strength, 3) the standard density PANs have similar CTEs except that there is less shrinkage with the spun PAN in the with-ply and across-ply directions, and 4) the low-density materials have CTEs similar to rayon.

**Thermal Analysis** - The thermal analysis was conducted using the same design criteria used on HPM. The HPM design criteria applicable to the Block II nozzle are:

- Main ablator thickness must be greater than or equal to twice the erosion plus 1.25 times the char thickness
- Steel structural components cannot experience a temperature rise greater than 10<sup>0</sup>F during motor firing
- Steel structural components cannot exceed 450<sup>0</sup>F at splashdown (splashdown assumed to occur at 400 sec)

Using the gas temperatures and pressures from the NASA-Lewis program, the 1-D ablation rate and boundary layer thermochemical properties were calculated as a function of surface temperature based on equilibrium-controlled surface reactions. These calculations were done using Aerotherm's Chemical Equilibrium (ACE) computer program. Each ACE run also calculated the Prandtl number, Schmidt number, and the static enthalpy for the given conditions.

The thermochemistry regions were chosen primarily to include only locations where the ratio of Stanton number for mass transfer to Stanton number for heat transfer,  $C_m/C_H$ , was nearly constant. The value of  $C_m/C_H$  was determined for all locations of the phenolic cloth surface material by the relationship:

$$C_m/C_H = (Pr/Sc)^{2/3}$$

where:

$C_m$  = Local Stanton number for mass transfer

$C_H$  = Local Stanton number for heat transfer

Pr = Local Prandtl number

Sc = Local Schmidt number

The local values of Pr and Sc were obtained from the local ACE solution.

Recovery enthalpy was used as the driving force for convective heat transfer at all locations analyzed. The value of recovery enthalpy was determined by the relationship:

$$H_R = H_S + Pr^{1/3} (H_C - H_S)$$

where:

$H_R$  = Local recovery enthalpy (Btu/lbm)

$H_S$  = Local static enthalpy

$H_C$  = Chamber enthalpy

$Pr$  = Local Prandtl number

$Pr^{1/3}$  = Recovery factor for turbulent flow

The values of radiation flux were calculated based on the equation:

$$Q_r = \epsilon r T_s^4$$

where:

$Q_r$  = Incident radiation heat flux (Btu/ft<sup>2</sup>-sec)

$r$  = Stefan-Boltzmann constant ( $4.7611 \times 10^{-13}$  Btu/ft<sup>2</sup>-sec-°R<sup>4</sup>)

$T_s$  = Local average static temperature of combustion products (°R)

$\epsilon$  = Emissivity of local combustion products [ $1 - \exp(-0.808\rho D \%Al/16)$ ]

$\rho$  = Local density of combustion products including condensed species (lbm/ft<sup>3</sup>)

$D$  = Local flow diameter (in.)

$\%Al$  = Percent aluminum in propellant combustion (whole number)

Convective heat transfer coefficients were computed using the gas dynamics turbulent boundary layer program. These were then adjusted to account for regions of severe particle impingement observed on previous HPM firings.

The average heat transfer coefficients for each location were then varied as a function of the predicted pressure trace following the relation:

$$h/C_{p1} \times (P(\theta)/P_{\text{Chamber Avg}})^{0.8} = h/C_{p2}$$



where:

$h/C_{p1}$  = Average value from a particular axial location

$h/C_{p2}$  = Value used in the computer input

$P(\theta)$  = Pressure at time  $\theta$

A flow chart that illustrates the analysis procedure is shown in Figure 54.

ORIGINAL PAGE IS  
OF POOR QUALITY

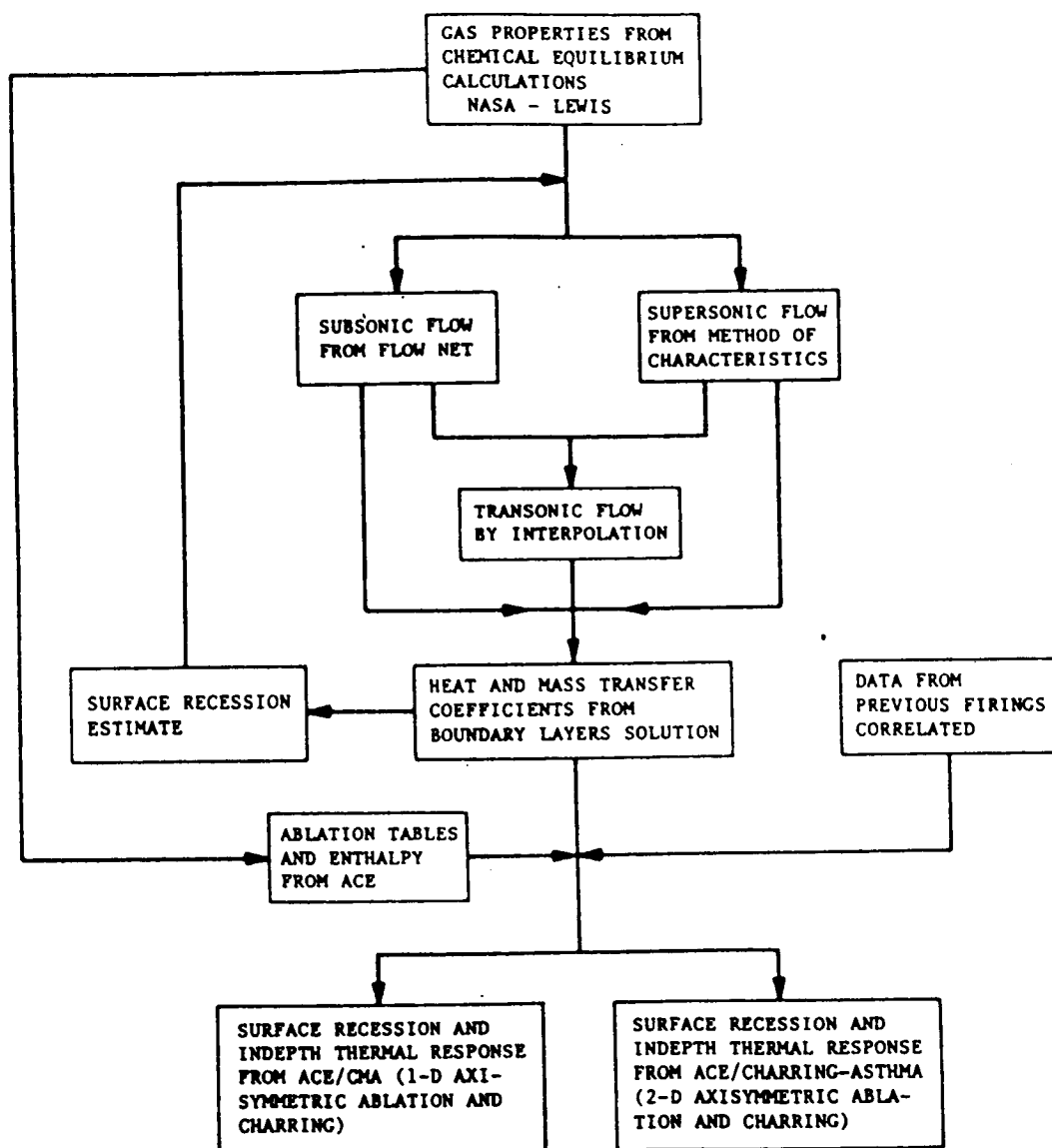


Figure 54 . Thermal Analysis Flow Chart

### 3.7 PROPELLANT

Four Class 1.3 composite propellant formulations were evaluated in the Block II SRM trade studies:

- TP-H1148 -- The current Space Shuttle SRM propellant was used as the baseline control and others were compared with it.
- TP-H3340 -- This propellant is used on the Star 37X space motor. It provided increased  $I_{sp}$  (larger payloads) and has demonstrated high reliability using an 89 percent solids loading in HTPB polymer..
- DL-H396 (88 percent Solids HTPB) -- This propellant is being developed under company-sponsored programs to provide more payload capability at lower cost. The extensive experience base acquired with other HTPB propellants (Peacekeeper Stage I motor, Mk 70 and Mk 104 Standard Missile motors, PAM-D II and Star 37X motors, Patriot, Mark 36) was used to establish trade-offs during development.
- DL-H397 -- A propellant which produces less than 1 percent HCl in the exhaust is being developed by Morton Thiokol. This Clean Propellant Program is funded by AFRPL.

DL-H396 (HTPB) propellant is selected for the Block II SRM. It is a modified Peacekeeper Stage I propellant which is also similar to TP-H3340 Star 37X space motor propellant. Ferric oxide ( $Fe_2O_3$ ) burn rate catalyst is added to the DL-H396 formulation to achieve burn rate requirements for both the heads-up and heads-down flight modes; triphenyl bismuth (TPB) cure catalyst is added to reduce the cure time to 4 days, as in the TP-H1148 PBAN propellant. SRM performance with DL-H396 propellant will prove as reliable as with other HTPB propellants and offer potential for significant performance gain in the heads-up configuration. DL-H396 propellant is a zero cards hazards Class 2 (DOT Class B) (Class 1.3) propellant with essentially the same safety characteristics as TP-H1148 propellant. In addition to improved performance, DL-H396 propellant has nearly the same processing characteristics (short mix time, minimal labor, and energy requirements) as TP-H1148 propellant at a lower raw material cost per pound. DL-H396 propellant offers the potential for higher mechanical properties, improved performance, reduced cost, and minimal technical risk.

### 3.7.1 REQUIREMENTS

Propellant candidates for the Block II SRM must satisfy the baseline requirements listed in CPW1-3300 for Space Shuttle HPM specifications (CPW1-3600 for the RSRM):

- a. Maintain integrity for storage periods of 5 years at a temperature range of 35° to 95°F or at a temperature exposure as low as -7°F during transportation and handling.
- b. Meet performance requirements over a propellant mean bulk temperature range of 40° to 90°F.
- c. Provide a composite formulation capable of being bonded to the applicable chamber via appropriate insulation, liner, and other inert items.
- d. Propellants shall meet the requirements of hazard classification 1.3 as defined in the Army material Command Regulation Safety Manual AMCR 385-100, or DoD Contractor's Safety Manual for Ammunition, Explosives, and Related Dangerous Materials, DoD 4145.26. The SRM segments shall have a DOT explosive classification of Class B.
- e. Propellant weight: minimum of 1,104,714 lb.
- f. The safety factor for propellant physical properties and propellant/liner bond shall be 2.0 minimum during storage and launch, with the exception that the propellant safety factor shall be 1.4 for the forward segment.

The current Space Shuttle TP-H1148 propellant and the Star 37X space motor TP-H3340 propellant satisfy all the CPW1-3600 requirements. Although no extensive aging data are available for DL-H396 propellant, it is very similar to other HTPB propellants and will satisfy the CPW1-3600 requirements. Extensive aging data show HTPB propellants (Peacekeeper Stage I and Star 37X) similar to the DL-H396 formulation to maintain their integrity for periods greater than 5 years.

DL-H397 (<1 percent HCl) propellant is not as far along in its development so it is uncertain whether it will meet the baseline requirements. No similar propellant is in production; therefore, no database is available for comparison.

Additional criteria for selecting the optimum propellant(s) were established from interactions between reliability, raw materials, performance, processing, and cost elements. Data were acquired from:

- Thermochemical calculations (density and impulse).
- Comparison to similar known propellants (burn rate, exponent,  $\pi_k$ , rheology, mechanical properties, aging safety, hazards, raw material handling and storage, and propellant processing).
- Vendor contacts (raw material storage cost and availability).
- Facility planning (safety, cost, and availability).

These data were used to determine the interactions and trades between elements. These trade studies were input to the design and analysis study for propellant selection and motor performance.

### 3.7.2 PROPELLANT EXPERIENCE BASE

Over the past 20 years, Morton Thiokol has accumulated extensive experience with PBAN and HTPB propellants. Millions of pounds of PBAN and HTPB propellants have been consistently manufactured to meet performance specifications. Table 29 lists the production programs which provide a large database of PBAN and HTPB experience: a testament to the reliability of PBAN and HTPB propellants options for the Block II SRM.

**Table 29. Major Production Programs for PBAN and HTPB Propellants**

<u>Major Program</u>	<u>Propellant Type</u>	<u>Propellant Produced (lb)</u>
AGILE/MALEMUTE	HTPB	18,000
IPSM/PAM-D II	HTPB	260,000
HARM	HTPB	400,000
Peacekeeper Stage I	HTPB	6,000,000
Standard Missile (Mark 104)	HTPB	1,000,000
Patriot	HTPB	1,700,000
Minuteman	PBAN	122,000,000
Poseidon	PBAN	31,500,000
Shuttle SRM	PBAN	103,000,000

TP-H1148 Space Shuttle propellant and TP-H3340 Star 37X space motor propellant have proven reliable and offer virtually no technical risk. Over 100M lb of TP-H1148 and 100K lb of TP-H3340 propellants have been consistently manufactured to meet performance requirements. Both propellants have excellent aging characteristics, as demonstrated with long-term sample and motor aging programs.

DL-H396 (lower cost HTPB) propellant, recently developed under a company-sponsored program, is similar to Peacekeeper Stage I and TP-H3340 propellants and offers minimal technical risk. Although no aging data are available, the ingredients are similar to TP-H3340 and Peacekeeper Stage I, which have excellent aging characteristics. DL-H396 is a modified Peacekeeper Stage I formulation containing lower cost R-45HT/HTPB polymer, nonspherical Al, bimodal AP, and aziridine bonding agent. DL-H396 will be as reliable as other proven HTPB propellants. It has been consistently manufactured on smaller scales to meet the performance requirements of the Block II SRM propellant.

The clean (low HCl) propellant DL-H397, developed under an AFRPL-funded program, currently offers a higher technical risk than TP-H1148, TP-H3340, and DL-H396 propellants. This propellant contains sodium nitrate ( $\text{NaNO}_3$ ) oxidizer, and no propellant production program exists using  $\text{NaNO}_3$ . Although DL-H397 propellant has demonstrated high-performance reliability in small-scale mixes and small motor testing, the experience and database are limited. It is difficult to assess long-term aging characteristics since no carton sample or motor aging program has been established. The difficulty in quantifying the performance reliability of DL-H397 propellant has reduced its emphasis as a candidate for the Block II SRM.

### **3.7.3 PROPELLANT RAW MATERIALS**

The compositions for the four candidate propellants are given in Table 30.

Table 30 . Basic Candidate Propellant Compositions

<u>Raw Material</u>	<u>Weight Percent</u>			
	<u>TP-H1148</u> <u>(HPM)</u>	<u>TP-H3340</u>	<u>DL-H396</u>	<u>DL-H397</u>
PBAN/Epoxy Binder	14.00	---	---	---
HTPB/Isocyanate Binder	---	11.00**	12.00**	10.00
DOA	---	---	---	2.00
Aluminum	16.00	18.00	19.00	19.00
AP	69.72*	71.00	68.90*	39.50
NaNO <sub>3</sub>	---	---	---	29.00
Fe <sub>2</sub> O <sub>3</sub>	0.28*	---	0.10*	0.25*
Al <sub>2</sub> O <sub>3</sub>	---	---	---	0.25*

\*Varied for burning rate control.

\*\*Aziridine bonding agent, HX-752.

Raw materials used in each candidate propellant are readily available at quantities to support a launch rate of 15 flights per year. Raw material storage facilities are similar for all propellants. There are no significant trade-offs between TP-H1148 and DL-H396 or TP-H3340 raw materials; however, DL-H397 raw material processing costs are currently much higher.

The important elements and properties of propellant raw materials are listed in Table 31. The raw materials for the Block II SRM propellant candidates are very similar so safety hazards are very similar. TP-H1148 raw material elements are used as a baseline to determine trade-offs with raw material elements of other propellant candidates.

**Table 31. Propellant Raw Material Elements**

<u>Elements</u>	<u>Specs and Goals</u>	<u>TP-H1148 (HPM)</u>	<u>TP-H3340</u>	<u>DL-H396</u>	<u>DL-H397</u>
Cost/lb	< TP-H1148	Baseline	↗	→	→
Grinding	Minimum	Baseline	→	→	↑
Availability	15 launches/yr	Baseline	→	→	→
Storage	Use existing facilities	Baseline	→	→	→
Handling	Minimum	Baseline	↗	→	↑
Specifications	Similar to TP-H1148	Baseline	→	→	→
Quality Control	Similar to TP-H1148	Baseline	→	→	↑

↑ Greater than TP-H1148  
 ↗ Slightly greater than TP-H1148  
 → Same as TP-H1148  
 ↘ Slightly less than TP-H1148

TP-H1148 propellant raw material cost serves as a baseline for comparison. TP-H3340 propellant raw material cost per pound is 26 percent higher because it contains R-45M/ HTPB polymer, spherical aluminum, and an aziridine bonding agent. These materials are more expensive than PBAN polymer and nonspherical aluminum, and TP-H1148 propellant does not contain bonding agents. TP-H3340 raw material processing costs will be slightly greater because three oxidizer sizes must be handled compared with two sizes for both TP-H1148 and DL-H396 propellants. Additional oxidizer weigh-up and handling increases labor costs and raw material processing time.

DL-H396 propellant raw material costs are slightly less than TP-H1148 propellant. The DL-H396 binder system uses R-45HT/HTPB polymer. R-45HT polymer is at least 50 percent less costly than PBAN or R-45M/HTPB polymer. HTPB propellants generally require bonding agents to achieve acceptable mechanical properties. Aziridine bonding agents (HX-752) are expensive and tend to offset the cost advantage of the R-45HT polymer. If an aziridine bonding agent is used, processing costs are equivalent to those of TP-H1148. Bonding agent influence on propellant processing is discussed further in the processing section.



The propellant raw material cost per pound for DL-H397 is less than TP-H1148. DL-H397 contains R-45HT/HTPB polymer, Tepanol bonding agent, and sodium nitrate ( $\text{NaNO}_3$ ) oxidizer which are relative low cost materials. DL-H397 raw material processing costs are currently much higher than TP-H1148 propellant because more of the solids are ground.  $\text{NaNO}_3$  may also require drying prior to use. Because DL-H397 propellant is not far along in its development, it was eliminated from further consideration at this point in the trade studies. Since the propellant is being developed under the AFRPL Clean Propellant Program, the DL-H397 could be considered in the future because of its potential to reduce HCl emissions.

The number of raw materials to be inspected increases the quality assurance efforts from TP-H1148 to DL-H396 to TP-H3340 to DL-H397. No unusual specifications exist for any of propellant raw materials. Specifications for all raw material of each propellant candidate are already established.

#### 3.7.4 PROPELLANT PERFORMANCE

Critical propellant properties which determine performance are the internal ballistics properties ( $r_b$ ,  $n$ ,  $\pi_k$ ,  $\sigma_p$ ,  $I_{sp}$ ), mechanical properties ( $\sigma_m$  and  $\epsilon_m$ ), hazards classifications, and aging characteristics. The performance properties for each candidate propellant are listed in Table 32. The specifications and goals for the Block II SRM propellant are the same as TP-H1148 propellant. Improvements in mechanical properties, density-impulse, and castability (processibility) above TP-H1148 are desirable.

The mechanical properties for TP-H1148, TP-H3340, and DL-H396 propellants meet or exceed the specification. TP-H3340 propellant has higher strain capabilities at stresses which slightly exceed specification. DL-H396 propellant has better mechanical properties than TP-H1148 propellant. TP-H1148 propellant properties typically exceed SRM mechanical property requirements. All three propellants meet the hazards requirement in specification CPW1-3600. TP-H1148, TP-H3340, and DL-H396 are zero cards, Class 1.3 composite propellants. This hazard classification is equivalent to the DOT explosive classification of Class B.

Table 32. Propellant Performance

Property	Spec and Goal	TP-H1148	TP-H3340	DL-H396
Internal Ballistics				
Burn Rate ( $r_b$ ) (in./sec) 1000 psi	0.42-0.47	0.42-0.47 (w/Fe <sub>2</sub> O <sub>3</sub> )	0.27-0.31 (w/o Fe <sub>2</sub> O <sub>3</sub> ) 0.42-0.46 (w/Fe <sub>2</sub> O <sub>3</sub> )	0.34-0.38 (w/o Fe <sub>2</sub> O <sub>3</sub> ) 0.42-0.46 (w/Fe <sub>2</sub> O <sub>3</sub> )
Burn Rate Exponent (n)	0.35	0.35	0.31 0.36 (w/Fe <sub>2</sub> O <sub>3</sub> )	0.36 0.38 (w/Fe <sub>2</sub> O <sub>3</sub> )
Burn Rate Temp ( $\pi_k$ ) %/°F	≤ 0.11	0.11	0.11	0.11*
Density (lb/in. <sup>3</sup> )	0.0641	0.0641	0.0656	0.0651
Impulse (Isp) lbf-sec/lbm	278.14	278.14	280.11	280.04
Mechanical Properties				
Stress ( $\sigma_m$ ) psi	80	110	96	>150
Strain ( $\epsilon_m$ ) %	>30	36	65	>40
Hazards	0 Cards, Class 1.3	0 Cards, Class 1.3	0 Cards, Class 1.3	0 Cards, Class 1.3
Aging	Maintain in- tegrity for 5 years	Exceeds spec	Exceeds spec	Exceeds spec*

\*Exceeds spec by analogy

TP-H1148 and TP-H3340 propellants have excellent aging characteristics. They maintain their performance and mechanical integrity for at least 5 years. DL-H396 is very similar to TP-H3340 and Peacekeeper Stage I propellant and should maintain its integrity for 5 years.

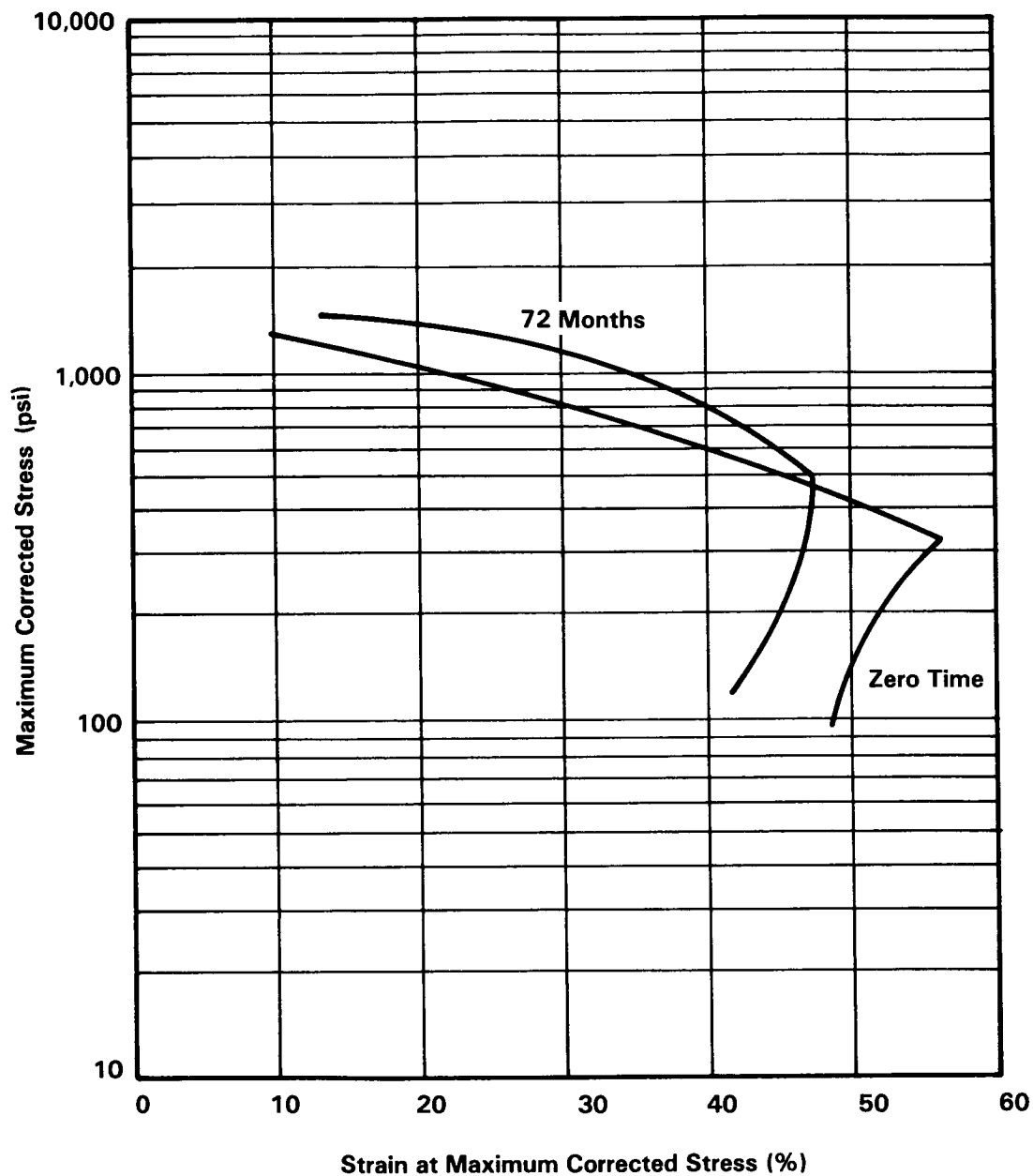
The main difference between DL-H396 and Peacekeeper Stage I or TP-H3340 propellants is the HTPB polymer. DL-H396 propellant uses R-45HT/HTPB polymer instead of the R-45M/HTPB polymer used in most HTPB propellant production programs. No production program currently exists at Morton Thiokol which uses R-45HT/HTPB polymer, so extensive aging data are unavailable. R-45HT and R-45M polymers are in the same HTPB polymer family and will age in propellants similarly. Slight differences in physical properties between R-45HT and R-45M polymers (hydroxyl number and viscosity) should not affect propellant aging characteristics. DL-H396 propellant containing R-45HT polymer will maintain its integrity during storage and transportation, as do R-45M propellants.

R-45HT polymer is produced with the same manufacturing facilities as R-45M polymer. R-45HT and R-45M post-production treatment (workup) is the same. R-45HT, a commercially-produced polymer at high rates, is manufactured at a high temperature (HT) to increase the input of the product.

HTPB propellants using R-45M polymer exhibit excellent aging stability. An 88 percent solids HTPB propellant (TP-H1139) containing the aziridine bonding agent (same basic formulation as DL-H396 except for R-45M versus R-45HT) was aged 72 months at 77°F.<sup>(1)</sup> Stress levels increased only moderately with some loss in strain (Figure 55). Real-time aging data for TP-H1139 propellant show that stress levels (Figure 56) increase moderately (18 percent in 6 years) with minor loss in strain levels (9 percent in 6 years) (Figure 57). Since R-45HT and R-45M polymers are nearly identical and of the same polymer family, DL-H396 will age as well as R-45M propellants (TP-H1139). Zero time strain levels for DL-H396 propellant are greater than 40 percent, and strain capabilities will be greater than 30 percent after 6 years, assuming similar strain reductions with time found for TP-H1139.

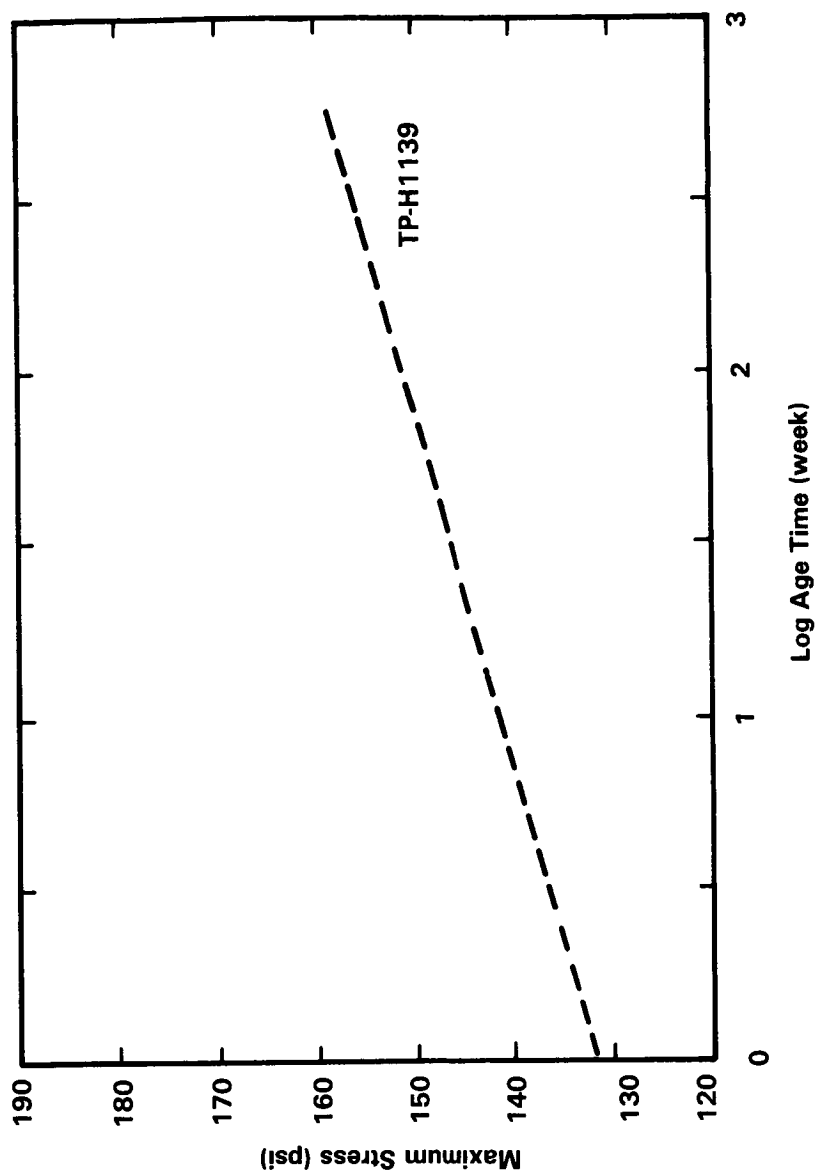
---

<sup>1</sup>A. Grant Christiansen, "Aging of HTPB Propellants," Morton Thiokol/Wasatch Operations, Brigham City, UT, AFRPL-TR-79-88, Pub No. 79580



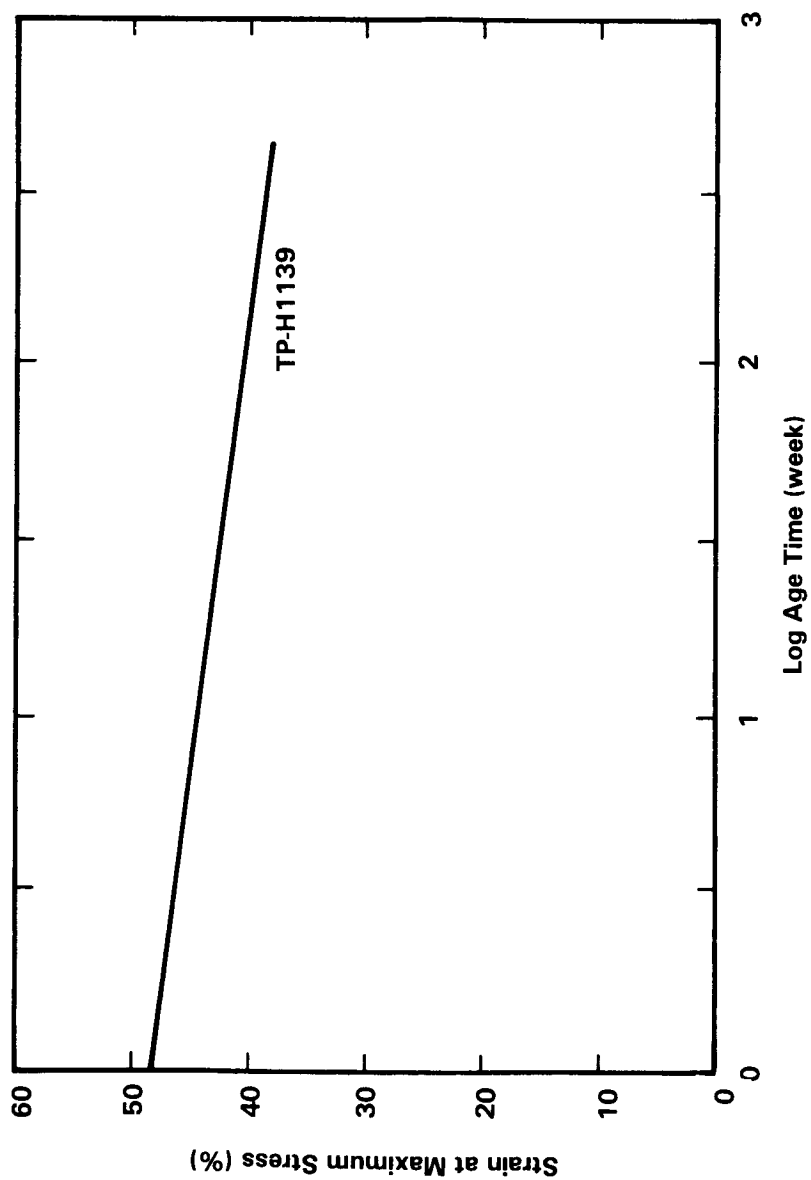
87354-12C

Figure 55. Uniaxial Failure Envelopes for TP-H1139 Propellant--  
Mix 8657001, Aged 72 Months at 77°F



87354-128

Figure 56. Comparison of Aging Effects on Uniaxial Maximum Stress for HTPB Propellant--  
Aged at 77°F, Tested at 77°F and Ambient Pressure, 2 In./Min Crosshead Rate



87354-12A

Figure 57. Comparison of Aging Effects on Strain at Maximum Stress for HTPB Propellant--  
Aged at 77°F, Tested at 77°F and Ambient Pressure, 2 In./Min Crosshead Rate

Service life predictions have been reported for MLRS propellant grain which contains R-45HT polymer. Martin and Siron<sup>(2)</sup> report variations in MLRS propellant properties indicate the MLRS motor should withstand a 20-year scenario at a 97 percent confidence level.

Propellant burn rate tailoring studies were performed to determine the best approach to increase the burn rate of DL-H396 and TP-H3340 propellants. A higher burn rate is required for both propellants to meet the thrust-time requirements in the CPW1-3600 specifications or for the Space Shuttle heads-up SRM. The Block II SRM burn rate requirement for DL-H396 and TP-H3340 propellants is 0.42 ips at 1,000 psi to match the heads-down thrust-time trace. DL-H396 and TP-H3340 should also provide the necessary performance to allow the Space Shuttle STS to fly in a heads-up configuration if the burn rate is increased to 0.46 ips for DL-H396 and 0.45 ips for TP-H3340 at 1,000 psi. The measured burn rate for DL-H396 without catalyst is 0.36 ips with a 0.36 exponent at 1,000 psi. The burn rate for TP-H3340 is 0.28 ips with a 0.31 exponent at 1,000 psi with no catalyst. Burn rate tailoring predictions were based on data generated from:

- Space Shuttle SRM propellant tailoring experience
- The development of HTPB propellants for ballistic missiles
- Development of Class 1.3 composite propellants for Small ICBM
- Preliminary development of DL-H396 in the pint and 1-gallon mixer

The burn rate requirements for DL-H396 and TP-H3340 propellants (Table 33) will depend on whether the motor performance must match the thrust-time trace specified in CPW1-3600 or the thrust-time trace for the heads-up configuration. Propellant burn rate tailoring trades will be established to determine the best approach to meet the performance requirements in CPW1-3600 and for the heads-up configuration.

---

<sup>2</sup>Donald L. Martin and Robert E. Siron, "Service Life Predictions of the MLRS Propellant Grain," U.S. Army Missile Command, Redstone Arsenal, AL, Report CPIA Pub 390, Vol. III, February 1984.

Table 33. Propellant Burn Rate Tailoring

<u>APPROACH</u>	<u>ADVANTAGE(S)</u>	<u>DISADVANTAGE(S)</u>	<u>TECHNICAL RISK</u>
INCREASING GRD AP FRACTION	LOWER COST.	POOR PROCESSIBILITY. HIGHER BURN RATE VARIABILITY. RIGOROUS STANDARDIZATION.	HIGH
FINER AP	EASILY PROCESSED. No $\text{Fe}_2\text{O}_3$ HANDLING OR STORAGE.	HIGHER EXPONENT. MORE EXPENSIVE. CLASS 1.1 OXIDIZER. HIGHER BURN RATE VARI- BILITY. RIGOROUS STANDARDIZATION.	MINIMAL TO MEDIUM
$\text{Fe}_2\text{O}_3$ CATALYST	EXTENSIVE DATABASE. LESS BURN RATE VARIABILITY. EASIER STANDARDI- ZATION. LOWER COST.	EXPONENTS INCREASE SLIGHTLY.	MINIMAL TO NONE



Increasing the ground AP fraction, using finer AP and  $\text{Fe}_2\text{O}_3$  catalyst were three approaches evaluated to tailor burn rate. Each approach, shown in Table 34, is traded against other critical propellant properties, including exponent, processibility, cost, material availability, and experience. The best approach meets both burn rate requirements with a minimal effect on exponent, without adversely affecting processibility, and is not cost prohibitive.

DL-H396 is an 88 percent solids/19 percent Al propellant with a bimodal AP distribution of 200/20 micron. Increasing the ground fraction of AP in DL-H396 will not raise the burn rate enough without causing processing problems and reducing potlife. Increasing the 20-micron ground AP fraction in a DL-H396-type propellant, enough to achieve the +60 mils required in burn rate, would result in high end-of-mix (EOM) viscosities and reduce potlife. Figure 58 shows that the 20-micron AP fraction must be approximately 42 percent to achieve the 0.42 ips burn rate required to duplicate HPM performance. This would result in an EOM viscosity of approximately 30 kP. This will reduce useful potlife since a viscosity of or less than 40 kP is generally required for efficient casting.

Replacing 20-micron AP with 9-micron particles and increasing the ground 9-micron fraction will raise the burn rate to meet the requirement; however, the pressure exponent for burn rate increases dramatically. Figure 59 shows how the exponent increases with increasing burn rate as the 9-micron fraction is increased. A ground/ unground ratio of 37/63 should meet the burning rate requirement of 0.42 ips at 1,000 psi; the burn rate exponent will probably be high, approximately 0.46.

DL-H396-type propellants with a 200/9-micron bimodal AP distribution are easily processed (EOM viscosities, 10 kP) and should meet the burn rate requirement, but the exponents are high and 9-micron AP is more expensive to attain than 20-micron AP. When the ground AP fraction is of a particle size less than 15-micron, it becomes a Class 1.1 material. This requires a batch type grinding operation which is done in a more remote facility than the continuous grinding operation used for 20-micron AP. Grinding AP to an average particle size less than 15-micron is a hazardous operation which is labor and time intensive,

Table 34. Burn Rate (ips) Requirement at 1,000 psi

<u>PROPELLANT</u>	<u>TYPICAL</u>	"HEADS-DOWN" CEI-THRUST	"HEADS-UP" THRUST
		<u>TIME PROFILE</u>	<u>TIME-PROFILE</u>
TP-H1148	0.43	0.43	0.46
DL-H396	0.36	0.42	0.45
TP-H3340	0.28	0.42	0.45

DL-H396 AND TP-H3340 BURN RATE MUST BE INCREASED TO MEET BOTH THRUST TIME PROFILES; TP-H1148 BURN RATE MUST BE INCREASED TO MEET "HEADS-UP" REQUIREMENTS.

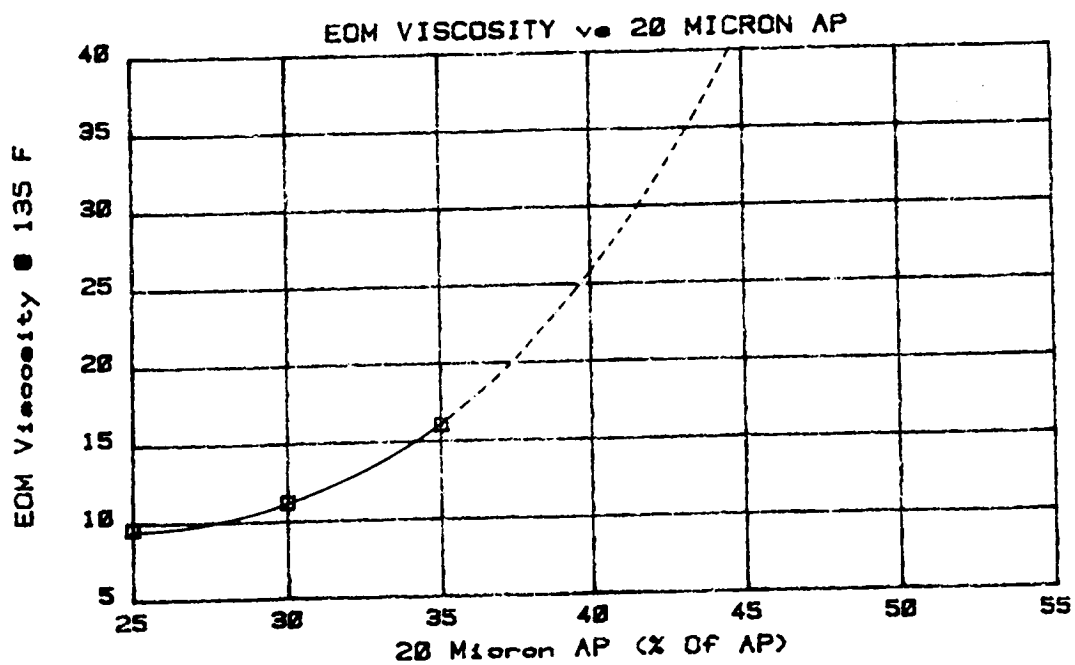
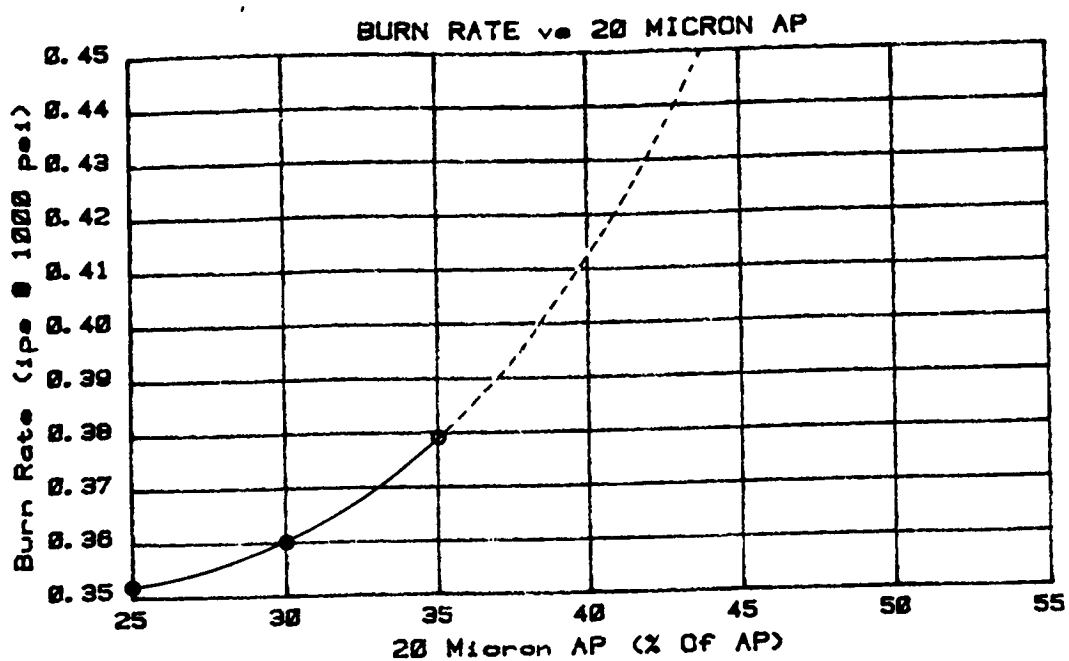


Figure 58 . Increasing Ground AP Fraction to Achieve 0.42-ips Burn Rate Results in Higher EOM Viscosities

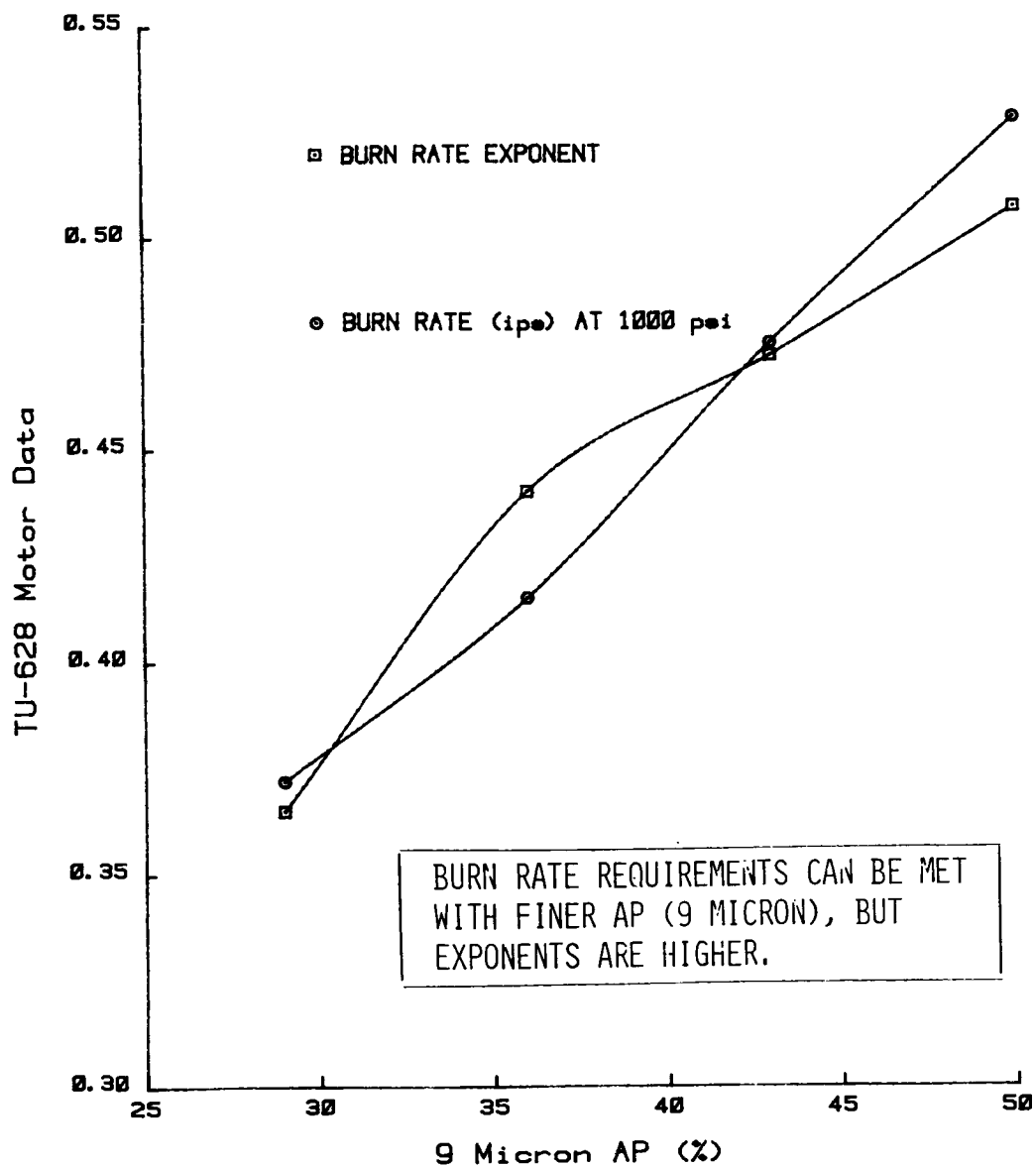


Figure 59 . Effect of Ground AP on Burn Rate and Exponent in 88 percent Solids/19 percent Al DL-H396 Propellant with 200/9 Micron AP

resulting in higher grinding costs. Higher grinding costs and exponents for 200/9-micron bimodal AP distributions make this approach unattractive for meeting the higher burn rate requirement.

Iron oxide was evaluated as a burn rate catalyst. A large database exists for  $\text{Fe}_2\text{O}_3$  as a catalyst in large boosters since it is used in TP-H1148 propellant. Two types of  $\text{Fe}_2\text{O}_3$  are used: Type I used in the SRM igniter has a larger surface area ( $8.1 \text{ m}^2/\text{gm}$ ); Type II ( $5.1 \text{ m}^2/\text{gm}$ ) used in the SRM propellant.

Space Shuttle SRM propellant tailoring studies using Types I and Type II  $\text{Fe}_2\text{O}_3$  report a slightly higher burning rate effect for Type I  $\text{Fe}_2\text{O}_3$ . TP-H1148 burning rate, shown in Figure 60, increases from 0.347 to 0.444 ips (+97 mils) with 0.13 percent Type I  $\text{Fe}_2\text{O}_3$  and from 0.347 to 0.428 ips (+81 mils) with 0.13 percent Type II  $\text{Fe}_2\text{O}_3$ . Exponent also increased from 0.26 to 0.32 (+0.06) with 0.13 percent Type I  $\text{Fe}_2\text{O}_3$ .

The burn rate versus  $\text{Fe}_2\text{O}_3$  relationship for DL-H396-type propellants was established during a company-sponsored program. Figure 61 shows that a burn rate of 0.42 ips at 1000 psi can be achieved with less than 0.1 percent Type II  $\text{Fe}_2\text{O}_3$ . An average burn rate exponent of  $0.38 \pm 0.02$  has been measured for Type II  $\text{Fe}_2\text{O}_3$ . The required Type II  $\text{Fe}_2\text{O}_3$  levels to duplicate HPM burn rates is approximately 0.03 to 0.07 percent and levels of 0.10 to 0.15 percent provide for the heads-up burn rate.

Using  $\text{Fe}_2\text{O}_3$  catalyst will allow burn rate to be tailored to meet the requirements without changing AP grind ratios.  $\text{Fe}_2\text{O}_3$  will have less of a detrimental effect on processibility at these levels (0.1 percent). Using  $\text{Fe}_2\text{O}_3$  to control burn rate (for standardization) allows the AP grind ratio to be fixed for optimum processing, rheology, and mechanical properties.

Standardizing DL-H396 propellant burn rate with  $\text{Fe}_2\text{O}_3$  should result in the same motor-to-motor burn rate variability experienced with the Space Shuttle SRM's. The SRM burn rate variability within three standard deviations is 3.0 percent by standardizing with  $\text{Fe}_2\text{O}_3$  at a fixed ground/unground AP ratio. Using the same standardization methods for DL-H396 propellant at a fixed ground/unground AP ratio will minimize motor-to-motor burn rate variability and make it

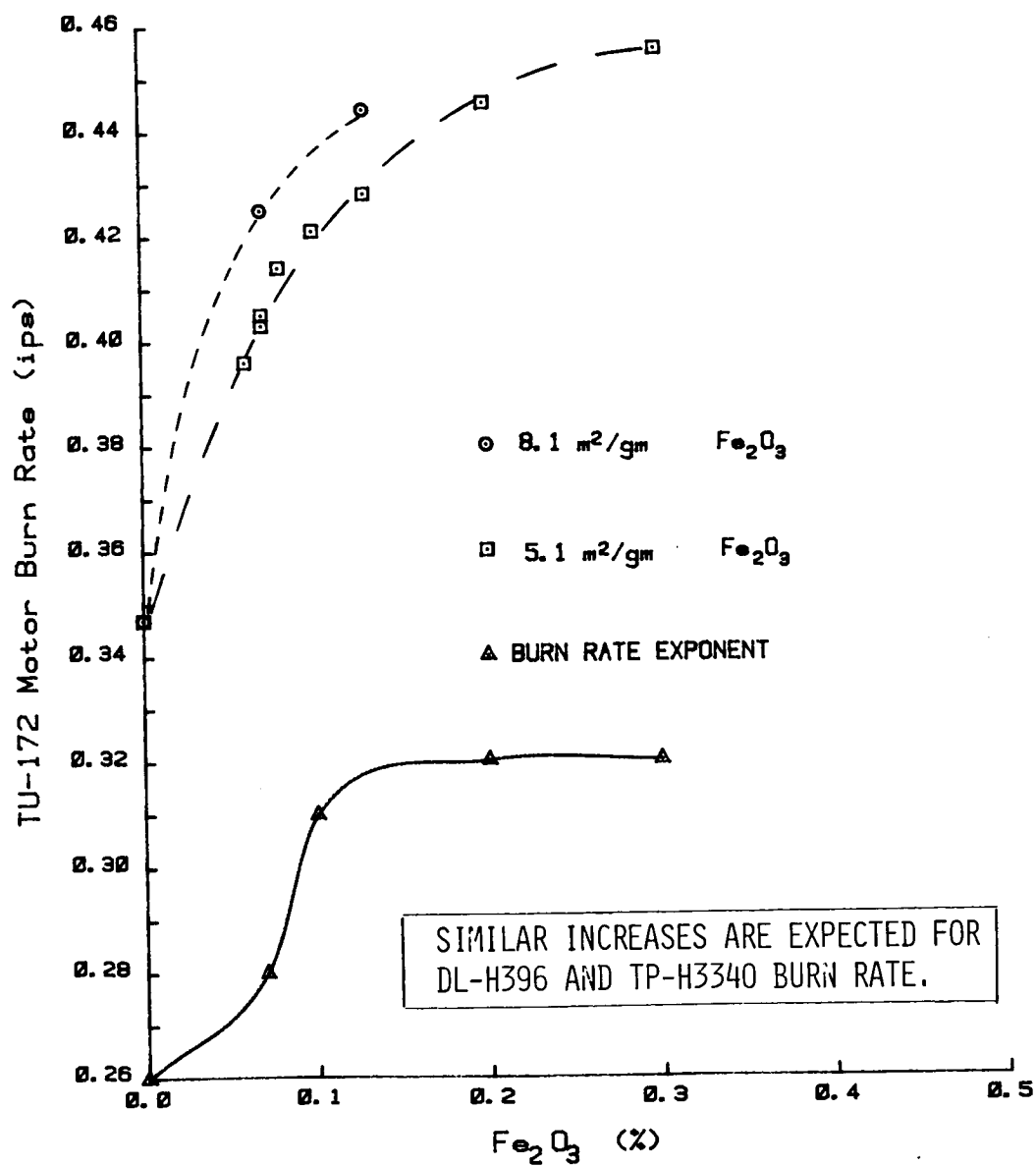


Figure 60. Burn Rate Versus  $\text{Fe}_2\text{O}_3$  in Space Shuttle Propellant (1,000 psi at 60°F)

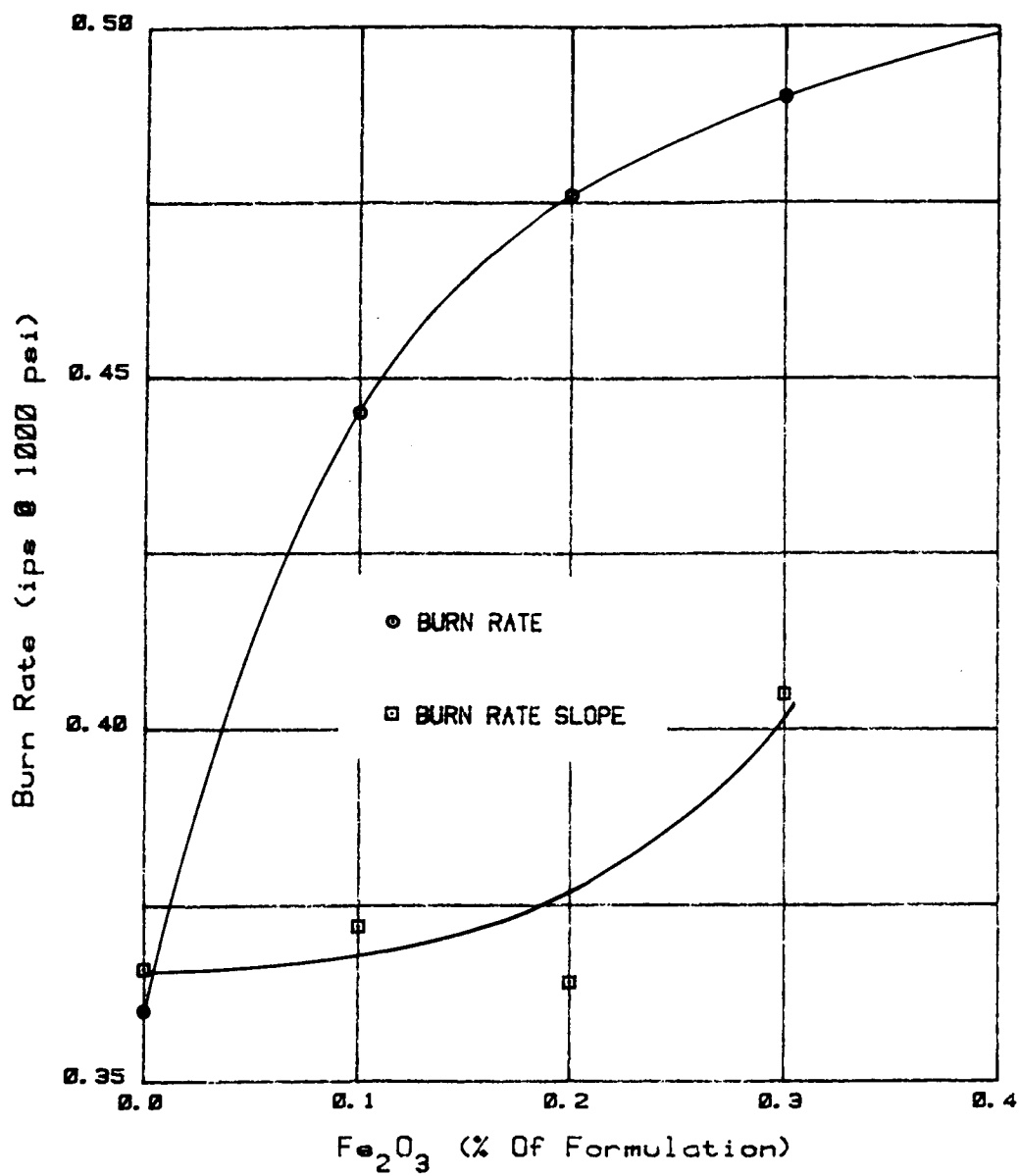


Figure 61 . Burn Rate Requirements For "Heads-Down" and "Heads-Up" Flight Modes Achieved With <0.2 Percent, Type II,  $\text{Fe}_2\text{O}_3$ , DL-H396-Type Propellant

possible to optimize propellant processing, rheology, and mechanical properties. Addition of  $\text{Fe}_2\text{O}_3$  to the DL-H396 formulation to achieve burn rate requirements offers minimal to no technical risk.

$\text{Fe}_2\text{O}_3$ , Type II, is a readily available materials at relatively low cost (less than \$1.00/lb).  $\text{Fe}_2\text{O}_3$  will have a minor impact on propellant cost since low levels (approximately 0.1 percent) are necessary to achieve the required burn rate in DL-H396 propellant.

TP-H3340 is an 89 percent solids/18 percent Al propellant with a trimodal AP distribution of 400/200/18 micron. The burn rate at 1,000 psi is 0.28 ips with a 0.31 exponent, well below the burn rate requirement of 0.42 at 1,000 psi to match the thrust-time profile in CPW1-3600. The burn rate must be raised 0.14 ips (140 mils) to meet the thrust-time requirement. Increasing the ground 18-micron AP fraction, and decreasing the 400-micron coarse fraction will not raise the burn rate enough to meet the requirement. Figure 62 shows that for a 400/200/50 micron trimodal distribution, increasing 50-micron from 10 to 25 percent only raised the burning rate 0.025 ips (+25 mils). Finer 18-micron AP would increase the burning rate more than 50 micron AP, but the maximum increase expected would be 0.03 ips (+30 mils). Increasing the 18-micron AP fraction significantly in a trimodal 400/200/18 micron AP distribution would certainly cause processing problems (high EOM viscosities).

Adding  $\text{Fe}_2\text{O}_3$  to increase burn rate, as was done with DL-H396-type propellants, would be the best approach. The trimodal distribution of AP could be fixed to optimize processing, rheology, and mechanical properties.  $\text{Fe}_2\text{O}_3$  addition is also an easy way to consistently standardize burn rate. Higher levels of  $\text{Fe}_2\text{O}_3$  will be necessary to meet burn rate requirements for TP-H3340 than for DL-H396 because the burn rate without catalyst is lower.

Using  $\text{Fe}_2\text{O}_3$  to raise the burn rate of TP-H3340 from 0.28 to 0.42 ips (+140) offers a higher technical risk. Higher levels of  $\text{Fe}_2\text{O}_3$  (0.5 to 1.5 percent) are required to achieve a 140-mil increase in burn rate. Addition of this much fine  $\text{Fe}_2\text{O}_3$  could cause processing problems in a higher solids level (89 percent) propellant. Addition of high levels of  $\text{Fe}_2\text{O}_3$  also degrades propellant energy ( $I_{sp}$ ).



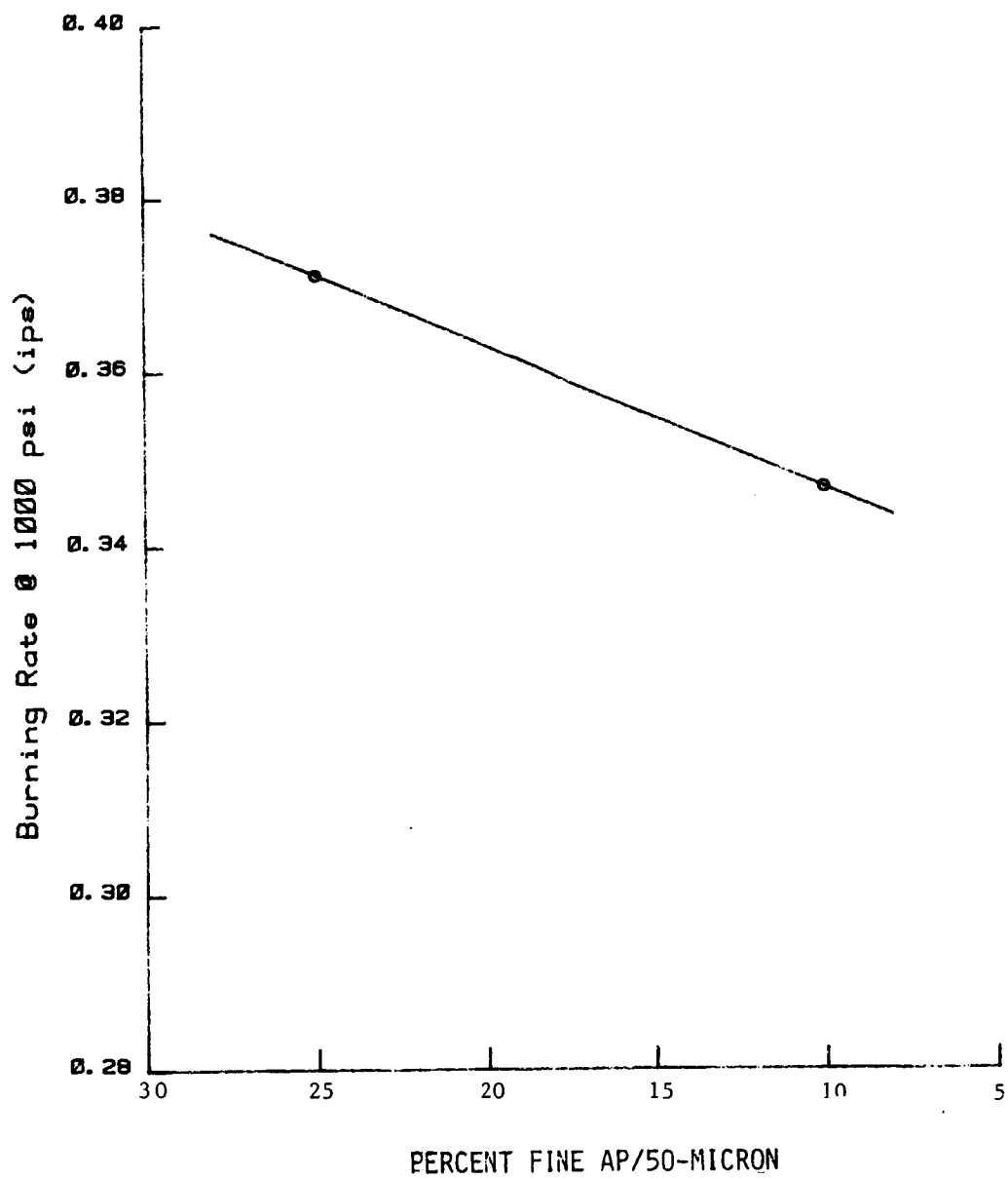


Figure 62. Effect of Ground AP on Burn Rate and Exponent in Trimodal 400/200/50 AP Distribution

The propellant burn rates necessary to fly in a heads-up configuration are higher than the burn rates needed to match the thrust-time profile in CPW1-3600. The burn rate for TP-H1148 must be increased from 0.43 to 0.46 ips at 1,000 psi, from 0.36 to 0.46 ips at 1,000 psi for DL-H396, and from 0.28 to 0.45 ips at 1,000 psi for TP-H3340. Figure 63 shows that 0.6 percent Type II  $\text{Fe}_2\text{O}_3$  will be required to achieve the 0.46 ips burn rate at 1,000 psi for TP-H1148 propellant. TP-H1148 propellant can be easily processed containing up to 1.0 percent  $\text{Fe}_2\text{O}_3$ .

Very high levels of  $\text{Fe}_2\text{O}_3$  may be required to raise the burn rate of TP-H3340 from 0.28 to 0.45 ips (170 mils). Processing difficulties could be significant at the higher levels of  $\text{Fe}_2\text{O}_3$  required to meet this burn rate. Higher  $\text{Fe}_2\text{O}_3$  levels necessary for TP-H3340 to meet its burn rate requirement will further degrade propellant performance ( $I_{sp}$ ). Therefore, the technical risks for achieving the necessary burn rate for a heads-up configuration are greater for TP-H3340.

### **3.7.5 PROPELLANT PROCESSING**

The three candidate propellant formulations were compared assuming a batch mixing process to support a Space Shuttle SRM II production rate. The current TP-H1148 propellant served as a baseline formulation and the cost and processing parameters of the other formulations were compared to it. The other two formulations were TP-H3340 and DL-H396. All three of these formulations are physical rate limited (i.e., mixing is required only to wet the solids and produce a homogeneous mixture). The TP-H3340 and DL-H396 formulations were compared to the TP-H1148 propellant in terms of mix cycle time, processibility, labor and energy requirements, and safety.

The mix cycles developed for TP-H3340 and DL-H396 propellants have times of 50 to 55 min. This is equivalent to the mix cycle time for TP-H1148 propellant. TP-H1148 oxidizer is preblended (bimodal AP) and added to a premix of curing agent, polymer, aluminum, and ferric oxide. The desired processing temperature and minimum viscosity is achieved approximately 30 to 40 min after oxidizer addition is completed. Homogeneity is achieved in less than 10 min after oxidizer addition.

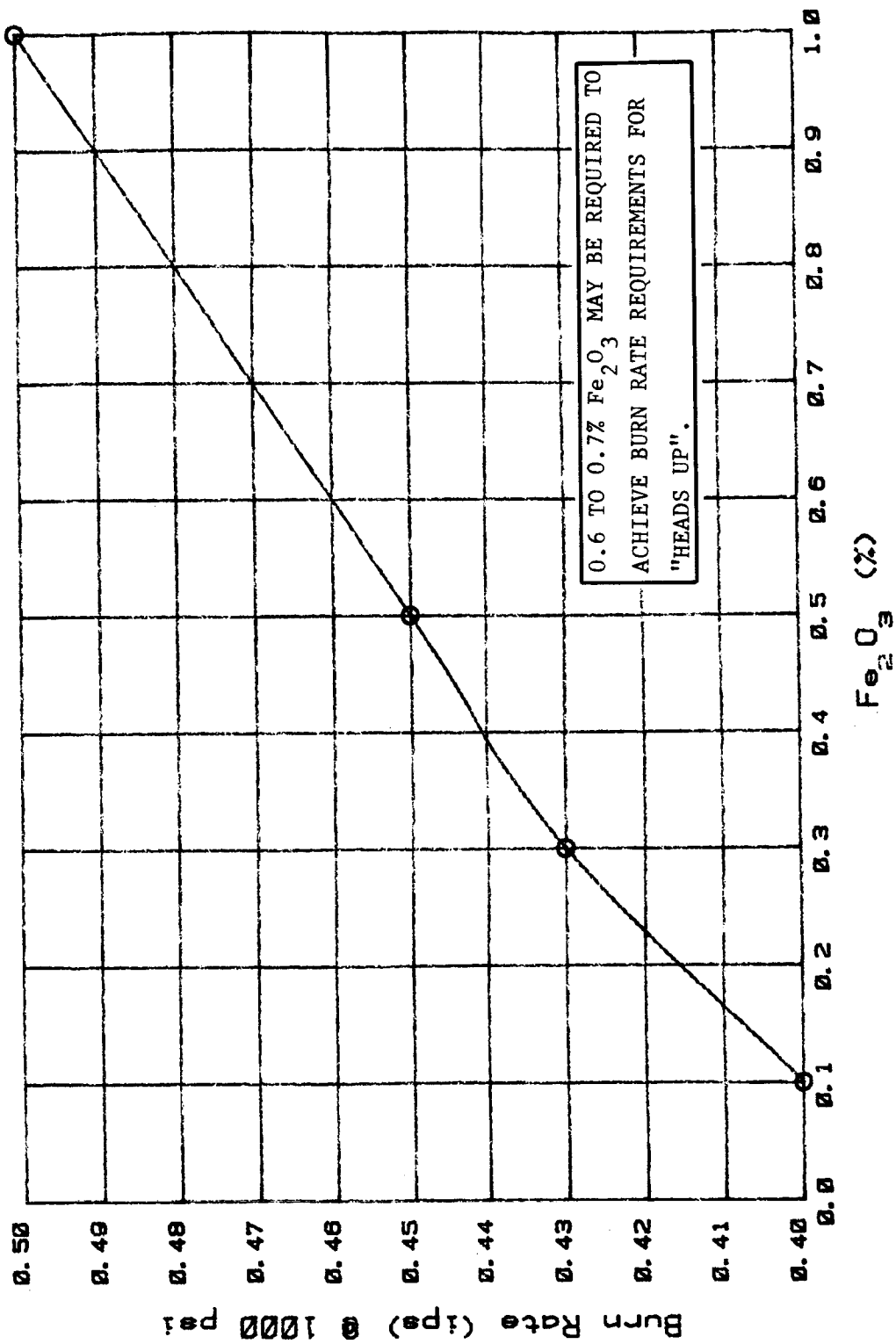


Figure 63. TP-H1148 Burn Rate Versus  $\text{Fe}_2\text{O}_3$  (5-in. CP Data)

TP-H3340 propellant oxidizer (trimodal AP) is added to a premix of polymer, curing agent, aluminum, and bonding agent as with TP-H1148 propellant. The only difference between TP-H3340 and TP-H1148 propellants is that a trimodal AP distribution is used which requires a third oxidizer fraction to be handled, stored, weighed, and transported. This has a minor impact on labor costs for TP-H3340. The mix time is essentially equivalent to TP-H1148 (50 to 55 min) so the time to achieve homogeneity and minimum viscosity is nearly identical.

The DL-H396 mix cycle time is very similar to that of TP-H1148 and TP-H3340. The oxidizer is added to a premix of polymer, aluminum, bonding agent, ferric oxide, and a triphenyl bismuth quick-cure catalyst. The IPDI curative, however, is added when the oxidizer addition is complete instead of in the premix. The mix cycle time of 50 to 55 min is the same as TP-H1148 and TP-H3340. Minimum propellant viscosity and homogeneity is achieved at mix times similar to TP-H1148.

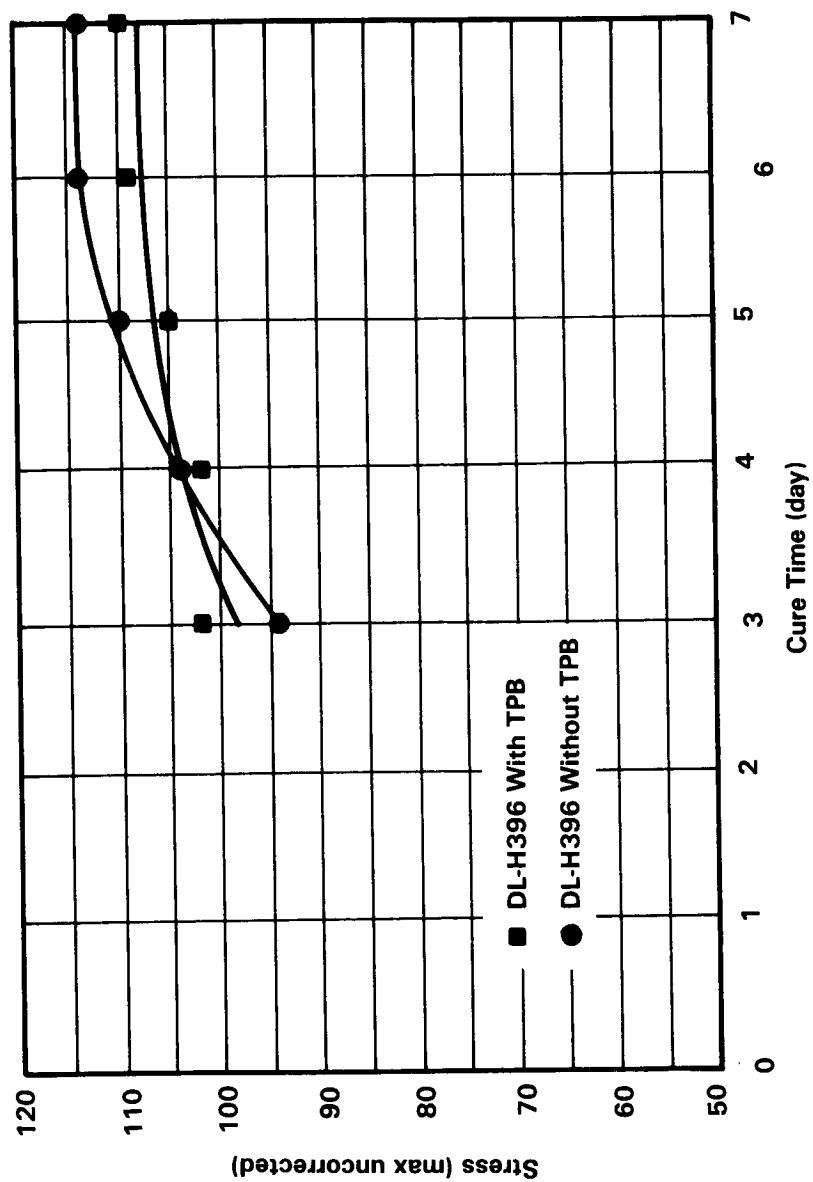
#### **3.7.5.1 Processibility**

The DL-H396 propellant formulation has a bimodal oxidizer distribution that is virtually identical with the oxidizer distribution in TP-H1148 propellant. The mix cycle calls for late IPDI addition (after oxidizer addition). Triphenyl bismuth (TPB) cure catalyst is sprinkled on top of the premix prior to raising the mix bowl and feeding the oxidizer. The intermediate propellant viscosities and EOM viscosities are better than those for TP-H1148 propellant. The mix cycle using late IPDI addition with TPB yields a 3.5- to 4.0-hr potlife, as shown in Table 35, which is equivalent to that of TP-H1148 propellant. The late IPDI addition mix cycle produces potlives of 6 hr when no TPB is added and 4 hr with TPB. The TPB content in the formulations producing these potlives was 0.005 percent. The propellant potlife can be tailored by adjustments in the TPB content as shown in Figure 64. The TPB in DL-H396 propellant shortens the propellant cure requirements. Figure 65 shows that the addition of the quick cure TPB shortens the cure time to 3 to 4 days.

Addition of the IPDI to the premix in TP-H3340 formulation improves the solids wetting and helps reduce the intermediate viscosities. The trimodal oxidizer fraction used in TP-H3340 propellant reduces the interstitial voids in

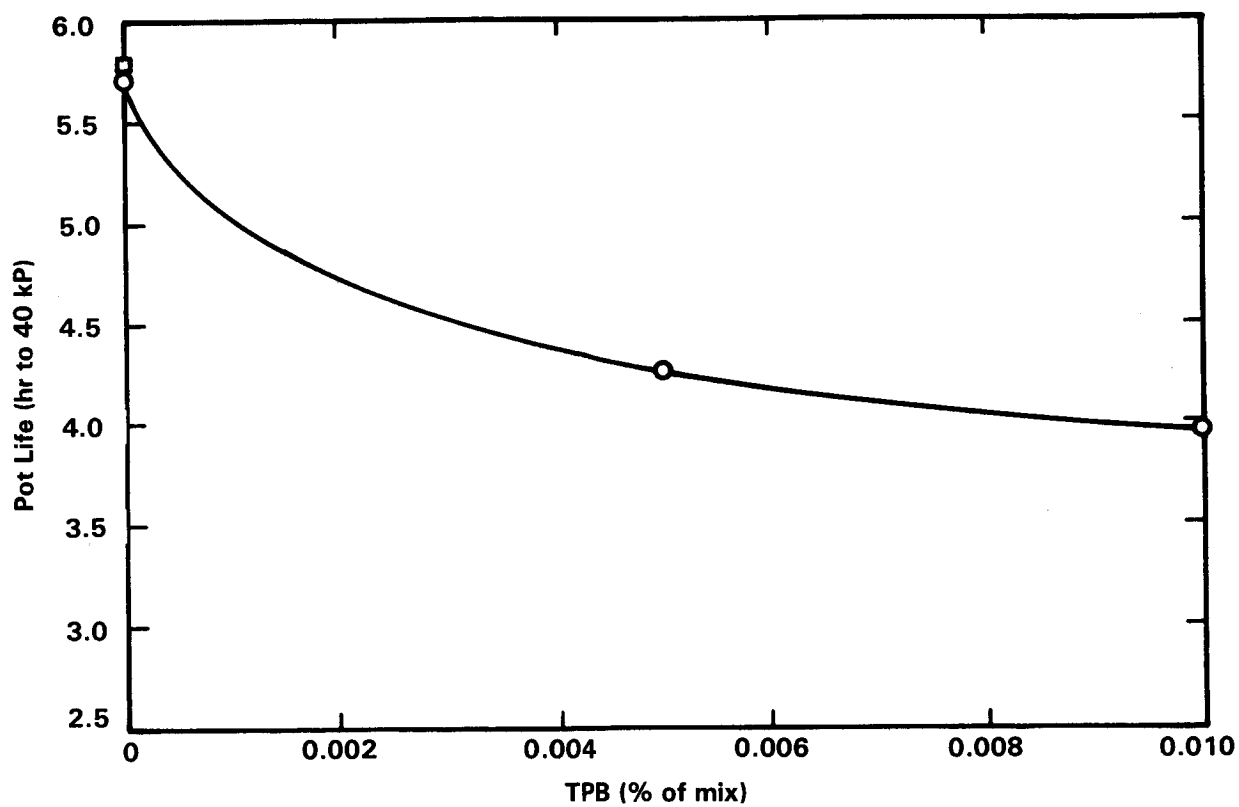
Table 35 . Propellant Processing Comparison

	<u>TP-H3340</u>	<u>SHUTTLE TP-H1148</u>	<u>DL-H396</u>
MIX TIME, MINUTES	55	55	55
EOM VISCOSITY, KP	12	15-20	12
POTLIFE (W/O TPB)	8	4	6
POTLIFE (W/TPB)	--	--	4



87354-13C

Figure 64. Addition of TPB Cure Catalyst Shortens Cure Time of DL-H396 Propellant--  
Tooling Could Be Removed After 3-4 Days of Cure at 135°F



87354-138

Figure 65. DL-H396 Propellant Pot Life Can Be Tailored by Adjustments in TPB Content

the propellant and significantly reduces intermediate propellant viscosities. This formulation is much easier to process than the other two candidate formulations. The potlife of TP-H3340 is 8 hr while that of DL-H396 and TP-H1148 formulations typically have 4- to 6-hr potlives. The longer potlife of TP-H3340 is due to the HTPB polymer R-45M. The R-45M polymer has a lower functionality than the R-45HT polymer used in DL-H396 propellant. The longer potlife of TP-H3340 propellant reduces the likelihood of scrapping a mix due to expiration of the potlife before the propellant is cast into the motor. The lower viscosities of TP-H3340 during casting operations will also reduce the time required to cast the propellant.

Each of the candidate propellant formulations possesses acceptable apparent viscosities at high and low shear rates. The apparent viscosities of propellants at various shear rates are important in the casting of an SRM. The propellant should have an acceptable apparent viscosity at low shear rates (e.g., less than 70 kP at 0.041/sec) and a low apparent viscosity at high shear rates (e.g., less than 35 kP at 0.37/sec). A low apparent viscosity at a high shear rate allows the propellant to flow quickly through a slit plate. Casting the propellant through the slit plate is essential in order to remove any entrained air bubbles and prevent void formation in the propellant grain. Propellant which flows quickly at high shear rates minimizes casting time. A propellant viscosity below 70 kP at low shear rates is necessary in order for the propellant to flow outward and fill the motor once it has passed through the slit plate.

TP-H3340 and DL-H396 propellants possess better casting characteristics than does TP-H1148 propellant. Higher casting rates can be achieved with both of these propellants because of their lower EOM viscosities and superior or equivalent potlives. Both propellants also have rheological properties which are conducive to vacuum casting, i.e., high casting rates at high shear rates. Previous experience with TP-H1148 propellant has shown that high casting rates are required when vacuum casting a motor to prevent void formation. The static head of the propellant provides the necessary pressure to force entrapped air out of the motor grain.

Previous studies with PBAN propellants have indicated that propellant rise rates in the motor below about 4 in./hr result in the void formation in the



grain. TP-H1011 (a PBAN formulation) propellant samples have been cast at rise rates of 2 and 6 in./hr. Numerous voids were found in samples cast at 2 in./hr. This is evidence that the static head on the cast propellant was not sufficient to force pockets of entrapped air out of the motor grain. The static head required is a function of the propellant density and the viscosity of the propellant when it is cast. The exact rise rates that would need to be met to ensure elimination of voids for each propellant candidate would need to be determined.

### **3.7.5.2 Labor and Energy Costs**

Labor requirements for mixing TP-H3340 and DL-H396 propellants are comparable to those for TP-H1148. The formulation used in TP-H1148 helps keep labor and energy costs to a minimum. TP-H3340 has some additional labor requirements because it has three oxidizer fractions to handle, weigh, and transport. DL-H396 has two oxidizer fractions, like TP-H1148, so handling and labor requirements are similar.

Energy requirements to process TP-H3340 and DL-H396 propellants are nearly equivalent to TP-H1148 when aziridine bonding agents are used. HTPB propellants generally require bonding agents to achieve acceptable mechanical properties. If the bonding agent is Tepanol, then the processing times are chemical rate limited. Mix times for chemical rate limited propellants are much longer than for TP-H1148 propellant. This is because ammonia is liberated from the reaction between Tepanol and AP, and sufficient time must be allowed to remove ammonia. Further, the propellant mix must be heated to 160°F to complete the reaction and to remove all the gas formed. This increases labor costs (longer mixing time) and energy requirements (higher mix temperature).

TP-H3340 and DL-H396 use HX-752, an aziridine bonding agent, which does not liberate ammonia. Their processing times are physical rate limited so their mix times are equivalent to TP-H1148. The major trade-off is that aziridines are more expensive than the Tepanol bonding agent. This increases propellant raw material cost per pound compared with Tepanol-containing HTPB propellants. This is more than offset by the increased labor and energy requirements necessary to process HTPB propellants containing Tepanol.

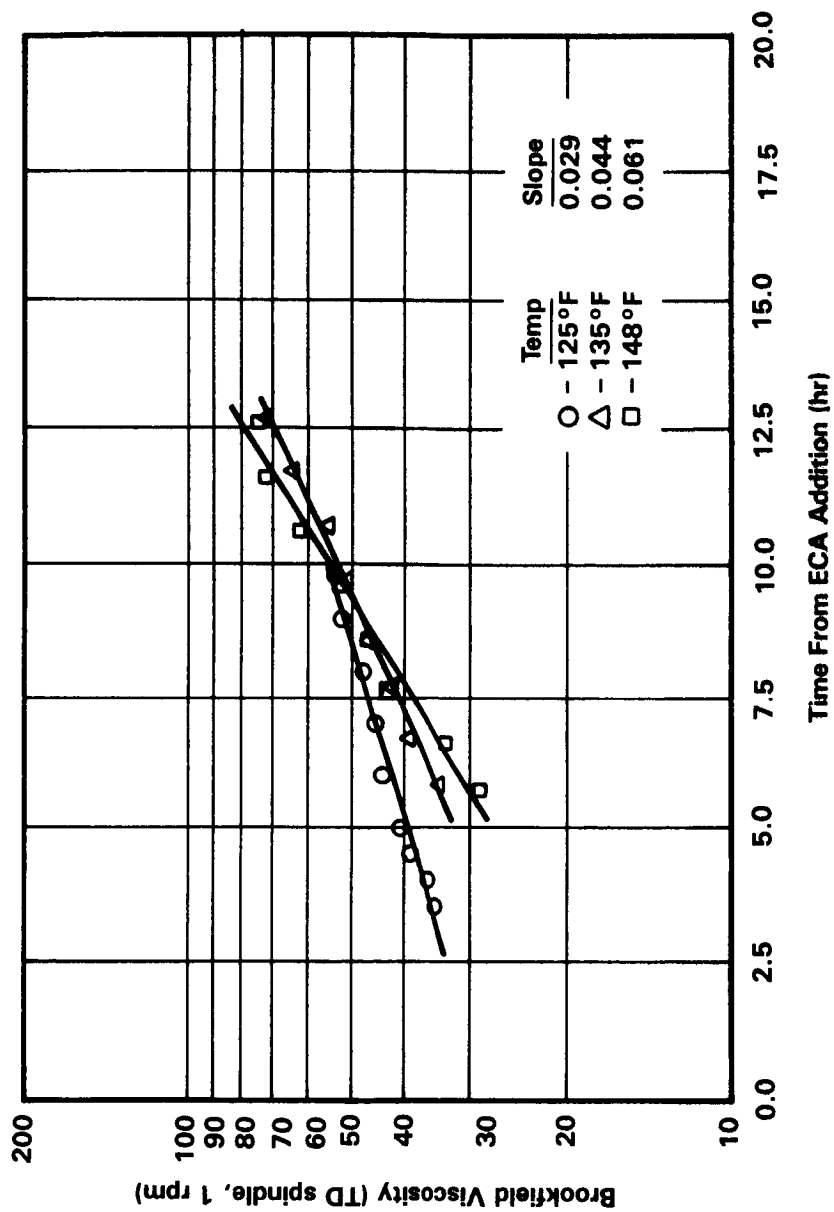
The temperature at which a physical rate limited propellant is processed and cast is selected to obtain acceptable EOM viscosities and potlives which provide adequate time after EOM to cast the propellant. As propellant EOM temperatures are increased, the EOM viscosities decline, but the potlife is usually shortened. This trade-off is illustrated for TP-H1148 propellant in Figure 66 . Few propellant formulations can be processed below 125°F because the EOM viscosity may already exceed 40 kP . A mix temperature that is extremely high (above 150°F) may shorten the potlife to less than 4 hr, and the propellant may cease to flow before casting is completed. Adequate EOM viscosities and potlives are achieved for TP-H1148 propellant at 135°F. The optimum processing temperature for TP-H3340 and DL-H396 propellants is also at 135°F. Because these formulations are mixed for the same amount of time and at the same temperature, the energy requirements will be the same.

### 3.7.5.3 Safety

The safety characteristics and properties of TP-H3340 and DL-H396 are nearly identical with TP-H1148 and TP-H1011 (Minuteman). Each of these propellants has been tested to determine ignition sensitivity to impact, friction, electrostatic discharge, and autoignition. Uncured and cured propellant formulations of TP-H3340 and DL-H396 were found to be comparable to TP-H1148 and TP-H1011 in ignition sensitivity. The ignition sensitivity of the intermediate products of TP-H3340 and DL-H396 were also found to be comparable to those for TP-H1148 and TP-H1011. The major difference between the formulations in terms of safety is that the TP-H3340 and DL-H396 formulations contain IPDI. Isocyanates are extremely toxic while the ECA curative used in TP-H1148 propellant is only moderately toxic. Extreme precautions are required for the storage and handling of isocyanates to prevent injury to personnel. However, safe isocyanate handling and storage procedures have already been established because of other production programs (Peacekeeper Stage I, Standard Missile, PAM DII, etc.).

### 3.7.6 CONCLUSION

Four composite propellants (zero cards, Class 1.3) were evaluated in the SRM trade studies; TP-H1148, DL-H396 (HTPB), and TP-H3340 propellants meet the baseline requirements specified in CPWI-3600. DL-H397 (low HCl) is not as far



87354-13A

Figure 66 . Effect of Sample Temperature on Slope of Pot Life Curves for TP-H1148 Propellant (Mix AB5154)

along in the development as the other candidates so its emphasis during the Block II SRM trade studies was reduced.

TP-H1148 propellant, used as the HPM formulation, has proven reliable and offers no technical risk. However, TP-H1148 does not offer as much potential for performance gains as offered by DL-H396 propellant. TP-H3340 propellant is not as attractive as either DL-H396 or TP-H1148 propellant because of higher raw material costs and difficulty in achieving required burn rates. Further,  $\text{Fe}_2\text{O}_3$  concentration greater than 1.0 percent may be required to meet burn rate requirements for the heads-up configuration. This amount of  $\text{Fe}_2\text{O}_3$  significantly reduces propellant impulse limiting the potential for performance gains. Processing problems could also be encountered due to the large fraction of fine  $\text{Fe}_2\text{O}_3$  necessary to achieve burn rates. TP-H3340 propellant has a slightly higher technical risk than either TP-H1148 or DL-H396 propellant.

DL-H396 (HTPB) propellant was selected as the formulation for the Block II SRM. Its reliability is based on similarity to other HTPB propellants. The processing characteristics of the DL-H396 formulation are nearly identical to those of TP-H1148 propellant and the raw material costs are less. It offers a significant potential for performance gains in the heads-up configuration.

The best approach for DL-H396 to achieve burn rate requirements with DL-H396 propellant is to add  $\text{Fe}_2\text{O}_3$  (as with TP-H1148 propellant). The low  $\text{Fe}_2\text{O}_3$  levels required (0.05 to 0.15 percent) allow the oxidizer grind ratio to be fixed, achieving optimum processing, rheology, and mechanical properties. Addition of  $\text{Fe}_2\text{O}_3$  is an easy way to standardize burn rate and to control the motor-to-motor burn rate variabilities similar to TP-H1148.

The raw materials used in DL-H396 propellant are readily available to support 15 launches per year. No unusual specification, handling, processing, or storage of DL-H396 raw materials are required. The selection of DL-H396 propellant for the Block II SRM offers potential for significant performance gains at minimal to no technical risk.

### 3.8 LINER

The liner selected to bond the DL-H396 propellant grain to the silica-filled NBR insulated case is identified as UF-2155. Its selection was based on its ability to form strong bonds to the propellant and insulation substrates and its successful use with HTPB propellants in many other rocket motors, e.g., Peacekeeper, Standard Missile Mk 104, PAM DII Space Motor. The formulation of UF-2155 liner is shown in Table 36.

**Table 36. Composition of UF-2155 Liner**

<u>Ingredient</u>	<u>Function</u>	<u>Composition (Weight Percent)</u>
R-45M	Polymer	} 62.71
IPDI	Curative	
HX-868	Bonding Agent	3.39
Thermax	Reinforcing Filler	33.9
Cab-O-Sil	Process Aid	0.6 to 6 parts/100 parts*

\*Adjust as required to obtain desired viscosity.

The bond strength between the NBR insulation and UF-2155 liner is much greater than the bond between the liner and DL-H396 propellant. The mode of failure in the DL-H396 propellant/UF-2155 liner/NBR insulation system is a cohesive failure in the propellant. This is the same failure mode exhibited with specimens from the present RSRM configuration; i.e., the failure occurs in the TP-H1148 propellant cohesively rather than at the STW5-3224 liner/insulation bondline. The bond strength is greater than the cohesive strength of the propellant adjacent to the propellant/liner bondline. Consequently, as long as the DL-H396 propellant is as strong or stronger than the TP-H1148 propellant, the present criterion for bond strength corresponds to the relative strengths of the propellants.

With the present Shuttle grain configuration, a design safety factor of 2.0 is maintained. Since the DL-H396 propellant has greater stress and strain capability than TP-H1148 propellant, the design safety margin is assured with the Block II SRM design configuration.

### 3.8.1 BOND STRENGTH

An even stronger bond in the peel mode has been demonstrated between NBR/UF-2155/DL-H396 propellant than that obtained with STW4-2621/STW5-3224/TP-H1148 propellant, the present SRM configuration. A comparison of the two configurations is listed in Table 37.

Table 37. Bond Strength Comparison

<u>Test Specimen</u>	<u>DL-H396/UF-2155/ V-45</u>	<u>TP-H1148/STW5-3224/ STW4-2621</u>
<u>90-deg Peel (pli)</u>	23	13
Failure Mode		
Liner Cohesive (%)	100	--
Propellant Cohesive (%)	--	100
<u>Tensile Adhesion (psi)</u>	142	95
Failure Mode		
Liner Cohesive (%)	--	--
Propellant Cohesive (%)	100	100

### 3.8.2 COMPATIBILITY

The similarity of the liner polymeric backbone to that used in the propellant and insulation ensures the substrates will be compatible. For the Block II configuration, an HTPB is used in DL-H396 propellant and UF-2155 liner. The NBR insulation is also made of butadiene (acrylonitrile copolymer) which, with the aid of sulfur, is vulcanized at a high temperature and pressure. For the present Shuttle configuration, the liner and propellant have polybutadiene with carboxyl terminations for effecting a low-temperature cure. The same NBR is used with silica filler to form a compatible insulation substrate.

Other processes ensure a compatible liner bond. The substrates are dried and meticulously cleaned prior to the liner application. An even precise thickness is obtained with the sling liner process. The liner applied to the NBR surface is partially cured prior to vacuum casting the propellant into the motor cavity. To counteract the tendency for the isocyanate curative to diffuse from

the propellant to the liner, an aziridine compound is added in small quantities to the UF-2155 liner. By diffusion into the propellant this bonding agent stiffens the propellant and promotes a strong bond.

The liner bond compatibility is further assured by selecting an optimum curative (NCO)-to-polymer (-OH) stoichiometric ratio. This selection is achieved by a standardization procedure carried out when any new lot of raw material is introduced into the UF-2155 liner formulation. The optimum liner thickness is also selected based on a standardization procedure. Since the liner replaces propellant, a minimum thickness compatible with bond strength is selected.

### **3.8.3 MAINTENANCE OF BOND INTEGRITY WITH TIME**

UF-2155 liner has been successfully used for bonding various propellants to insulated motor cases. An example of how well the UF-2155 liner maintains bond integrity is presented in Figure 67 for tensile adhesion and Figure 68 for 90-deg peel adhesion after 1 year storage at 145°F. This example represents the bond integrity for the Standard Missile, a Navy tactical missile. The high-temperature environment simulates long-term ambient storage by a factor of 16, i.e., 1 year at 145°F is equivalent to 16 years at ambient. The failure mode of test specimens was consistently at the propellant/liner interface with grains of propellant adhering to the liner and some liner adhering to the exposed propellant.

Since the Block II SRM configuration requires as good or better aging behavior than the present configuration, the behavior of the STW5-3224/TP-H1148 bond with time at 135°F is also shown in Figures 67 and 68. The peel and stress levels are much lower than those obtained with the Standard Missile, the example used for comparison. However, we expect the improvements in 90-deg peel and tensile adhesion experienced with the Standard Missile can be duplicated with the Block II SRM Shuttle configuration which will have the same HTPB binder.

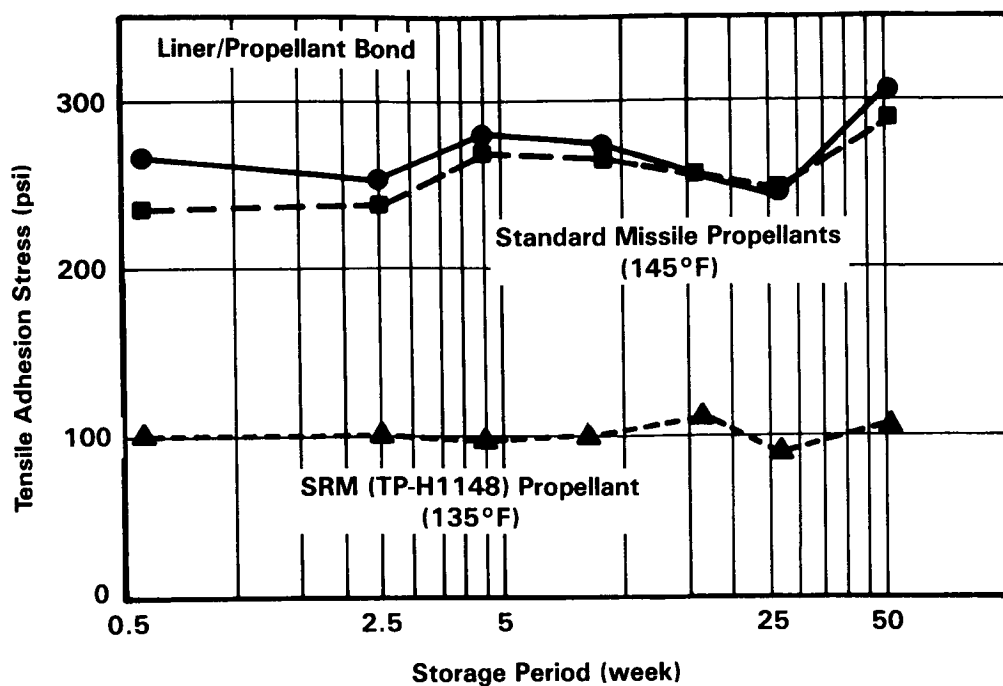


Figure 67. Effect of Accelerated Aging on Tensile Adhesion

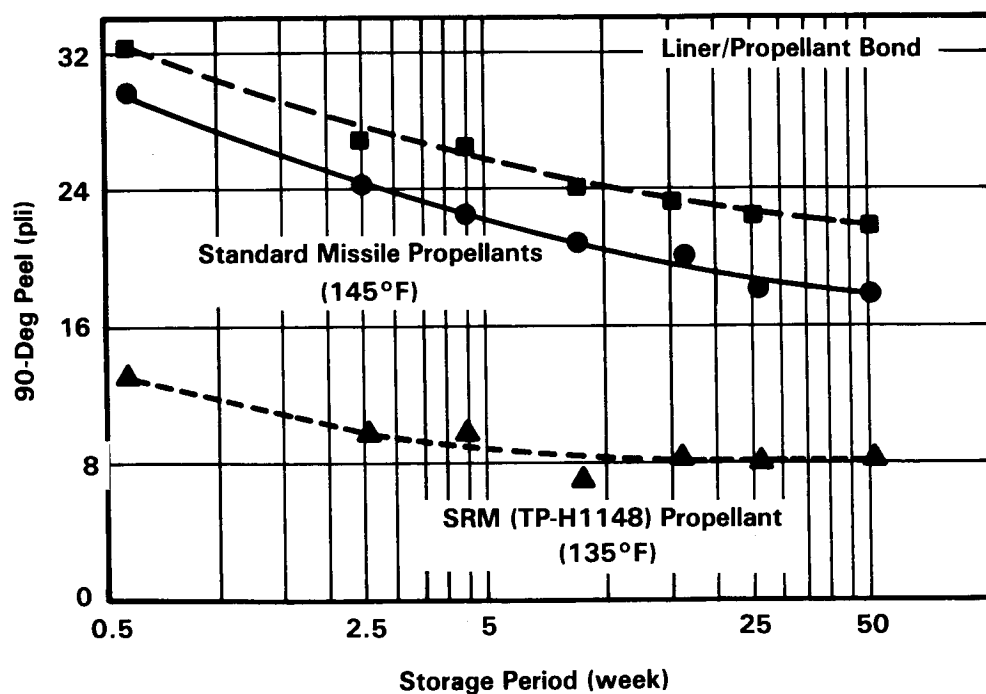


Figure 68. Effect of Accelerated Aging on 90°F Peel Adhesion



### 3.8.4 PREVIOUS APPLICATIONS

Morton Thiokol recommends the liner, UF-2155, to take advantage of the experience and reliable performance of this liner in bonding the propellant grains to the insulated case for various motor production contracts:

- a. PAM-DII. UF-2155 liner reliably bonds the TP-H1202 propellant grain to an EPDM insulated case. This motor is used to lift payloads from the Shuttle bay into the desired orbit and operates in a high vacuum environment.
- b. Peacekeeper Stage I. UF-2155 liner reliably bonds the TP-H1207C propellant grain to an EPDM insulated case.
- c. Standard Missile. UF-2155 liner bonds both the TP-H1205C and TP-H1206C sustain and boost grains to the polyisoprene insulated case.

The process for applying the UF-2155 liner to an insulated case is well characterized. It has been used to bond the HTPB propellant grains over the last 10 years.

### 3.8.5 CASTABLE INHIBITOR

The aft end of the propellant grain on Block II center and forward segments will be inhibited to control the burning surface area just as it is done in the HPM configuration. An off-the-shelf liner, UF-2153, which has the thixotroping agent Cab-O-Sil removed, will be used to inhibit DL-H396 burning. The formulation of this liner/inhibitor is listed below:

Table 38. Formulation for UF-2153 Inhibitor

<u>Ingredient</u>	<u>Function</u>	<u>Composition (weight percent)</u>
R-45M Triethanol amine	Polymer Cross-linker	80
DDI 1410 Titanium oxide	Curative Filler	20

UF-2153 was selected to inhibit the end of the DL-H396 grain segment because of its rapid cure, and because it will bond well to the DL-H396 partially-cured propellant. After about 40 hr propellant cure, the UF-2153 inhibitor will be poured into a cavity formed at the top of the segment grain. UF-2153 inhibitor without Cab-O-Sil is very fluid, will fill the cavity, and cure to a solid consistency with continued cure of the DL-H396 grain. Since the UF-2153 castable inhibitor contains the same binder as the propellant, strong bonds are assured.

The bond and rheological behavior of the UF-2153 castable inhibitor (liner) is well characterized, since it is used to bond TP-H1159 propellant grain to a phenolic insulation in the HARM missile. TP-H1159 propellant contains an IPDI-cured HTPB polymer as does DL-H396.

### **3.9 INSULATION DESIGN**

The current HPM internal insulation system design is based on thermal properties, char, and material erosion characteristics of asbestos/silica-filled NBR.

Because of possible carcinogenic effects associated with asbestos-containing materials, it is necessary to develop and qualify replacement materials.

Presently, a study is under way to replace all asbestos-containing materials in the RSRM which will consider the development, testing, analysis, and design efforts required to develop and qualify an asbestos-free SRM. The results from this study at the date of this report have influenced the Block II SRM design.

This study, the Asbestos Replacement Study Plan, will not be completed until early 1987; the insulation design described for the Block II SRM may be improved after that time. It is the intent of the Block II study to increase reliability while analyzing different replacement materials by ensuring that previous SRM experience is reflected in the determination of safety factors at various locations in the motor. Particular emphasis is placed on the insulation configuration at the field assembly joints between segments and at the nozzle attachment joint where the insulation provides thermal protection to critical pressure seals.

#### **3.9.1 REQUIREMENTS AND SCOPE OF STUDY**

The following guidelines for internal insulation design are taken from CEI specification CPW1-3600 which defines the redesign criteria.

The Block II SRM internal insulation system, consisting of case side wall thermal insulation, stress relief flaps, and propellant grain inhibitors, use component design configurations as defined in this report. Post-test and post-flight verification of insulation compliance with design safety factor requirements shall be based on a comparison of material-affected depth against minimum design thickness.

Case insulation adjacent to metal part field joints have a minimum safety factor of 2.0. The case insulation has a minimum safety factor of 1.5, assuming normal motor operation and a safety factor of 1.2 assuming loss of a castable

inhibitor. Case insulation in sandwich construction regions (aft dome and center segments, aft end) have a minimum safety factor of 1.5. Insulation is designed to be capable of withstanding 12 sec of early exposure. Insulation remaining at the end of action time shall be greater than or equal to the amount of material required for thermal protection. Insulation performance shall be calculated using actual prefire and postfire motor operation insulation thickness measurements. Compliance with safety factor requirements shall be calculated using minimum insulation design thickness.

The insulation is designed to ensure that the mechanical properties of the case are not degraded by flight and/or subsequent thermal soak for worst-case PMBT over a range of 40° to 90°F. The safety factor for the physical properties of the insulation/liner bond will be a minimum of 2.0 during the life of the SRM. The bond safety factor is based on the bond strength of the bondline.

### **3.9.2 SUMMARY OF SELECTED DESIGN**

The insulation subsystem for the SRM Block II includes chamber insulation, propellant stress relief flaps, forward-facing inhibitors, and aft-facing castable inhibitors. The insulation configuration protects each case segment during motor operation, reentry, and subsequent recovery. The case internal insulation subsystems include: primary insulation, forward-facing (full-web) propellant grain inhibitors, aft-facing (partial-web) inhibitors, and propellant grain stress relief flaps.

The materials selected for use as internal insulation are silica-filled NBR (SIL/NBR) and carbon fiber-filled ethylene propylene diene monomer (CF/EPDM). SIL/NBR is used as the primary insulation in the forward and center segments. It is also used as a bonding aid and for thermal protection in the aft segment. A layer of CF/EPDM is used under the propellant stress relief flaps in the aft end of the center segments. CF/EPDM is the primary insulation in the entire aft segment. It is sandwiched between two thin layers of SIL/NBR. The purpose of this CF/EPDM is to improve the ablation resistance of the insulation surface in these locations.

These two materials were selected because of the extensive experience with them in the HPM. Neither one uses asbestos fillers, and their respective thermal properties and erosion characteristics are quite adequate for their particular applications. Other nonasbestos insulation elastomers are in the development stage and, ultimately, SRMs using them might show even better payload capacity potential for the STS. However, for reliability and schedule purposes, Morton Thiokol recommends the simple approach herein described.

#### **3.9.2.1 Forward Segment**

The forward segment insulation is designed primarily to protect the SRM case during motor operation based on the 11-point star-center perforate (CP) propellant grain configuration. The insulation material to be used is SIL/NBR. This segment includes a propellant stress relief flap and a full-web castable inhibitor on the aft face of the propellant grain.

The propellant stress relief flaps are designed to reduce insulation-liner-propellant bondline loads induced at propellant grain termination surfaces following propellant cure, thermal shrinkage, and during SRM pressurization.

#### **3.9.2.2 Center Segments**

The SRM configuration requires the use of two center segments. The insulation and propellant grain configuration of the two segments are identical to maintain their interchangeability. The insulation configuration in the center segments includes a full-web, forward-facing NBR inhibitor and a partial-web castable inhibitor on the aft face of the propellant grain. The segments also include a propellant stress relief flap in the aft portion of the segments. The primary insulation material will be SIL/NBR. A layer of CF/EPDM will be used under the propellant stress relief flap to reduce erosion in this region.

The inhibitors provide thermal protection to the propellant grain, thus preventing ignition and burning perpendicular to the inhibitor surface. The forward-facing, full-web propellant inhibitor is fabricated as an integral part of the casting segment insulator. The aft-facing, partial-web inhibitor is cast

on the aft face of the propellant during cure. The inhibitor materials provide a chemically compatible stratum to which the liner/propellant is bonded.

### **3.9.2.3 Aft Segment**

The aft segment insulation is designed primarily to protect the aft SRM case during motor operation. This segment consists of a forward-facing inhibitor, the primary case insulation, and a propellant stress relief flap in the aft dome region of the segment. The primary insulation material used is CF/EPDM sandwiched between two thin layers of SIL/NBR. The two layers of NBR will be used to ensure an adequate bond at both the case/insulation interface and the insulation/liner/propellant interface. The current bond systems involving NBR provide a chemically compatible stratum with the liner/propellant system and also produces rubber tearing bonds (the failure occurs cohesively near the bond) at the case/insulation interface. The layer of NBR between the CF/EPDM and the case is also designed to provide the necessary thermal protection to the case. The current SRM involves an NBR/liner/propellant bond system interface. The forward-facing inhibitor and the propellant relief flap will be fabricated using SIL/NBR.

### **3.9.2.4 Nozzle-to-Case Insulation**

The RSRM team performs postfire analysis and evaluation on all flight motors. Postfire inspection of flight motors 16A<sup>(1)</sup> and 24A<sup>(2)</sup> revealed extensive damage to the primary O-ring at the nozzle-to-case joint. Postfire inspections also showed soot behind the primary O-ring on flight motors 13A, 15A, 15B, 18A, and 23A. Postfire delaminations also showed heat-affected primary O-rings but no damage to the O-ring) on flight motors 6A, 6B, and 19B.

---

<sup>1</sup>S. Rodgers, "SRM Significant Problem Report, Report Number DR4-5/49 (21 day), Secondary O-ring Erosion in the Nozzle-to-Case Joint on Mission 51-B (SRM16A)," TWR-15091-2, 26 July 1985.

<sup>2</sup>F. Adams, "SRM Postflight Hardware Inspection Report for STS/61C (SRM L024), Part 1 of 2 parts KSC Inspection," TWR-15412-1, 24 January 1986.

The postfire inspection results from the current SRM were used to establish the Block II SRM insulation design concept at the nozzle-to-case attachment joint. The Block II design changes the existing field joint at the nozzle/aft dome to a welded joint, with insulation laid up over the entire aft dome and fixed housing. A new factory-installed joint is created at the cylinder-to-aft dome tangent point. This new joint is similar to the other cylindrical field joints and eliminates a field joint in a very turbulent erosive environment in the motor.

#### **3.9.2.5 Field Joint Insulation**

Postfire inspections done by the RSRM team revealed extensive damage to the primary O-ring. The secondary O-ring was heat-affected in the center field joint of flight motor 15B. Postfire examinations also showed soot behind the primary O-ring on flight motors 15A (forward field joint), 22A (center field joint), and 22A (aft field joint). Other flight motors that showed damaged O-rings, after postfire examination, were 2B, 10A, 13B, and 24A. The aft field joint of flight motor 25B is blamed for the Shuttle Challenger accident.

The postfire inspection results from the RSRM team were evaluated by the Block II study team. The field joint had experienced problems that culminated in the Challenger accident and therefore it became necessary to redesign a more reliable joint.

The Block II-proposed field joint changes the existing putty-filled labyrinth configuration to a more reliable J-seal type configuration. The J-seal allows sealing to occur at the insulation, thus restricting the flow of hot erosive gases to the O-ring sealing region. This is the same concept approved for the RSRM.

#### **3.9.3 DISCUSSION**

The selection of insulation materials reconciles such seemingly opposed design considerations and requirements as inert weight versus safety factor and improved materials versus proven reliability. The priority assigned to each factor is generally determined by advanced technology, development, and state-of-the-art

designs. However, in the SRM, as in any case-bonded solid propellant rocket motor, factors related to basic motor reliability and structural integrity (insulation-liner-propellant composite bond integrity, for example) always command highest priority.

Filled rubber insulation materials as a class have completely dominated the internal chamber insulation field for many years. Reliability, design, and fabrication versatility are the characteristics of filled NBR (and rubber insulation generally) that led to its establishment as the industry-wide standard. With these materials, design and manufacturing activities are not constrained by specific component manufacturing techniques, as is the case with reinforced-phenolic materials. Structurally, integral rubber components can be: (1) laid up in place, cured, and bonded in one operation; (2) laid up on a mandrel (male or female), cured, and machined to the required configuration and thickness, then secondarily bonded in place; or (3) high-pressure molded using standard matched metal, closed-die molding techniques, and secondarily bonded in place. The first approach (in-place layup and cure) is our selected Block II SRM insulation fabrication approach. this selection is based on the following rationale:

- a. **Reliability** -- This approach eliminates the secondary bonding operation otherwise required at the critical case-to-insulation interface.
- b. **Experience** -- This fabrication method is used to insulate the majority of the large steel case space booster motors built by Morton Thiokol, Inc.
- c. **Cost Effectiveness** -- The tooling required to support this approach is minimal and substantially less expensive than that required to support either of the alternate methods (no long-lead-time tools are required).
- d. **Versatility** -- This approach offers the minimum reaction time to implement required insulation design modifications with the lowest tooling impact.

Although material vendors presently supply far more uncured, calendered, filled NBR material than they do the other candidate materials, the same mixing and calendering equipment is used to manufacture all candidate materials. However, in the quantities required to support the SRM program, supplier experience in processing NBR is a clear advantage.



Evaluation of candidate material cost effectiveness was based on basic material cost, present availability status (multiple vendor competitive bidding), estimated installed material cost, and related experience and process development factors.

The evaluation demonstrates a substantial advantage of filled NBR over the other candidate materials. The final determining factor leading to selection of silica-filled NBR was its prior successful usage and proven bond compatibility with the selected liner-propellant system. Therefore, the selection of SIL/NBR and CF/EPDM as primary insulator materials is based on evaluation of candidate material usage and demonstrated reliability, processibility, and installed cost, performance, and availability.

### **3.9.3.1 Asbestos Replacement**

The HPM insulation performance database was used to design the Block II SRM insulator using a combination of silica-filled NBR and carbon fiber-filled EPDM. The design criteria and methods used in the current design have been outlined.<sup>(3,4,5)</sup> The SRM insulation performance database consists of data from DM-5, QM-4, DM-6 (FWC), STS-8A, STS-8B, STS-9A, STS-9B, STS-10A, STS-10B, STS-16A, and STS-22B, which constitutes all HPM and FWC internal insulation performance data currently available. With these data an average material loss rate and an average exposure time for each longitudinal inspection station was calculated. A standard deviation of the average material loss rates (motor-to-motor) was also calculated. The material-affected rate of silica-filled NBR has been determined to be approximately 1.3 times the material-affected rate of asbestos/silica-filled NBR. This scale-up factor was determined from other large

---

<sup>3</sup>A. Neilson and K. Speas, "Preliminary Assessment of Space Shuttle Performance for the High Burn Rate Heads-Up Design," TWR-14920.

<sup>4</sup>N. Eddy, "High Performance SRM Internal Insulation Design Report, Revision B," TWR-13065, 11 September 1984.

<sup>5</sup>Prime Equipment Contract End Item Detail Specification, "Performance Design and Verification Requirements, Space Shuttle Solid Rocket Motor Block II, CPW1-1900 for Space Shuttle Solid Rocket Motor Project," Specification CPW1-3600, 25 November 1986.

motor firings and recent subscale motor testing. This scale-up is an estimate and is valid only in low-erosion environments such as the forward and center segments of the SRM. Subscale testing indicates that this scale-up factor is conservative.

To use the HPM insulation database, a second scale-up factor is required because the Block II design uses an HTPB propellant rather than the current PBAN propellant. The aerothermal environment associated with SRM operation is directly related to the chamber pressure, chamber temperature, and the composition of the combustion gases. The chamber temperature and combustion gas composition are functions of the propellant formulation and are relatively insensitive to the chamber pressure. Chamber pressure, however, is fixed by the nozzle throat area and the propellant grain design which is established by the motor design. Chamber pressure and nozzle throat area fixes the mass flow rate, in conjunction with the grain geometry and the internal case/nozzle configuration; this defines the local mass flow rate per unit area and Mach number. In addition, the overall design and internal ballistics establishes the exposure time of the internal case insulation at the various station locations.

The controlling parameter for convective heat transfer and mass transfer is the mass flow rate per unit area ( $\rho V = \dot{m}/A$ ) which, for a particular propellant, is fixed by the operating pressure and the motor geometry. In the motor chamber, the flow is subsonic and therefore the static pressure and temperature are essentially the chamber conditions, which results in high radiative heating rates. In general, radiative heating dominates in the chamber except for specific areas depending upon the motor design. In a submerged nozzle configuration, relatively high subsonic Mach numbers can be induced in the aft dome area which leads to correspondingly high convective heating. In addition, slots and fins in the grain design can lead to high erosion rates resulting from particle impingement induced by confined directed flow conditions.

As discussed above, the chamber temperature is a function of the propellant formulation and as such is strongly dependent on the aluminum content. The erosion, and hence the insulation design, is only affected by the percent solids as it affects the operation temperature, except for isolated particle impingement conditions. In the case of carbon derivative materials such as CF/EPDM, the

oxidation characteristics of the combustion gases will result in additional erosion due to chemical reactions. In the case of silica-filled materials such as silica-filled NBR, the primary erosion mechanism is due to melting and therefore the loss rate should be directly proportional to the total heating rates, radiative and convective.

In the past Morton Thiokol conducted an extensive study to correlate material erosion with propellant and aerothermal environments. This study included the effects of seven propellants with widely varying chemical formulations and five motor configurations. As a result of this study the following correlation was developed:

$$E_n = (\bar{P}_c/\bar{P}_r)^{1.11} (T_c/T_r)^{3.69} (\beta/\beta_r)^{0.44}$$

where:

$E_n$  = Erosion index

$\bar{P}_c$  = Average chamber pressure

$T_c$  = Chamber temperature

$\beta$  = Oxidation blowing parameter

The subscript values are the corresponding parameters for a reference propellant (r) and motor configuration (c). In the above relation the pressure term represents the convective heating, the temperature term the radiative heating, and the  $\beta$  term the chemical reaction effects. For the Block II design two different propellants are being considered: a high burn rate PBAN formulation and a low-cost HTPB propellant. The PBAN propellant is a modified version of the current HPM formulation in which the iron oxide content has been increased from 0.3 to 0.66 percent. The following is a listing of the motor operation parameters of interest for insulation performance assessment.

	<u>HPM</u>	<u>Block II PBAN</u>	<u>Block II HTPB</u>
Chamber Pressure (psi)	650	731	728
Chamber Temperature (°K)	3,387	3,387	3,511
Blowing Parameter ( $\beta$ )	0.107	0.106	0.095
Burn Time (sec)	122	113	116

Substituting these data in the foregoing equation for the erosion index the effect of propellant on insulation performance is compared with the current HPM insulation design. The results are summarized in the following table for both CF/EPDM and silica-filled NBR insulation. The change in motor action time is also factored into the following data.

Performance Index		
	<u>PBAN</u>	<u>HTPB</u>
CF EPDM	1.06	1.17
Silica-Filled NBR	1.06	1.23

The data indicate that in the case of the PBAN propellant the insulation requirements will increase by 6 percent over the existing HPM design for both the CF/EPDM and the silica-filled NBR insulation systems. For the HTPB propellant, the CF/EPDM requirement increases by 17 percent and the silica-filled NBR by 23 percent. The large increase for the HTPB propellant design is because of the difference in chamber temperature, 3,511°K compared with 3,387°K for PBAN propellant. The indicated increase is mitigated by the lower blowing parameter associated with the HTPB propellant. Since the silica-filled NBR is primarily a melting process, the effect of the blowing parameter was not included in the design of that insulation.

This scale-up factor, along with the 1.3 asbestos/silica NBR-to-silica NBR scale-up was applied to the HPM material loss rate data using the following formula:

$$\text{MLR} = (\text{scale-up} * \text{average MLR}) + (3 * \text{standard deviation})$$

Recent subscale testing indicates that in low-velocity environments the standard deviation of the material loss rate data exhibited by silica NBR is not any greater than the standard deviation of material loss rate data for asbestos/silica NBR.

The following criteria were used to determine the design thickness of the insulator at each longitudinal station location in the motor.

a. **Insulation Design Equation**

$$DT = SF (ET * MLR), SF = 1.5$$

b. **Case Wall Insulation Design-Castable Inhibitor Failure**

$$DT = SF (ET_{inhib} * MLR_{inhib}) \quad SF = 1.2$$

c. **Thermal Protection**

$$DT = (MLR * ET) + TP$$

d. **Twelve-second Early Exposure**

$$DT = MLR (ET + 12 \text{ sec})$$

e. **Minimum Design Thickness**

$$DT = 0.090 \text{ minimum}$$

DT = Design thickness

SF = Safety factor

ET = Exposure time

MLR = Scaled up material loss rate ( $\bar{X} + 3 \text{ sigma}$ )

$ET_{inhib}$  = Exposure time in the event of castable inhibitor failure

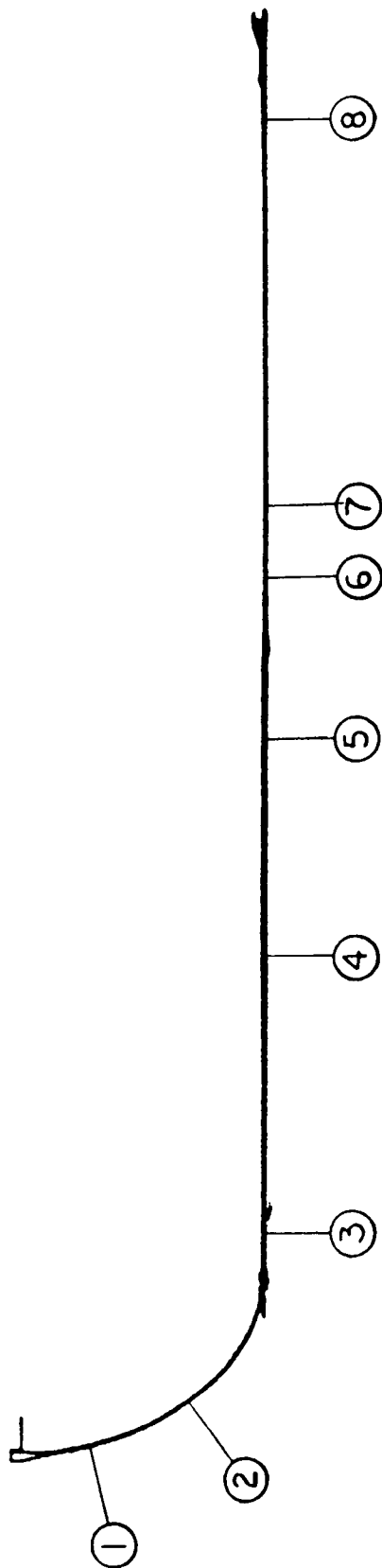
$MLR_{inhib}$  = Material loss rate in the event of castable inhibitor failure

TP = Thermal protection required (200°F maximum case temperature)

The maximum value derived from the five design criteria tests was used as the new minimum design thickness at the specified longitudinal location. Figures 69 through 72 show the minimum design thicknesses at part of the inspection stations in each segment. Also shown are the average scaled-up material loss rates and safety factors and the average +3 times the standard deviation material loss rates and safety factors. Table 39 shows the weight impact study of the insulation thicknesses in comparison to the current HPM design and performance assuming noninterchangeable center segments. Table 40 shows the same data assuming interchangeable center segments.

### 3.9.3.1.1 Case Insulation Alternatives

Different types of available insulation materials were evaluated along with filled rubbers. A list of filled rubbers that have been tested and will be



#### FORWARD SEGMENT

STATION NO.  
LONGITUDINAL LOCATION

#### HPM DESIGN

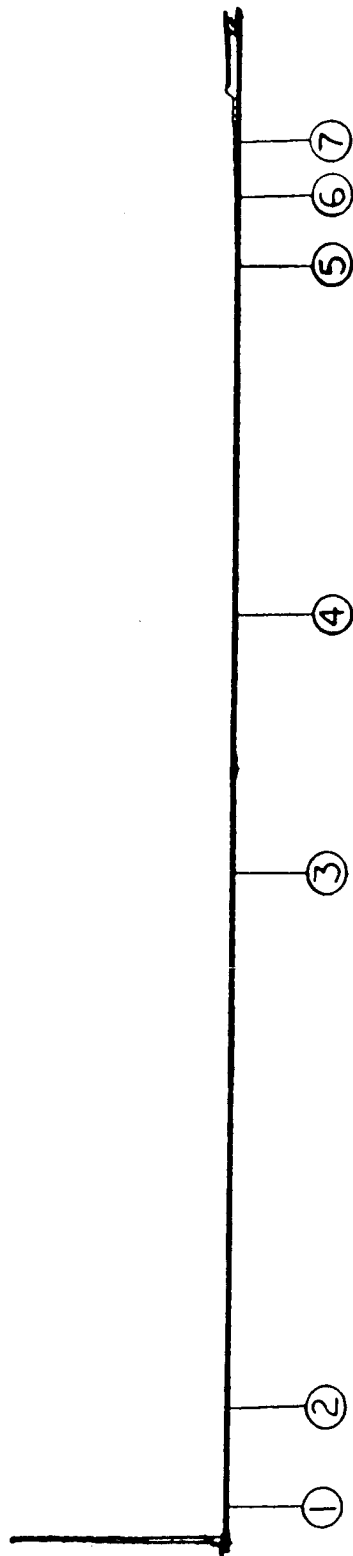
EXPOSURE TIME-SECONDS	1	2	3	4	5	6	7	8
MINIMUM DESIGN THICKNESS-INCHES	100.0	100.0	100.4	100.7	99.3	39.5	1.1	9.5
AVE MATERIAL AFFECTED RATE-MILS/SEC	0.475	0.493	0.510	0.574	0.628	0.360	0.133	0.500
AVE SAFETY FACTOR	1.440	1.233	1.430	1.890	1.500	0.930	0.000	0.000
X+3S MATERIAL AFFECTED RATE-MILS/SEC	3.30	4.00	3.55	3.02	4.22	9.80	*	*
X+3S SAFETY FACTOR	2.430	2.622	2.450	2.880	3.810	4.260	0.000	0.000
	1.95	1.88	2.07	1.98	1.66	2.14	*	*

#### BLOCK II DESIGN

MINIMUM DESIGN THICKNESS-INCHES	0.544	0.553	0.547	0.616	0.686	0.346	0.090	0.381
AVE MATERIAL AFFECTED RATE-MILS/SEC	2.203	1.887	2.188	2.892	2.295	1.423	0.000	0.000
AVE SAFETY FACTOR	2.47	2.93	2.49	2.12	3.01	6.15	*	*
X+3S MATERIAL AFFECTED RATE-MILS/SEC	3.193	3.275	3.208	3.882	4.605	4.753	0.000	0.000
X+3S SAFETY FACTOR	1.70	1.69	1.70	1.58	1.50	1.84	*	*

\*No material loss

Figure 69. Forward Segment Design

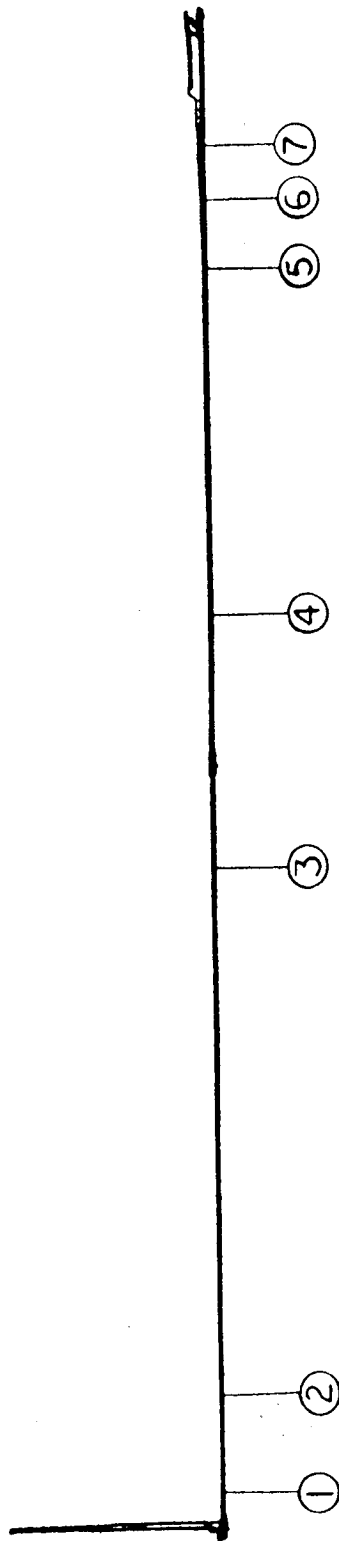


#### FORWARD CENTER SEGMENT

STATION NO.	1	2	3	4	5	6	7
LONGITUDINAL LOCATION	316.0	298.0	214.1	126.0	71.5	44.6	30.7
<b>HPM DESIGN</b>							
EXPOSURE TIME-SECONDS	0.3	1.6	2.6	7.6	9.1	10.6	4.8
MINIMUM DESIGN THICKNESS-INCHES	0.090	0.090	0.130	0.150	0.170	0.360	0.750
AVE MATERIAL AFFECTED RATE-MILS/SEC	0.000	0.000	0.000	0.000	0.800	0.490	0.980
AVE SAFETY FACTOR	*	*	*	*	23.40	69.64	16.11
X+3S MATERIAL AFFECTED RATE-MILS/SEC	0.000	0.000	0.000	5.640	4.490	5.800	3.950
X+3S SAFETY FACTOR	*	*	*	3.52	4.17	5.88	5.18
<b>BLOCK II DESIGN</b>							
MINIMUM DESIGN THICKNESS-INCHES	0.090	0.090	0.090	0.150	0.186	0.376	0.878
AVE MATERIAL AFFECTED RATE-MILS/SEC	0.000	0.000	0.000	0.000	1.224	0.750	1.499
AVE SAFETY FACTOR	*	*	*	*	16.74	47.55	12.32
X+3S MATERIAL AFFECTED RATE-MILS/SEC	0.000	0.000	0.000	5.640	4.914	6.060	3.569
X+3S Safety Factor	*	*	*	3.52	4.17	5.88	5.18

\* No Material loss

Figure 70. Forward Center Segment Design



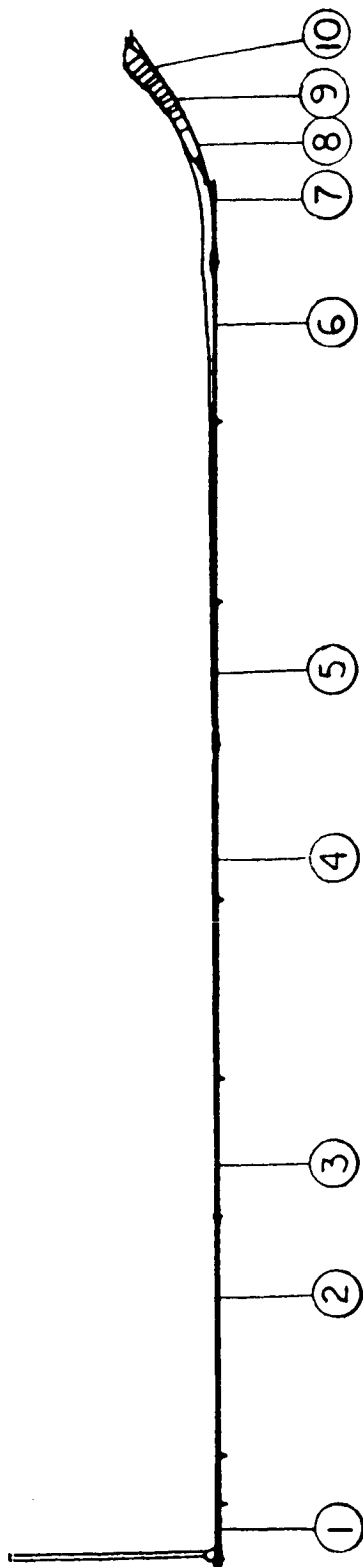
# AFT CENTER SEGMENT

STATION NO. LONGITUDINAL LOCATION	1	2	3	4	5	6	7
HPM DESIGN							
EXPOSURE TIME-SECONDS	0.1	0.9	0.8	6.4	8.2	9.8	47.0
MINIMUM DESIGN THICKNESS-INCHES	0.090	0.090	0.130	0.150	0.170	0.360	0.750
AVE MATERIAL AFFECTED RATE-MILS/SEC	0.000	0.000	0.490	3.920	4.320	3.390	4.260
AVE SAFETY FACTOR	*	*	324.73	5.99	4.80	10.89	3.75
X+3S MATERIAL AFFECTED RATE-MILS/SEC	0.000	0.000	8.590	6.020	8.100	6.690	9.510
X+3S SAFETY FACTOR	*	*	18.52	3.90	2.56	5.52	1.68
BLOCK II DESIGN							
MINIMUM DESIGN THICKNESS-INCHES	0.090	0.090	0.113	0.149	0.210	0.185	0.830
AVE MATERIAL AFFECTED RATE-MILS/SEC	0.000	0.000	0.750	5.998	6.610	5.187	6.518
AVE SAFETY FACTOR	*	*	185.19	3.89	3.57	3.65	2.71
X+3S MATERIAL AFFECTED RATE-MILS/SEC	0.000	0.000	8.850	8.098	10.390	8.487	11.768
X+3S SAFETY FACTOR	*	*	15.69	2.88	2.46	2.23	1.50

\*No material loss

Figure 71. Aft Center Segment Design





#### AFT SEGMENT

STATION NO.

LONGITUDINAL LOCATION

	1	2	3	4	5	6	7	8	9	10
	373.0	322.0	283.9	202.5	158.5	75.0	40.0	24.3	17.3	10.7

#### HPM DESIGN

EXPOSURE TIME-SECONDS

MINIMUM DESIGN THICKNESS-INCHES

AVE MATERIAL AFFECTED RATE-MILS/SEC

AVE SAFETY FACTOR

X+3S MATERIAL AFFECTED RATE-MILS/SEC

X+3S SAFETY FACTOR

	15.4	12.9	16.2	28.9	35.2	49.8	75.7	90.1	101.5	116.8
	0.400	0.380	0.450	0.730	0.880	1.800	2.600	2.793	3.522	4.636
	0.750	5.860	7.530	8.460	9.130	8.510	12.510	11.270	13.450	20.490
	34.63	5.40	3.69	2.99	2.74	4.25	2.75	2.75	2.58	1.94
	7.380	10.360	12.780	11.610	11.830	13.130	15.480	17.110	17.560	22.680
	3.52	3.06	2.17	2.18	2.11	2.75	2.22	1.81	1.98	1.75

#### BLOCK II DESIGN

MINIMUM DESIGN THICKNESS-INCHES

AVE MATERIAL AFFECTED RATE-MILS/SEC

AVE SAFETY FACTOR

X+3S MATERIAL AFFECTED RATE-MILS/SEC

X+3S SAFETY FACTOR

	0.222	0.273	0.396	0.566	0.707	1.089	2.052	2.571	3.022	4.584
	0.878	6.856	8.810	9.898	10.682	9.957	14.801	13.174	15.737	23.973
	16.40	3.31	2.78	1.98	1.88	2.20	1.86	2.17	1.89	1.64
	7.508	11.356	14.060	13.048	13.382	14.577	18.311	19.024	19.847	26.163
	1.92	2.00	1.74	1.50	1.50	1.50	1.50	1.50	1.50	1.50

Figure 72. Aft Segment Design

Table 39. Preliminary Weight Impact Study for Silica/NBR

INSULATION PERFORMANCE* = 130% ASBESTOS/SILICA NBR	INSULATION ADDED, LBS	PROPELLANT LOST, LBS	PAYLOAD IMPACT, LBS
EQUIVALENT S.F. (Use the same S.F. as in current SRM)	6,326	8,692	1,711
2.0 S.F. (Decrease the areas above 2.0, increase the areas below 2.0)	-73	-53	+10
1.5 S.F. (Decrease the areas above 1.5, increase the areas below 1.5)	-2057	-2826	+556
2.0 MINIMUM S.F. (No change to areas above 2.0, increase the areas below 2.0)	6,196	8,513	-1,676
1.5 MINIMUM S.F. (No change to areas above 1.5, increase the areas below 1.5)	2,273	3,123	-614

\*SILICA NBR (V-45) -- PERFORMANCE CHANGES BASED ON LIMITED SUBSCALE AND MINUTEMAN F/S DM TEST DATA UP TO 10 MILS/SEC. EXTRAPOLATED IN THE 10 TO 30 MILS/SEC RANGE.

Table 40. Preliminary Sandwich Weight Impact Study for Silica/NBR  
Using Interchangeable Center Segments

INSULATION PERFORMANCE\* = 130% ASBESTOS NBR

	<u>INSULATION ADDED, LBS</u>	<u>PROPELLANT LOST LBS</u>	<u>PAYLOAD IMPACT, LBS</u>
EQUIVALENT S.F. (Use the same S.F. as in current SRM)	6,313	8,674	1,708
2.0 S.F. (Decrease the areas above 2.0, increase the areas below 2.0)	704	967	-190
1.5 S.F. (Decrease the areas above 1.5, increase the areas below 1.5)	-1455	-1999	+393
2.0 MINIMUM S.F. (No change to areas above 2.0, increase the areas below 2.0)	6,196	8,513	-1,676
1.5 MINIMUM S.F. (No change to areas above 1.5, increase the areas below 1.5)	2,273	3,123	-614

\*SILICA NBR (V-45) --- PERFORMANCE CHANGES BASED ON LIMITED SUBSCALE AND MINUTEMAN F/S  
DM TEST DATA UP TO 10 MILS/SEC. EXTRAPOLATED IN THE 10 TO 30 MILS/SEC RANGE.

tested is in Table 41. Other alternatives include trowelable filled mastics, castable and sprayable materials, and reinforced phenolics.

**Reinforced Phenolics.** The rigid and semirigid reinforced phenolic materials, which possess excellent erosion resistance, were considered potential candidates for aft dome insulation. These materials have limited use because of high raw material costs, component fabrication and assembly costs, and because of technical problems of fabricating and installing components of the size and weight required. Component fabrication (both one-piece or segmented) using this type material requires costly, high-pressure, matched metal molding dies, thus incurring a large expenditure early in the program.

The Asbestos Replacement Study Team is currently conducting tests (see Section 3.9.3.2.1) on an elastomerized carbon phenolic material (manufactured by U. S. Polymeric Corp.) that would (if tests are conclusive) replace the CF/EPDM in the high erosive area in the aft dome. To date these tests are inconclusive and therefore this concept is not included as a candidate in the Block II SRM design.

**Trowelable Mastics and Sprayable Materials.** The trowelable mastics and sprayable materials that offer a potentially low installed cost were eliminated as candidate primary chamber insulation materials because production experience and demonstrated reliability in large motor programs are lacking. The use of trowelable mastic materials that have received the widest usage has been limited to demonstration motors. Fabrication of insulation components using these high-viscosity materials has been limited generally to the "in-place" method, which involves applying one or more layers of the material directly to the case interior surface to obtain the required thickness.

Our experience with viscous mastic materials has identified a basic problem with air entrapment. This problem has precluded extensive use of these materials in production motors. Motors insulated with trowelable mastic materials have required extensive work to inspect, identify, and repair voids and porous defect areas. A program to develop improved material processing properties, inspection methods, and repair procedures would involve substantial effort and associated costs and project risk.

ORIGINAL PAGE IS  
OF POOR QUALITY

Table 41. SRM Asbestos-Free Insulation Development

(12/09/86)

Test Number	Polymer	FORMULATION Fillers	ACTION TIME	AVG. PRESSURE	MATERIAL AFFECTED RATES (mils./sec.)		
					LOW	MEDIUM	HIGH
+ 401	NR	Asbestos/Silica (Std)	23.84	857.2	.003	.04-.09	.09-.15
	NR	Silica			2.2	7.7	9.7
	NR	Silica			2.9	11.9	30.8
+ 402	NR	Asbestos/Silica (Std)	12.06	822.5	2.8	12.8	26.1
	NR	Silica			3.4	9.4	11.8
	NR	Silica			4.2	16.4	34.9
+ 403	NR	Asbestos/Silica (Std)	6.95	833.0	4.2	15.2	32.9
	NR	Silica			3.3	9.6	16.1
	NR	Silica			3.7	17.9	42.3
107	NR	Asbestos/Silica (Std)	12.13	808.5	2.8	13.9	39.2
	NR	Carbon Fibers 27%			2.7	8.6	21.4
	NR	Carbonized Rayon cloth			4.5	11.0	26.6
108	NR	Asbestos/Silica (Std)	11.55	849.8	4.5	13.7	19.6
	IR	Kevlar/Silica			3.0	9.6	15.7
	IR	Fire Retardant			4.3	16.2	32.9
+ 109	NR	Asbestos/Silica (Std)	11.90	821.3	2.3	24.0	52.5
	NR	Asbestos/Silica (Std)			3.1	7.9	13.5
	NR	Asbestos/Silica (Std)			2.9	8.1	15.0
110	NR	Asbestos/Silica (Std)	11.71	826.6	3.1	8.1	16.0
	IR/EPDM	Kevlar/Silica/Dechlorane			7.9	7.9	15.5
	IR/EPDM	Kevlar/Silica/Dechlorane			3.5	9.8	25.0
+ 111	NR	Asbestos/Silica (Std)	11.35	798.8	3.6	8.5	17.1
	NR	Glass/Phenolic			3.4	8.9	13.9
	NR	Glass/Phenolic			(glass phenolic)	15.9	15.0
112	NR	Asbestos/Silica (Std)	12.12	835.9	3.4	8.9	14.8
	EPDM	Carbon Fiber (27%)			2.6	4.0	22.2
	EPDM	Carbonized Rayon Cloth			4.5	12.5	24.8
113	NR	Asbestos/Silica (Std)	11.3	853.7	3.5	6.3	15.6
	NR	Kynol/Silica/Dechlorane			3.1	8.9	13.3
	IR/EPDM	Kevlar/Silica/Dechlorane			5.6	17.1	53.8
114	NR	Asbestos/Silica (Std)	11.3	853.7	3.8	6.8	7.5
	NR	Kevlar/Talc/Flame Ret.			3.1	8.9	13.3
	NR	Kevlar/Talc/Flame Ret.			5.6	17.1	53.8
115	NR	Asbestos/Silica (Std)	11.3	853.7	3.8	6.8	7.5
	NR	Silica/Kynol/Flame Ret.			3.1	8.9	13.3
	NR	Silica/Kynol/Flame Ret.			5.6	17.1	53.8

+ Conducted to evaluate the performance characteristics of high-mach test chamber.

\* Test Standard STW4-2621 calender direction was parallel to gas flow.

Table 41. SRM Asbestos-Free Insulation Development (Cont)

Test Number	Polymer	FORMULATION Fillers	ACTION TIME	AVG. PRESSURE	MATERIAL AFFECTED RATES (mils/sec.)		
					LOW	MEDIUM	HIGH
116	NBR NBR NBR	Asbestos/Silica (Std) Kevlar/Talc/CF/Flame Ret. Kevlar/Talc/Kynol/Flame Ret.	12.15	788.2	.003	.04-.09	.09-.15
117	NBR NBR EPDM	Asbestos/Silica (Std) Silica/Kynol/CF/Flame Ret. Kevlar/Talc/Flame Ret.					
118	NBR EPDM EPDM	Asbestos/Silica (Std) Kevlar/Talc/Kynol/Flame Ret. Kevlar/Talc/CF/Flame Ret.					
119	NBR VMQ VMQ	Asbestos/Silica (Std) Kevlar/Silica Kynol/Silica					
120	NBR EPDM EPDM	Asbestos/Silica (Std) Silica Kevlar/Silica					
121	NBR CSM/EPDM CSM/EPDM	Asbestos/Silica (Std) Silica Kevlar (1/4")/Silica					
122	NBR CSM/EPDM CSM/EPDM	Asbestos/Silica (Std) Kevlar/Talc Kevlar/Silica					
123	NBR CSM/EPDM CSM/EPDM	Asbestos/Silica (Std) Silica Silica/Phthalocyanine					
124	NBR EPDM NBR	Asbestos/Silica (Std) Kevlar/Silica Kevlar/Silica					
125	NBR	Asbestos/Silica (Std) ARN116 Improvement ARN117 Improvement					
126	NBR	Asbestos/Silica (Std) ARN118 Improvement ARN119 Improvement					
127	NBR CSM/EPDM CSM/EPDM	Asbestos/Silica (Std) Silica/Rayon (Mgo) Silica/Rayon (alumina)					

ORIGINAL PAGE IS  
OF POOR QUALITY

Table 41. SRM Asbestos-Free Insulation Development (Cont)

Test Number	Polymer	FORMULATION Fillers	ACTION TIME	AVG. PRESSURE	(12/09/86)		
					MATERIAL AFFECTED RATES (mils/sec.)		
					LOW	MEDIUM	HIGH
128	NBR SBR SBR	Asbestos/Silica (Std) Kevlar/Silica/Flame Ret. Kevlar/Silica/Kynol/Flame Ret.			.003	.04-.09	.09-.15
129	NBR SBR SBR	Asbestos/Silica (Std) Improvements on 128 Improvements on 128					
130	NBR	Asbestos/Silica (Std) Qualify best candidates Qualify best candidates					
131	NBR	Asbestos/Silica (Std) Qualify best candidates Qualify best candidates					

ORIGINAL PAGE IS  
OF POOR QUALITY

### **3.9.3.2 Nozzle-to-Case Insulation**

The Block II baseline design for the aft dome insulation eliminates the existing field joint at the nozzle and creates a new factory-installed joint at the cylinder-to-aft dome tangent point (Figures 73 through 75). To eliminate the need of extensive tests involving a new CF/EPDM-to-case bond system, a thin layer of SIL/NBR will be used between the CF/EPDM and the case. Analysis requires a maximum CF/EPDM thickness of approximately 5 inches.

The Block II design modifies the method in which the existing aft dome and segment are insulated and propellant is cast. A summary of the new procedure is included in Section 3.9.4.

#### **3.9.3.2.1 Nozzle /Aft Dome Alternatives**

The SRM Asbestos Replacement Study Team is in the process of conducting a series of subscale tests to evaluate different candidate materials. The test section (Figure 76) is attached to an end-burning, seventy-pound charge (SPC) motor which provides burn times from 10 to 85 sec. The test section is designed with low-, medium-, and high-velocity regions so effects can be evaluated at different Mach numbers. Each test evaluates three materials: a baseline asbestos/silica-filled NBR and two candidate materials.

An NBR-filled, carbonized, rayon-cloth phenolic (R2121), provided by U. S. Polymeric, has shown promising erosion data. Char motor performance data are shown in Tables 42 and 43 and in Figures 77 through 80. An EPDM filler will also be tested later in the program.

Although a final decision on these materials cannot be included in this Block II final report, serious consideration is given to these promising data.

### **3.9.3.3 Field Joint Insulation**

A number of joint insulation configurations have been evaluated to determine an insulation joint configuration which will best meet the requirements of protecting the steel case hardware and the primary and secondary O-ring seals during



ORIGINAL PAGE IS  
OF POOR QUALITY

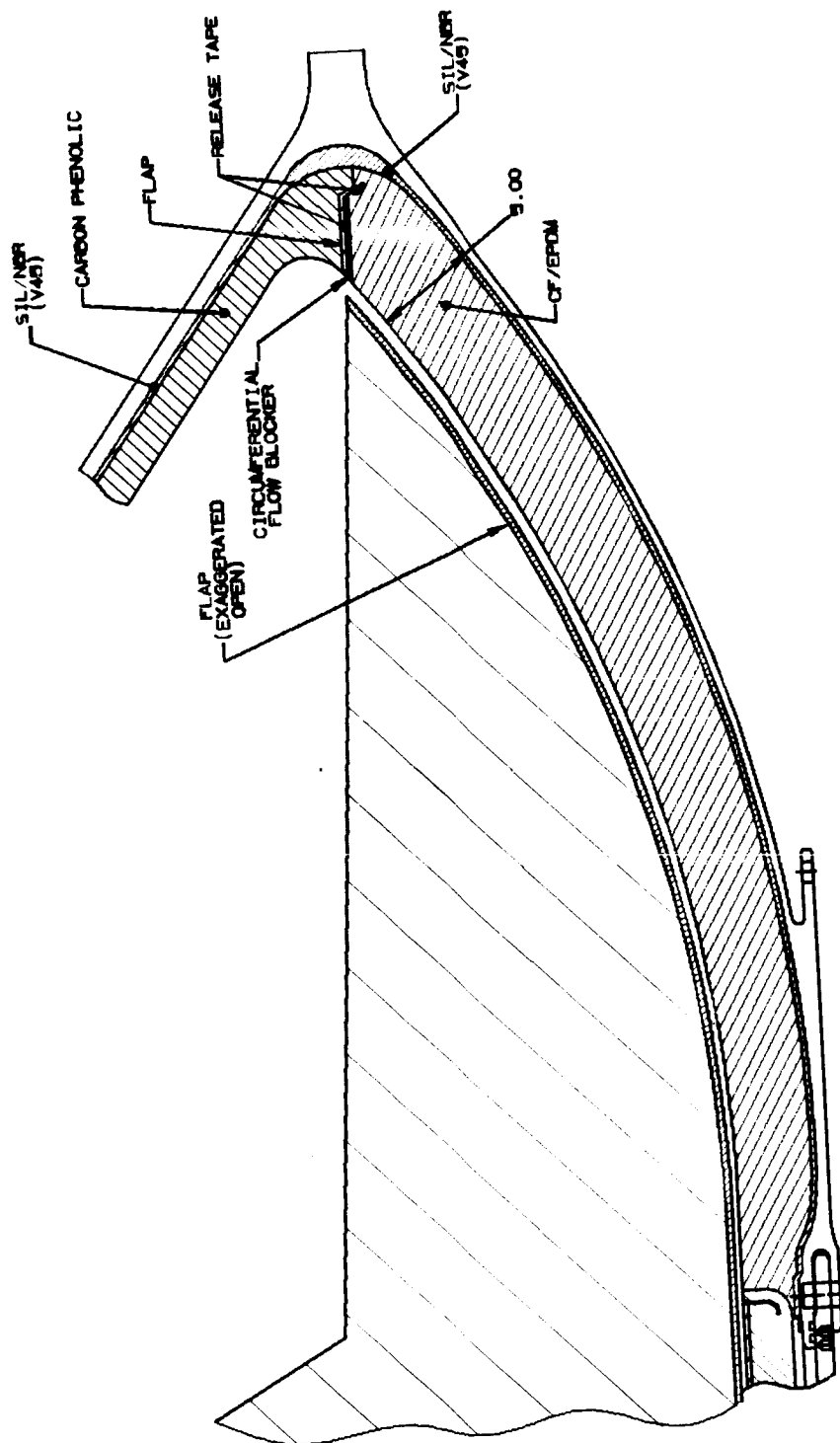


Figure 73. Insulated Aft Dome

ORIGINAL PAGE IS  
OF POOR QUALITY

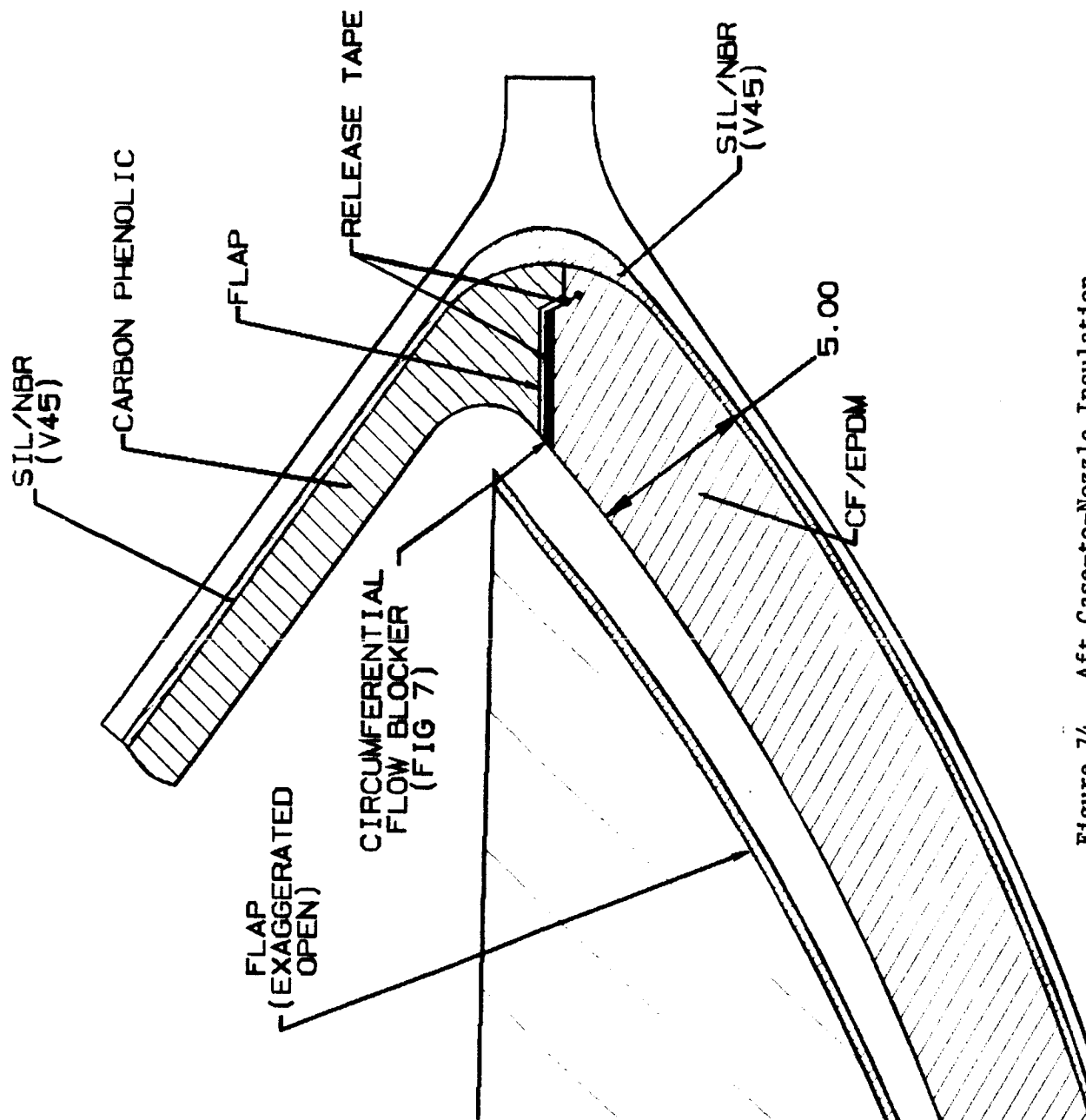


Figure 74. Aft Case-to-Nozzle Insulation

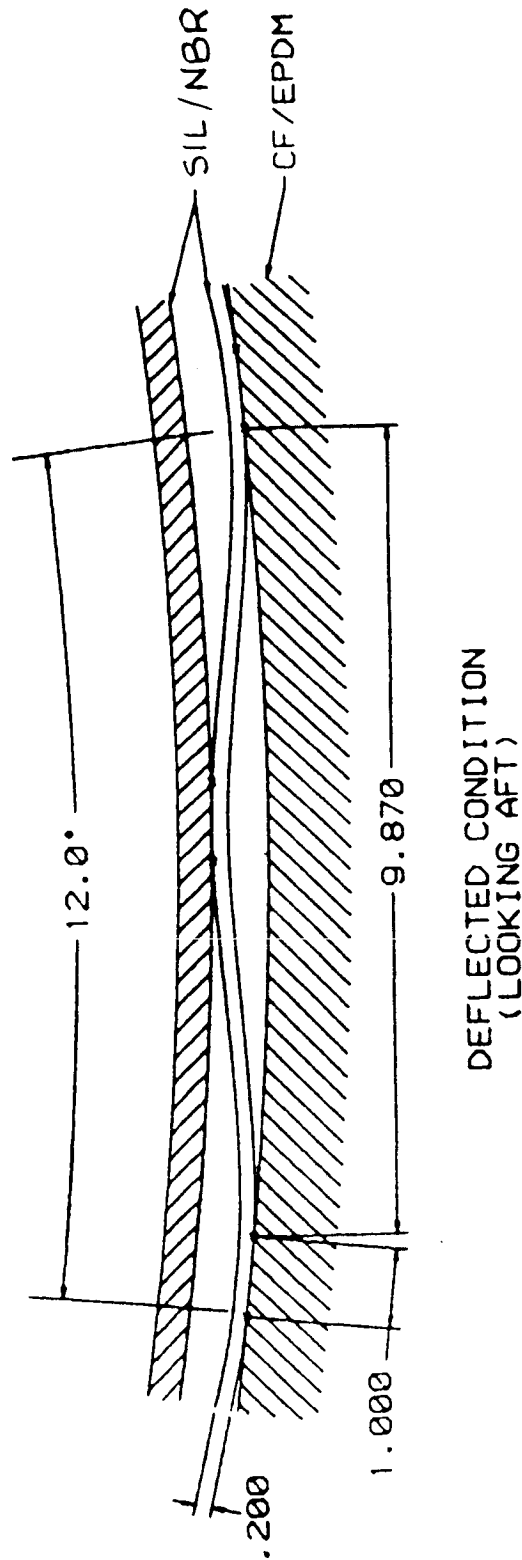


Figure 75. Circumferential Flow Blocker (baffle)

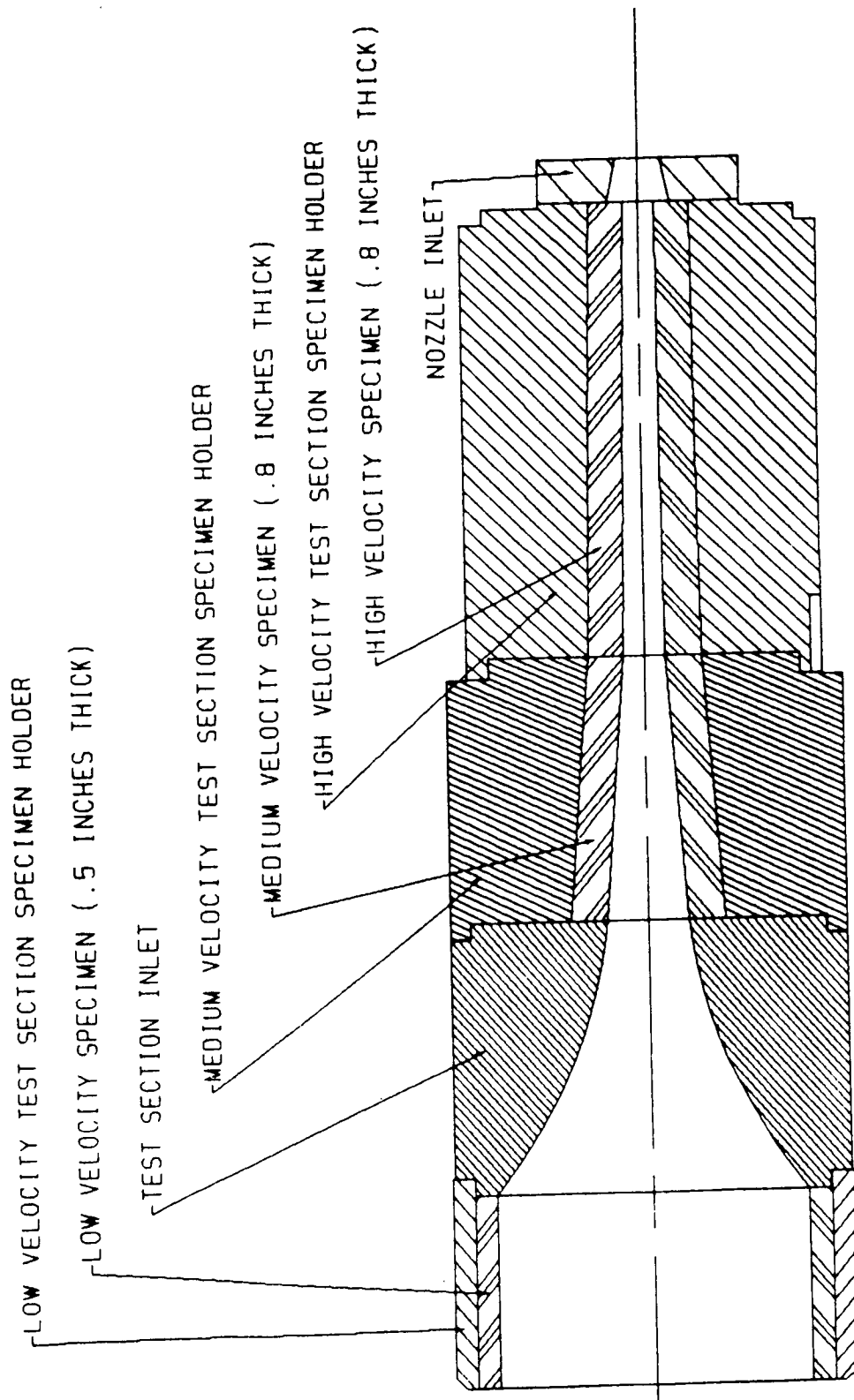


Figure 76. Insulation Test Section of 70-lb Charge Char Motor

Table 42. Insulation Material and Process Development--Char Motor Performance

MORTON THIOKOL Inc. - Wasatch Operations

CHARMOTOR No. ARN107 DATE: 11/03/86 PROPELLANT: TP-H1148

PRELIMINARY TEST RESULTS

AVERAGE PRESSURE: 808.50 psia  
ACTION TIME: 12.13 seconds

MATERIALS TESTED:

STANDARD: STW4-2621  
SAMPLE #1: NBR-27  
SAMPLE #2: R2121

- NBR/Asbestos/Silica - a V44-type insulation supplied by Kirkhill  
- NBR/Carbon Fiber filler - Similar to CFF/EPDM: supplied by U.S. Polymer  
- NBR/Carbon Cloth - an insulation candidate supplied by U.S. Polymer

PHYSICAL PROPERTY DATA:

	Tensile psi	Elong. -----	Tear pli	Density g/cc	Thermal Cond.	Specific Heat	Shore "A"
--	----------------	-----------------	-------------	-----------------	------------------	------------------	--------------

STANDARD:	1302	130	330	1.282	0.136	0.373	79
-----------	------	-----	-----	-------	-------	-------	----

SAMPLE #1:

SAMPLE #2:

MAT'L AFFECTED RATE (mils/sec.):		(NBR-27)		(R2121)	
Mach No.	=	.003	.06	.003	.06
STANDARD:		2.7	8.5	2.7	8.5
SAMPLE:		4.5	11.0	4.5	13.5
(Difference)		1.7	2.5	1.7	5.0
			5.5		-2.0

OBSERVATIONS & CONCLUSIONS:

Both candidate materials were relatively good performers in the lower Mach range. The carbonized rayon cloth candidate looked superior in the high velocity region; however, severe delamination was observed in the low velocity samples.

ORIGINAL PAGE IS  
OF POOR QUALITY

ORIGINAL PAGE IS  
OF POOR QUALITY

Table 43. Char Motor Performance--Motor No. ARN 107

DATE: 11/03/86 PROPELLANT: TP-H1148 PRESSURE: 808.5 psia. TIME: 12.13 sec.

MAR Summary for all pieces in each section.												
DATA POINT	DISTANCE ALONG CHAMBER		Std. Dev.	NBR-27	Std. Dev.	R2121	Std. Dev.	(STM4-2621) STANDARD		AVERAGE Radius	AREA RATIO a/a*	MACH No. Rav basis
	STM4-2621 V44 type	in.)						MAX	MIN			
LOW												
1	0.5	2.50	0.61	3.74	0.42	3.41	1.82	3.32	1.49	3.523	214.612	0.0027
2	1.0	2.59	0.51	4.10	0.29	1.21	3.56	3.22	1.92	3.519	214.115	0.0027
3	1.5	2.70	0.53	4.34	0.23	1.48	3.68	3.53	1.98	3.521	214.296	0.0027
4	2.0	2.71	0.24	4.49	0.10	2.89	2.93	2.89	2.24	3.523	214.544	0.0027
5	2.5	2.87	0.28	4.60	0.28	4.20	2.43	3.16	2.42	3.525	214.863	0.0027
6	3.0	2.90	0.33	4.83	0.43	5.37	1.89	3.34	2.45	3.528	215.217	0.0027
7	3.5	2.84	0.45	5.14	0.53	5.35	1.48	3.46	2.32	3.527	215.099	0.0027
MEDIUM												
1	6.5											
2	8.8											
3	10.5	5.61	0.39	8.95	0.87	12.28	1.34	6.03	5.10	0.947	15.516	0.0384
4	11.3	6.75	0.76	10.59	0.15	12.08	1.86	7.54	5.73	0.894	13.812	0.0431
5	12.0	7.32	0.91	10.28	0.44	12.59	1.37	8.06	6.04	0.836	12.084	0.0493
6	12.8	7.89	0.60	10.49	0.47	13.39	1.59	8.51	7.08	0.780	10.517	0.0567
7	13.5	8.66	0.80	10.82	0.30	13.81	1.03	9.58	7.63	0.723	9.040	0.0660
8	14.3	8.44	0.95	11.83	0.62	14.76	0.86	9.61	7.30	0.669	7.747	0.0770
9	15.0	10.27	0.65	11.90	1.32	15.14	0.94	10.77	9.36	0.616	6.556	0.0911
10	15.8	13.51	0.46	13.02	1.08	15.84	1.21	14.00	12.89	0.569	5.606	0.1068
HIGH												
1	17.0	13.45	2.46	16.82	0.34	16.62	3.45	15.92	10.99	0.542	5.085	0.1179
2	18.0	16.88	1.35	17.70	0.63	18.43	2.44	18.23	15.53	0.541	5.060	0.1185
3	19.0	18.37	1.24	20.78	1.15	20.22	1.00	19.61	17.12	0.541	5.069	0.1183
4	20.0	21.01	0.16	24.88	0.89	19.89	0.92	21.17	20.86	0.543	5.089	0.1178
5	21.0	22.10	1.32	27.18	1.95	20.35	1.26	23.42	20.78	0.537	4.993	0.1201
6	22.0	23.21	0.52	28.54	1.92	20.03	1.27	23.73	22.70	0.529	4.842	0.1239
7	23.0	23.27	1.53	30.83	2.17	21.40	0.04	24.81	21.74	0.520	4.666	0.1287
8	24.0	25.44	1.53	31.34	1.77	20.75	0.18	26.97	23.92	0.507	4.446	0.1352
9	25.0	25.50	2.27	32.87	1.48	20.66	0.42	27.77	23.23	0.496	4.252	0.1415
10	26.0	24.27	2.10	35.36	0.56	17.65	0.52	26.37	22.18	0.489	4.127	0.1458

STM4-2261 - NBR/Asb/Silica - supplied by Kirkhill Rubber Co.  
NBR-27 - NBR/Carbon Fiber filled - supplied by U.S. Polymeric.  
R2121 - NBR/Carbonized Rayon Cloth - supplied by U.S. Polymeric

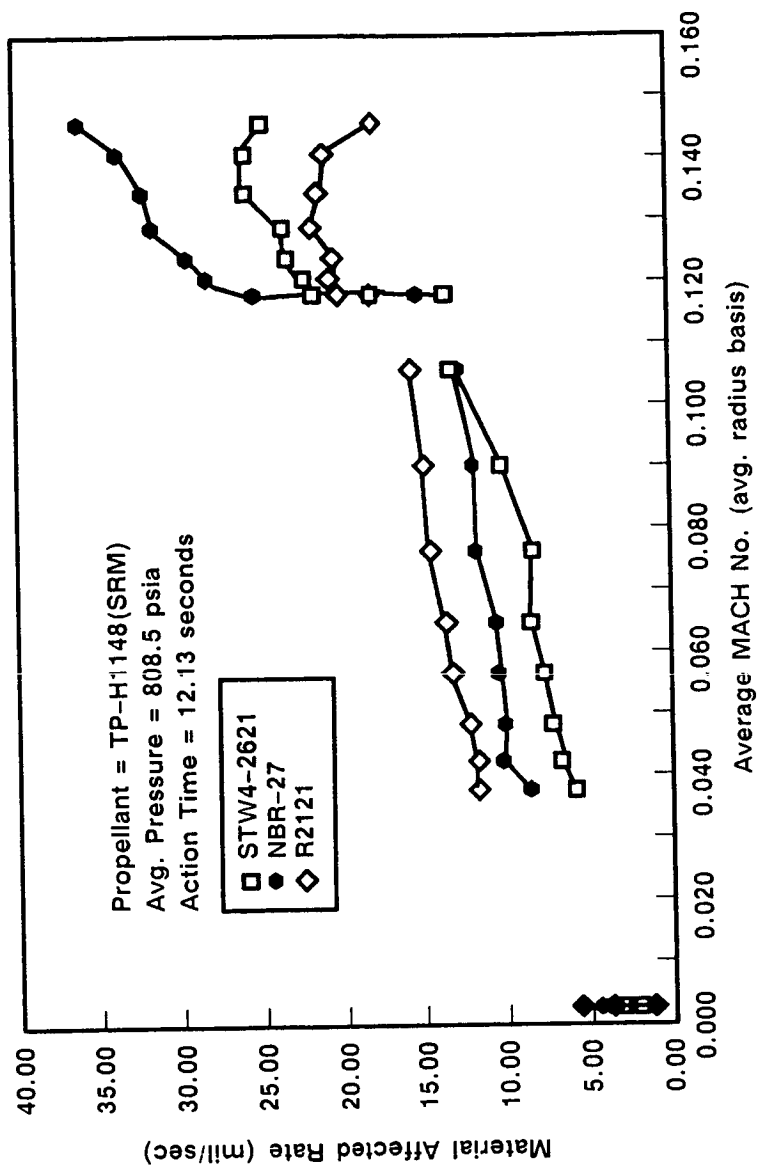


Figure 77. Material Affected Rate Versus Mach Number--Char Motor No. 107

A004664a

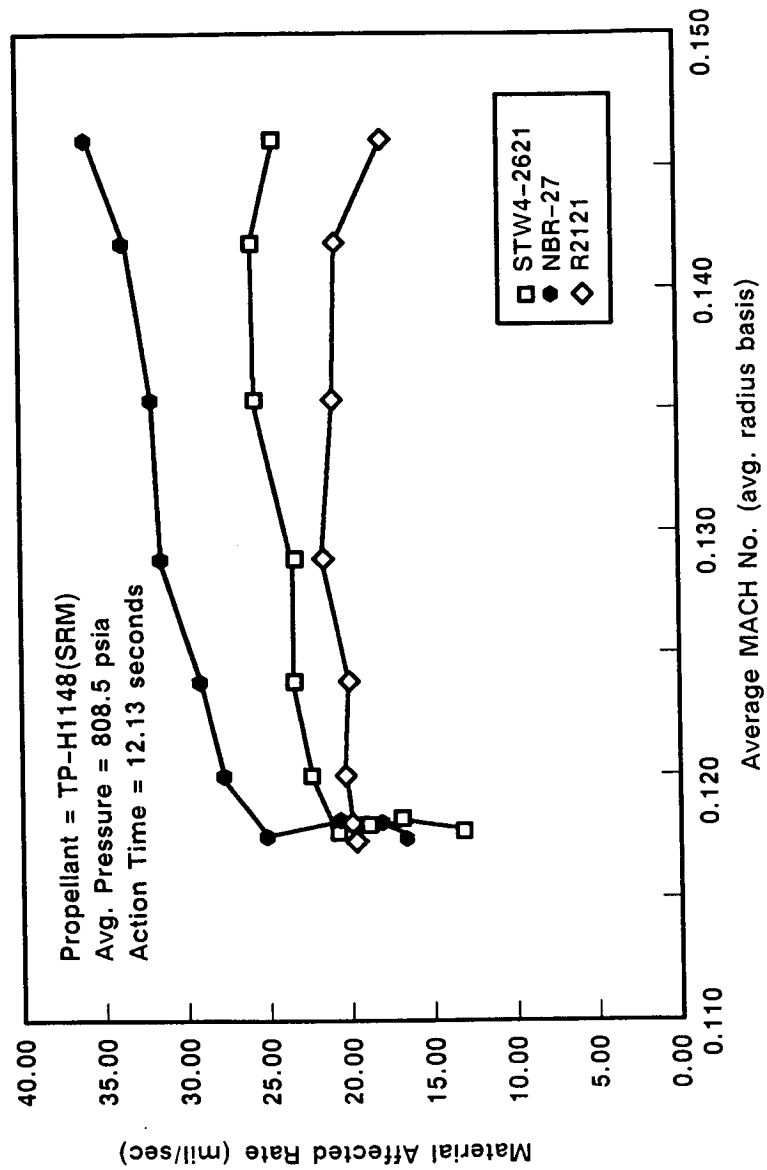


Figure 78. Material Affected Rate (High Velocity) --Char Motor No. 107



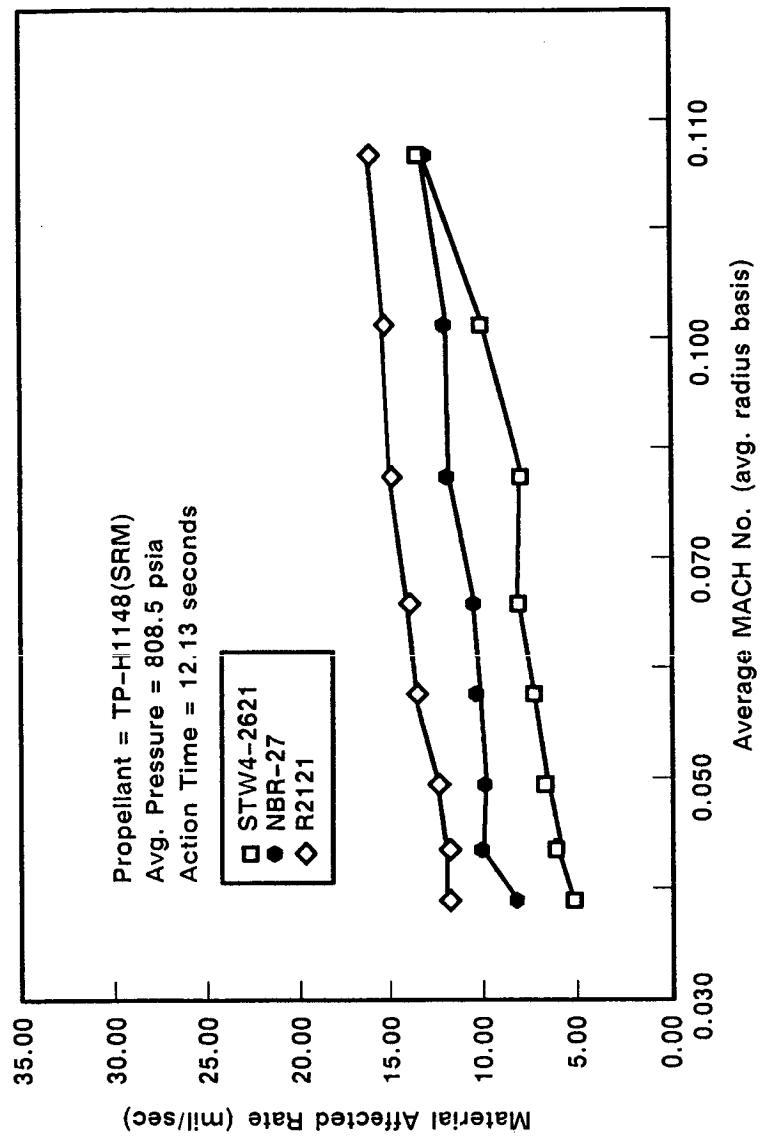


Figure 79. Material Affected Rate (Medium Velocity) --Char Motor No. 107

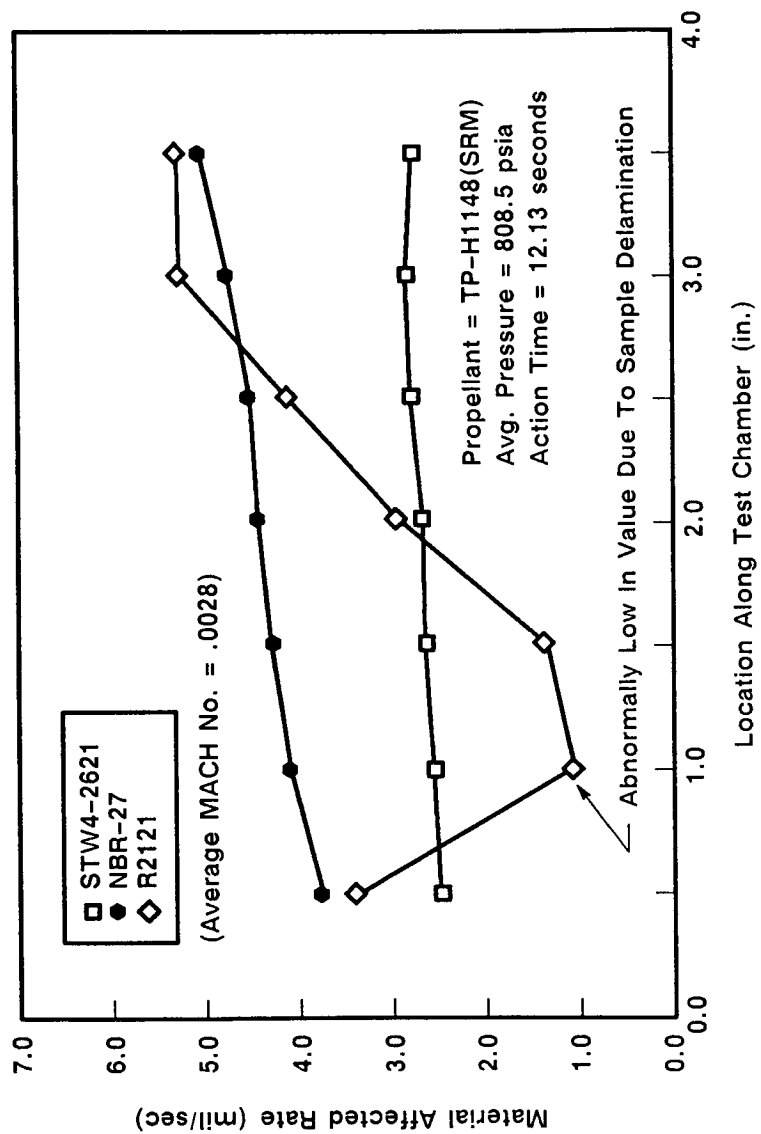


Figure 80. Material Affected Rate (Low Velocity) --Char Motor No. 107

motor operation. The design approach selected for the Block II design is an unvented system which prevents gas flow within the joint.

The baseline field joint insulation configuration is referred to as the J-seal (Figure 81). This configuration incorporates use of a thin adhesive bondline. The J-seal configuration is fabricated with the inboard leg of the tang insulation in a deflected condition. Upon assembly this leg provides contact with the clevis insulation to assure that the gap between the tang and the clevis insulation is closed off. The deflection leg of the tang insulation is designed to assure that, under worst-case thermal conditions and manufacturing tolerances, contact between the tang and clevis insulation is maintained. The deflection leg was designed for:

- a. At 90°F the nominal flap gap at assembly will be 0.075 inch.
- b. Based on thermal variations in the propellant grain and motor pressurization effects, 0.250 in. of deflection is incorporated into the design.
- c. To assure that contact always occurs between the tang and clevis joint insulation on assembly, an additional 0.100 in. of deflection is incorporated into the design.
- d. A minimum flap deflection gap of 0.050 in. is incorporated into the design to assure that the deflection flap pressurizes first at motor ignition, more rapidly than a leak path within the joint.
- e. The J-seal configuration is designed so that upon motor pressurization the deflection flap is pressurized, forcing the deflected leg against the clevis insulation, sealing off any leak paths within the joint, and reducing the amount of free volume deep in the joint.

An adhesive system is used to bond the deflected leg of the tang insulation to the clevis insulation on assembly. The adhesive system recommended for the case field joint is a pressure-sensitive adhesive. This adhesive, which has a thickness of 2 to 5 mils, is applied to assure a bond over the length identified in Figure 81. Application of the pressure-sensitive adhesive will probably be accomplished at the factory just prior to segment shipment. A protective backing remains on the adhesive to assure there is no contamination. Prior to assembly the protective backing is removed, leaving the bonding material for mating.

An alternate adhesive system uses a mastic-type adhesive. With the mastic material, the tang and clevis insulation outboard of the tip of the J-seal

ORIGINAL PAGE IS  
OF POOR QUALITY

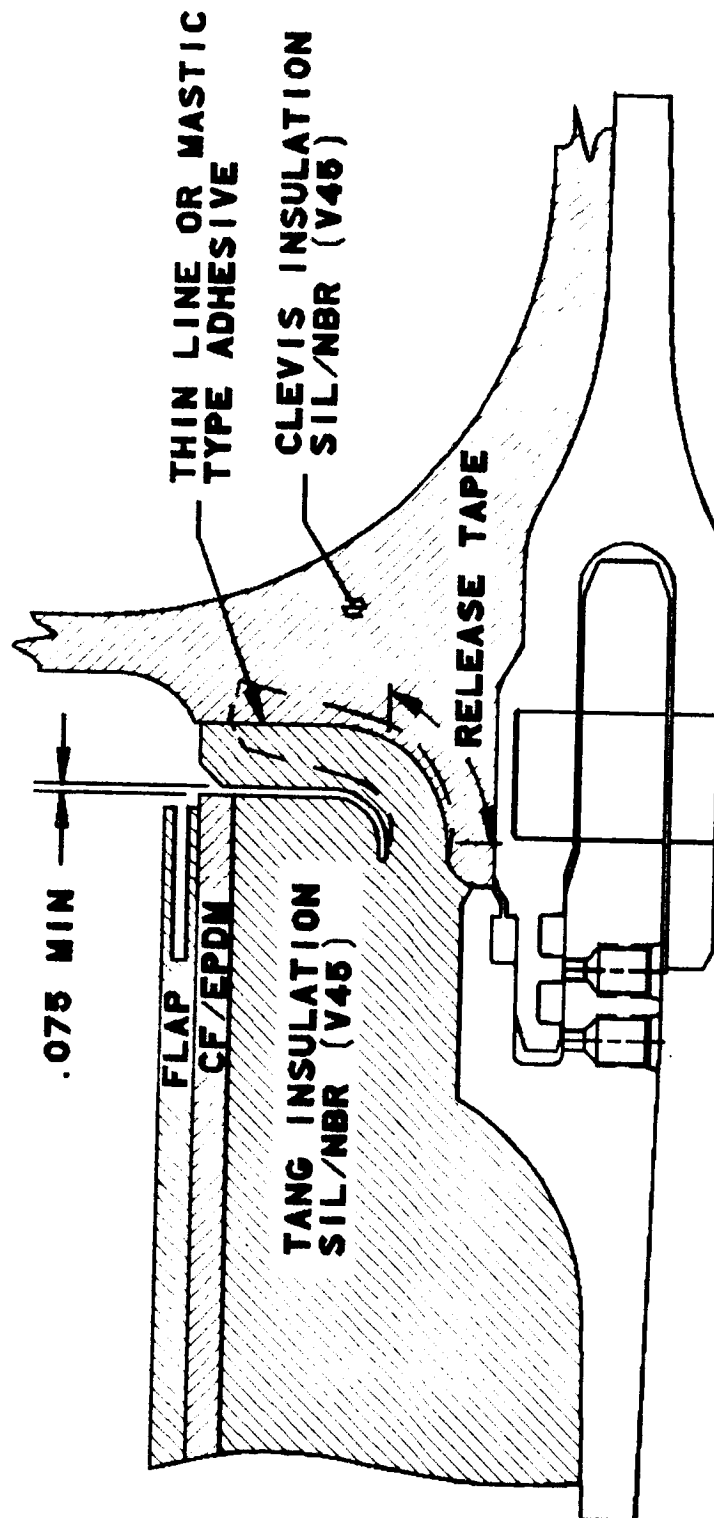


Figure 81. Bonded J-Seal

deflection flap is covered with a Teflon tape or FEP film to assure there is no bonding. This provides an area where joint deflection may occur and reduces the forces required for disassembly of segments. This type of adhesive system would be applied at KSC just prior to segment mating.

#### 3.9.3.3.1 Field Joint Alternatives

A number of other joint configurations have been evaluated to determine their attributes for protecting the field joints and seals during motor operation. An overview of the primary designs that were evaluated is presented in Figure 82. Figures 83 through 88 show designs considered, with their accompanying pros, cons, and brief reason as to why they were not selected. Designs outlined in Figures 83, 85, and 86 have been tested successfully in subscale motors as part of the RSRM effort and reports are available.<sup>(4)</sup>

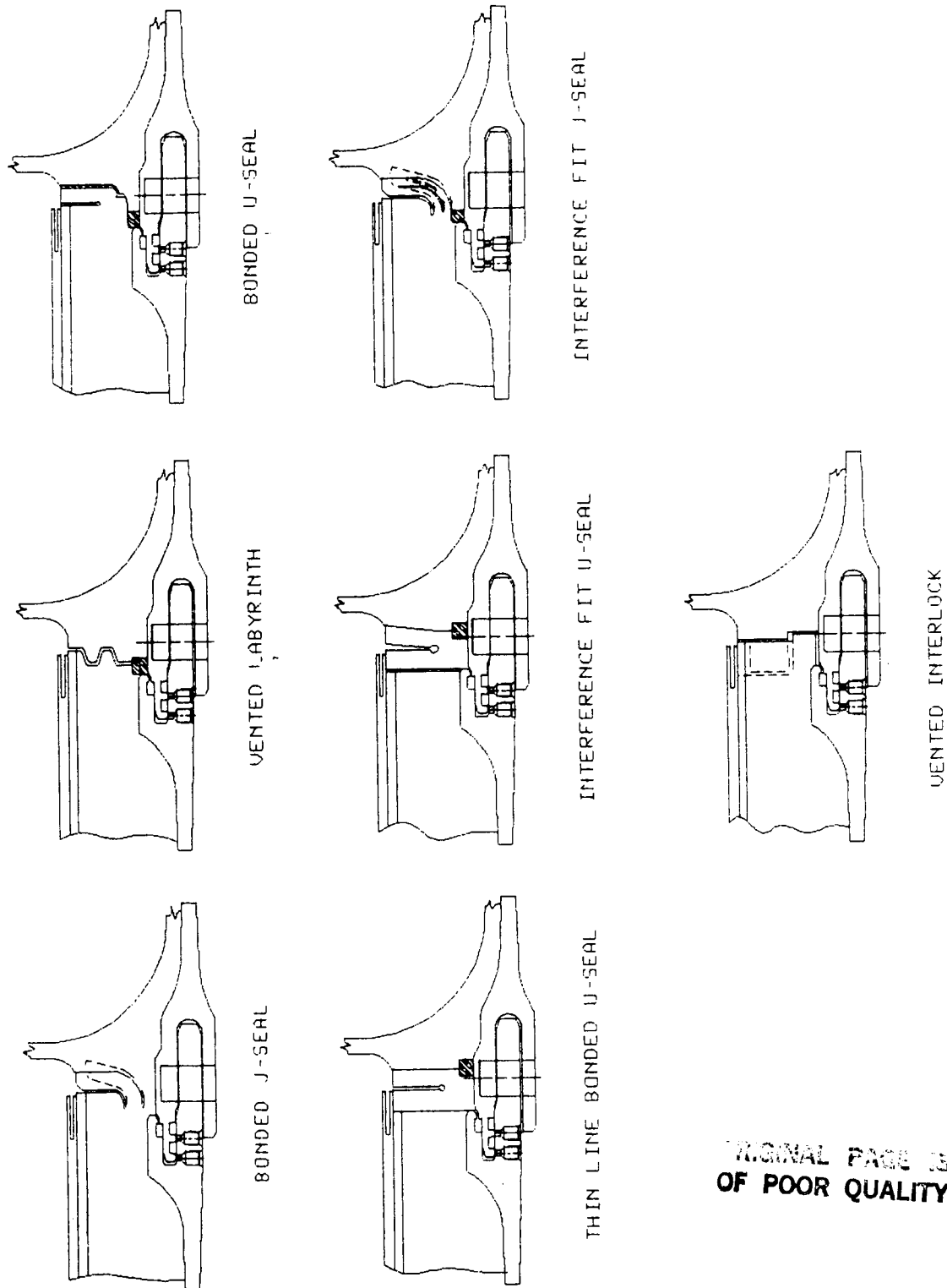
**J-Seal Flap Stiffener.** The J-Seal configuration selected as the baseline for the Block II SRM requires the use of bonding/sealing materials to ensure actuation of the J-seal flap during motor pressurization. An alternative design (Figure 87) has been evaluated should the bonded seal develop problems.<sup>(5)</sup> This design features a metal stiffener embedded in the J-seal flap for forcing the flap firmly against the clevis insulation. This concept will be tested as part of the redesign effort.

The potential advantage in this type of a design is the elimination of any adhesive in the joint while maintaining positive pressure between the J-seal flap and the clevis insulation interface. This flap stiffener concept also allows for compressed air, at the base of the J-seal, to escape without sacrificing the integrity of the seal.

---

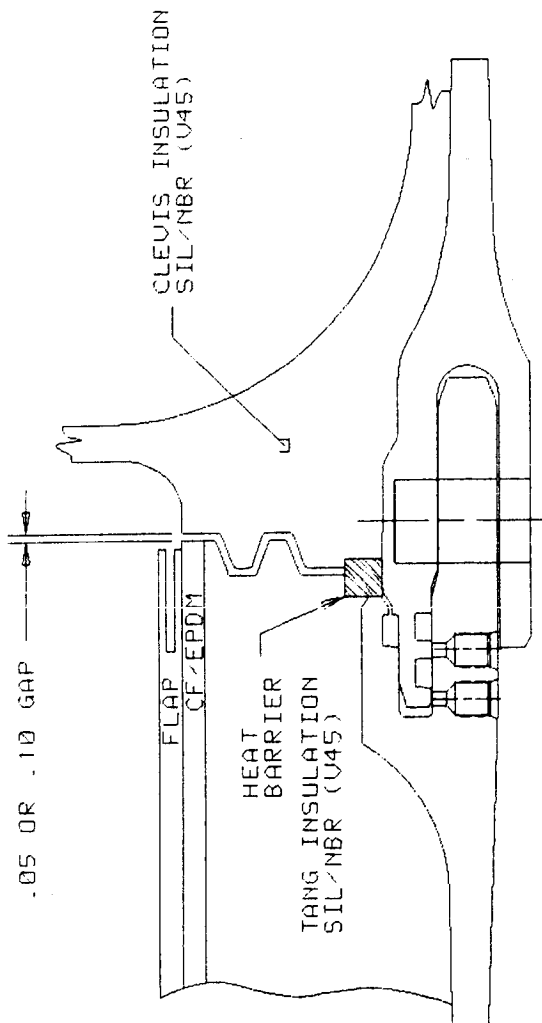
<sup>4</sup>Ibid, page 3-201.

<sup>5</sup>J. F. Miller, "Space Shuttle SRM J-Seal Stiffener Design Concept," TWR-16003, 30 November 1986.



ORIGINAL PAGE IS  
OF POOR QUALITY

Figure 82. Overview of Field Joint Trade Study



PROS:

COOLS HOT GAS MEASUREABLY AHEAD  
OF CAPTURE FEATURE O-RING  
ALLOWS PRESSURIZATION OF O-RING

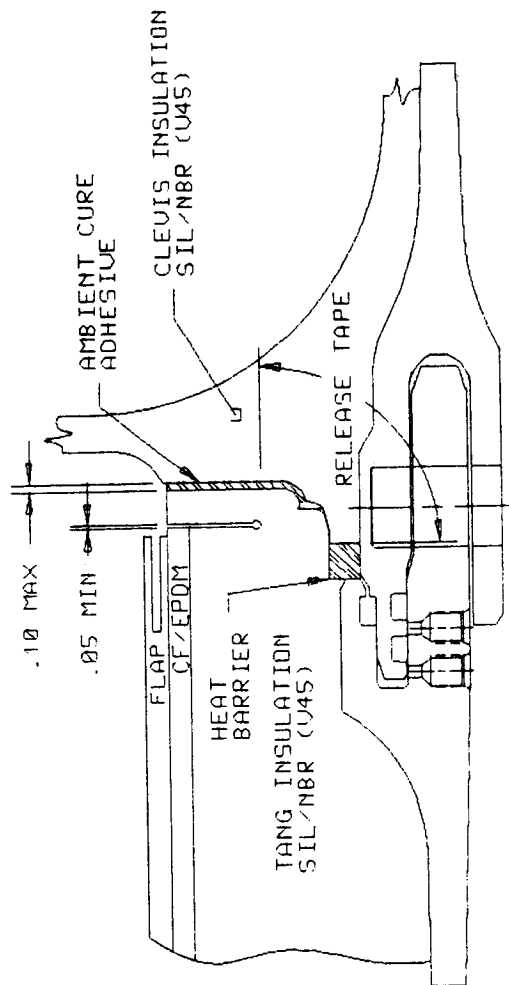
CONS:

DIFFICULT TO FABRICATE  
VERY DIFFICULT TO MAINTAIN INTEGRITY  
OF GAP (ESP. RAMPED REGIONS)  
SLUMP OF PROPELLANT CAUSES IRREGULAR  
OPENING OF GAP THUS ALLOWING  
HOTTER THAN NORMAL GAS INTO  
OPENING  
IF GAP IS CLOSED IRREGULARLY,  
IMPINGEMENT FLOW COULD RESULT

COMMENTS: NOT CONSIDERED BECAUSES OF DIFFICULTIES IN FABRICATION.  
IF THE GAP OPENS OR CLOSES IRREGULARLY HOT GAS MAY  
DAMAGE THE HEAT BARRIER AND THUS CAUSE UNWANTED  
HOT GAS IN THE SEAL REGION

ORIGINAL PAGE IS  
OF POOR QUALITY

Figure 83. Vented Labyrinth



PROS:

ALLOWS FOR SEAL AT THE INSULATION  
MOTOR PRESSURE TENDS TO  
SEAL THE U-SEAL TO CLEVIS  
INSULATION  
GAP IS NOT ADVERSELY AFFECTED  
BY JOINT ROTATION  
U-SEAL IS SIZED TO WITHSTAND  
FULL MOTOR DURATION

CONS:

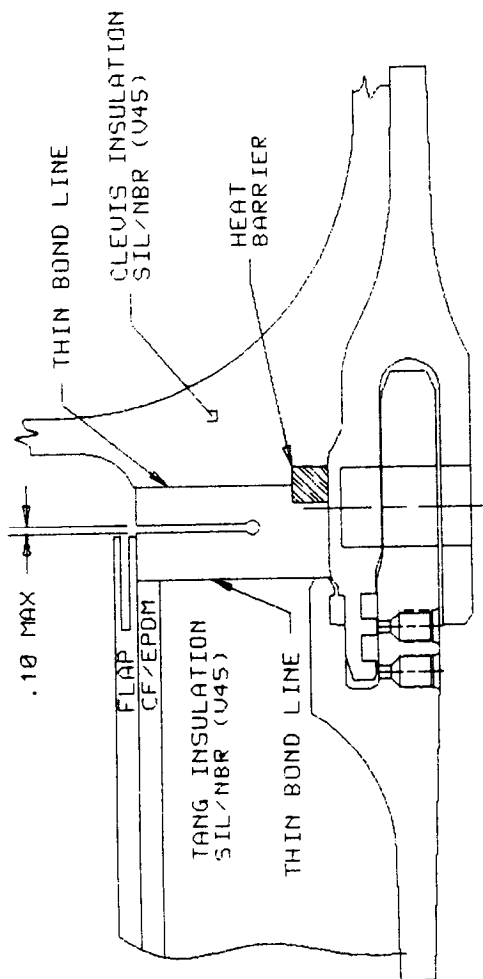
ADHESIVE AT U-SEAL TO CLEVIS  
INSULATION MAY CAUSE BUILDUP  
OF COMPRESSED AIR AT BASE OF  
U-SEAL  
COMPRESSED AIR MAY CAUSE A  
BLOWHOLE IN ADHESIVE AND  
THUS A POSSIBLE GAS PATH  
TO SEAL REGION  
NO CONSIDERATION FOR INTERFERENCE  
AT U-SEAL TO CLEVIS INSULATION

COMMENTS: NOT CONSIDERED BECAUSE THERE IS  
TOO MUCH POSSIBILITY OF BUILDUP OF COMPRESSED AIR  
AT THE BASE OF THE U-SEAL

Figure 84. Bonded U-Seal



ORIGINAL PAGE IS  
OF POOR QUALITY



PROS:

ALLOWS FOR SEAL AT THE INSULATION

MOTOR PRESSURE TENDS TO SEAL THE U-SEAL TO CLEVIS INSULATION

GAP IS NOT ADVERSELY AFFECTED BY JOINT ROTATION

U-SEAL IS SIZED TO WITHSTAND FULL MOTOR DURATION

THIN BOND LINE ON TANG SIDE ALLOWS FOR SEPARATION OF SEGMENTS WITHOUT MACHINING NEW TANG INSULATION

CONS:

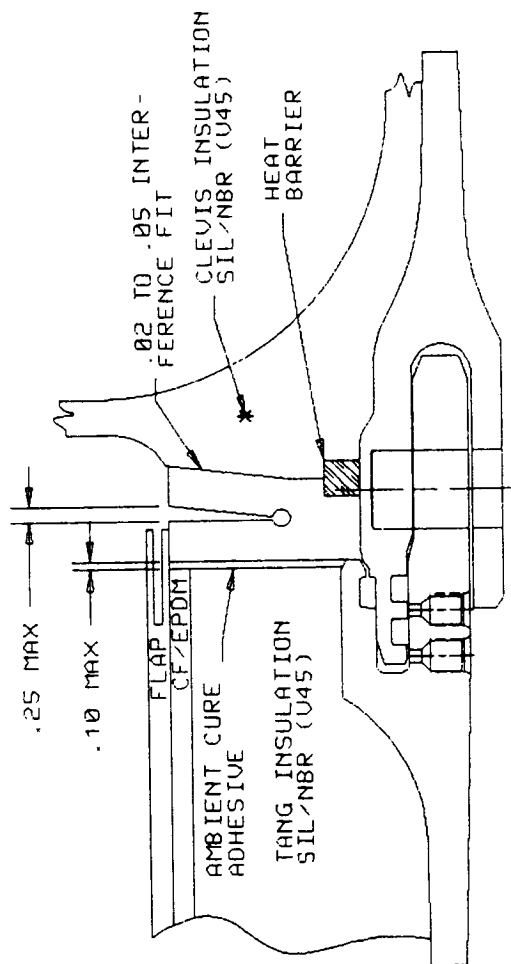
ADHESIVE AT U-SEAL TO CLEVIS INSULATION MAY CAUSE BUILDUP OF COMPRESSED AIR AT BASE OF U-SEAL

COMPRESSED AIR MAY CAUSE A BLOWHOLE IN ADHESIVE AND THUS A POSSIBLE GAS PATH TO SEAL REGION

NO CONSIDERATION FOR INTERFERENCE AT U-SEAL TO CLEVIS INSULATION

COMMENTS: NOT CONSIDERED BECAUSE DOES NOT ALLOW FOR SLUMP HEAT DIFFERENTIALS ETC.

Figure 85. Thin Line Bonded U-Seal



PROS:

ALLOWS FOR SEAL AT THE INSULATION

MOTOR PRESSURE TENDS TO SEAL THE U-SEAL TO CLEVIS INSULATION

GAP IS NOT ADVERSELY AFFECTED BY JOINT ROTATION

U-SEAL IS SIZED TO WITHSTAND FULL MOTOR DURATION

CONS:

THICK BOND LINE MAY ERODE WHEN FLAP HAS BEEN ERODED

WILL BE DIFFICULT TO MAINTAIN INTEGRITY OF U-RING ON FULL SCALE SEGMENTS

COMMENTS: NOT CONSIDERED BECAUSE DOES NOT ALLOW FOR U-RING INSTALLATION INTEGRITY

Figure 86. Interference Fit U-Seal

ORIGINAL PAGE IS  
OF POOR QUALITY

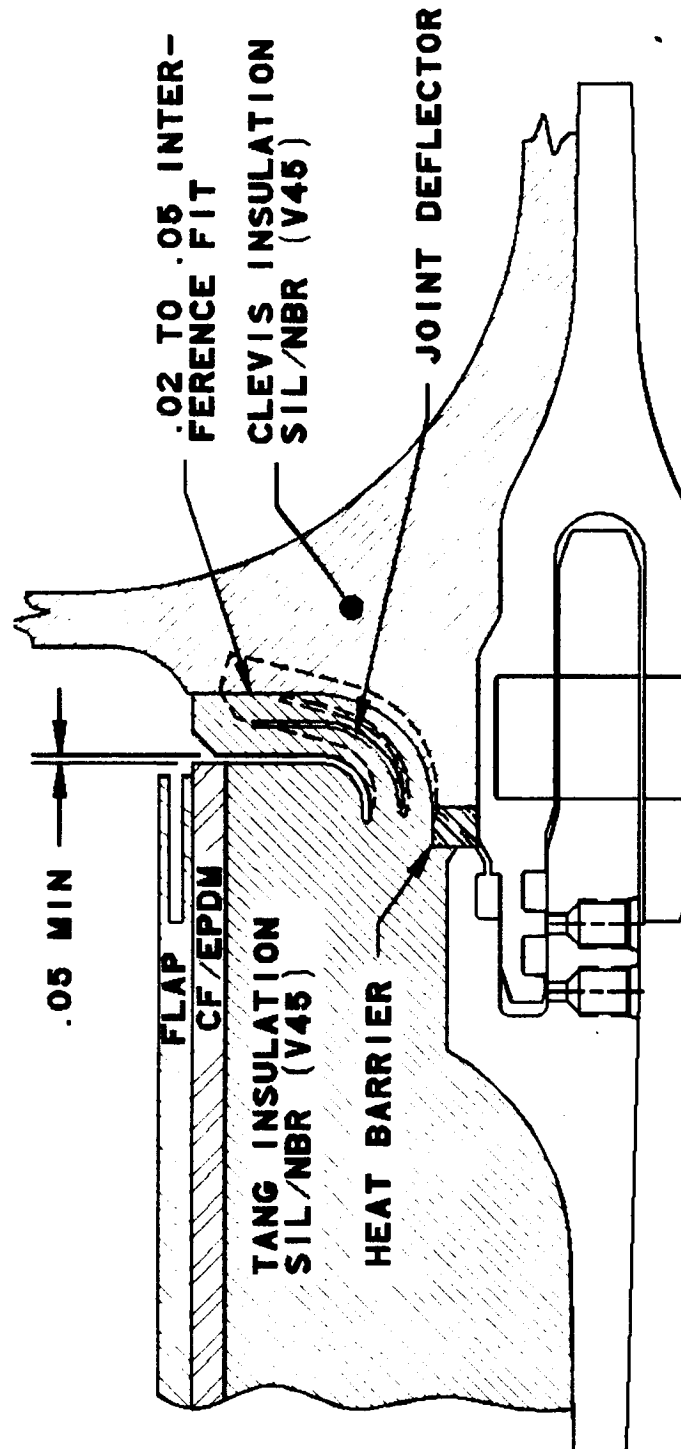


Figure 87. Interference Fit J-Seal

ORIGINAL PAGE IS  
OF POOR QUALITY

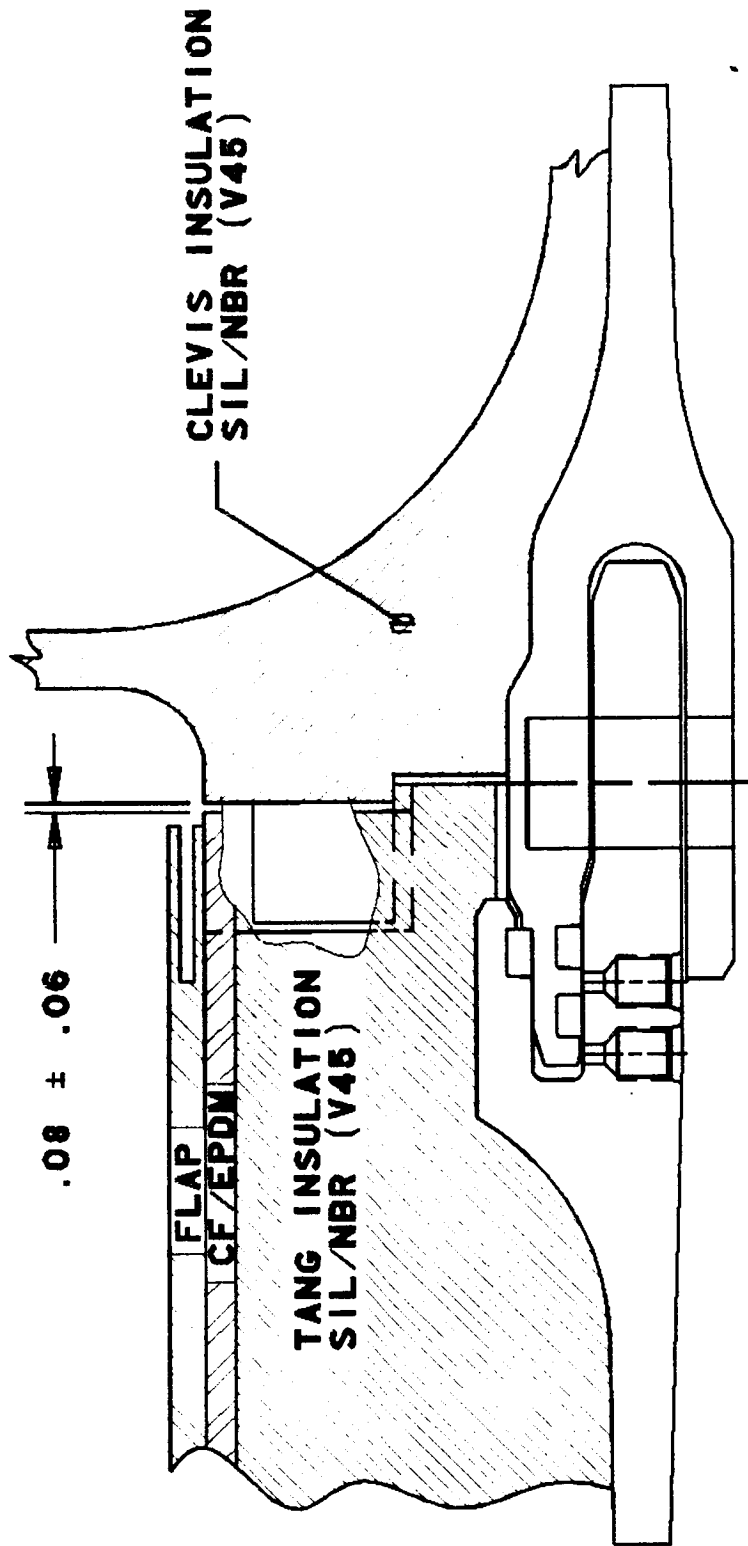


Figure 88. Vented Interlock

**Vented Interlock.** A vented interlock design, as defined in Figure is also being carried as an alternate to the baseline J-seal configuration. The vented interlock configuration allows for uniform pressurization at the capture feature upon ignition. It incorporates a series of 18 circumferential interlocking protrusions and recess areas on the tang and clevis insulation. Upon assembly each protrusion mates up to a corresponding recess area to form a restriction within the joint. Pressurization to the capture feature occurs through gaps (0.20 to 0.40 in.) located between the end of each protrusion and the recess area. The length of the protrusions is designed so that upon assembly a minimum gap of 0.02 in. would exist between the protrusion and recess area. This was designed to assure that no potential case/insulation debond problems are created due to an interference problem. Upon motor pressurization the tang and clevis insulations deflect away from each other, forming a wider joint gap. The interlocks are designed to assure that under worst-case gap conditions approximately 50 percent of the interlock blocking feature remains to restrict flow.

**Heat Barrier.** As part of the RSRM effort, both Morton Thiokol and MSFC have conducted preliminary conservative analyses to evaluate the severity of circumferential flow within the O-ring groove in the capture feature of the current baseline case field joint. These conservative analyses assumed two leak paths through the insulation bond and an O-ring groove modeled as a smooth tube. These analyses predicted flow velocities on the order of 100 ft/sec. The assumption that a pressure differential exists, driving gas flow for full motor burn, produced unacceptable capture feature heating.

Other internal joint potential heating mechanisms that could be of concern are gas impingement and the accumulation of slag particles on seals and metal parts. Extensive slag and molten aluminum oxide accumulations might cause unacceptable thermal degradation.

Heat barriers are a proposed alternative solution to these potential thermal degradation issues. As part of the RSRM effort, heat barriers are being evaluated to protect the seals and metal parts from thermal degradation due to circumferential flow, hot gas jet impingement, slag impingement, and slag accumulation.

The barriers would likely be positioned between joint insulation surfaces, as close to the metal parts as practical. Figures 83 through 87 show typical heat barrier locations.

The function of the barriers would be to provide an extra measure of thermal protection to pressure vessel seals and metal parts. This extra protection would not be required under normal motor and joint operating conditions, but it could substantially improve metal parts and seal survivability in case of anomalous performance. The scenarios addressed include:

- a. Jet impingement, single and multiple leak paths through the insulation joints.
- b. Circumferential flow, low-velocity hot gas circulation occurring in the insulation joint.

Heat barrier materials may be divided into four categories: refractories, sacrificial coolants, intumescent, and composites of the three. The following is a brief discussion of the materials in terms of these four categories.

- a. Refractories are capable of surviving the high-temperature, high-pressure, and chemically reactive environment for the duration of the motor burn. Refractories are potentially good, continuous flow blockers by virtue of their survivability. However, their performance at higher temperature might make them incompatible with surrounding materials. At high temperatures they may conduct heat into adjacent insulation, inducing thermal degradation.
- b. Coolant materials serve to remove energy from hot gases invading the joints. These ablative materials remove energy from the gases through absorbed latent heat, heats of fusion, boiling, and sublimation, as well as off-gassing, producing cool volumes of mixing gas.
- c. Intumescent materials are being evaluated as a part of the coolant development effort. Commercially available intumescent swell to 150 times their initial volume. In addition to swelling, they may function as ablative coolants. Teflon, although not thought of as being intumescent, swells by a small percentage when heated.
- d. Composites of coolant fillers in refractory matrices are designed to survive the SRM environment while providing a gas cooling function. Binder materials serve to hold coolants in refractory matrices.

Initial heat barrier material screening has been performed. A large number of possible materials are being procured and evaluated for selection by the RSRM team. This list includes:

- a. Knitted tungsten wire, 0.5- by 0.5-inch. The wire diameter is 0.0045-inch. the density is approximately 15 percent.
- b. Knitted stainless steel, 0.5- by 0.5-inch. The wire diameter is 0.0045-inch. The density is 20 percent.
- c. Knitted stainless steel, 0.5- by 0.5-inch. The wire diameter is 0.0045-inch. The density is 10 percent.
- d. Knitted stainless steel, 0.5- by 0.5-inch. The wire diameter is 0.0045-inch. The density is 30 percent.
- e. Filament wound graphite fiber with Vamac<sup>®</sup> rubber binder, 0.5- by 0.5-inch.
- f. Filament wound Kevlar fiber with Vamac<sup>®</sup> rubber binder, 0.5- by 0.5-inch.
- g. Teflon-impregnated carbon fiber braid, 0.5-inch.
- h. Braided virgin Teflon, 0.5- by 0.5-inch.
- i. Corrugated Grafoil tape, 0.5- by 0.015-inch.
- j. Woven ceramic cloth on knitted stainless steel hollow core, 0.5-in. diameter with 0.5-in. tail.
- k. Reticulated vitreous carbon, ring samples, 12-in. OD by 8-in. ID by 1.0-in. height. Pore sizes of 45 and 100 pores per linear inch.
- l. Reticulated vitreous carbon coated with nickel, ring samples, 1.5-in. OD by 0.75-in. ID by 1.0-in. height. Pore sizes of 10 and 80 pores per linear inch.
- m. Reticulated silica carbide, ring samples, 12-in. OD by 8-in. ID by 1.0-in. height, and 1.5-in. OD by 0.75-in. ID by 1.0-in. height. Pore sizes of 10, 45, 80, and 100 pores per linear inch.
- n. Compressed aluminum foam, 0.55-in. by 0.4-inch. 80 pores per linear inch.
- o. Aluminum foam coated with Teflon, a compressed bar, 0.55- by 0.4-inch at 80 pores per linear inch, and a ring, 1.5-in. OD by 0.75-in. ID by 1.0-in. height at 40 pores per linear inch.

These materials are being subjected to hot gas impingement test as part of the RSRM effort. Capability of these materials and the necessity for any additional heat barriers will be established in the ongoing test programs and results can be incorporated in a final Block II SRM, if necessary.

### 3.9.4 MANUFACTURING PROCESS ALTERATIONS

Both manual and semimechanized layup techniques will be used to rubber insulate the Block II SRM casting segments. The primary insulation is a silica-filled NBR used in varying thicknesses up to 0.200 inch. Quantities of carbon fiber-filled EPDM will also be used in high erosion areas of the center segments and the aft segment. Uncured NBR extrusions will be procured for use in the layup where irregularly shaped pieces are needed which are normally applied in the thicker insulation area of the segment joints.

The major modification to existing HPM insulation installation occurs in the aft dome. The aft dome will be insulated by manually laying up precut pieces of NBR and carbon fiber-filled EPDM. SIL/NBR is layed up as a substrate over the entire aft dome and nozzle fixed housing. Then CF/EPDM will be laid up over the aft dome in a series of "debulking" operations. This will be accomplished by laying up approximately one-third of the required thickness; then the entire unit will be vacuum bagged. This minimizes entrapped air and compresses the rubber. This operation will be repeated until the required design thickness is achieved, with allowance for curing shrinkage. Then the premachined nozzle carbon phenolic insulator will be attached and again the entire unit will be vacuum bagged, autoclave cured, and inspected as a separate part.

Insulations for the aft dome stress relief flap will be installed and vulcanized in a contoured tooling/casting dome (Figure 88) with appropriate release materials. The bonding of the propellant to the flap will be accomplished during the propellant casting of the aft segment. The tooling/casting dome will be used to establish the aft dome propellant and flap contour. Upon removal of the tooling dome, the outside material line (OML) or inside of the relief flap will be measured. The measurement will be compared to the inside material line (IML) of the insulated aft dome. The insulated aft dome IML will then be machined to ensure proper stress relief and joint pressurization prior to mating and installation to the aft segment (Figure 89).



ORIGINAL PAGE IS  
OF POOR QUALITY

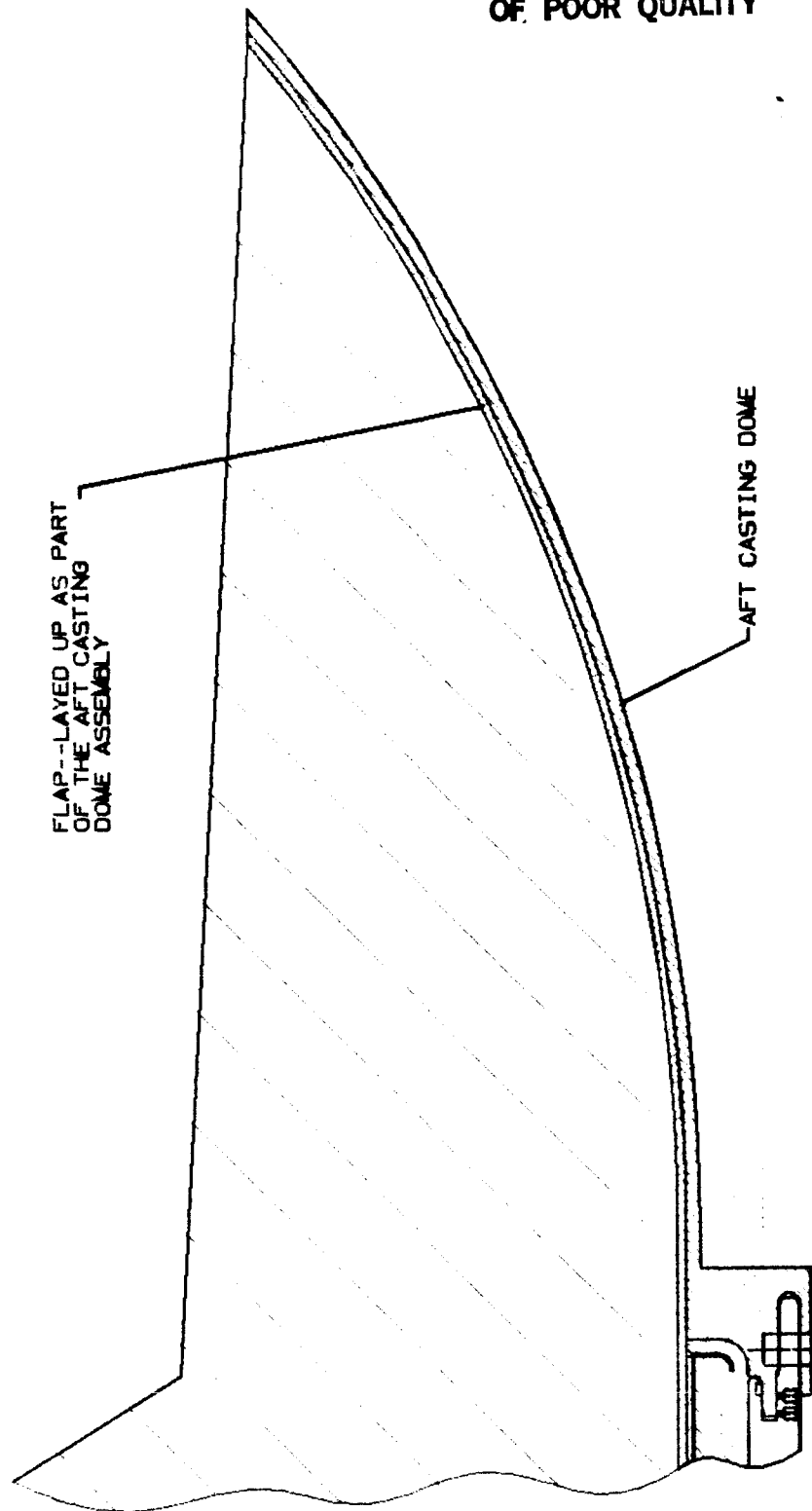


Figure 89. Casting Dome Assembly

ORIGINAL PAGE IS  
OF POOR QUALITY

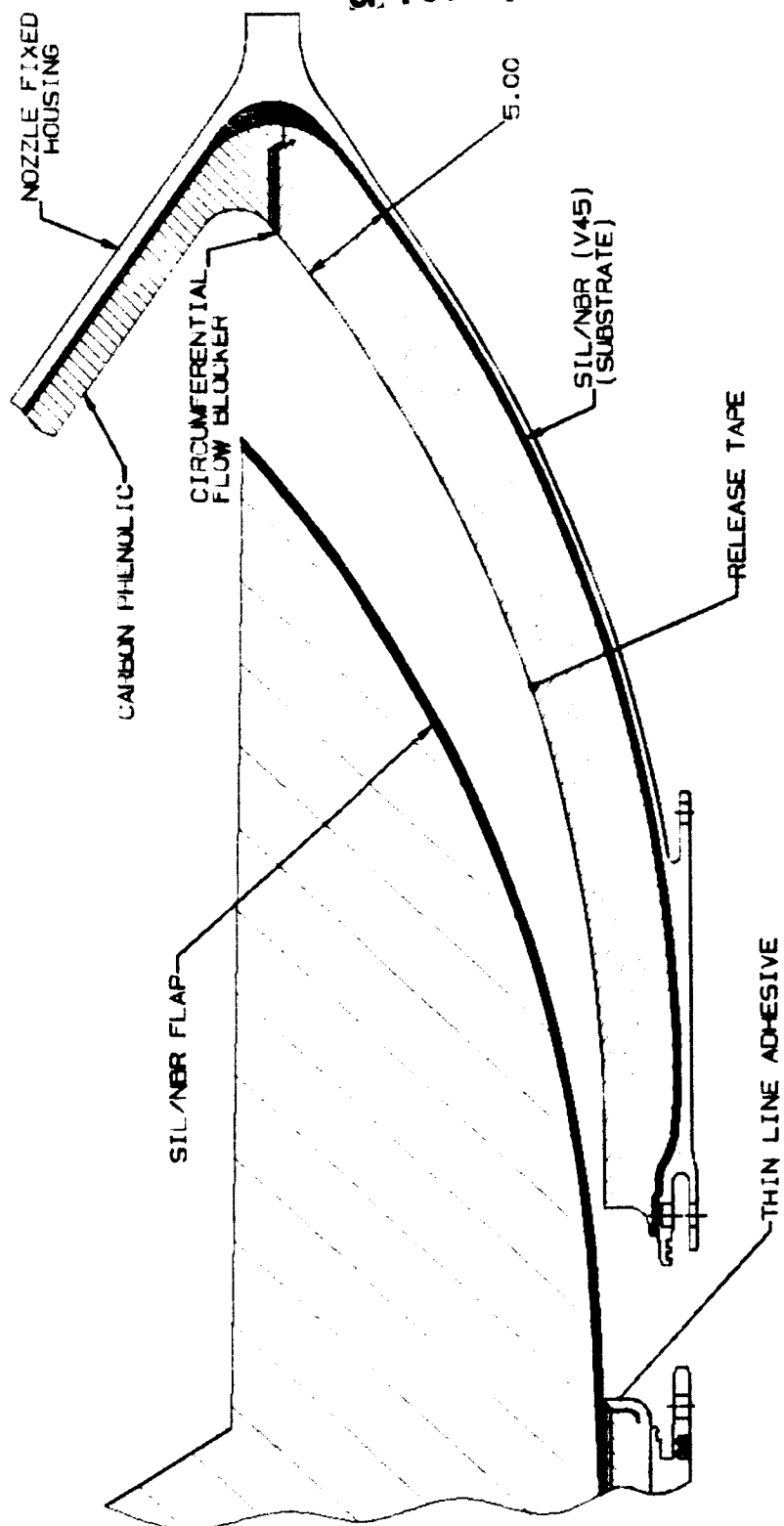


Figure 90. Nozzle Assembly-to-Aft Segment

PRECEDING PAGE BLANK NOT FILMED

### 3.10 IGNITER

The current HPM ignition system consists of an internally mounted pyrogen igniter and initiator and an externally mounted safety and arming (S&A) device. The performance of the ignition system has been satisfactory in all qualification tests and flights and no major design changes are required. The Block II ignition studies were centered on increasing the reliability of the system while maintaining the same basic configuration. Improvements for the Block II SRM ignition system will consist of shortening the igniter chamber to reduce inert weight, and eliminating potential leak paths by using more reliable attachment and sealing methods.

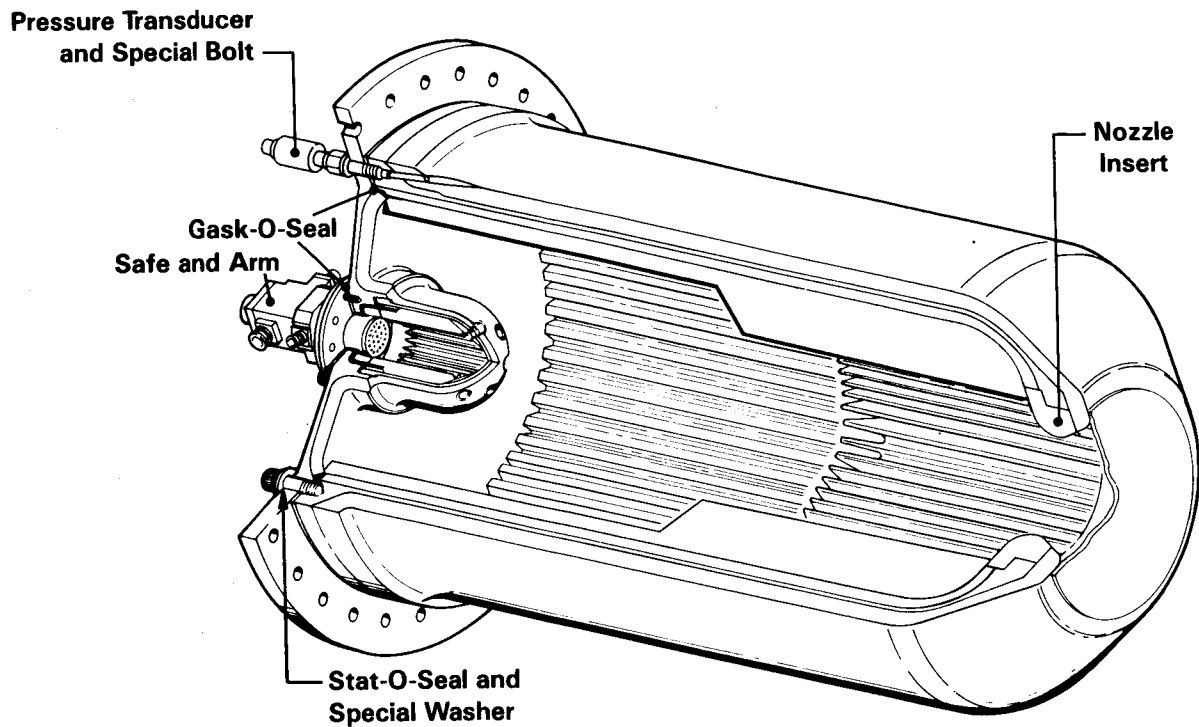
#### 3.10.1 DISCUSSION

The HPM igniter has a 40 starpoint propellant grain. Twelve inches of starpoints were cut down during development testing to reduce initial surface area which decreased the ignition shock and mass flow rate. The igniter chamber was not changed to account for the reduction in the propellant volume, so igniters were cast in chambers with reduced starpoints. The Block II SRM igniter chamber length will be reduced by 8.6 in. by removing the cutback and adding 3.5 in. of full length starpoints. The total weight savings for the chamber, internal, and external insulation will be approximately 60 lb.

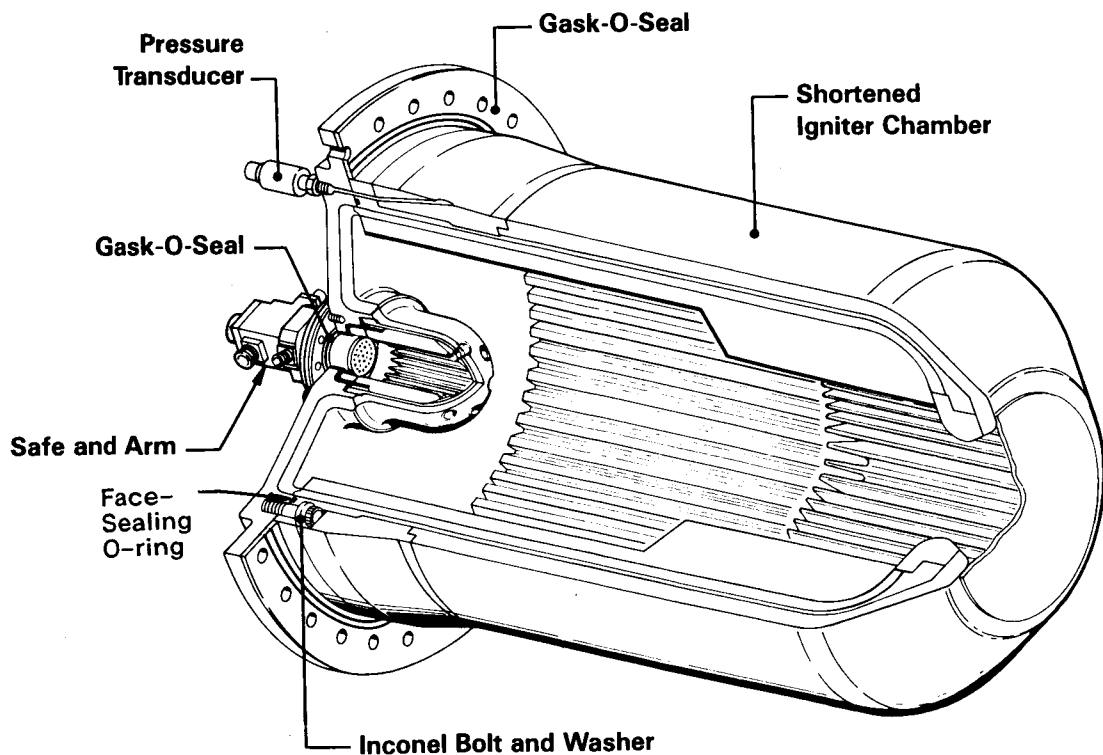
Other design changes included in the Block II SRM igniter are shown in Figure 91.

1. Change the direction of the attach bolts between the igniter adapter and the igniter chamber.
2. Replace the inner Gask-O-Seal<sup>®</sup> (adapter to chamber joint) with an O-ring seal.
3. Remove environmental seals between S&A/igniter adapter and igniter/forward dome. (Gask-O-Seal<sup>®</sup> will remain, and will be made of 321 stainless steel instead of cadmium-plated 4130 steel.)
4. Eliminate vacuum putty in joint areas.

### Present HPM Ignition System Configuration



### Block II SRM Ignition System Configuration



87354-9A

Figure 91. Comparison of Current and Block II SRM Ignition Systems

5. Liner used on SRM cases (STW5-3229) will be used for the improved igniter.
6. Eliminate six environmental seals on the igniter initiator nozzle parts.

These changes will eliminate 41 seals from the igniter assembly by eliminating seals at attach bolts, special bolts, and inner Gask-O-Seal<sup>®</sup> and replacing them with a face-sealing O-ring.